Dibenzo-30-crown-10: Synthetic optimization and studies of the binding conformation and efficacy

Hanlie Ronèl Wessels

Dissertation submitted to the faculty of the Virginia Polytechnic Institute and State University in partial fulfilment of the requirements for the degree of

Doctor of Philosophy
In
Chemistry

Harry W. Gibson, Chair
Richard D. Gandour
Tijana Z. Grove
David G. I. Kingston

15 February 2018
Blacksburg, VA

Keywords: crown ethers, DB30C10, paraquat, rotaxane, poly(pseudorotaxane), binding conformation

Dibenzo-30-crown-10: Synthetic optimization and studies of the binding conformation and efficacy

Hanlie R. Wessels

ABSTRACT

Dibenzo-30-crown-10 (**DB30C10**) is one of the first-generation macrocyclic hosts discovered by Pedersen. Crown ethers originally attracted attention due to their ability to encapsulate metal cations and render them soluble in organic solvents. These studies helped to launch host-guest chemistry as a discipline within supramolecular chemistry. Crown ethers form complex molecules containing organic cations and neutral organic molecules. Additionally, they form components in supramolecular architectures such as catenanes, rotaxanes, and supramolecular polymers. They have been used as selective hosts in diverse applications such as wastewater treatment, switchable catalysis, therapeutic agents, sensors, molecular machines, and stimuli responsive materials ("smart polymers"). Despite the vigorous research activity in the field, **DB30C10** has received surprisingly little attention. **DB30C10** was reported in 1967 and has been commercially available since 1992; however, it has been mostly overlooked as a host in favour of smaller crown ethers such as **DB24C8**, **B15C5**, **18C6** and **15C5**.

Herein we present an improved synthetic route that improves the yield of the cyclization step in the synthesis of **DB30C10** from 25% to 88% enabling us to prepare multiple grams of the material without the use of pseudo high-dilution techniques. The same methodology was applied to three other crown ethers with similar improvement in yield.

Four new rotaxanes based on the **DB30C10**-paraquat binding motif were used to investigate the binding conformation of **DB30C10** and paraquat. The new rotaxanes were characterized by ^{1}H, ^{13}C and 2D-NOESY NMR, mp, and HRMS. A single crystal X-ray structure of one of the [2]rotaxanes was obtained. To our knowledge, this is the first crystal structure of a rotaxane based on this particular binding motif. This result illustrated that **DB30C10** was a suitable host for the construction of supramolecular systems and polymers.

Our eventual goal is to use **DB30C10** in the construction of supramolecular polymers with novel topologies. Therefore, the relative threading efficiency of **DB30C10** in solution had to be determined. A series of segmented polyurethane poly(pseudorotaxanes) with paraquats in the backbone were synthesized with different crown ether or cyptand hosts. The threading efficiency was determined by ^{1}H NMR.

Dibenzo-30-crown-10: Synthetic optimization and studies of the binding conformation and efficacy

Hanlie R. Wessels

GENERAL AUDIENCE ABSTRACT

Supramolecular chemistry is loosely defined as “chemistry beyond the molecule”, that is the study of interaction between molecules. This field is broad and includes material science, biochemistry, self-assembly, host-guest chemistry, molecular recognition and more. Examples of self-assembly in Nature includes the tertiary structure of proteins and helical shape of DNA. Examples of host guest chemistry and molecular recognition include an enzymes interaction with only a specific substrate. The enzyme is the host and the substrate would be the guest.

Crown ethers were discovered in 1967 by Pedersen at DuPont. This discovery generated a lot of interest because he discovered that these molecules bind to metal cations and can render the metal salts soluble in organic solvents. Moreover, specific crown ethers show a preference for specific metal cations. No synthetic molecule has been able to do this before. The field expanded to include a large number of synthetic host molecules that can bind to all kinds of guests. The ability to design and make host guest pairs that interact with each other preferentially soon led to applications like sensors for specific metal ions, removing radioactive caesium from waste water, targeted drug delivery, and stimuli-responsive, or “smart”, materials. In 2016 the Nobel Prize in chemistry was awarded for the design and synthesis of molecular machines. Crown ethers are often used as component in these systems.

Dibenzo-30-crown-10 (**DB30C10**) is a molecule in the crown ether family. It was discovered in 1967, but very little study has been done on it compared to other crown ethers. In this dissertation we describe a new synthesis for **DB30C10** that has fewer steps, does not require cumbersome purification and significantly increases the yield of the final step from 25% to >80%. Our synthesis enables us to make multiple grams of **DB30C10** and three other crown ethers.

Because **DB30C10** is a large and flexible molecule, it can bind with our guest of interest (paraquat) in various ways. It can fold over the rigid guest making a “taco” complex, or the guest can presumably thread through the cavity of the host to make a pseudorotaxane. No conclusive proof of the latter binding conformation has been found. Since the guests needs to be threaded through the host system in order for the complex to be used in construction of supramolecular systems, it is imperative to investigate the binding mode of **DB30C10** with paraquat. We did this by designing and synthesizing four new rotaxanes (see figure below). The rotaxanes were isolated and analysed. In order to be a rotaxane the guest must be threaded through the host and is then trapped with blocking groups. This allows it to be differentiated from transient taco species that might form in

solution. Our rotaxanes were analysed by ^{1}H, ^{13}C and 2D NOESY NMR, melting point, HRMS and one of them was analysed by X-ray diffraction.

The successful synthesis and analysis of these four rotaxanes demonstrated that the **DB30C10**/ paraquat system can be used for synthesis of supramolecular systems. The crystal structure of our rotaxane is the first crystal structure with this system.

In addition to knowing that paraquats can thread through the cavity of **DB30C10**, we would like to know how easily this happens in solution compared to other hosts. We did this by making poly(urethanes) with paraquat units in the backbone of the polymer. We made a model backbone polymer (with no hosts) and repeated the synthesis in the presence of five different host molecules. We determined the amount of host present in the polymer after purification by ^{1}H NMR.

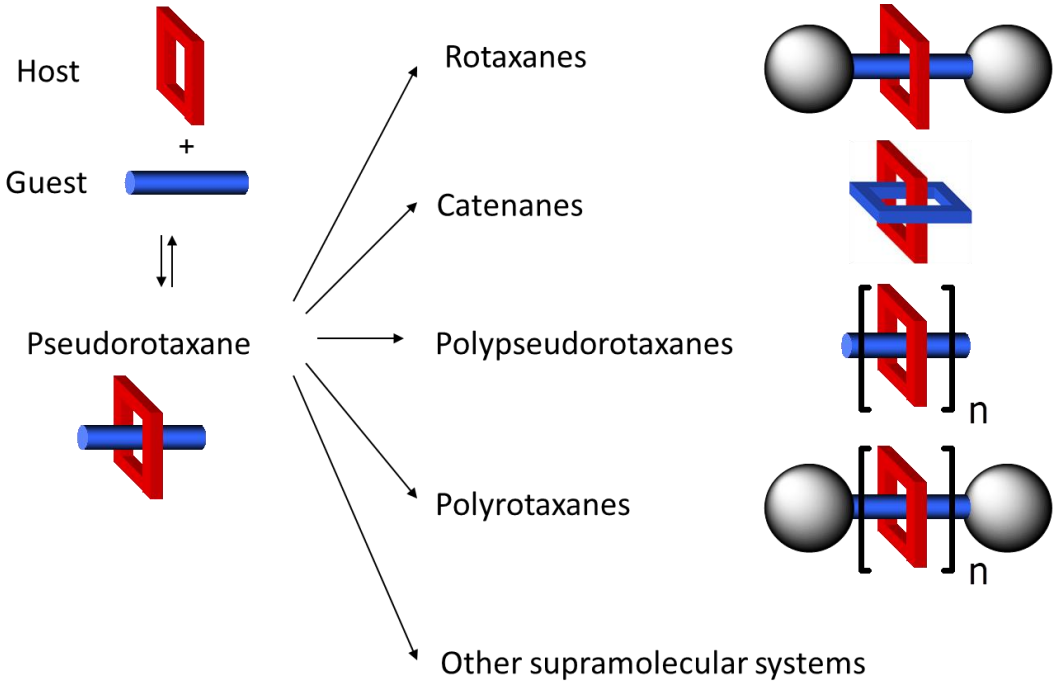

Dedication

To my husband Dr. Daniel Schoonover. I could never have done this without you

and

To all my students. You have made this endeavour worthwhile.

TABLE OF CONTENT

Chapter 1: Literature review

Supramolecular Chemistry

Traditionally, chemistry has been concerned with molecules whose constituent atoms are connected by covalent bonds, and how to connect atoms in a way that is useful. Supramolecular chemistry is concerned with assemblies of multiple molecules. Lehn, one of the fathers of supramolecular chemistry, notes that one can draw a distinction between super- and supra-molecular chemistry. He defines a supermolecule or "übermoleküle"[1] as an entity that is composed of discrete, well defined oligomeric species that is a result of intermolecular association between a few components. Lehn broadly defines supramolecular chemistry as the "chemistry of molecular assemblies beyond the molecule"[2] and more specifically as the assembly of multiple components into an array that has defined organization and specific characteristics.[1] Areas that have been studied under the umbrella of supramolecular chemistry include host-guest chemistry, self-assembly, molecular recognition, biology (recognition in the form of enzymes, and various forms of receptors, replication and transcription of DNA, self-association of DNA, protein folding, etc.), inorganic chemistry, polymer science (supramolecular polymers), material science, photochemistry and electronics in the form of molecular devices, physics, mathematics (topology) and nanochemisty (as synthetic molecules can reach sizes of tens of nanometers).[3]

Bonding Interactions in Supramolecular chemistry

Supramolecular chemistry is concerned with species connected by bonds other than covalent bonds. The types of interactions that hold supramolecular species together

include: ion-dipole interactions, dipole-dipole interactions, hydrogen bonding, pi-pi interactions, charge transfer interactions, electrostatic forces, van der Waals forces, and hydrophobic-hydrophilic or solvation effects.

Hydrogen bonds are particularly important in the organization of supramolecular structures.[2-3] This was recognized as early as 1931 upon examination of the structure of complex biological and natural molecules.[4] IUPAC recommends[5] that a hydrogen bond be defined as an attractive interaction between hydrogen atoms attached to a donor that is more electronegative than hydrogen itself and an atom or molecular fragment that acts as the acceptor. Examples of donor species include C-H, N-H, O-H, S-H, P-H, and X-H (where X denotes a halogen). Examples of acceptor species include N, O, P, S, the halogens, as well as areas of high electron density such as alkenes, alkynes, aromatic systems and transition metals.[3] Bond strengths for hydrogen bonds range from 1-60 kJ/mol for normal hydrogen bonds and up to 120 kJ/mol for extremely acidic species.[2] Hydrogen bonds can be characterized with a variety of techniques including IR, Raman and microwave spectroscopy, NMR spectroscopy, and by X-ray and neutron diffraction.[4, 6] A variety of geometries has been described (Figure 1.1). The strongest hydrogen bond has the hydrogen and the hydrogen bond acceptor at an angle of 150-180 ^{o}.[6] Examples of other geometries include bent, bifurcated, trifurcated, cyclic, cyclic dimer, and three cantered bifurcated.

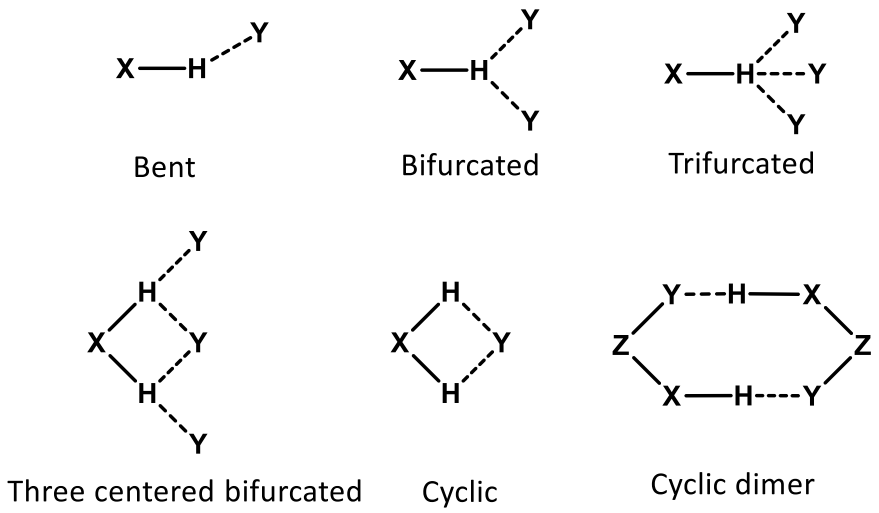

Figure 1.1. Hydrogen bonding geometries. X is a hydrogen bond donor and Y is the hydrogen bond acceptor.

π-π Interactions are very important in the assembly of supramolecular structures, but are rather difficult to define clearly, and consequently have been a subject of debate. The two limiting attractive geometries for π-π interactions are the T-shaped or edge to face geometry and the offset stacked geometry.[3, 7] Two aromatic molecules stacked directly above one other experience repulsive forces due to their π-clouds. Hunter and Sanders proposed a simple theoretical model for the treatment of π-systems. Their model is based upon electrostatics and van der Waals forces (other forces that could be viewed as influencing aromatic interactions are London dispersion forces, desolvation, induction, and charge transfer interactions.) The system is regarded as an interaction between positive σ-framework and a negative π-cloud. Both regions can be treated as point charges and the distance between them is based on the experimental value for the quadrupole moment of benzene. This approach has been quite successful in explaining geometries found in a variety of systems.[7] This model explains changes in stacking interactions observed with aromatic systems with heteroatoms and systems polarized by electron withdrawing or electron donating

substituents. Systems with opposite polarization show an attractive interaction while systems of similar polarization show repulsive interactions.[7]

Mechanically interlocked molecules

The Gibson group is primarily concerned with host-guest chemistry and specifically of those molecules that contain mechanical bonds. These include pseudorotaxanes, rotaxanes and catenanes (Figure 1.2). Pseudorotaxanes consist of a relatively linear component threaded through a macrocyle. For true rotaxanes, the threaded part is terminated by bulky end groups that are too large to fit through the macrocyclic part, thus forming a thermodynamically stable species. Catenanes consist of two macrocyles that are physically interlocked in such a way that they cannot be dissociated from one another without breaking open one of the macrocyles.[2-3, 8-9] Some molecular knot structures (Figure 1.2) are also physically interlocked. Examples of this are the Borromean rings, structures that consist of three interlocked macrocyles. None of the rings are actually linked to one another and when one ring is cut the other two can be isolated.

From rotaxanes and molecular knots to catenanes

The exact origin of supramolecular chemistry seems to be rather obscure, and depends a great deal on what exactly one comprehends under the term supramolecular chemistry. Lehn credits Paul Ehrlich with introducing the concept of a receptor in 1903, which introduced the concept of fixation; Emil Fischer, with the introduction of the concept of recognition with his introduction of the famous “lock and key” model in 1894; and Alfred Werner with the introduction of the concept of coordination in 1893.[1-2] Thus, the foundations of supramolecular chemistry—fixation,

recognition and coordination—and therefore the birth of supramolecular chemistry according to Lehn's understanding, took place during the late 19th century.

Steed and Atwood takes the position that supramolecular chemistry is a relatively young field that traces its beginnings to the advent of host-guest chemistry. In particular, the development of macrocyclic chemistry, during the 1960's with work of Curtis, Busch, Jäger, and Pederson in the discovery and, synthesis of macrocyclic hosts for cations. He also adds Cram's work in macrocylic cyclophanes and Lehn's work on cryptands as pivotal to the development of supramolecular chemistry.[2]

Figure 1.2. Examples of supramolecular, interlocked molecules.

Catenanes are supramolecular structures, in that they are made up of molecules that are linked together without using covalent bonds. The tools used in their construction are also the tools of a supramolecular chemist (templation, self-assembly, molecular recognition, threading). Catenanes also fall under the field of molecular topology as objects of topological interest. In the strictest sense, topology is a field of mathematics, specifically a subfield of geometry that deals with the description of geometric forms. It differs from traditional Euclidean geometry, in that it does not deal with the description of angles, side lengths and areas; instead all objects are treated as being made out of infinitely flexible material and can be deformed in any way as long as lines or edges do not break or pass through one another during a deformation. Thus, topology is mainly concerned with the connectivities of objects.[9-10] Topology in turn grew out of knot theory, which was inspired by a hypothesis of a chemist, Lord Kelvin.

Lord Kelvin speculated that all matter was composed of knots floating in the ether. According to his theory atoms were vortex rings knotted and linked in different ways according to which element they were. His friend and physicist Peter Guthrie Tait then attempted to tabulate all known knots and links in an effort to create a periodic table.[9, 11] From Tait's various publications developed the field of knot theory, which is still studied today.

Topology came to the attention of various chemists who, inspired by the synthetic challenge of making molecular knots and links, then developed the field of chemical topology. Chemists like Wasserman and Frisch, Harrison and Harrison, Schill, Zilkha and Agam and Walba developed synthetic routes to catenanes (which represents a 2_1 link or a Hopf link, one of the simplest knots in knot theory) and rotaxanes based on statistical methods.[10] Being dependent on probability of threading, these methods were very low yielding, and topologically non-trivial molecules remained an academic curiosity until the developments of template strategies in the 1980s.[11]

Template strategies

The first high yield synthesis of a catenane by Dietrich-Buchecker, Suavage and Kern in 1984 (Scheme 1.1)[12] made use of the observation that Cu(1) adopted a tetrahedral coordination geometry and could organize bidentate ligands in a mutually orthogonal fashion. They prepared 2,9-di(*p*-hydroxyphenyl)-1,10-phrenanthroline from 1,10-phrenanthroline and lithioanisole. This compound was deprotected. In the presence of $Cu(CH_3CN_4)\cdot BF_4$, the phrenanthroline ligands form a very stable, red pseudo-tetrahedral complex that was reacted with the di-iodo derivative of penta(ethylene glycol) in DMF under high dilution conditions to yield the desired catenate in 27%. The

catenane was obtained after a ligand exchange reaction of the catenand with and excess KCN.

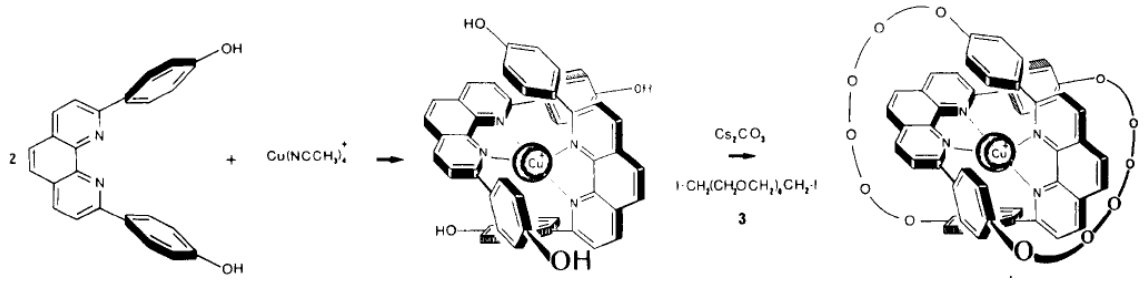

Scheme 1.1 Sauvage's one step synthesis of a catenand.[12] Figure reproduced from ref 11, Copyright 1984 with permission from American Chemical Society.

The yield was improved to 42% by performing the reaction is two steps (Scheme 1.2). A pseudorotaxane was formed between the preformed macrocycle and the deprotected phrenanthroline derivative before the cyclization reaction was performed.

2-3, 9, 13

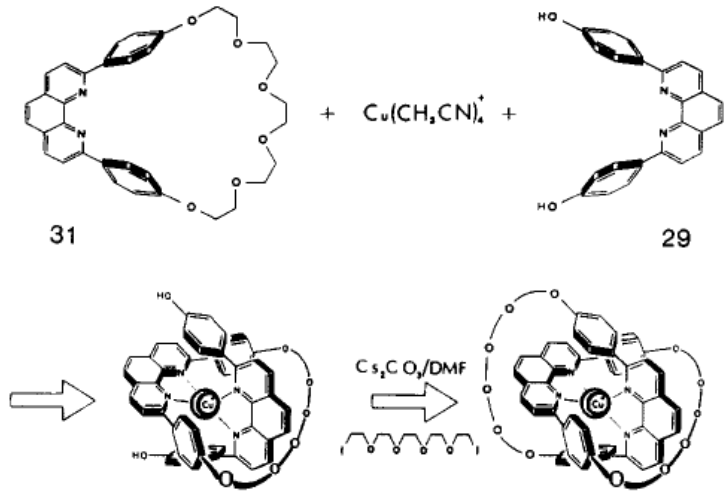

Scheme 1.2. Sauvage's two step strategy for catenand formation using a pre-formed macrocyle.[14] Reproduced from ref 13 Copyright (1983), with permission from Elsevier

Combining this metal templation strategy with intramolecular ring closing metathesis (RCM) with a ruthenium benzylidene catalyst yielded catenanes in 92%.[15]

In 1989 Stoddard reported[16] formation of a catenane in 71% yield. This catenane was formed by the reaction of a bipyridium derivative with *p*-dibromoxylene and bis(*para*-phenylene-34-crown-10) **BPP34C10** in acetonitrile. The catenane was isolated as a (tetra) hexafluorophosphate salt. The catenane was also obtained by stirring a mixture of *p*-dibromoxylene, 4,4'-bipyridine and **BPP34C10** in DMF for five days, though the yield was reduced to 18%. This self-assembly, or clipping, procedure indicates that there are several intramolecular forces at work that allow the components to recognize one another. Indeed, the X-ray crystal structure of the catenane shows evidence of π-π donor-acceptor stacking and edge-to-face interactions between the two interlocked rings. Charge transfer bands are observed in absorption and luminescent spectra and there is also significant electronic interaction between the two rings. This template clipping strategy has been used to make a wide variety of [2]catenanes (degenerate and non-degenerate) as well as bis-[2]catenanes and higher catenanes, including a [5]catenane.[3]

Template directed synthesis enabled the preparation of molecules with more complex topology. Selected examples include: the trefoil, or 3_1, knot[17-19] and the doubly interlocked [2]catenane, also known as a Solomon link or 4_1^2 link,[20] prepared by the Sauvage group; the Borromean ring (6_2^3) synthesized by the Stoddart group;[21] a pentafoil (5_1) knot,[22] star of David catenane (6_1^2),[23] and a molecular knot with eight crossings (8_{19} knot),[24] all synthesized by the Leigh group. In addition to being an intriguing synthetic challenge and the molecules being aesthetically pleasing, some of these knots have shown some interesting properties. Many of the knots are topologically chiral. They have no asymmetric centres or other elements of Euclidean chirality, but nevertheless have non-superimposable mirror images by virtue of their shape. It is possible to separate the isomers though chiral chromatography in some

cases, and some cases of asymmetric synthesis of the smaller knots have been described.[25] Some of the knots are strong and selective hosts for halide ions, particularly Cl^-, with binding constants on the order of 10^{10} M^{-1} in MeCN.[26] A molecular trefoil knot has been used as an asymmetric catalyst for Mukaiyama aldol reactions.[27] A pentafoil knot has been used as a switchable catalyst for Diels-Alder reactions and Micheal additions. The shape and efficacy of the catalyst depends upon which metal ions are bound to it. The catalyst exhibits allosteric control, which is a feature of many enzyme reactions.[28]

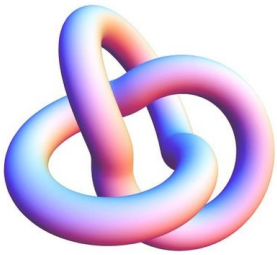

Trefoil knot (3_1)[29]

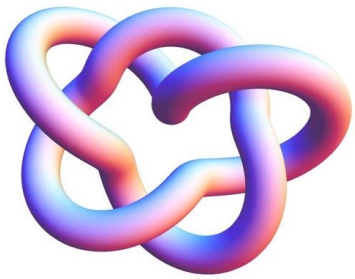

Pentafoil knot (5_1)[30]

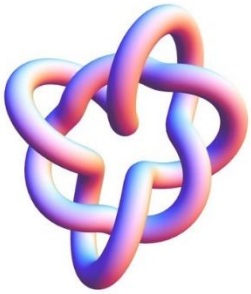

7_1 knot[31]

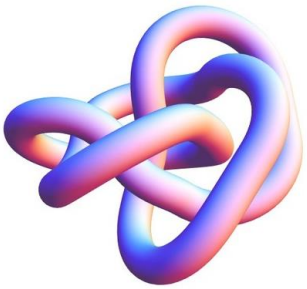

8_{19} knot[32]

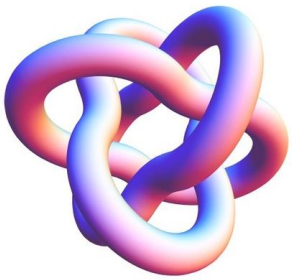

Borromean rings (6_2^3)[33]

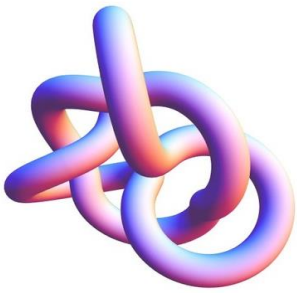

Star of David Catenane (6_1^2)[34]

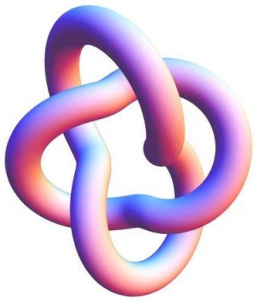

Solomon's knot (4_1^2)[35]

Figure 1.3. Examples of knots and links that have been synthesized by chemists.

The use of templates to induce a thermodynamically favoured association between the host and guest molecules has allowed the preparation of catenanes and rotaxanes in much higher yields than through statistical methods. This opened the field of molecularly interlocked molecules to serious study. Consequently, a great many rotaxane and catenane systems have been synthesized in the decades since the

templating strategy was first introduced. Fairly quickly, it was realized that the wheel component in a rotaxane could move between two degenerate binding sites on the axles component – a molecular shuttle.[36] The motion of the two interlocked rings in catenanes and the motion of a wheel along an axle component in rotaxanes suggested an ideal platform for building molecular devices.[37] The motion can be controlled by chemical,[38] electrochemical,[39] and photochemical[40] means. By 1998 reviews were published by both the Stoddart[41-42] and Sauvage[41] groups describing a number of rudimentary molecular machines. In the two decades since, many more examples of more sophisticated molecular machines have been published.[43-46] Quite recently, unidirectional motion[47] has been established, enabling the production of molecular pumps and motors[48] as well as a simple peptide synthesizer.[49-50] Non-equilibrium systems that perform work have become possible.[51] Supramolecular polymers that move on a macro scale as a result of the concerted work of many molecular machines have also been produced.[52] A great many of these examples use rotaxanes and catenanes as integral parts of the design. Although other macrocycles like pillar[5]arenes, curcubiturils and cyclodextrins are used, as well as non-macrocycle based systems, a substantial number of examples use crown ethers as the host molecules.[53-56]

The Gibson group uses mostly crown ethers and crown ether based pyridyl cryptands as our hosts of choice. We therefore turn our attention to crown ethers as hosts in supramolecular chemistry, and more specifically to dibenzo-30-crown-10, an underrepresented example of the dibenzo crown ethers.

Dibenzo-30-crown-10 (DB30C10)

The synthesis of **DB30C10** was reported in Pederson's seminal 1967 paper, in which it is referred to as compound XXXVIII (**DB30C10**). The crown ether was synthesized by method W with 1-butanol as solvent and the product was obtained as a mixture of **DB30C10** and **B15C5** in 51% yield with at least 6% of the mixture being **DB30C10**. This crown ether was thus reported, but not isolated or characterized in this paper.[57]

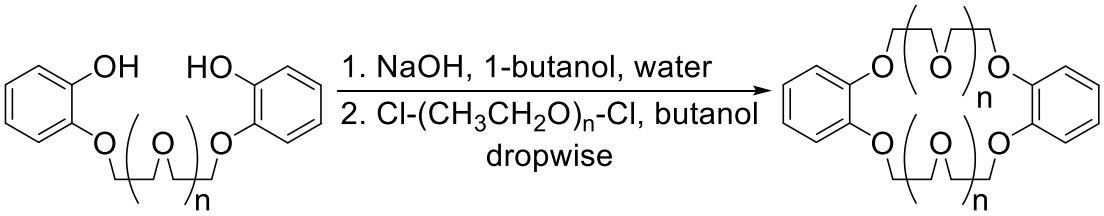

Scheme 1.3. Synthesis W was recommended by Pedersen as the most versatile method by which to synthesize crown ethers with 2 or more benzene rings.

The crystal structure of a complex between KI and **DB30C10** was published in 1970. The crystal structure showed the ethyleneoxy arms of the crown ether wrapped around the potassium ion.[58] In 1972, the same authors published the crystal structure of **DB30C10** along with the crystal structure of **DB30C10** with K^+ in the cavity. The crown ether undergoes a rather dramatic change in conformation between its complexed and uncomplexed from. Pedersen is thanked for his gift of the crown ether by the author of this paper.[59]

Most of the early studies of crown ethers were focused on the complexation behaviour of the crown ethers with alkali earth metal ions (Na^+, K^+ Ce^+), lanthanides, barium, polyatomic ion clusters (perchlorates and H_3O^+) in various solvents. The spectroscopic, conductive and physical properties of these complexes were investigated. The Gibson group focus on crown ethers and their complexation of organic cations, chiefly in respect to molecular architectures and the construction of supramolecular polymers.

These early studies therefore lie outside the scope of this dissertation. We will confine our attention to the literature that describes **DB30C10**'s binding geometry or its use in interlocked supramolecular systems and selected examples of its use as in host-guest chemistry applications.

Colquhoun et al. discovered that crown ethers act as second sphere coordination ligands of crown ethers with transition metal complexes in 1981. They published a crystal structure of the complex between **DB30C10** and $[Pt(bipy)(NH_3)_2]^{2+}[PF_6]^{-}{}_2$ (Figure 3 b). The complex was stabilized by relatively few hydrogen bonds, and was apparently stabilized by π-π interactions between the aromatic rings of the host and guest. They noted that a solution of and $[Pt(bipy)(NH_3)_2]^{2+}[PF_6]^{-}{}_2$ became strongly coloured with the addition of **DB30C10** and that a strong absorption appeared at λ_{max} ~ 350 nm, indicating charge transfer interactions. They also noted noticeable upfield shifts in the ^{1}H NMR spectrum of the aromatic protons in both the host and guest of the complex.[60] It should be noted that the formation of charge transfer complexes between paraquat and electron donating ions (Br^-, I^-, and ferrocyanide ions) had been reported previously.[61] The shift in proton resonances in the ^{1}H NMR spectra of paraquat and diquat when complexed with I^-, $Fe(CN)_6^{4-}$ and $Fe(CN)_6^{3-}$ had also been reported.[62]

In 1983, the same authors reported that **DB30C10** also forms a 1:1 complex with diquat bis(hexafluorophosphate). They noted the colour change, the upfield chemical shifts in the NMR spectra and that **DB30C10** rendered the diquat soluble in CH_2Cl_2. They also reported the X-ray crystal structure and the association constant of the complex (K_a = 17.5 x 10^3 M^{-1}, in acetone).

Calquhuon et al. published the crystal structure of **DB30C10**·$[Rh(cod)(NH_3)_2]^+$ (Figure 1.3 e) which illustrates another binding conformation of **DB30C10**. The aromatic rings do not appear to participate in the bonding interactions to any appreciable extent. The crown ether adopts what the authors call a V-shape, and the guest chiefly interacts with the ethyleneoxy units.[63]

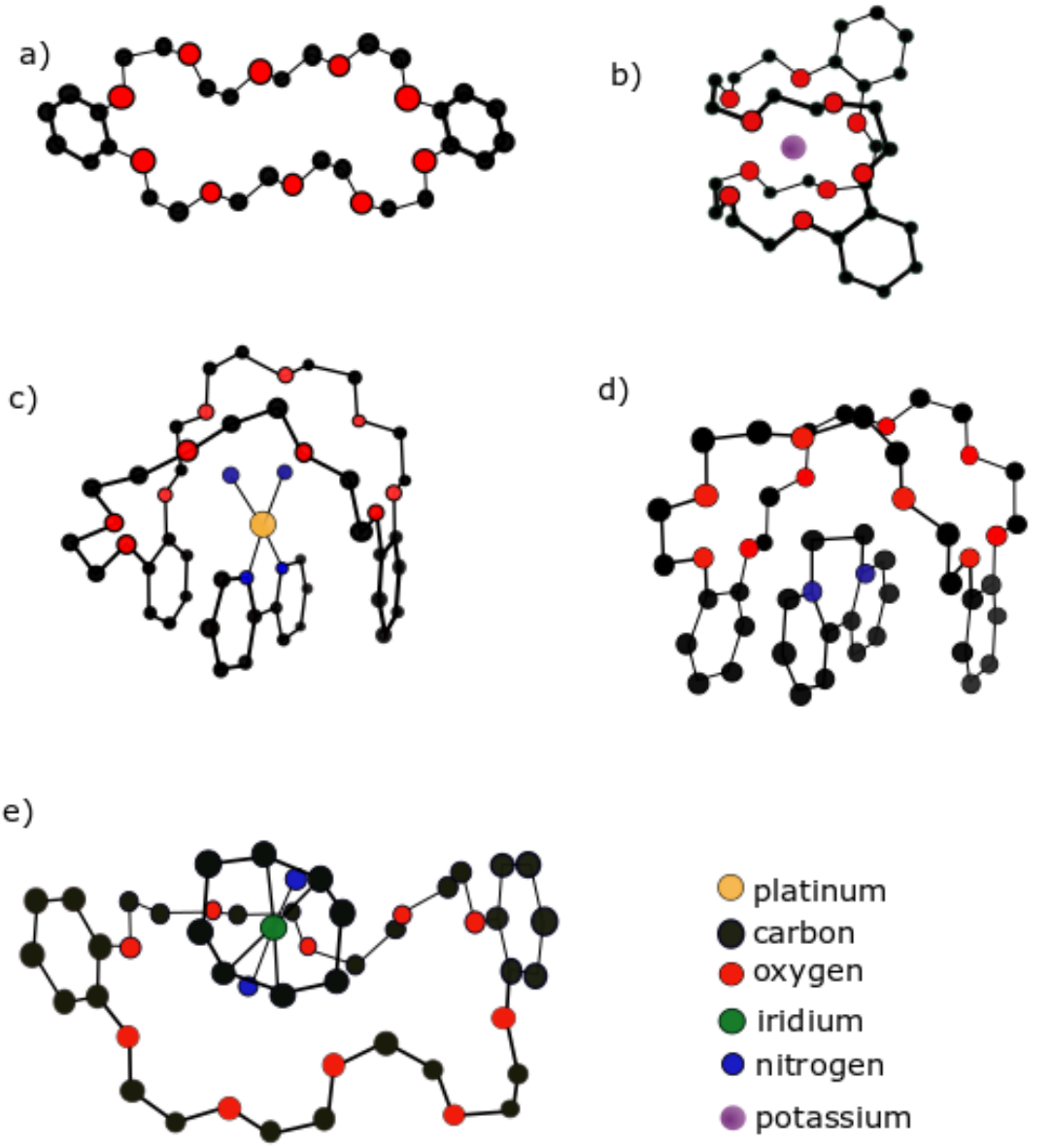

Figure 1.3. Crystals structure of (a) **DB30C10**[59] and its complexes with (b) K^+,[58] (c) $[Pt(bpy)(NH_3)_2]^{2+}[PF_6]^-_2$ [60] and with (d) diquat, [64] (e) $[Rh(cod)(NH_3)_2]^+$.[63] These crystal structures illustrate the conformational flexibility of **DB30C10.** Figure adapted form a) ref 58 with permission of The Royal Society of Chemistry b) ref 57 The Royal Society of Chemistry c) ref 59 John Wiley & Sons Ltd d) ref 63 with permission of The Royal Society of Chemistry and e) ref 62 with permission of The Royal Society of Chemistry. Figure generated using Inkscape.

A molecular mechanics and dynamics study undertaken by Grootenhuis and Kollman, published in 1989, was able to produce energy minimized structures of complexes between **DB30C10** and Li^+, Na^+, K^+, Rb^+ and Cs^+ that closely resembled the published crystal structures. They were also able to accurately model the preference of **DB30C10** for K^+ over Na^+ with their first solvation sphere model with MeOH as their chosen solvent.[65]

Semnani et al. reported the formation of charge transfer complexes between the neutral electron deficient compounds tetracyanoethylene and 2,3-dichloro-5,6-dicyanobenzoquinone and dibenzo crown ethers. They reported that the addition of KCl to the solutions increased the stability of the complexes with the neutral guests.[66]

A [3]pseudorotaxane with two **DB30C10** units and an axle containing two ammonium centres, a *p*-xylene spacer and relatively bulky 3,5-(t-Bu)$_2$C$_6$H$_3$CH$_2$ stoppers was synthesized by means of slippage synthesis (the ring component “slips over” the blocking group of the axles component with heating) in 1997. Crystals suitable for X-ray crystallography were obtained. The crystal structure showed that the crown ethers adopted a more open conformation, almost S-shaped (Figure 1.4 a). The complex is stabilized by H-bonding interactions between the ammonium centre and the ethyleneoxy arms, as well as π-π interactions between the catechol rings of the crown ether and the *p*-xylene spacer.[67]

In 2008 syntheses of *cis*- and *trans*-**DB30C10** diol were published. The binding constants with paraquat and diquat for each isomer were obtained by UV-vis titration in acetone. Crystal structures for the two isomers with diquat were obtained, but not with paraquat. The geometry is very much like that of unfunctionalized **DB30C10** with diquat, that is to say, the crown ethers fold around the guest, the only difference being

that the *cis*-**DB30C10** isomer incorporated a water molecule into the complex to form a “supramolecular cryptand”, which the *trans*-cryptand did not do.[68] Later the same year, Pederson et al. published a high yield synthesis of *cis*(4,4’)-di(carbomethoxybenzo)-30-crown-10 and its conversion to a pyridyl cryptand. The crystal structure of the empty cryptand shows that the crown ether part is pre-organized in the c- or taco-shape which the crown ether adopts when forming complexes with diquat (Figure 1.4 b). This is given as one of the reasons that the binding constants between the cryptand and paraquat and diquat are two orders of magnitude higher than the association constants between **DB30C10** and the same guests. The crystal structure of the complex between the pyridyl cryptand and paraquat shows that the crown ether part is in the taco shape.[69]

Christinat et al. attempted to make a rotaxane with 1,2-di(4’-pyridyl)ethylene as guest and **DB30C10** as ring component. This study is interesting in that the guest is neutral, and the synthesis is under thermodynamic control. The yields were quite good (67% using 1,5-dinaphto-38-crown-10 as the wheel component and 63% for **BPP34C10**) and the rotaxane was boron based. Catechol, 3,5-bis(trifluoromethyl)phenylboronic acid, 1,2-di-(4’-pyridyl)ethylene and the crown ether combined with toluene and refluxed using a Dean Stark trap. The boronic acid and catechol combined to form the boronic ester, which functioned as the blocking group. The 1,2-di-(4’-pyridyl)ethylene) formed a dative bond with the boron of the boronic ester. This bond was reversible, and dissociation of the B-N bond allowed the crown ether to thread unto the axle to form a rotaxane. Attempts to use **DB30C10** as wheel component did not result in crystals suitable for X-ray crystallography. Replacing the axle component (1,2-di-(4-pyridyl)ethylene) with the more rigid 4,4’-bipyridine did yield suitable, though low

quality, crystals, but the structure showed the crown ether wrapped around the axle – the rotaxane did not form, only the pseudorotaxane taco structure (Figure 1.4 c).[70]

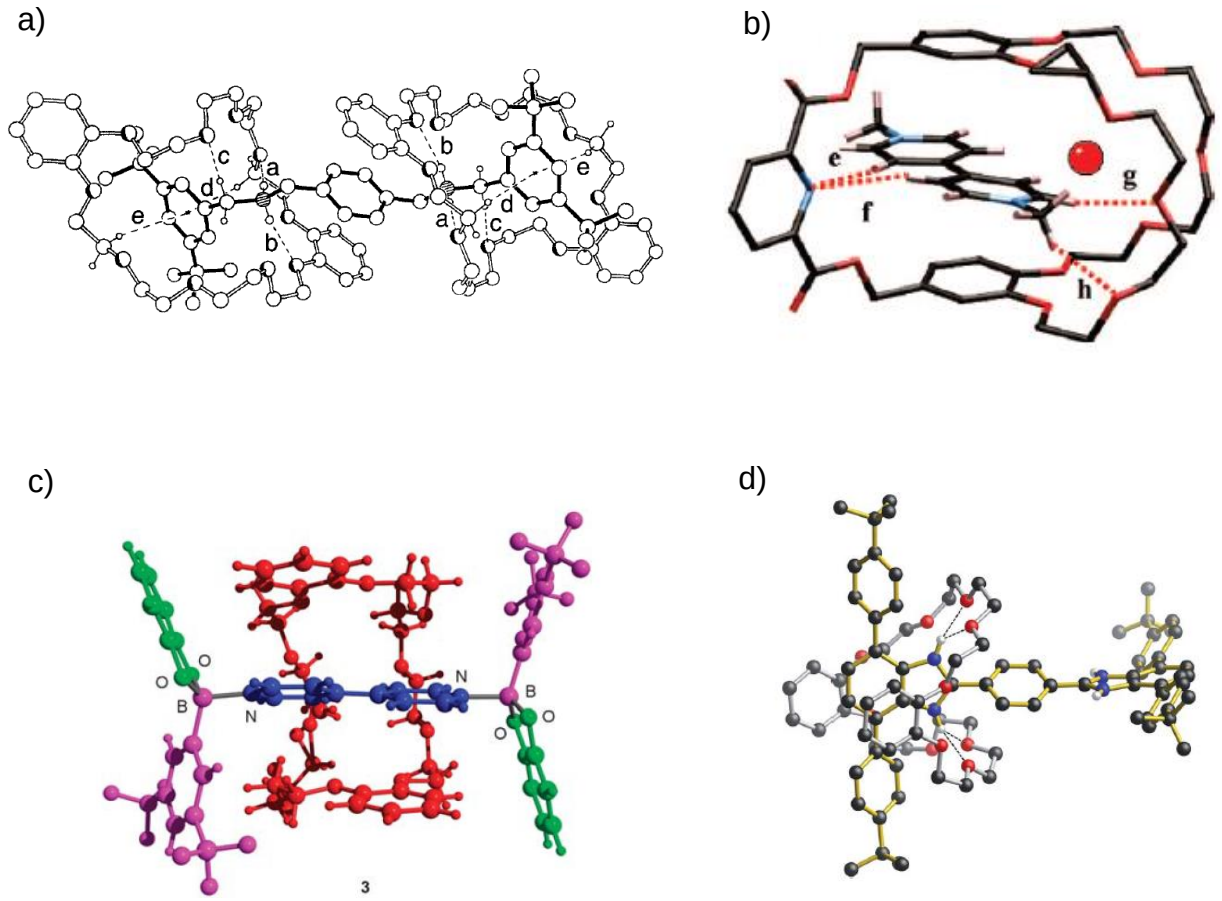

Figure 1.4. Crystal structures of (a) complex between two **DB30C10** and a bisammonium cation guest[67] (b) a pyridyl cryptand derived from **DB30C10** and paraquat[69] (c) boron based psuedorotaxane with 4,4'-bipyridine as axle and **DB30C10** folded around the host[70] (d) ball and stick representation of the crystal structure of biz(benzimidazolium) rotaxane.[71] Figures reproduced from a) ref 66 Copyright (1998), with permission from Elsevier b) ref 68 Copyright (2008) American Chemical Society c) ref 69 with permission of The Royal Society of Chemistry d) ref 70 with permission of The Royal Society of Chemistry.

A true rotaxane with a bis(benzimidazolium) axle and **DB30C10** as wheel component was published in 2012. The rotaxane was prepared by reacting a preformed [2]pseudorotaxane containing a terminal aldehyde with an equivalent of 1,2-diamino-3,6-di(4'-tert-butylphenyl)benzene followed by oxidation with $ZnCl_4$ and treatment with

trimethylamine. These rotaxanes can be neutral, cationic or dicationic, and the shuttling of the hosts between the two benzimidazolium stations was discussed. Once again, the crown ether seems to be folded in the taco conformation, but the benzimidazolium axle protruded through the “back” of the ethyleneoxy arms (Figure 1.4 d).[71] To the best of our knowledge, this is the only example of a rotaxane with **DB30C10** as the wheel component in the literature at present.

Another, mainly computational, paper studying the complexation between a series of benzimidazolium-alkane guests and **DB30C10** was published in 2015.[72] The guests include two benzimidazoliums directly linked to each other and guests with alkylene linkers (from methylene to butylene) between the benzimidazolium units. Monte Carlo simulations showed that the conformation of the crown ether was highly dependent on the length of the spacer units, with the n=0 and n=1 in pseudorotaxane conformations (s-shaped and taco shaped respectively) while the guests n=2 through n=4 linkers cradled in the crown ether. The crown ether adopts a more c- or taco-shaped conformation in the case of guests with ethylene and propylene linkers and a more open, or V-shaped conformation with the benzimidazolium guest with the butylene linker. The calculations show H-bonds only between the N-H of the protonated imidazolium and the O of the ethyleneoxy units of the crown ether, a total of 4 H-bonds. Their single point Monte Carlo FMO calculation in the DFT/B3LYP/6-31G* functional showed overlap between the HOMO on the catechol rings and the LUMO concentrated on the axle of the guest overlaps. In the case for the guests with longer linkers, the authors allege that there was sufficient interaction between the HOMO-1, HOMO-2 and LUMO+1, LUMO+2 orbitals to justify the conformations produced. The authors offer ^{1}H NMR, with very small chemical shift changes, NOESY and HRMS

spectra as experimental support. No crystal structures were included. It is worth noting that all the complexes did not have the same counter ions.[72]

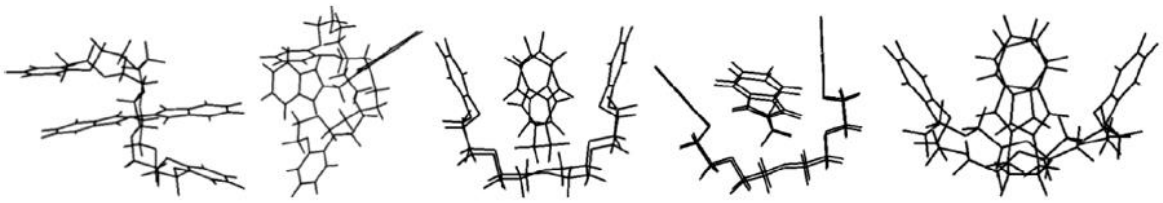

Figure 1.5. Structures produced by Monte Carlo global minimizations for complexes between **DB30C10** and various bisimidazolium-alkane guests.[72] From left to right the guest that have two benzimidazolium units directly linked and the guests with the methylene, ethylene, propylene, and butylene linkers. Reproduced from ref 71 Copyright (2015), with permission from Elsevier.

From the above discussion we can safely conclude that the conformation of **DB30C10** is highly dependent upon the type of guest. The cavity is large and the ethyleneoxy arms are quite flexible, affording the host some ability to adapt to the guest and change its binding conformation to maximize favourable binding interactions. It is therefore important to determine the binding conformation with a particular guest and not make assumptions about the structure of the complex.

We now turn our attention to selected applications of **DB30C10**, such as potentiometric sensors for various organic compounds, some polymers incorporating **DB30C10**, the synthesis of a new host based on the crown ether, and catenanes incorporating **DB30C10** as one of the rings. As mentioned above, we will not mention studies of complexes with inorganic ions.

Several types of potentiometric sensors making use of crown ether's ability to complex selectively various molecules have been developed. Moody et al. developed a series of liquid membrane ion selective electrodes (ISE) that are based on crown ethers. The membranes are made of poly(vinyl chloride), and crown ethers are used as the neutral

carrier of the ions. An appropriate plasticizing solvent and a liquid ion exchanger is used (or not). They conclude that **DB30C10** forms a good sensor for diquat, but not so much with paraquat.[73-74] The same group also published a study wherein various polyethers were studies as ISE's for guanidinium ions. **DB30C10** was tested and while the sensor worked, they recommended the smaller, more rigid bis(*meta*-phenylene)-26-crown-8 for this purpose.[75] Other examples using **DB30C10** include a sensor for primaquine (a malaria drug)[76] and a sensor for the neurotransmitters serotonin, dopamine and epinephrine.[77] The sensors for serotonin and epinephrine were the first examples of sensors for these molecules. The sensors were sensitive, were insensitive to up to 500-fold molar excess of uric and ascorbic acid (which interfere with potentiometric methods), stable over 2.5 months, fast and the dopamine and epinephrine sensors were able to quantify these neurotransmitters in pharmaceutical preparations, and compared well with the official method in the British Pharmacopoeia.

A study by Ashton et al. in 1997 showed that crown ethers and 9-(anthracenyl)methylammonium and 9-(anthracenyl)benzylammonium tetrakis(hexafluorophosphate) salts formed complexes in CH_2Cl_2. Of particular interest was their finding that the dibenzo crown ethers (**DB18C6**, **DB24C8** and **DB30C10**) had fluorescence arising from the aromatic groups completely quenched by complexation with guests. The anthracene units of the guest were sensitized at the same time.[78] The complexation is, of course, reversible based on whether the guest is protonated or not. This fluorescence quenching upon complexation that can turned on and off based on the pH of the solution can be used for the construction of supramolecular sensors.

In a similar vein, Schild et al. found that ruthenium(II) dyads and triad with paraquat units as sensitizers showed a remarkable increase (up to 2×10^4) in the charge

separated life times upon complexation with crown ethers, notably **DB30C10**. The authors attributed the large increase in charge separated lifetimes to a change in the reorganization energy.[79]

The change of reduction potentials of paraquats undergo when forming charge transfer complexes with **DB30C10** was explored to a limited extent in a study performed at an Australian university in 2013. The authors made an ionic liquid from 4,4'-bipyridine and tosylated tri(ethylene glycol) monomethyl ether. The authors noted that counter ions had an effect on both the colours and the melting points of the materials. The iodide salt was orange, the sulphonate salt pale yellow, and the TFSI salt colourless. The ionic liquids formed charge transfer complexes with electron rich materials (**DB30C10**, tetrathiafulvalene, and 2-methoxynaphtalene). As expected the TFSI salt changed from colourless to yellow when mixed with **DB30C10** and the ^{1}H NMR spectrum showed chemical shifts for both the paraquat and crown ether peaks (as opposed to the uncomplexed materials). The paraquat containing TFSI salt was more difficult to reduce when complexed with **DB30C10**. Although UV spectra, DSC traces, ^{1}H NMR and cyclic voltammetry data were reported, it was not done in a systematic fashion. The authors seemed mainly interested in the fact that the TFSI salt of the ionic liquid's melting point drops from 68.8 ºC to -42.2 ºC when mixed with 2-methoxynapthalene — the materials form a deep eutectic solvent.[80]

Crown ethers have been investigated for their anti-tumor potential. Since the early discovery, comparisons have been made between crown ether complex formation and natural ionophore valinomycin. Especially a large crown ether like **DB30C10** is flexible and can completely encapsulate the metal ion in its hydrophilic cavity while presenting a more hydrophobic exterior. This property led to investigations of crown ethers' anti-

proliferative and anti-tumor activity. **DB30C10** showed μM IC_{50} values against 5 cancer cell lines in one study.[81]

Aside from the **DB30C10**-based pyridyl cryptand mentioned above, **DB30C10** has been used as the basis of another new type of host. The host contains two **DB30C10** units linked together with triptycene units to make a macrocycle with large central cavity - 10.89 × 8.23 $Å^2$ for the empty macrocycle. The two **DB30C10** units make up the sides of the macrocycle. This host is interesting because it contains three macrocycles in one molecule. The two **DB30C10** sides still function as hosts and the large central cavity can also accommodate guests.[82] The paper that first describes the synthesis also describes the 1:2 complex formation between the new host and two 9-(anthracylmethyl)benzylammonium salt guests. The crystal structure of the complex shows that the anthracyl rings are arranged parallel to each inside the large cavity. The complex also undergoes a change in fluorescence intensity when Ba^{2+} ions are added to the solution, making this a barium selective fluorescence sensor.[83] A later paper describes the formation of 1:2 complexes between the host and paraquat derivatives. One of the crystal structures shows two paraquat guests inside with the large central cavity with a PF_6^- ion neatly between them. The PF_6^- ion appears to be engaging in H-bonding with the ethyleneoxy units as well as in anion-π stacking with the bipyridinium rings.[84] The authors also demonstrated that the host forms complexes with a variety of guests, including 11 different paraquat derivatives (besides the 4 mentioned in the 2011 paper), diquat, and a 2,7-diazapyrenium salt. The identity of the guest had a large influence on the binding geometry. Even changes as seemingly small as a halogen in the 4 position of the bromobenzyl paraquat derivatives had a large effect on the binding geometry. The 4-chloro and 4-bromo derivatives formed 1:1 complexes with the benzyl groups protruding out of the cavity, while the 4-fluoro

derivative formed a 1:2 complex with the benzyl groups protruding out of the cavity and almost orthogonal to the pyridinium rings. The crystal structures of the various host guest complexes show that the central cavity changes size and shape depending on the guest. This behaviour is an example of substrate induced fit with an artificial host molecule.[82]

Examples of **DB30C10** incorporated into polymers and supramolecular polymers are few. This is rather astonishing considering the plethora of supramolecular polymers based on crown ethers that have been synthesized.[55, 85-87] In one example from 2006, the authors made a series of polymers with dibenzo crown ethers **DB18C6**, **DB21C7**, **DB24C8** and **DB30C10** in the backbone. The aliphatic spacer units were derived from dicarboxylic acids (sebacic, 1,12-dodecanedicarboxylic, hexadecanedioic or 1,4-phenylene diacetic acids). The polymers were prepared by Friedel-Crafts reaction in Eaton's reagent (phosphorus pentoxide in methanesulfonic acid, 0.8:10, w/w) in a one-step reaction. The resulting high molecular weight polymers were reduced to transform the ketone carbonyls into CH_2 groups by triethylsilane in trifluoroacetic acid media. All the polymers were characterized by ^{1}H and ^{13}C NMR, IR, DSC and their morphologies were studied by X-ray scattering and scanning electron microscopy.[88]

Another example is a daisy chain polymer wherein the heteroditopic monomer consists of **DB30C10** linked to a paraquat unit by a CH_2 spacer unit.[89] This is very similar to a system that the Gibson group published in 1998[90] in which **BMP32C10** was used as the host instead of **DB30C10**. No attempt was made to determine the molecular weight of the **DB30C10** polymers, but the authors did demonstrate, by recording the ^{1}H NMR, that the monomer forms aggregates as the solution concentration increases. They also obtained a double logarithmic plot of specific viscosity vs monomer concentration that shows a sharp increase in the slope from 1.11 to 2.03 at approximately 70 mM. The

authors also showed through space interactions between the paraquat and the crown by 2D NOESY NMR and they obtained an SEM image of a fibre drawn from high concentration solution. They also demonstrated that the aggregate formation/ polymerization was reversible. They could induce polymerization and depolymerization by adding K^+ ions and **DB18C6**, respectively.

A catenane using **DB30C10** was synthesized by Yuki et al.[91] A pseudorotaxane between **DB30C10** and a dibenzyl ammonium salt functionalized with terminal alkyne groups was formed. The cyclization reaction to form the second macrocycle was performed by a metal free click reaction between a homoditopic nitrile *N*-oxide and alkyne groups on the functionalized benzylammonium guest. Comparisons were made between the [2]catenanes wherein the ammonium site was protonated and deprotonated, acetylated and deacetylated as well as comparisons between the **DB24C8** (which was synthesized in order to optimize the conditions of the click reaction) and the **DB30C10** catenanes. The **DB24C8** catenane did not deprotonate under the same conditions as the **DB30C10**. **DB24C8** could also apparently not pass over the acetylated *sec*-ammonium site and seemed to rotate slowly on the NMR time scale. The **DB30C10**, being larger, was not hindered by the acetylation and rotated faster relative to the NMR time scale.

An elegant recent publication used both **DB30C10** as the macrocycle in the formation of catenanes and rotaxanes that function as molecular rotors and pumps that respond to pulses of a chemical fuel.[48] The rotors/ pumps were operated by addition of a chemical fuel, an aliquot of trichloroacetic acid, which decarboxylated under basic conditions to give $CHCl_3$ and CO_2. Several model systems were synthesized to demonstrate the operation of each step. A [2]catenane rotor was then synthesized in 24 synthetic steps. The catenane had a dibenzylammonium binding site next to a

disulfide blocking group which was locked (stable) in acidic conditions, but labile in basic conditions. Next along the circular track was a triazolium site, followed by a hydrazone blocking group that was locked under basic conditions, but labile under acidic conditions. When the catenane was placed in a solution with 4:1 trichloroacetic acid: triethyl amine, the solution was acidic and the dibenzylammonium site was protonated. The hydrazone barrier exchanged via transient aldehyde and the **DB30C10** was moved to the dibenzylammonium site. The triethylanime catalyzed the decarboxylation of the trichloroacetic acid over the course of 17 hours. Eventually, the trichloroacetic acid had been converted into CO_2 and $CHCl_2$ so that the solution was basic enough to deprotonate the dibenzylammonium site. The **DB30C10** had no affinity for this site and bound preferentially to the triazolium group. The hydrazone barrier was “locked” so that the **DB30C10** could not move counterclockwise to get to the triazolium. The disulfide barrier underwent exchange with disulfides in the solution through thiolate catalysis. The **DB30C10** moved clockwise to the thermodynamically preferred binding site. Each fuel pulse enabled 360 º directional rotation and there was no build-up of organic salts that would occur with sequential addition of acids and bases to drive the operation of the rotor. The systems operated with repeated fuel pulses with no apparent loss or damage, except that the hydrazone exchange became slower as the solution was diluted by the generation of chloroform.

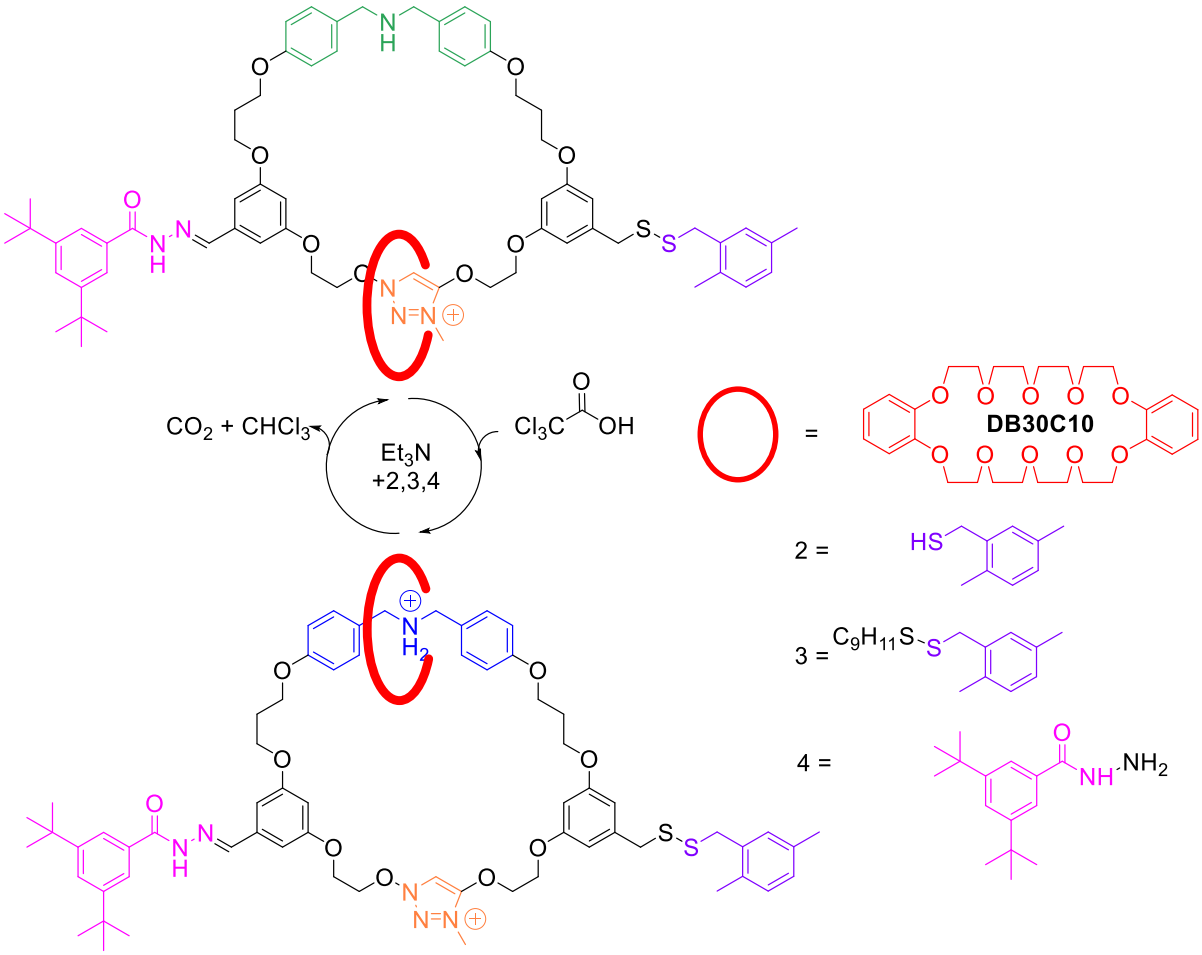

Scheme 1.3. Operation of a molecular motor through addition of fuel pulses.

A [3] catenane with two hydrazone groups, two dibenzylammonium sites, two disulfide blocking groups, two triazole groups and two **DB30C10** units was also isolated. It operates under the same principles and each fuel pulse causes both crown ethers to move around the track in a directional manner. A rotaxane that can pump up to four crown ethers on to the axles was also synthesized.

Motivation for this thesis

A review of the literature shows that **DB30C10** is shockingly underrepresented, especially compared to other crown ethers. The basic synthesis of **DB30C10** was described in 1967 and has not been substantially improved since. This can be

explained, in part, by the fact that the early studies were mostly analytical and the crown ether was obtained directly from Pedersen at Du Pont, and later from the Stoddart group. By 1992, **DB30C10** was commercially available. However, the fact that the synthesis was patented and commercialized shows that there was, and is, interest in this larger crown ether.

Because **DB30C10** is large and flexible, it can adopt a variety of binding conformations depending on the host. Examining the various crystal structures and computer generated minimum energy conformations, at least five distinct binding conformations can be identified. The only crystal structures of **DB30C10** with paraquat shows the host folding around the paraquat in a taco conformation and not threaded through the crown ether to form a pseudorotaxane.

Despite its apparent neglect as a host, **DB30C10** has found diverse applications. Excluding studies with metal ions, **DB30C10** has been used in selective sensors for paraquat, diquat, primaquine, guanidinium ions, and neurotransmitters. It has also been used essentially as an additive to increase charge separated lifetimes in ruthenium dyads and triad, and to modulate the properties of paraquat containing ionic liquids. **DB30C10** shows antitumor activity against multiple cell lines and has been used in the development of two new hosts. It has also been used in polymers and catenanes, although there are far fewer examples than other types of crown ethers.

In this dissertation we describe an improved synthesis of **DB30C10** (chapter 2), formation of four new rotaxanes with **DB30C10** as the wheel component and paraquat as the guest in order to determine the binding conformation of **DB30C10** with paraquat (chapter 3) and the formation of several segmented polyurethane

poly(pseudorotaxanes) with paraquat in the backbone to explore the relative binding of **DB30C10** compared to other common crown ethers in solution (chapter 4).

References

1. Lehn, J.-M., *Supramolecular Chemisty, Concepts and Perspectives*. VCH: 1995.
2. Steed, J. W.; Atwood, J. L., *Supramolecular chemistry*. second ed.; John Wiley & Sons: 2009.
3. Lindoy, L. F.; Atkinson, I. M., *Self-Assembly in Supramolecular Systems*. The Royal Society of Chemistry: 2000; Vol. 7.
4. Jeffrey, G. A., *An Introduction to Hydrogen Bonding*. Oxford University Press: 1997.
5. Arunan, E.; Desiraju, G. R.; Klein, R. A.; Sadlej, J.; Scheiner, S.; Alkorta, I.; Clary, D. C.; Crabtree, R. H.; Dannenberg, J. J.; Hobza, P.; Kjaergaard, H. G.; Legon, A. C.; Mennucci, B.; Nesbitt, D. J., Definition of the hydrogen bond (IUPAC Recommendations 2011). *Pure Appl. Chem.* **2011,** *83*, 1637-1641.
6. Desiraju, G. R., A bond by any other name. *Angew. Chem. Int. Ed.* **2011,** *50*, 52-59.
7. Hunter, C. A.; Lawson, K. R.; Perkins, J.; Urch, C. J., Aromatic interactions. *J. Chem. Soc., Perkin Trans. 2* **2001**, 651-669.
8. Vogtle, F., *Supramolecular Chemistry*. John Wiley & Sons: 1991.
9. *Molecular Catenanes, Rotaxanes and Knots A Journey Through the World of Molecular Topology*. Wiley-VCH: 1999.
10. Breault, G. A.; Hunter, C. A.; Mayers, P. C., Supramolecular Topology. *Tetrahedron* **1999**, 5265-5293.
11. Forgan, R. S.; Sauvage, J.-P.; Stoddart, J. F., Chemical Topology: Complex Molecular Knots, Links, and Entanglements. *Chem. Rev.* **2011,** *111*, 5434-5464.
12. Dietrich-Buchecker, C. O.; Sauvage, J. P.; Kern, J. M., Templated synthesis of interlocked macrocyclic ligands: the catenands. *J. Am. Chem. Soc.* **1984,** *106*, 3043-3045.
13. Wu, C.; Lecavalier, P. R.; Shen, Y. X.; Gibson, H. W., Synthesis of a rotaxane via the template method. *Chem. Mater.* **1991,** *3*, 569-572.
14. Dietrich-Buchecker, C. O.; Sauvage, J. P., Une Nouvelle Famille de Molecules: Let Metallo-Catenanes. *Tetrahedron Lett.* **1983,** *24*, 5095-5098.
15. Mohr, B.; Sauvage, J.-P.; Grubbs, R. H.; Weck, M., High-Yield Synthesis of [2] Catenanes by Intramolecular Ring-Closing Metathesis. *Angew. Chem. Int. Ed.* **1997,** *36*, 1308-1310.

16. Ashton, P. R.; Goodnow, T. T.; Kaifer, A. E.; Reddington, M. V.; Slawin, A. M. Z.; Spencer, N.; Stoddart, J. F.; Vicent, C.; Williams, D. J., A [2] Catenane Made to Order. *Angew. Chem. Int. Ed.* **1989,** *28*, 1396-1399.
17. Dietrich-Buchecker, C. O.; Guilhem, J.; Pascard, C.; Sauvage, J.-P., Structure of a Synthetic Trefoil Knot Coordinated to Two Copper(I) Centers. *Angew. Chem. Int. Ed.* **1990,** *29*, 1154-1156.
18. Dietrich-Buchecker, C. O.; Sauvage, J.-P., A synthetic Molecular Trefoil Knot. *Angew. Chem. Int. Ed.* **1989,** *28*, 189-192.
19. Dietrich-Buchecker, C. O.; Sauvage, J.-P.; De Cian, A.; Fischer, J., High-yield Synthesis of a Dicopper(I) Trefoil Knot Containing 1,3-Phenylene Groups as Bridges between the Chelate Units. *J. Chem. Soc. Chem. Commun.* **1994,** *0*, 2231-2232.
20. Nierengarten, J.-F.; Dietrich-Buchecher, C.; Sauvage, J.-P., Synthesis of a Doubly Interlocked [2]-Catenane. *J. Am. Chem. Soc.* **1994,** *116*, 375-376.
21. Chichak, K. S.; Cantrill, S. J.; Pease, A. R.; Chiu, S.-H.; Cave, G. W. V.; Atwood, J. L.; Stoddart, J. F., Molecular Borromean Rings. *Science* **2004,** *304*, 1308-1312.
22. Ayme, J.-F.; Beves, J. E.; Leigh, D. A.; McBurney, R. T.; Rissanen, K.; Schultz, D., A synthetic molecular pentafoil knot. *Nat. Chem.* **2012,** *4*, 15-20.
23. Leigh, D. A.; Pritchard, R. G.; Stephens, A. J., A Star of David catenane. *Nat. Chem.* **2014,** *6*, 978-982.
24. Danon, J. J.; Krüger, A.; Leigh, D. A.; Lemonnier, J.-F.; Stephens, A. J.; Vitorica-Yrezabal, I. J.; Woltering, S. L., Braiding a molecular knot with eight crossings. *Science* **2017,** *355*, 159-162.
25. Fielden, S. D. P.; Leigh, D. A.; Woltering, S. L., Molecular Knots. *Angew. Chem. Int. Ed.* **2017,** *56*, 11166-11194.
26. Ayme, J.-F.; Beves, J. E.; Campbell, C. J.; Gil-Ramírez, G.; Leigh, D. A.; Stephens, A. J., Strong and Selective Anion Binding within the Central Cavity of Molecular Knots and Links. *J. Am. Chem. Soc.* **2015,** *137*, 9812-9815.
27. Gil-Ramírez, G.; Hoekman, S.; Kitching, M. O.; Leigh, D. A.; Vitorica-Yrezabal, I. J.; Zhang, G., Tying a Molecular Overhand Knot of Single Handedness and Asymmetric Catalysis with the Corresponding Pseudo-D_3-Symmetric Trefoil Knot. *J. Am. Chem. Soc.* **2016,** *138*, 13159-13162.
28. Marcos, V.; Stephens, A. J.; Jaramillo-Garcia, J.; Nussbaumer, A. L.; Woltering, S. L.; Valero, A.; Lemonnier, J.-F.; Vitorica-Yrezabal, I. J.; Leigh, D. A., Allosteric initiation and regulation of catalysis with a molecular knot. *Science* **2016,** *352*, 1555-1559.
29. DesignByNumbers Prime Knot: 3_1 (trefoil knot). https://www.thingiverse.com/thing:216667.
30. DesignByNumbers Prime Knot: 5_1. https://www.thingiverse.com/thing:216674.

31. DesignByNumbers Prime Knot: 7_1. https://www.thingiverse.com/thing:216692.
32. DesignByNumbers Prime Knot: 8_19. https://www.thingiverse.com/thing:216812.
33. DesignByNumbers Prime Link: 6_3_2. https://www.thingiverse.com/thing:216688.
34. DesignByNumbers Prime Link: 6_2_1. https://www.thingiverse.com/thing:216681.
35. DesignByNumbers Prime Link: 4_2_1. https://www.thingiverse.com/thing:216673.
36. Anelli, P. L.; Spencer, N.; Stoddart, J. F., A Molecular Shuttle. *J. Am. Chem. Soc.* **1991,** *113*, 5131-5133.
37. Armaroli, N.; Balzani, V.; Collin, J.-P.; Gaviña, P.; Sauvage, J.-P.; Ventura, B., Rotaxanes Incorporating Two different Coordinating Units in Their Thread: Synthesis and Electrochemically and Photochemically Induced Molecular Motions. *J. Am. Chem. Soc.* **1999,** *121*, 4397-4408.
38. Bissell, R. A.; Córdova, E.; Kaifer, A. E.; Stoddart, J. F., A chemically and electrochemically switchable molecular shuttle. *Nature* **1994,** *369*, 133-137.
39. Livoreil, A.; Dietrich-Buchecker, C. O.; Sauvage, J.-P., Electrochemically Triggered Swinging of a [2]-Catenate. *J. Am. Chem. Soc.* **1994,** *116*, 9399-9400.
40. Ashton, P. R.; Ballardini, R.; Balzani, V.; Boyd, S. E.; Credi, A.; Gandolfi, M. T.; Gómez-López, M.; Iqbal, S.; Philp, D.; Preece, J. A.; Prodi, L.; Ricketts, H. G.; Stoddart, J. F.; Tolley, M. S.; Venturi, M.; White, A. J. P.; Williams, D. J., Simple Mechanical Molecular and Supramolecular Machines: Photochemical and Electrochemical Control of Switching Processes. *Chem. Eur. J.* **1997,** *3*, 152-170.
41. Sauvage, J.-P., Transition Metal-Containing Rotaxanes and Catenanes in Motion: Toward Molecular Machines and Motors. *Acc. Chem. Res.* **1998,** *31*, 611-619.
42. Philp, D.; Stoddart, J. F., Self-Assembly in Natural and Unnatural Systems. *Angew. Chem. Int. Ed.* **1996,** *35*, 1154-1196.
43. Cheng, C.; Stoddart, J. F., Wholly Synthetic Molecular Machines. *ChemPhysChem* **2016,** *17*, 1780-1793.
44. Kay, E. R.; Leigh, D. A., Rise of the Molecular Machines. *Angew. Chem. Int. Ed.* **2015,** *54*.
45. Abendroth, J. M.; Bushuyev, O. S.; Weiss, P. S.; Barrett, C. J., Controlling Motion at the Nanoscale: Rise of the Molecular Machines. *ACS Nano* **2015,** *9*, 7746-7768.
46. Erbas-Cakmak, S.; Leigh, D. A.; McTernan, C. T.; Nussbaumer, A. L., Artificial Molecular Machines. *Chem. Rev.* **2015,** *115*, 10081-10206.
47. Kistemaker, J. C. M.; Štacko, P.; Visser, J.; Feringa, B. L., Unidirectional rotary motion in achiral molecular motors. *Nat. Chem.* **2015,** *7*, 890-896.

48. Erbas-Cakmak, S.; Fielden, S. D. P.; Karaca, U.; Leigh, D. A.; McTernan, C. T.; Tetlow, D. J.; Wilson, M. R., Rotary and linear molecular motors driven by pulses of a chemical fuel. *Science* **2017,** *358*, 340-343.

49. Lewandowski, B.; De Bo, G.; Ward, J. W.; Papmeyer, M.; Kuschel, S.; Aldegunde, M. J.; Gramlich, P. M. E.; Heckmann, D.; Goldup, S. M.; D'Souza, D. M.; Fernandes, A. E.; Leigh, D. A., Sequence-Specific Peptide Synthesis by an Artificial Small-Moleucule Machine. *Science* **2013,** *339*, 189-193.

50. De Bo, G.; Kuschel, S.; Leigh, D. A.; Lewandowski, B.; Papmeyer, M.; Ward, J. W., Efficient Assembly of Threaded Molecular Machines for Sequence-Specific Synthesis. *J. Am. Chem. Soc.* **2014,** *136*.

51. Cheng, C.; McGonigal, P. R.; Schneebeli, S. T.; Li, H.; Vermeulen, N. A.; Ke, C.; Stoddart, J. F., An artificial molecular pump. *Nat. Nanotechnol.* **2015,** *10*, 547-553.

52. Du, G.; Moulin, E.; Jouault, N.; Buhler, E.; Giuseppone, N., Muscle-like Supramolecular Polymers: Integrated Motion from Thousands of Molecular Machines. *Angew. Chem. Int. Ed.* **2012,** *51*, 12504-12508.

53. Xue, M.; Yang, Y.; Chi, X.; Yan, X.; Huang, F., Development of Pseudorotaxanes and Rotaxanes: From Synthesis to Stimuli-Responsive Motions to Applications. *Chem. Rev.* **2015,** *115*, 7398-7501.

54. Langton, M. J.; Beer, P. D., Rotaxane and Catenane Host Structures for Sensing Charged Guest Species. *Acc. Chem. Res.* **2014,** *47*, 1935-1949.

55. Zhen, B.; Wang, F.; Dong, S.; Huang, F., Supramolecular polymers constructed by crown ether-based molecular recognition. *Chem. Soc. Rev.* **2012,** *41*, 1621-1636.

56. Arunachalam, M.; Gibson, H. W., Recent developments in polypseudorotaxanes and polyrotaxanes. *Prog. Polym. Sci* **2014,** *39*, 1043-1073.

57. Pedersen, C. J., Cyclic Polyethers and Their Complexes with Metal Salts. *J. Am. Chem. Soc.* **1967,** *89*, 7017-7036.

58. Bush, M. A.; Truter, M. R., The Crystal Structures of Three Alkali-metal Complexes wiht Cyclic Polyethers. *Chem. Commun.* **1970**, 1439-1440.

59. Bush, M. A.; Truter, M. R., Crystal Structures of Complexes between Alkali-metal Salts and Cyclic Polyethers. Part IV. The Crystal Structures of Dibenzo-30-crown-I0 (2,3: 17,18-di benzo-I ,4,7,10,13,16,19,22,25,28-decaoxacyclotriaconta-2,17-diene) and of its Complex with Potassium Iodide. *J. Chem. Soc., Perkin Trans. 2* **1972,** *0*, 345-350.

60. Colquhoun, H. M.; Stoddart, J. F.; Williams, D. J.; Wolstenholme, J. B.; Zarzycki, R., Second Sphere Coordination of Cationic Platinum Complexes by Crown Ethers- The X-Ray Crystal

Structure of IPt(bpy)(NH,), Dibenzo[3O]crown-10]$^{2+}$[PF_6]$_2^-$. $x$$H_2O$ (x = 0.6)'*. *Angew. Chem. Int. Ed.* **1981,** *20*, 1051-1053.

61. Nakahara, A.; Want, J. H., Charge-Transfer Complexes of Methylviologen. *J. Phys. Chem* **1963,** *67*, 496-498.

62. Haque, R.; Coshow, W. R.; Johnson, L. F., Nuclear Magnetic Resonance Studies of Diquat, Paraquat and Their Charge-Transfer Complexes. *J. Am. Chem. Soc.* **1969,** *91*, 3822-3827.

63. Colquhoun, H. M.; Doughty, S. M.; Stoddart, J. F.; Slawin, A. M. Z.; Williams, D. J., Second-sphere Co-ordination of Cationic Rhodium Complexes [Rh(L)($NH)_3]_2$ by Dibenzo-3n-crown-n Ethers [n = 6-42; L = cyclo-octa-l,5-diene (cod) or norbornadiene (nbd)]. Solution l ^{1}H Nuclear Magnetic Resonance Spectroscopic Studies and X-Ray Crystal Structures of [Rh(cod)$(NH_3)_2$*db-21-c-7][PF_6], [Rh(nbd)$(NH_3)_2$*db-24-c-8] [PF_6], and [{Rh(cod)($NH_3)_2$),*db-36-c-l2][$PF_6]_2$ *. *J. Chem. Soc. Dalton Trans.* **1986**, 1639-1652.

64. Colquhoun, H. M.; Goodings, E. P.; Maud, J. M.; Stoddart, J. F.; Williams, D. J.; Wolstenholme, J. B., Complex Formation between Dibenzo-3n-crown-n Ethers and the Diquat Dication. *J. Chem. Soc., Chem. Commun.* **1983,** *0*, 1140-1142.

65. Grootenhuis, P. D. J.; Kollman, P. A., Molecular Mechanics and Dynamics Studies of Crown Ether-Cation Interactions: Free Energy Calculations on the Cation Selectivity of Dibenzo-18-crown-6 and Dibenzo-30-crown-10. *J. Am. Chem. Soc.* **1989,** *111*, 2152-2158.

66. Semnani, A.; Shamsipur, M., Spectroscopic study of charge transfer complexes of some benzo crown ether with p-acceptors DDQ and TCNE in dichloromethane solution. *Spectrochimica Acta* **1993,** *49A*, 411-415.

67. Ashton, P. R.; Fyfe, M. C. T.; Schiavo, C.; Stoddart, J. F.; White, A. J. P.; Williams, D. J., A New Slippage Synthesis. *Tetrahedron Lett.* **1998,** *39*, 5455-5458.

68. He, C.; Shi, Z.; Zhou, Q.; Li, S.; Li, N.; Huang, F., Syntheses of *cis*- and *trans*-Dibenzo-30-Crown-10 Derivatives *via* Regioselective Routes and Their Complexations with Paraquat and Diquat. *J. Org. Chem.* **2008,** *75*, 5872-5880.

69. Pederson, A. M. P.; Ward, E. M.; Schoonover, D. V.; Slebodnick, C.; Gibson, H. W., High-Yielding, Regiospecific Synthesis of cis(4,4')-Di(carbomethoxybenzo)-30-crown-10, Its Conversion to a Pyridyl Cryptand and Strong Complexation of 2,2'- and 4,4'-Bipyridinium Derivatives. *J. Org. Chem.* **2008,** *73*, 9094-9101.

70. Christinat, N.; Scopelliti, R.; Severin, K., Boron-based rotaxanes by multicomponent self-assembly. *Chem. Commun.* **2008**, 3660-3662.

71. Zhu, K.; Vukotic, N.; Noujeim, N.; Loeb, S. J., Bis(benzimidazolium) axles and crown ether wheels: a versatile templating pair for the formation of [2]rotaxane molecular shuttles. *Chem. Sci.* **2012,** *3*, 3265-3271.

72. Ghosh, S.; Chaudhuri, T.; Padmanaban, E.; Mukhopadhyay, C., The idiosyncrasies of (BBIM-alkane)DB30C10 MIMs. *J. Mol. Struct.* **2015,** *1097*, 6-14.

73. Moody, G. J.; Owusu, R. K.; Thomas, J. D. R., Liquid Membrane Ion-selective Electrodes for Diquat and Paraquat. *Analyst* **1987,** *112*, 121-127.

74. Moody, G. J.; Owusu, R. K.; Thomas, J. D. R., Studies on Crown Ether Based Potentiometric Sensors for 4,4'-Dipyridinium and Related Dications. *Analyst* **1988,** *113*, 65-69.

75. Assubaie, F. N.; Moody, G. J.; Thomas, J. D. R., Comparitive Study of Polyether-type Neutral Carriers for the Potentiometric Sensing of Guanidinium Ions. *Analyst* **1989,** *114*, 1545-1550.

76. Saad, B. B.; Zahid, Z. A.; Rahman, S. A.; Ahmad, M. N., Primaquine-selective Electrodes Based on Macrocyclic Crown Ethers. *Analyst* **1992,** *117*, 1319-1321.

77. Elmosallamy, M. A. F.; Saber, A. L., Recognition and Quantification of Some Monoamines Neurotransmitters. *Electroanalysis* **2016,** *28*, 2500-2505.

78. Ashton, P. R.; Ballardini, R.; Balzani, V.; Gómez-López, M.; Lawrence, S. E.; Martínez-Díaz, M. V.; Montali, M.; Piersanti, A.; Prodi, L.; Stoddart, J. F.; Williams, D. J., Hydrogen-Bonded Complexes of Aromatci Crown Ethers with (9-Anthracenyl)methylammonium Derivatives. Supramolecular Photochemistry and Photophysics. pH-Controllable Supramolecular Switching. *J. Am. Chem. Soc.* **1997,** *119*, 10641-10651.

79. Schild, V.; van Loyen, D.; Dürr, H.; Bouas-Laurent, H.; Turro, C.; Wörner, M.; Pokhrel, M. R.; Bossmann, S. H., Tuning the Charge-Separated Lifetimes of Ruthenium(II)polypyridyl-Viologen Dyads and Ruthenium(II)polypyridyl-Viologen Triads by the Formation of Supramolecular Assemblies with Crown Ethers. *J. Phys. Chem. A* **2002,** *106*, 9149-9158.

80. Gunaratne, H. Q. N.; Nockemann, P.; Olejarz, S.; Reid, S. M.; Seddon, K. R.; Srinivasan, G., Ionic Liquids with Solvatochromic and Charge-Transfer Functionalities Incorporating the Viologen Moeity. *Aust. J. Chem.* **2013,** *66*, 607-611.

81. Marjanovic, M.; Kralj, M.; Supek, F.; Frkanec, L.; Piantanida, I.; Šmuc, T.; Tusek-Božic, L., Antitumor Potential of Crown Ethers: Structure-Activity Relationships, Cell Cycle Disturbances, and Cell Death Studies of a Series of Ionophores. *J. Med. Chem.* **2007,** *50*, 1007-1018.

82. Han, Y.; Cao, J.; Li, P.-F.; Zong, Q.-S.; Zhao, J.-M.; Guo, J.-B.; Xiang, J.-F.; Chen, C.-F., Complexation of Triptycene-Derived Macrotricyclic Polyether with Paraquat Derivatives, Diquat, and a 2,7-Diazapyrenium Salt: Guest-Induced Conformational Changes of the Host. *J. Org. Chem.* **2013,** *78*, 3235-3242.

83. Zhao, J.-M.; Zong, Q.-S.; Chen, C.-F., Complexation of Triptycene-Based Macrotricyclic Host towards (9-Anthracylmethyl)benzylammonium Salt: A Ba^{2+} Selective Fluorescence Probe. *J. Org. Chem.* **2010,** *75*, 5092-5098.

84. Guo, J.-B.; Han, Y.; Cao, J.; Chen, C.-F., Formation of 1:2 Host-Guest Complexes Based on Triptycene-Derived Macrotricycle and Paraquat Derivatives: Anion-π Interactions between PF_6^- and Bipyridinium Rings in the Solid State. *J. Org. Chem.* **2011,** *13*, 5688-5691.

85. Wang, X.-Q.; Wang, W.; Wang, Y.-X.; Yang, H.-B., Supramoleuclar Polymers Constructed through Self-sorting Host-Guest Interactions. *Chem. Lett.* **2015,** *44*, 1040-1046.

86. Wei, P.; Yan, X.; Huang, F., Supramolecular polymers constructed by orthogonal self-assembly based on host–guest and metal–ligand interactions. *Chem. Soc. Rev.* **2015,** *44*, 815-832.

87. Li, S.-L.; Xiao, T.; Lin, C.; Wang, L., Advanced supramolecular polymers constructed by orthoganol self-assembly. *Chem. Soc. Rev.* **2012,** *41*.

88. Zolotukhin, M. G.; Hernández, M. d. C. G.; Lopez, A. M.; Fomina, L.; Cedillo, G.; Nogales, A.; Ezquerra, T.; Rueda, D.; Colquhoun, H. M.; Fromm, K. M.; Ruiz-Treviño, A.; Ree, M., Film-Forming Polymers Containing in the Main-Chain Dibenzo Crown Ethers with Aliphatic (C_{10}-C_{16}), Aliphatic-Aromatic, or Oxyindole Spacers. *Macromolecules* **2006,** *39*, 4649-4703.

89. Chen, R.; Zhou, Q.; zhang, B.; Wu, J.; Ye, Y.; Dai, G.; Jiang, H., K^+ Responsive Supramolecular Polymer Constructed by Dibenzo-30-Crown-10/Paraquat-Based Molecular Recognition. *J. Polym. Sci. Part A: Polym. Chem.* **2015,** *53*, 1178-1181.

90. Yamaguchi, N.; Nagvekar, D. S.; Gibson, H. W., Self-Organization of a Heteroditopic Molecule to Linear Polymolecular Arrays in Solution. *Angew. Chem. Int. Ed.* **1998,** *37*, 2361-2364.

91. Yuki, T.; Koyama, Y.; Matsumura, T.; Takata, T., Click Annulation of Pseudo[2]rotaxane to [2]Catenane Exploiting Homoditopic Nitrile *N*-Oxide. *Org. Lett.* **2013,** *15*, 4438-4441.

Chapter 2: Multi-gram syntheses of four crown ethers using K^+ as templating agent.

ABSTRACT

Dibenzo-30-crown-10 (**DB30C10**, **1c**), dibenzo-24-crown-8 (**DB24C8**, **1a**), 4-carbomethoxydibenzo-24crown-8 (**1b**) and a new crown ether, 4-carbomethoxydibenzo-30-crown-10 (**1d**), were synthesized by a simple, high yielding, three step method. Potassium ions from the highly soluble KPF_6 were employed to template the cyclization step, which resulted in very high isolated yields (80-90%).

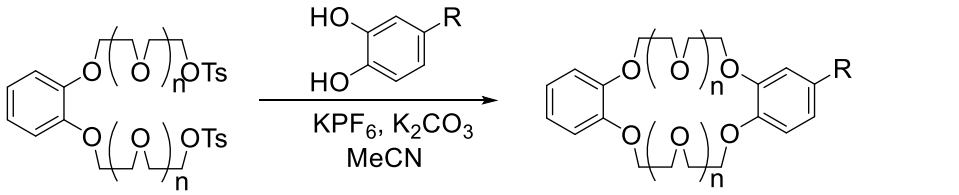

1a R= H, n = 2, 87%
1b R= COOMe, n = 2, 90%
1c R= H, n = 3, 86%
1d R=COOMe, n = 3, 80%

Introduction

DB30C10 and **DB24C8** are useful components in the construction of mechanically interlocked molecules such as pseudorotaxanes,[1-7] rotaxanes,[2,8-11] catenanes,[9,8, 12-13] molecular shuttles,[10,14-15] and other molecular machines.[10,16-18] These crown ethers also have great utility as components in potentiometric sensors,[19-20] in selective complexation and extraction of ions,[21-22] in polymers,[23-30] and other stimuli-responsive materials.[31-33] **DB30C10** has anticoccidial activity.[34] Functionalized **DB24C8** has been used extensively

in more complicated supramolecular devices,[1-7,14-18,35-39] supramolecular polymers,[40-44] and self-healing supramolecular gels.[32]

DB30C10 is commercially available at ~$302/gram. Our research requires multiple grams of the material, which makes purchasing it cost prohibitive. A careful search of the literature revealed that most authors to date used the method published by Pederson in 1967 (**Scheme 1**).[(13)45-46] Pedersen did not isolate the **DB30C10** completely in his initial report, but claimed that his reaction mixture contained at least 6% of the desired crown.[(13a)46] To our knowledge, the highest cyclization yield that has been obtained using Pedersen's method to date is 25%.[(13b)45]

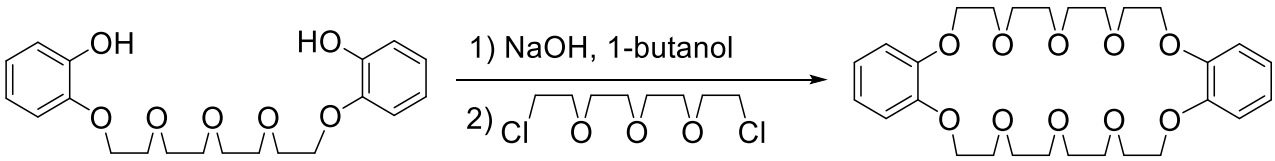

Scheme 2.1. **DB30C10** synthesis as outlined by Pedersen

None of the reports in the literature takes advantage of the fact that the final cyclization step in the syntheses of **DB30C10** and **DB24C8** can be templated with potassium ion, as was previously demonstrated in the syntheses of the *cis*-dicarbomethoxy derivatives.[47-48] Association constants for complexation between **DB24C8** and potassium ion in acetonitrile as measured by conductivity and solubility average 7.6 (±1.9) × 10^3 M^{-1}.[49-52] Similarly association constants for **DB30C10** with K^+ average 4.3 × 10^4 M^{-1}.[51, 53] Given these association constants, we thought it reasonable to suppose that potassium would be an effective templation agent for formation of **DB24C8** and **DB30C10**.

K_2CO_3 is often employed as the base in such cyclizations; however, its solubility in the organic solvents normally used is quite low, minimizing the effect of templation. Furthermore, the synthesis that gave the highest yield for **DB30C10**[45] uses a benzyl protecting group to make the diphenolic intermediate shown in **Scheme 2.1**. Since this crown ether is symmetrical, the use of a protecting group is wholly unnecessary. We designed the synthetic route depicted in **Scheme 2.2** to take advantage of templation by potassium ion in the form of the highly organic-soluble hexafluorophosphate salt and the symmetry of the desired **DB30C10**. Our route closely resembles that reported by Bruns et al. for the synthesis of 1,5-dinaptho-38-crown-10 (28 or 33%, syringe pump addition),[54] but with the exception that they did not use potassium ion templation in the form of KPF_6.

Knowing that the *cis*-dicarbomethoxy derivatives of both **DB30C10**[48] and **DB24C8**[47] can be templated with potassium, and that, unlike the dicarbomethoxy crown derivatives, the unsubstituted and monocarbomethoxy derivatives cannot form regio-isomers, we saw no reason that **DB24C8** and the 2-carbomethoxy derivatives of **DB30C10** and **DB24C8** could not be synthesized by the same route.

Indeed, this synthetic route requires only a single chromatographic step after the tosylation of **2a** and **2b**. The cyclization step essentially yields a single product: the crown ethers **1a**-**d**, which can easily be purified by washing or by ion exchange resin. In contrast, most untemplated cyclizations require two chromatography columns, or chromatography followed by recrystallization, to yield crown ethers of satisfactory purity.

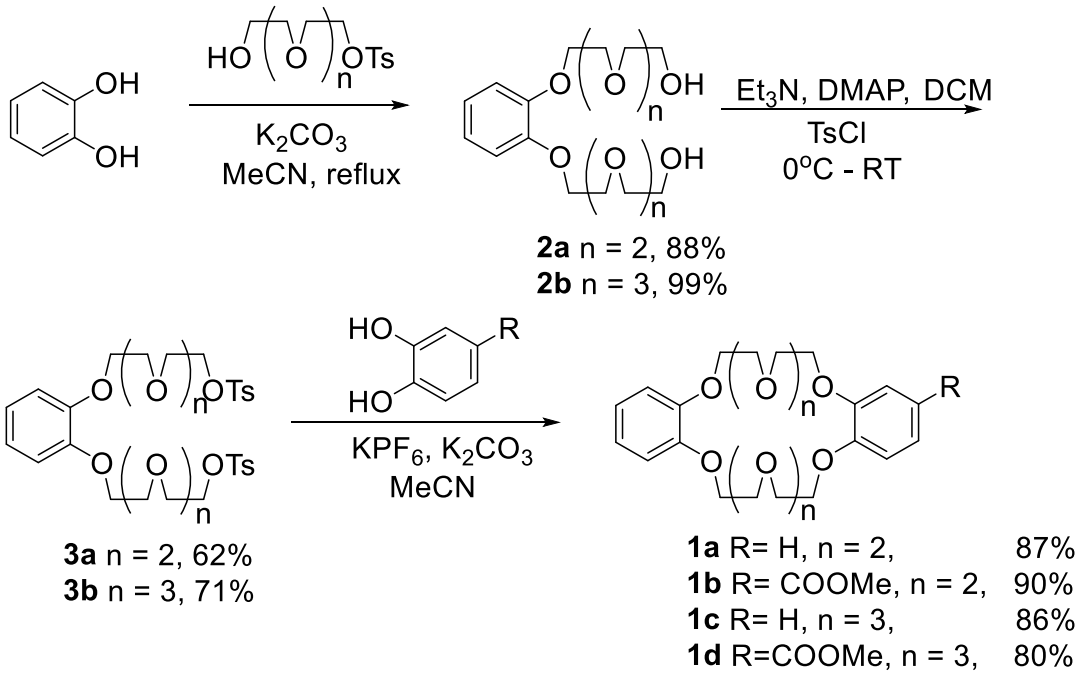

Scheme 2.2. Improved syntheses of crown ethers

Results and discussion

Diols **2a** and **2b** were prepared *via* Williamson ether synthesis with the monotosylate of the appropriate glycol and catechol, in MeCN with K_2CO_3 as base. Diol **2a** was tosylated by the dropwise addition of tosyl chloride in DCM to a solution of diol in DCM at 0 ˚C. Diol **2b** was tosylated by adding a solution of tosyl chloride in DCM to a cold solution of **2b**, trimethylamine and DMAP. The diols were purified by column chromatography to yield yellow oils. **DB30C10** was prepared by Williamson ether synthesis of ditosylate **3b** with catechol. K_2CO_3 was used as the base, and 1.2 equivalents KPF_6 were added as a templating agent by simple mixing without the use of a syringe pump. The concentrations of the two components were 44 mM. After four days at reflux, the crude solution's ^{1}H NMR

spectrum revealed no trace of the starting material and indicated almost exclusively the complex between **DB30C10** and K^+ (as compared to the ^1H NMR of a sample of commercial **DB30C10** mixed with KPF_6, (Supplementary info).

Removing the K^+ from **DB30C10** proved unexpectedly challenging. When the diester derivative of **DB30C10** was prepared using KPF_6 as template, the K^+ was removed by simply washing the DCM solution with water three times.[48] This was not the case with the parent **DB30C10**, as extensive water washing did not remove the K^+. Eventually the template was removed by washing with pyridinium hydrochloride solution to displace the K^+. The solution turned yellow, indicating the formation of a charge transfer complex between **DB30C10** and pyridinium hydrochloride.[55] The solution was then washed with 10% (w/v) NaOH, which led to the deprotonation of the pyridinium salt and subsequent decomplexation. The resulting solid was reasonably pure, but had a slight brown color that was removed by treatment with decolorizing carbon, followed by recrystallization from MeOH to yield **DB30C10** as a colorless solid in 86% yield. (The discoloration was only observed in one of the five batches prepared in this fashion. The recrystallization step was therefore omitted in the other batches).

The other crown ethers were prepared in a similar fashion. The carbomethoxy crown ethers **1b** and **1d** were washed with $NaHCO_3$, instead of 10% NaOH, to prevent hydrolysis of the esters. Both esters contained residual pyridine (^1H NMR), which was removed by drying under high vacuum or by passing the compound through a cation exchange resin.

The synthesis is amenable to multi-gram preparation of product, as up to 5 grams can be produced in a single reaction without undue difficulty, whereas multigram preparation is impractical for untemplated cyclizations. Note that, though syringe pump addition or high dilution is unnecessary, some attention should be paid to concentration. In more concentrated solutions (67 mM) some linear oligomers were formed. This led to a decrease in the yield of **1c** from 86% to 65%. This observation seems to indicate that the K^+ ion pre-organizes the ethylene glycol arms in a conformation favorable for ring closure, thereby lowering the entropic barrier to cyclization. However, with higher concentrations, the competing polymerization becomes more favorable.

Since the templation of the reaction between ditosylate and catechol does not produce significant by-products (save for oligomers at high concentration), we tested the efficacy of the templation by attempting a one-pot preparation of the crown ethers. Typically this method produces very poor yields (6-15%), for example, the one-pot preparation of bis(*m*-phenylene)-32-crown-10 and its derivatives.[56-57] The one-pot procedure was attempted for **DB24C8**. Tri(ethylene glycol) ditosylate, catechol, KPF_6, and K_2CO_3 were combined and allowed to reflux in MeCN for several days. **DB24C8** was easily isolated from the mixture by column chromatography in 36% yield. Although a yield of 43% has been reported in the one-step synthesis of **DB24C8**, that synthesis required much harsher conditions such as boiling DMSO and KOH.[58]

Conclusion

DB30C10, **DB24C8** and their corresponding 4-carbomethoxy derivatives were prepared by a facile, three step synthesis from relatively inexpensive starting materials using KPF_6 to template the cyclizations. The isolated yields of the final cyclization steps ranged from 80-90%. It is believed that the high yield and the lack of significant by-products is a result of the ethylene glycol arms "wrapping around" the K^+ ion. With the tosylated ends of the ethylene glycol arms positioned close together, the entropic barrier to ring closure is reduced. This arrangement favors ring closure over polymerization, the typical competing process in macrocyclizations of this kind. The method does not require special purification (except liquid-liquid extraction) or syringe pump addition. The syntheses require only a single chromatographic separation in the second step. Isolation of the crown ether is accomplished by washing or by treatment with ion exchange resin. This simple, economical, high yielding synthesis provides access to multiple grams of these valuable supramolecular building blocks.

Experimental

General: Compounds **2a**[13], **2b**[37]**, 3a**[13] and **3b**[35] were prepared according to literature procedures.

THF was dried by distillation over Na/benzophenone. DCM was dried by distillation over CaH_2, and pyridine was dried by distillation over molecular sieves. All other chemicals were used as received. Melting points were measured with a Mel-Temp II device in capillary tubes and are uncorrected. ^1H, ^{19}F and ^{13}C NMR spectra were obtained at

ambient temperature on JOEL Eclipse Plus 500 MHz, Varian Unity Plus or Varian MR 400 MHz spectrometers. ^{1}H NMR and ^{13}C spectra are corrected relative to residual solvent peaks. High-resolution mass spectra were obtained with an Agilent 6220 LCMS ESITOF spectrometer. Ion exchange was performed with Amberlite GC-120, strongly acid sulfonated cation exchange resin (RSO^{-} Na^{+}) 100-200 mesh. Column chromatography was performed with silica gel, 40-63 μm, 60 Å from Sorbent Technologies, or Flash Alumina-N from Agela Technologies.

Dibenzo-30-crown-10 (**1c**). Ditosylate **3b** (7.52 g, 9.75 mmol), catechol (7.07 g, 9.75 mmol) and KPF_6 (2.15 g, 11.7 mmol) were dissolved in MeCN (220 mL). N_2 (g) was bubbled through the solution for 20 min. The flask was wrapped in aluminium foil, and K_2CO_3 (8.08 g, 59 mmol) was added. The mixture was allowed to reflux under N_2 (g) for 4 days, allowed to cool to room temperature and evaporated under reduced pressure. The residue was partitioned between DCM and water. The DCM layer was washed with water 1x, pyridinium hydrochloride solution (1:1:1 pyridine: conc. HCl: water (v/v/v)) (5 x 20 mL), 10% (w/v) NaOH (20 mL), and water (1 x 20 mL). The organic layer was dried over Na_2SO_4, filtered, and evaporated *in vacuo* to yield a white solid, (4.50 g, 86%), mp 102.0-103.6 ˚C; lit. mp 106.0 - 107.5 °C.[13a] ^{1}H NMR (400 MHz, $CDCl_3$) δ 6.89 - 6.81 (m, 8H), 4.10 (t, *J* = 4 Hz, 8H), 3.82 (t, *J* = 4 Hz, 8H), 3.75–3.69 (m, 8H), 3.66-3.64 (m, 8H). ^{13}C NMR (101 MHz, $CDCl_3$) δ 149.1, 121.6, 114.6, 70.9, 70.7, 69.8, 69.2. ESI-TOF: $(M+H)^{+}$ *m/z* 537.2691 (found), 537.2694 (calculated for $C_{28}H_{40}O_{10}$), error -0.5 ppm.

4-Carbomethoxydibenzo-30-crown-10 (**1d**). Ditosylate **3b** (1.30 g, 1.70 mmol), methyl 3,4-dihydroxybenzoate (0.28 g, 1.7 mmol) and KPF_6 (0.38 g, 2.1 mmol) were dissolved in MeCN (100 mL). The solution was degassed with N_2 (g) and the flask was wrapped in foil to exclude light. K_2CO_3 (0.96 g, 7.0 mmol) was added and the mixture was heated at reflux for 7 days, allowed to cool to room temperature and filtered to remove the solids. The solvent was removed by rotary evaporation. The residue was dissolved in DCM and washed with pyridinium hydrochloride (1:1:1 pyridine: conc. HCl: water) (12 x 15 mL), water (15 mL), $NaHCO_3$ (sat.) (4 x 15 mL), and water (1 x 15 mL). The organic layer was dried over $MgSO_4$, filtered, and the solvent was removed by rotary evaporation. The white solid still had some pyridinium peaks in the ^1H NMR spectrum. The solid was dissolved in acetone and passed through an ion exchange resin. The solvent was removed to yield a white solid (0.80 g, 80%), mp 76-78 ˚C. ^1H NMR (400 MHz, $CDCl_3$) δ 7.64 (dd, *J* = 8, 2 Hz, 1H), 7.52 (d, *J* = 2 Hz, 1H), 6.88 (d, *J* = 2 Hz, 4H), 6.85 (d, *J* = 8 Hz, 1H), 4.19 (t, *J* = 4 Hz, 4H), 4.14 (t, *J* = 4 Hz, 4H), 3.92–3.86 (m, 11H), 3.80 - 3.75 (m, 8H), 3.70–3.66 (m, 8H). ^{13}C NMR (101 MHz, $CDCl_3$) δ 166.8, 152.9, 149.1, 148.3, 123.9, 122.9, 121.5, 114.7, 114.6, 112.4, 71.02, 70.98, 70.91, 70.7, 69.8, 69.6, 69.5, 69.18, 69.16, 69.15, 68.9, 51.9. ESI-TOF: $(M+H)^+$ *m/z* 595.2753 (found), 595.2749 (calculated for $C_{30}H_{42}O_{12}$), error 0.6 ppm.

4-Carbomethoxydibenzo-24-crown-8 (**1b**). Ditosylate **3a** (2.40 g, 3.50 mmol), methyl 3,4-dihydroxybenzoate (0.59 g, 3.5 mmol) and KPF_6 (0.78 g, 4.2 mmol) were dissolved in MeCN (110 mL). The solution was degassed by bubbling N_2 (g) through it. The flask

was wrapped in aluminium foil to exclude light, and K_2CO_3 (1.96 g, 14.0 mmol) was added. The mixture was heated at reflux under N_2 (g) for 5 days, allowed to cool to room temperature and the solids were filtered. The solvent was removed by rotary evaporation and the residue was dissolved in DCM. The solution was washed with pyridinium hydrochloride (12 x 15 mL), water (15 mL), $NaHCO_3$ (sat.) (4 x 15 mL), and water (1 x 15 mL), dried over $MgSO_4$, filtered, and the solvent was removed by rotary evaporation to yield a white solid (1.61 g, 90%), mp 86.0-87.5 ˚C. Lit. yield 40% (12.5 g by pseudo-high dilution in 3.5 L of DMF using K_2CO_3 as base and syringe pump addition of the two reactants), mp 83-85˚C.[59] The analogous ethyl ester was reportedly prepared in 56% yield (2.6 g) by slow (12 h) addition of the ditosylate in 500 mL of MeCN to a mixture of K_2CO_3 and the catechol derivative and in 1 L of MeCN.[35] ^{1}H NMR (400 MHz, $CDCl_3$) δ 7.64 (dd, *J* = 8, 2 Hz, 1H), 7.51 (d, *J* = 2 Hz, 1H), 6.90-6.86 (m, 4H), 6.84 (d, *J* = 8 Hz, 2H), 4.21-4.17 (m, 4H), 4.16 – 4.13 (m, 4H), 3.95-3.90 (m, 8H), 3.87 (s, 3H), 3.84 (s, 4H), 3.83 (s, 4H). ^{13}C NMR (101 MHz, $CDCl_3$) δ 166.8, 152.9, 148.95, 148.93,148.3, 123.9, 122.9, 121.4, 114.3, 114.1, 112.0, 71.5, 71.4, 71.3, 69.95, 69.8, 69.6, 69.5, 69.4, 69.39, 69.32, 51.9. ESITOF: $(M+H)^+$ *m/z* 507.2238 (found), 507.2225 (calculated for $C_{26}H_{34}O_{10}$), error 2.6 ppm.

Dibenzo-24-crown-8 (**1a**). Ditosylate **3a** (2.23 g, 3.2 mmol), catechol (0.36 g, 3.2 mmol) and KPF_6 (0.72 g, 3.9 mmol) were dissolved in MeCN (100 mL). Ar (g) was bubbled through the solution for 10 min. The flask was wrapped in aluminium foil to exclude light, and K_2CO_3 (1.78 g, 13 mmol) was added. The mixture was heated at reflux under Ar (g) for 3 days, allowed to cool to room temperature and the solids were filtered. The solvent

was removed by rotary evaporation and the purple residue was partitioned between DCM and water. The organic layer was washed with 1:1:1 pyridine: HCl: H_2O (10 x 20 mL), water (1 x 20 mL), 10% (w/v) NaOH (3 x 20 mL) and water (1 x 20 mL). The purple solution turned bright red when it was washed with the pyridinium•HCl solution and back to purple again with the NaOH washings. The organic layer was dried over $MgSO_4$ and activated carbon was added. The solution was filtered through *Celite*®, filtered again and the solvent was removed. The residual pyridine was removed by drying under high vacuum to yield a white solid (1.27 g, 87%), mp 100-102 ˚C. Lit. yield 43% (NaOH/DMSO), mp 102-103 ˚C.[19,21][58, 60] ^{1}H NMR (400 MHz $CDCl_3$, Figure S10) δ 6.88 (m, 8H), 4.15 (t, *J* = 4 Hz, 8H), 3.92 (t, *J* = 4 Hz, 8H), 3.83 (s, 8H). ^{13}C NMR (101 MHz, $CDCl_3$) δ 149.1, 121.5, 114.2, 71.4, 70.1, 69.5 ESITOF: $(M+H)^+$ *m/z* 449.2171 (found), 449.2174 (calculated for $C_{24}H_{32}O_8$), error 0.3 ppm.

One Step Synthesis of Dibenzo-24-crown-8. Catechol (1.01 g, 9.10 mmol), tri(ethylene glycol) ditosylate (4.16 g, 9.10 mmol) and KPF_6 (6.66 g, 36.0 mmol) were dissolved in MeCN (120 mL). N_2 (g) was bubbled through the solution for 20 min. The flask was wrapped in aluminium foil to exclude light, and K_2CO_3 (5.03 g, 36 mmol) was added. The mixture was heated at reflux under N_2 (g). After one week, the solution was allowed to cool to room temperature. The solvent was removed by rotary evaporation and the solid was partitioned between DCM and water (15 mL). The DCM layer was washed with water (3 x 15 mL), dried over Na_2SO_4, filtered, and the solvent was removed by rotary evaporation. The crude solid was purified by column chromatography (neutral alumina; 2:1 EtOAc:DCM, v:v). The fractions containing product were concentrated to yield a white

solid (0.74 g, 36%), mp 100-102 ˚C; lit. mp 102-103 ˚C.[19,21][58, 60] ^{1}H NMR (500 MHz, $CDCl_3$) δ 7.01 – 6.96 (m, 4H), 4.24 – 4.20 (m, 4H), 3.80 – 3.76 (m, 4H), 3.73 (s, 4H). ^{13}C NMR (101 MHz, $CDCl_3$) δ 150.1, 123.0, 118.1, 71.2, 70.0, 69.0.

References

1. Xue, M.; Yang, Y.; Chi, X.; Yan, X.; Huang, F., Development of Pseudorotaxanes and Rotaxanes: From Synthesis to Stimuli-Responsive Motions to Applications. *Chem. Rev.* **2015,** *115*, 7398-7501.
2. Arunachalam, M.; Gibson, H. W., Recent developments in polypseudorotaxanes and polyrotaxanes. *Prog. Polym. Sci* **2014,** *39*, 1043-1073.
3. Ghosh, S.; Chaudhuri, T.; Schmiedekamp, A. M.; Padmanaban, E.; Mukhopadhyay, C., A 2,2'-bis(benzimidazolium)-dibenzo[24]crown[8] rigid pseudorotaxane system. *Tetrahedron* **2014,** *70*, 6885-6893.
4. Madhy, V.; Das, S. K., Diverse Supramolecular Architectures Having Well-Defined Void Spaces Formed from a Pseudorotaxane Cation: Influential Role of Metal Dithiolate Coordination Complex Anions. *Cryst. Growth Des.* **2014,** *14*, 2343-2356.
5. Deska, M.; Kozlowska, J.; Sliwa, W., Rotaxanes and pseudorotaxanes with threads containing viologen units. *ARKIVOC* **2013**, 66-100.
6. Gibson, H. W.; Jones, J. W.; Zakharov, L. N.; Rheingold, A. L.; Slebodnick, C., Complexation Equilibria Involving Salts in Non-Aqueous Solvents: Ion Pairing and Activity Considerations. *Chem. Eur. J.* **2011,** *17*, 3192-3206.
7. Fyfe, M. C. T.; Stoddart, J. F., (Supra)Molecular systems based on crown ethers and secondary dialkylammonium ions *Adv. Supramol. Chem.* **1999,** *6*, 1-53.
8. Yuki, T.; Koyama, Y.; Matsumura, T.; Takata, T., Click Annulation of Pseudo[2]rotaxane to [2]Catenane Exploiting Homoditopic Nitrile *N*-Oxide. *Org. Lett.* **2013,** *15*, 4438-4441.
9. Tron, A.; Jacquot de Rouville, H.-P.; Ducrot, A.; Tucker, J. H. R.; Baroncini, M.; Credi, A.; McClenaghan, N. D., Photodriven [2]rotaxane-[2]catenane interconversion. *Chem. Commun.* **2015,** *51*, 2810-2813.

10. Zhu, K.; Vukotic, N.; Noujeim, N.; Loeb, S. J., Bis(benzimidazolium) axles and crown ether wheels: a versatile templating pair for the formation of [2]rotaxane molecular shuttles. *Chem. Sci.* **2012,** *3*, 3265-3271.
11. Ashton, P. R.; Fyfe, M. C. T.; Schiavo, C.; Stoddart, J. F.; White, A. J. P.; Williams, D. J., A New Slippage Synthesis. *Tetrahedron Lett.* **1998,** *39*, 5455-5458.
12. Niu, Z.; Gibson, H. W., Polycatenanes. *Chem. Rev.* **2009,** *109*, 6024-6046.
13. Zhao, Y.-L.; Liu, L.; Zhang, W.; Sue, C.-H.; Li, Q.; Miljanić, O. Š.; Yaghi, O. M.; Stoddart, J. F., Rigid-Strut-Containing Crown Ethers and [2]Catenanes for Incorporation into Metal-Organic Frameworks. *Chem. Eur. J.* **2009,** *15*, 13356-13380.
14. Busseron, E.; Coutrot, F., N-Benzyltriazolium as Both Molecular Station and Barrier in [2]Rotaxane Molecular Machines. *J. Org. Chem.* **2013,** *78*, 4099-4106.
15. Cao, Z.-Q.; Li, H.; Yao, J.; Zou, L.; Qu, D.-H.; Tian, H., A Perylene-Bridged Switchable [3]Rotaxane Molecular Shuttle with a Fluorescence Output. *Asian J. Org. Chem* **2015,** *4*, 212-216.
16. Ma, Y.-X.; Meng, Z.; Chen, C.-F., A Novel Pentiptycene Bis(crown ether)-Based [2](2)Rotaxane Whose Two DB24C8 Rings Act as Flapping Wings of a Butterfly. *Org. Lett.* **2014,** *16*, 1860-1863.
17. Li, H.; Li, X.; Wu, Y.; Ågrent, H.; Qu, D.-H., A Musclelike [2](2)Rotaxane: Synthesis, Performance, and Molecular Dynamics Simulations. *J. Org. Chem.* **2014,** *79*, 6996-7004.
18. Qu, D.-H.; Feringa, B. L., Controlling Molecular Rotary Motion with a Self-Complexing Lock. *Angew. Chem. Int. Ed.* **2010,** *49*, 1107-1110.
19. Elmosallamy, M. A. F., New potentiometric sensors for creatine. *Anal. Chim. Acta* **2006,** *564*, 253-257.
20. Lee, D.; Thomas, J. D. R., 4'-Picrylamino-5'-nitrobenzo-18-crown-6 as a sensing reagent in potassium ion-selective electrode membranes. *Talanta* **1994,** *41*, 901-907.
21. Agnihotri, P.; Suresh, E.; Ganguly, B.; Paul, P.; Ghosh, P. K., Study of the competitive binding of mixed alkali and alkaline earth metal ions with dibenzo-30-crown-10. *Polyhedron* **2005,** *24*, 1023-1032.
22. Saad, B. B.; Zahid, Z. A.; Rahman, S. A.; Ahmad, M. N., Primaquine-selective Electrodes Based on Macrocyclic Crown Ethers. *Analyst* **1992,** *117*, 1319-1321.
23. Lee, M.; Schoonover, D. V.; Gies, A. P.; Hercules, D. M.; Gibson, H. W., Synthesis of Complementary Host- and Guest-Functionalized Polymeric Building Blocks and Their Self-Assembling Behavior. *Macromolecules* **2009,** *42*, 6483-6494.

24. Gibson, H. W.; Ge, Z.; Jones, J. W.; Harich, K.; Pederson, A.; Dorn, H. C., Supramacromolecular chemistry: Self-assembly of polystyrene-based multi-armed pseudorotaxane star polymers from multi-topic C_{60} derivatives. *J. Polym. Sci. A. Polym. Chem.* **2009,** *47*, 6472–6495.

25. Zolotukhin, M. G.; Hernández, M. d. C. G.; Lopez, A. M.; Fomina, L.; Cedillo, G.; Nogales, A.; Ezquerra, T.; Rueda, D.; Colquhoun, H. M.; Fromm, K. M.; Ruiz-Treviño, A.; Ree, M., Film-Forming Polymers Containing in the Main-Chain Dibenzo Crown Ethers with Aliphatic (C_{10}-C_{16}), Aliphatic-Aromatic, or Oxyindole Spacers. *Macromolecules* **2006,** *39*, 4649-4703.

26. Gibson, H. W.; Ge, Z.; Huang, F.; Jones, J. W.; Lefebvre, H.; Vergne, M. J.; Hercules, D. M., Syntheses and Model Complexation Studies of Well-Defined Crown Terminated Polymers. *Macromolecules* **2005,** *38*, 2626-2637.

27. Gibson, H. W.; Farcas, A.; Jones, J. W.; Ge, Z.; Huang, F.; Vergne, M. J.; Hercules, D. M., Supramacromolecular self-assembly: Chain extension, star and block polymers via pseudorotaxane formation from well-defined end-functionalized polymers. *J. Polym. Sci. A. Polym. Chem.* **2009,** *47*, 3518-3543.

28. Gibson, H. W.; Yamaguchi, N.; Hamilton, L. M.; Jones, J. W., Cooperative Self-Assembly of Dendrimers via Pseudorotaxane Formation from a Homotritopic Guest Molecule and Complementary Monotopic Host Dendrons. *J. Am. Chem. Soc.* **2002,** *124*, 4653-4665.

29. Gibson, H. W.; Hamilton, L.; Yamaguchi, N., Molecular Self-assembly of Dendrimers, Non-covalent Polymers and Polypseudorotaxanes. *Polym. Adv. Technol.* **2000,** *11*, 791-797.

30. Yamaguchi, N.; Gibson, H. W., Non-covalent chemical modification of crown ether side-chain polymethacrylates with a secondary ammonium salt: a family of new polypseudorotaxanes. *Macromol. Chem. Phys* **2000,** *201*, 815-824.

31. Li, S.; Lu, H.-Y.; Shen, Y.; Chen, C.-F., A Stimulus-Response and Self-Healing Supramolecular Polymer Gel Based on Host–Guest Interactions. *Macromol. Chem. Phys.* **2013,** *214*, 1596-1601.

32. Zhang, M.; Yan, X.; Huang, F.; Niu, Z.; Gibson, H. W., Stimuli-Responsive Host–Guest Systems Based on the Recognition of Cryptands by Organic Guests. *Acc. Chem. Res.* **2014,** *47*, 1995-2005.

33. Lee, M.; Choi, U. H.; Colby, R. H.; Gibson, H. W., Ion Conduction in a Semicrystalline Polyviologen and Its Polyether Mixtures. *Macromol. Chem. Phys* **2015,** *216*, 344-349.

34. Brown, G. R.; Foubister, A. J., Anticoccidial Activity of Crown Polyethers. *J. Med. Chem.* **1983,** *26*, 590-592.

35. Diederich, F.; Echegoyen, L.; Gómez-López, M.; Kessinger, R.; Stoddart, J. F., The self-assembly of fullerene-containing [2]pseudorotaxanes: formation of a supramolecular C_{60} dimer *J. Chem. Soc., Perkin Trans. 2* **1999,** *0*, 1577-1586.

36. Zhu, X.-Z.; Chen, C.-F., A Highly Efficient Approach to [4]Pseudocatenanes by Threefold Metathesis Reactions of a Triptycene-Based Tris[2]pseudorotaxane. *J. Am. Chem. Soc.* **2005,** *127*, 13158-13159.

37. Wu, L.; He, Y.-M.; Fan, Q.-H., Controlled Reversible Anchoring of h6-Arene/TsDPEN-Ruthenium(II) Complex onto Magnetic Nanoparticles: A New Strategy for Catalyst Separation and Recycling. *Adv. Synth. Catal.* **2011,** *353*, 2915-2919.

38. Ding, Z.-J.; Zhang, Y.-M.; Teng, X.; Liu, Y., Controlled Photophysical Behaviors between Dibenzo-24-crown-8 Bearing Terpyridine Moiety and Fullerene-Containing Ammonium Salt. *J. Org. Chem.* **2011,** *76*, 1910-1913.

39. Li, H.; Zhang, H.; Zhang, Q.; Zhang, Q.-W.; Qu, D.-H., A Switchable Ferrocene-Based [1]Rotaxane with an Electrochemical Signal Output. *Org. Lett.* **2012,** *14*, 5900-5903.

40. Yamaguchi, N.; Gibson, H. W., Formation of Supramolecular Polymers from Homoditopic Molecules Containing Secondary Ammonium Ions and Crown Ether Moieties. *Angew. Chem. Int. Ed.* **1999,** *38*, 143-147.

41. Gibson, H. W.; Yamaguchi, N.; Jones, J. W., Supramolecular Pseudorotaxane Polymers from Complementary Pairs of Homoditopic Molecules. *J. Am. Chem. Soc.* **2003,** *125*, 3522-3533.

42. Gibson, H. W.; Yamaguchi, N.; Niu, Z.; Jones, J. W.; Slebodnick, C.; Rheingold, A. L.; Zakharov, L. N., Self-assembly of daisy chain oligomers from heteroditopic molecules containing secondary ammonium ion and crown ether moieties. *J. Polym. Sci. A. Polym. Chem.* **2010,** *48*, 975-985.

43. Li, S.; Zheng, B.; Chen, J.; Dong, S.; Ma, Z.; Huang, F.; Gibson, H. W., A hyperbranched, rotaxane-type mechanically interlocked polymer. *J. Polym. Sci. A. Polym. Chem.* **2010,** *48*, 4067-4073.

44. Wang, F.; Zhang, J.; Ding, X.; Dong, S.; Liu, M.; Zheng, B.; Li, S.; Wu, L.; Yu, Y.; Gibson, H. W.; Huang, F., Metal Coordination Mediated Reversible Conversion between Linear and Cross-Linked Supramolecular Polymers. *Angew. Chem. Int. Ed.* **2010,** *49*, 1090-1094.

45. Colquhoun, H. M.; Goodings, E. P.; Maud, J. M.; Stoddart, J. F.; Wolstenholme, J. B.; Williams, D. J., The Complexation of the Diquat Dication by Dibenzo-3*n*-crown-*n* Ethers. *J. Chem. Soc. Perkin Trans. II* **1985,** *0*, 607-624.

46. Pedersen, C. J., Cyclic Polyethers and Their Complexes with Metal Salts. *J. Am. Chem. Soc.* **1967,** *89*, 7017-7036.

47. Gibson, H. W.; Wang, F.; Bonrad, K.; Jones, J. W.; Slebodnick, C.; Zackharov, L. N.; Rheingold, A. L.; Habenicht, B.; Lobue, P.; Ratliff, A. E., Regioselective routes to disubstituted dibenzo crown ethers and their complexations. *Org. Biomol. Chem.* **2005,** *3*, 2114-2121.

48. Pederson, A. M. P.; Ward, E. M.; Schoonover, D. V.; Slebodnick, C.; Gibson, H. W., High-Yielding, Regiospecific Synthesis of cis(4,4')-Di(carbomethoxybenzo)-30-crown-10, Its Conversion to a Pyridyl Cryptand and Strong Complexation of 2,2'- and 4,4'-Bipyridinium Derivatives. *J. Org. Chem.* **2008,** *73*, 9094-9101.

49. Takeda, Y., Thermodynamic Study for Dibenzo-24-crown-8 Complexes with Alkali Metal Ions in Nonaqueous Solvents. *Bull. Chem. Soc. Jpn.* **1983,** *56*, 3600-3602.

50. Takeda, Y.; Kudo, Y.; Fujiwara, S., Thermodynamic Study for Complexation Reactions of Dibenzo-24-crown-8 with Alkali Metal Ions in Acetonitrile. *Bull. Chem. Soc. Jpn.* **1985,** *58*, 1315-1316.

51. Tawarah, K. M.; Mizyed, S. A., A conductance study of the association of alkali cations with 1,13-dibenzo-24-crown-8 in acetonitrile. *J. Solution Chem* **1989,** *18*, 387-401.

52. Izatt, R. M.; Pawlak, K.; Bradshaw, J. S.; Breuning, R. L., Thermodynamic and kinetic data for macrocycle interactions with cations and anions. *Chem. Rev.* **1991,** *91*, 1721-2085.

53. Massaux, J.; Roland, G.; Desreux, J. F., Solvation of the Potassium Ion Complexed with Dibenzo-30-crown-10. Transfer Activity Coefficients between Methanol and Various Solvents. *J. Solution Chem* **1982,** *11*, 549-555.

54. Bruns, C. J.; Basu, S.; Stoddart, J. F., Improved synthesis of 1,5-dinaphto[38]crown-10. *Tetrahedron Lett.* **2010,** *51*, 983-986.

55. Price, T. L. J.; Wessels, H. R.; Slebodnick, C.; Gibson, H. W., High-Yielding Syntheses of Crown Ether-Based Pyridyl Cryptands. *J. Org. Chem.* **2017,** *82*, 8117-8122.

56. Delaviz, Y.; Merola, J. S.; Berg, M. A. G.; Gibson, H. W., Syntheses, X-ray Structures, Complexation, and Thermal Stability Studies of Bis(5-carbomethoxy-1,3-phenylene)-(3*x* + 2)-crown-*x*-compounds. *J. Org. Chem.* **1995,** *60*, 516-522.

57. Gibson, H. W.; Nagvekar, D. S.; Yamaguchi, N.; Wang, F.; Bryant, W. S., Syntheses of Monofunctional Derivatives of m-Phenylene-16-crown-5, Bis(m-phenylene)-32-crown-10, and m-Phenylene-p-phenylene-33-crown-10. *J. Org. Chem.* **1997,** *62*, 4798-4803.

58. Kotlyar, S. A.; Gorodnyuk, V. P.; Grigorash, R. Y.; Chuprin, G. N., An Improved Method for Preparing Dibenzo Crown Ethers. *Russ. J. Gen. Chem.* **1998,** *68*, 1135-1138.

59. Yamaguchi, N.; Hamilton, L. M.; Gibson, H. W., Dendritic Pseudorotaxanes. *Angew. Chem. Int. Ed.* **1998,** *37*, 3275-3279.

60. Izatt, R. M.; Terry, D. P.; Nelson, D. P.; Chan, Y.; J., E. D.; Bradshaw, J. S.; Hansen, L. D.; Christensen, J. J., Calorimetric titration study of the interaction of some uni- and bivalent cations with benzo-15-crown-5, 18-crown-6, dibenzo-24-crown-8, and dibenzo-27-crown-9 in methanol-water solvents, at 25.degree.C and .mu. = 0.1. *J. Am. Chem. Soc.* **1976,** *98*, 7626-7630.

Supporting information: ^{1}H NMR, ^{13}C NMR and HRMS of crown ethers.

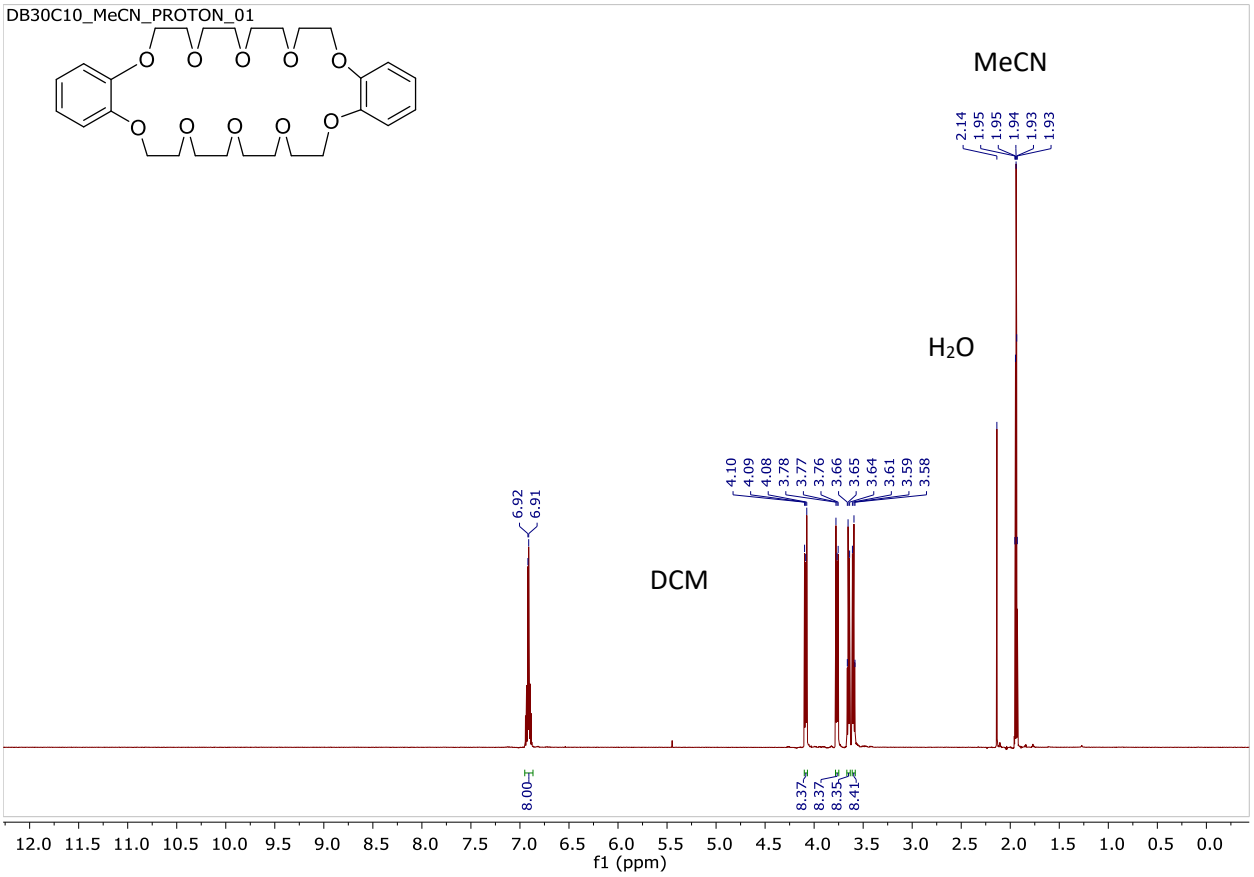

Figure 2.1. ^{1}H NMR spectrum of DB30C10 (**1c**) in CD_3CN at 400 MHz.

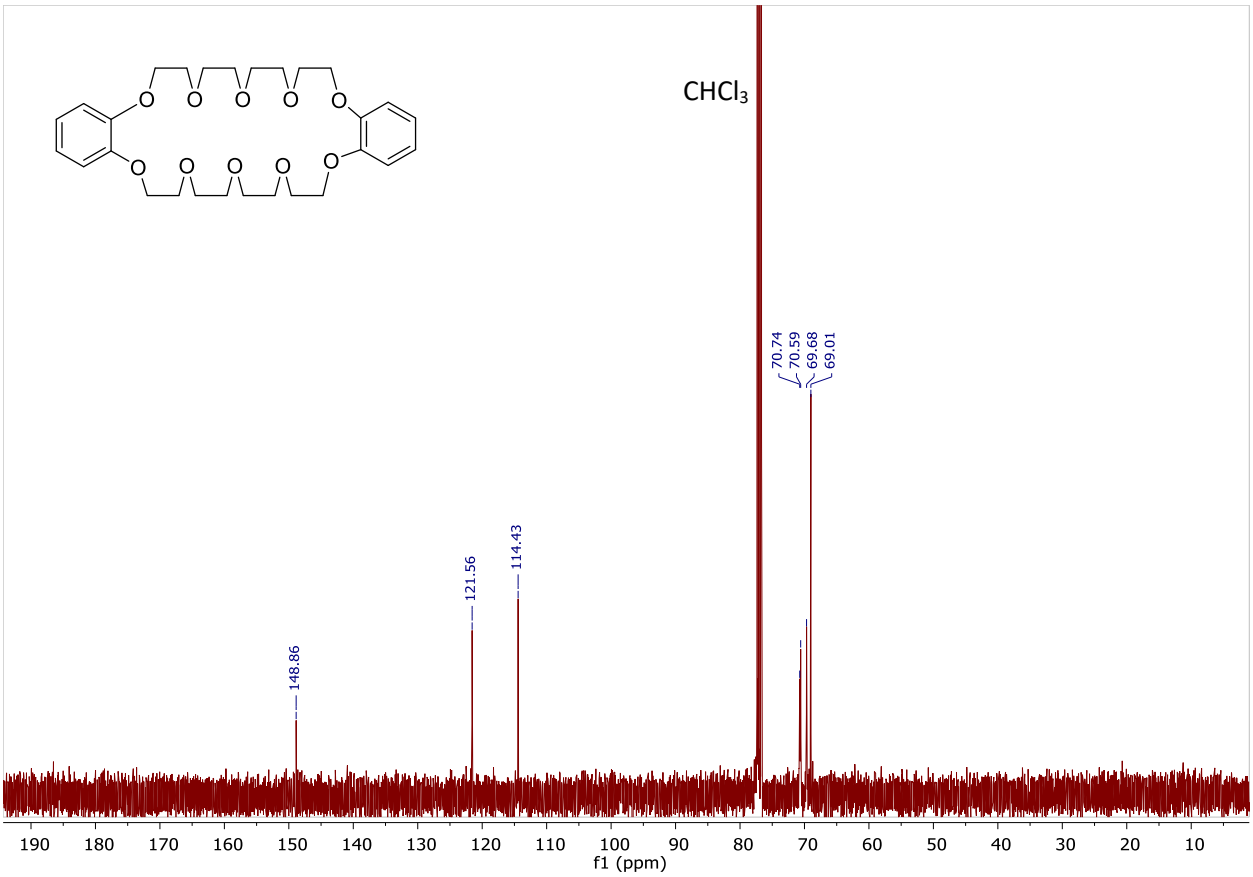

Figure 2.2. ^{13}C NMR spectrum of DB30C10 (**1c**) in $CDCl_3$ at 101 MHz.

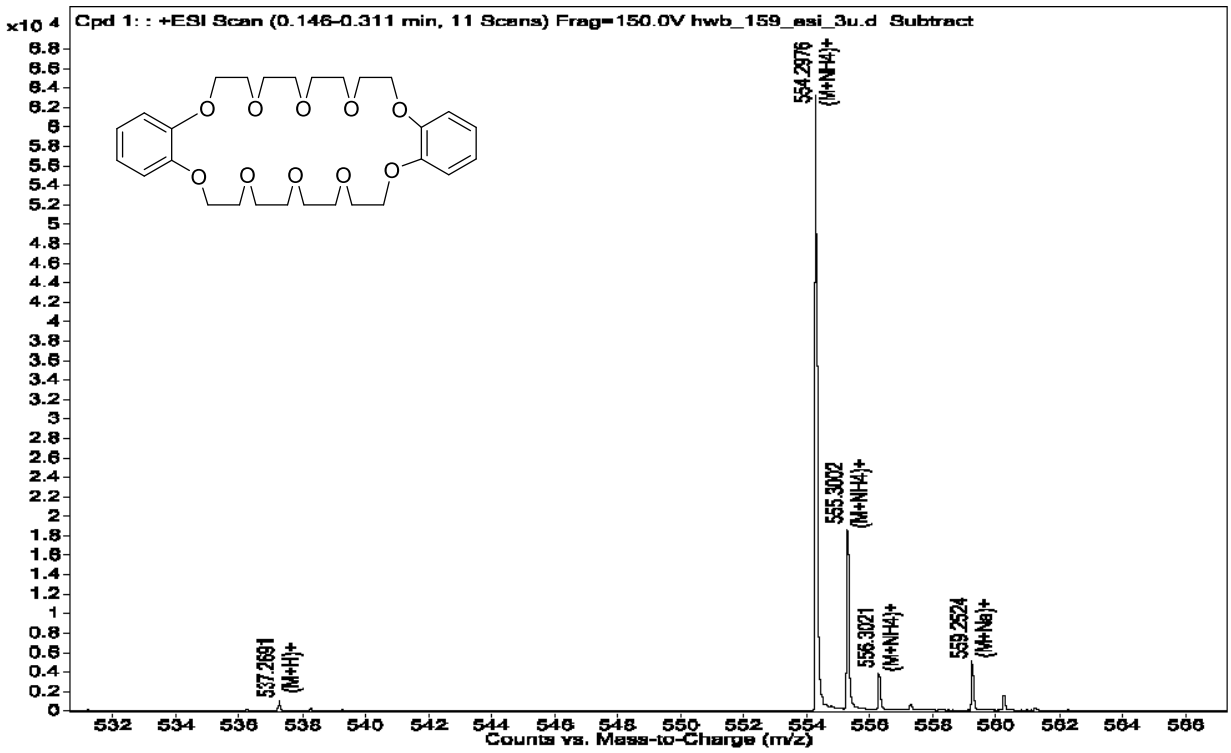

Figure 2.3. ESI-TOF HRMS of **DB30C10** (**1c**).

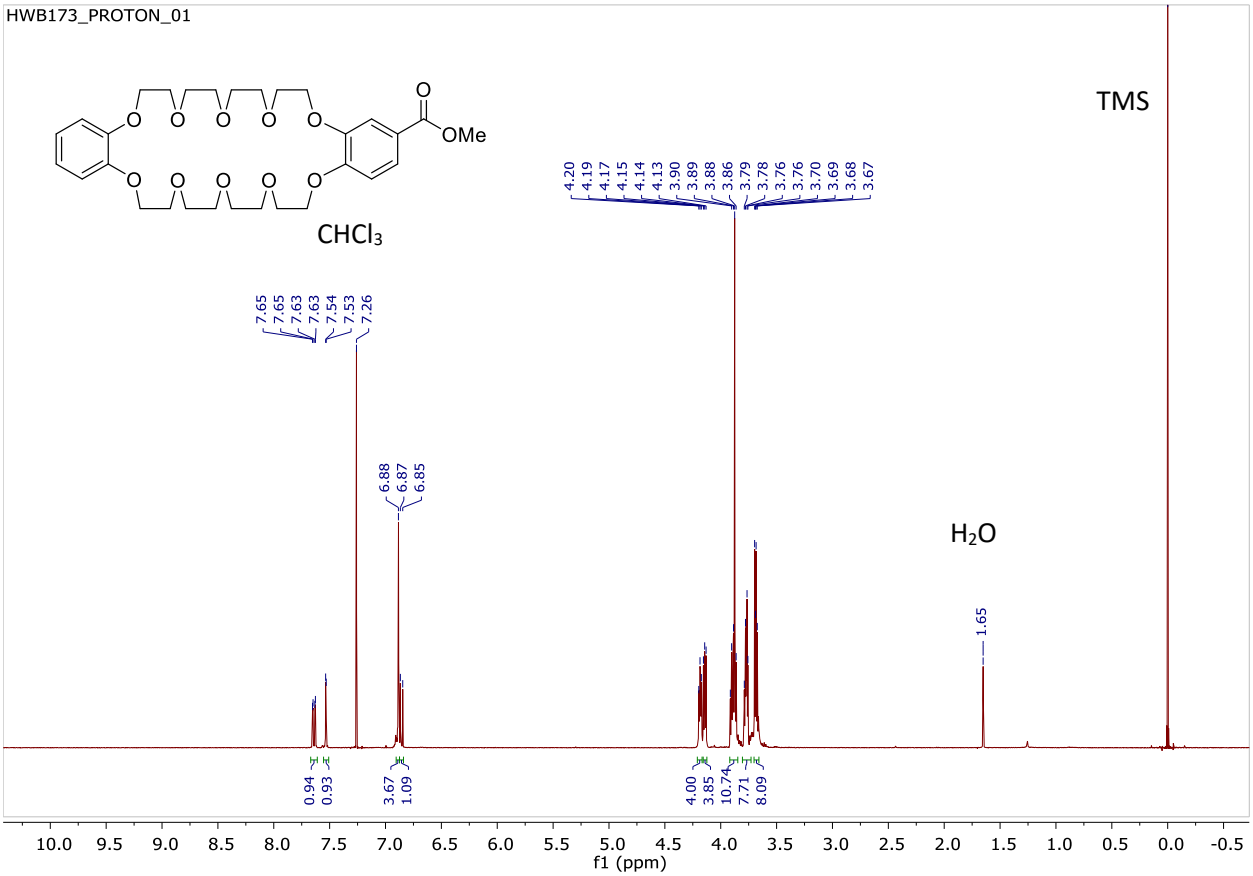

Figure 2.4. ^{1}H NMR spectrum of 4-carbomethoxydibenzo-30-crown-10 (**1d**) in $CDCl_3$ at 400 MHz.

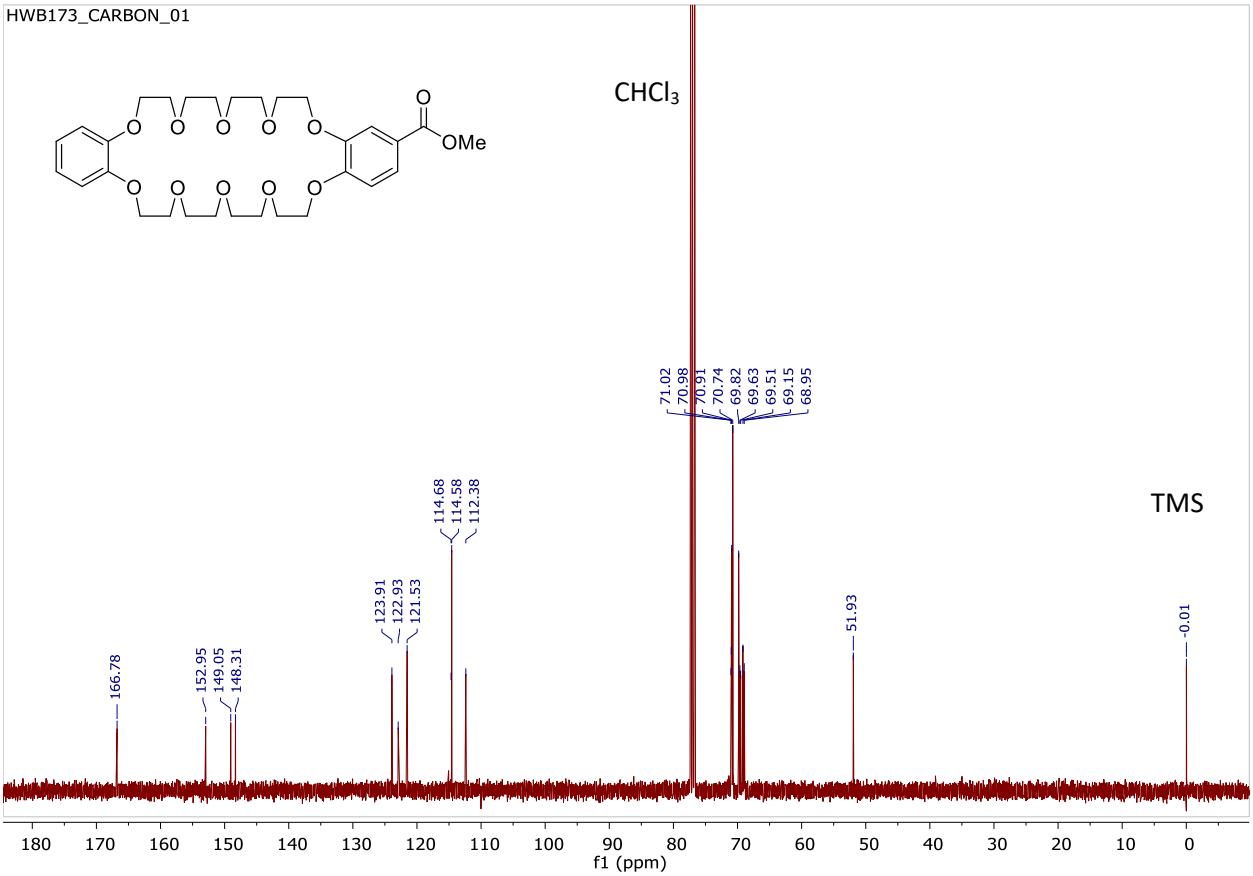

Figure 2.5. ^{13}C NMR spectrum of 4-carbomethoxydibenzo-30-crown-10 (**1d**) in $CDCl_3$ at 101 MHz.

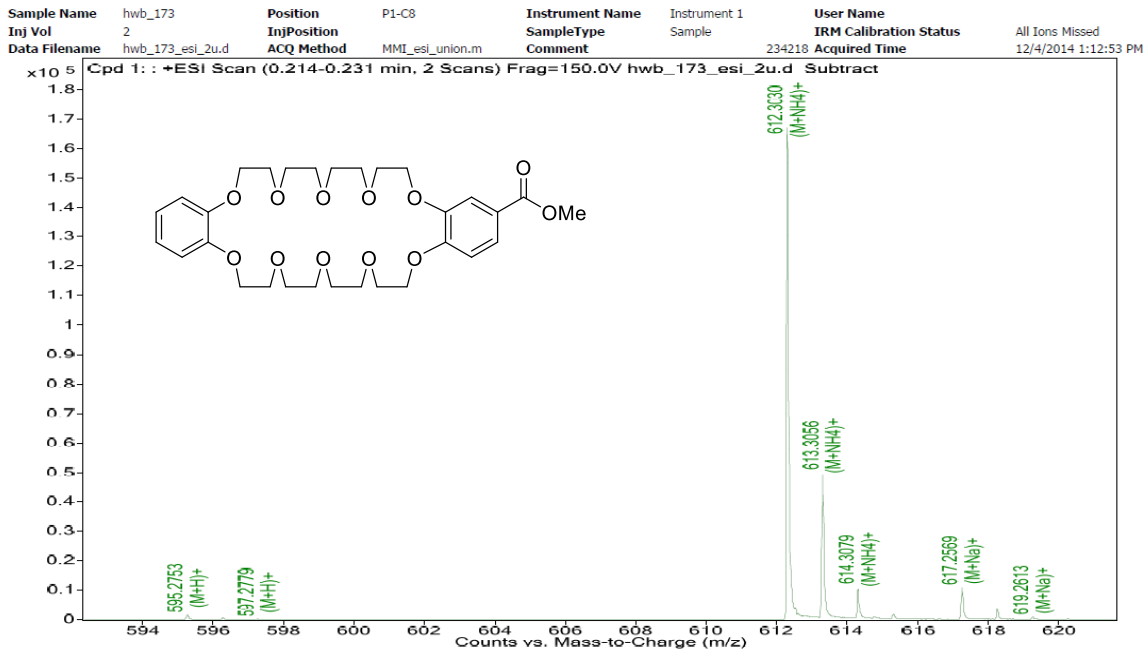

Figure 2.6. ESI-TOF HRMS of 4-carbomethoxydibenzo-30-crown-10 (**1d**).

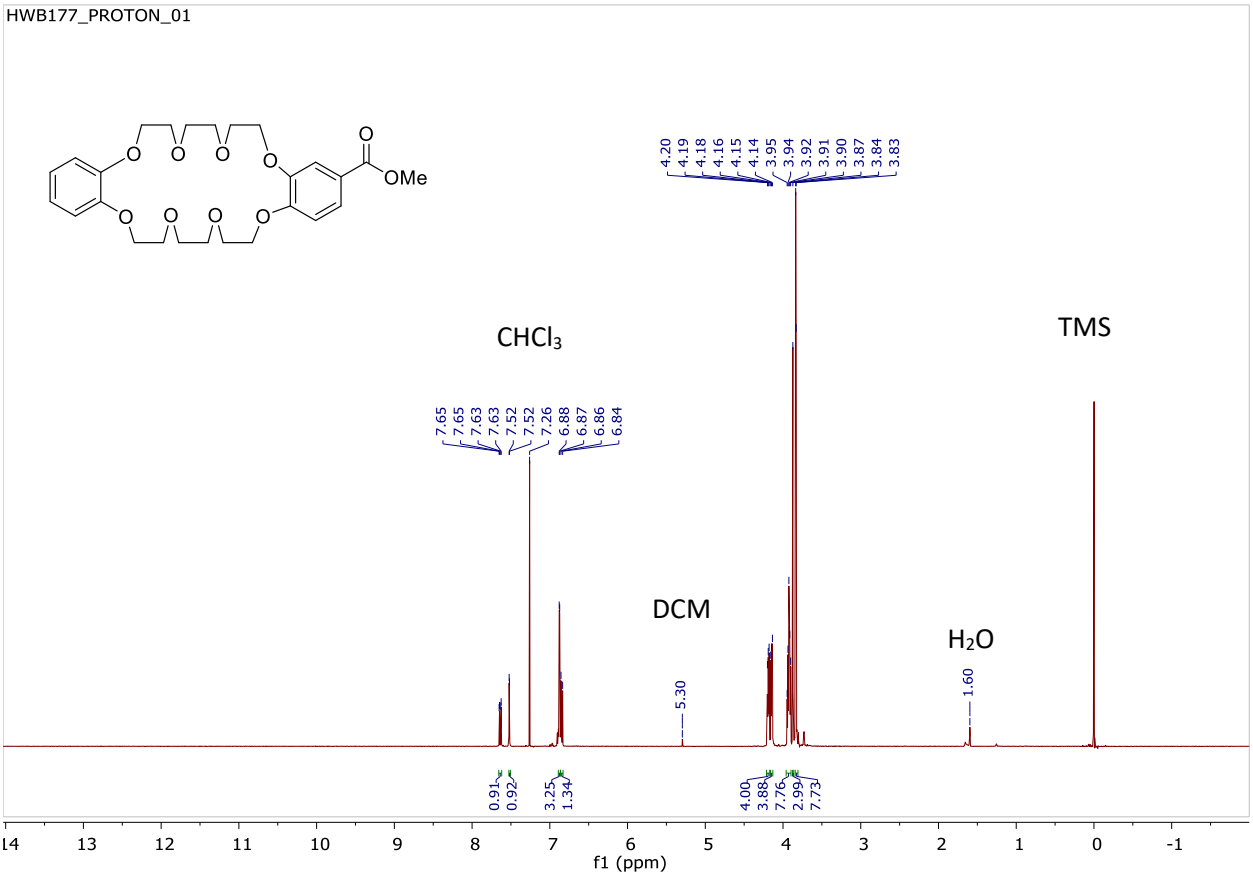

Figure 2.7. ^{1}H NMR spectrum of 4-carbomethoxydibenzo-24-crown-8 (**1b**) in $CDCl_3$ at 400 MHz.

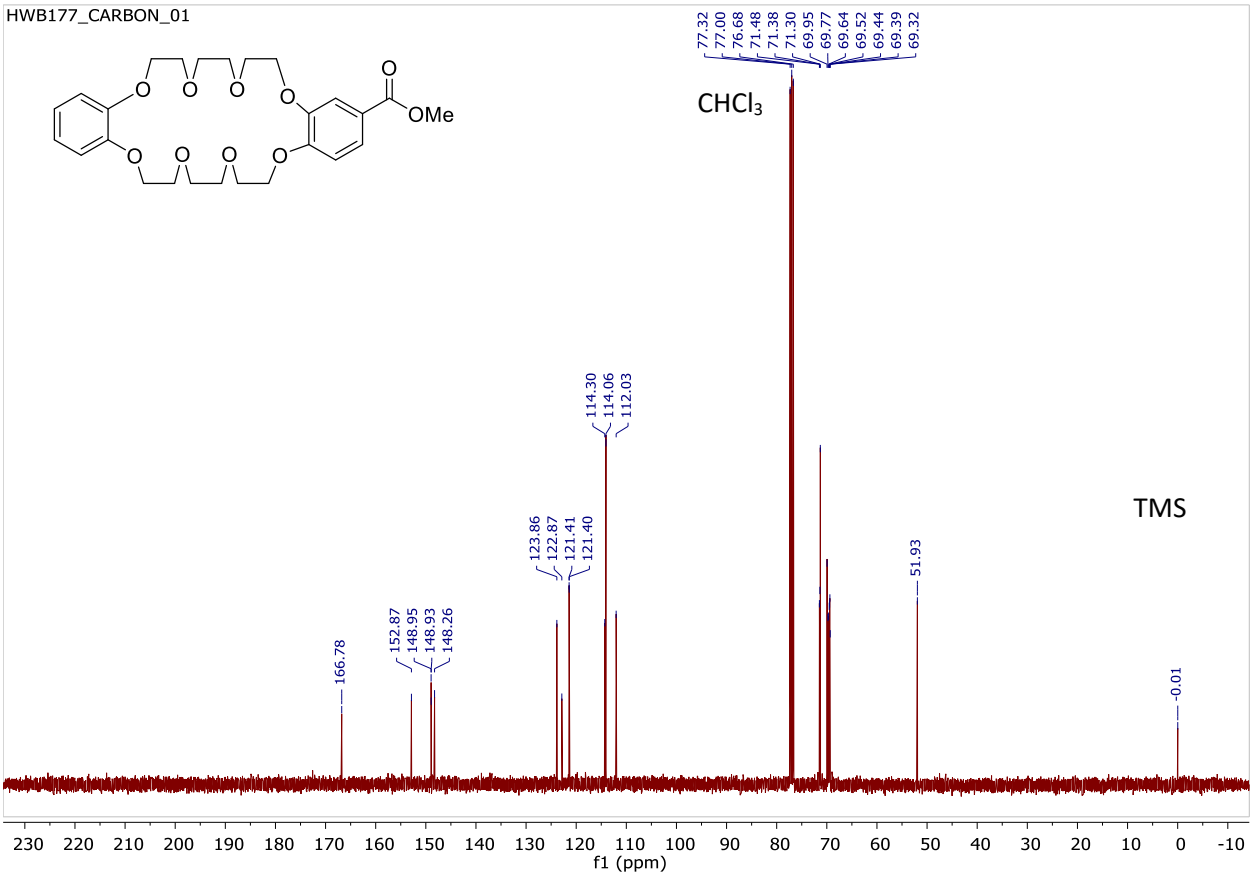

Figure 2.8. ^{13}C NMR spectrum of 4-carbomethoxydibenzo-24-crown-8 (**1b**) in $CDCl_3$ at 101 MHz.

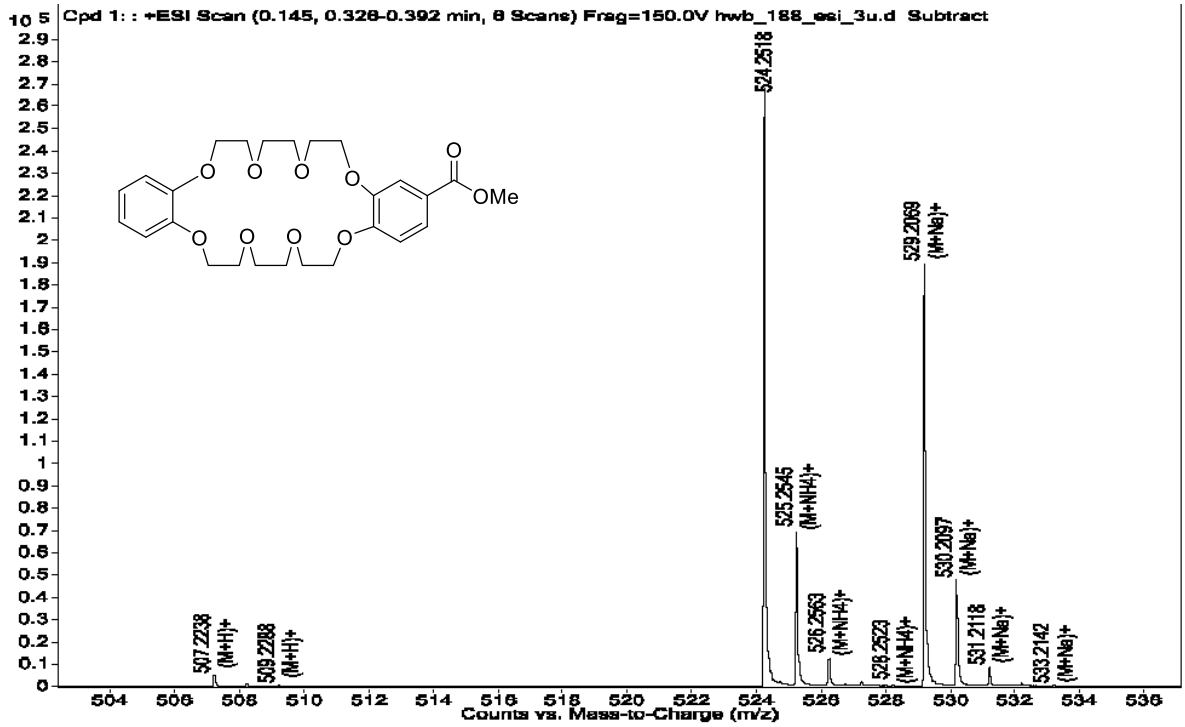

Figure 2.9. ESI-TOF HRMS of 4-carbomethoxydibenzo-24-crown-8 (**1b**).

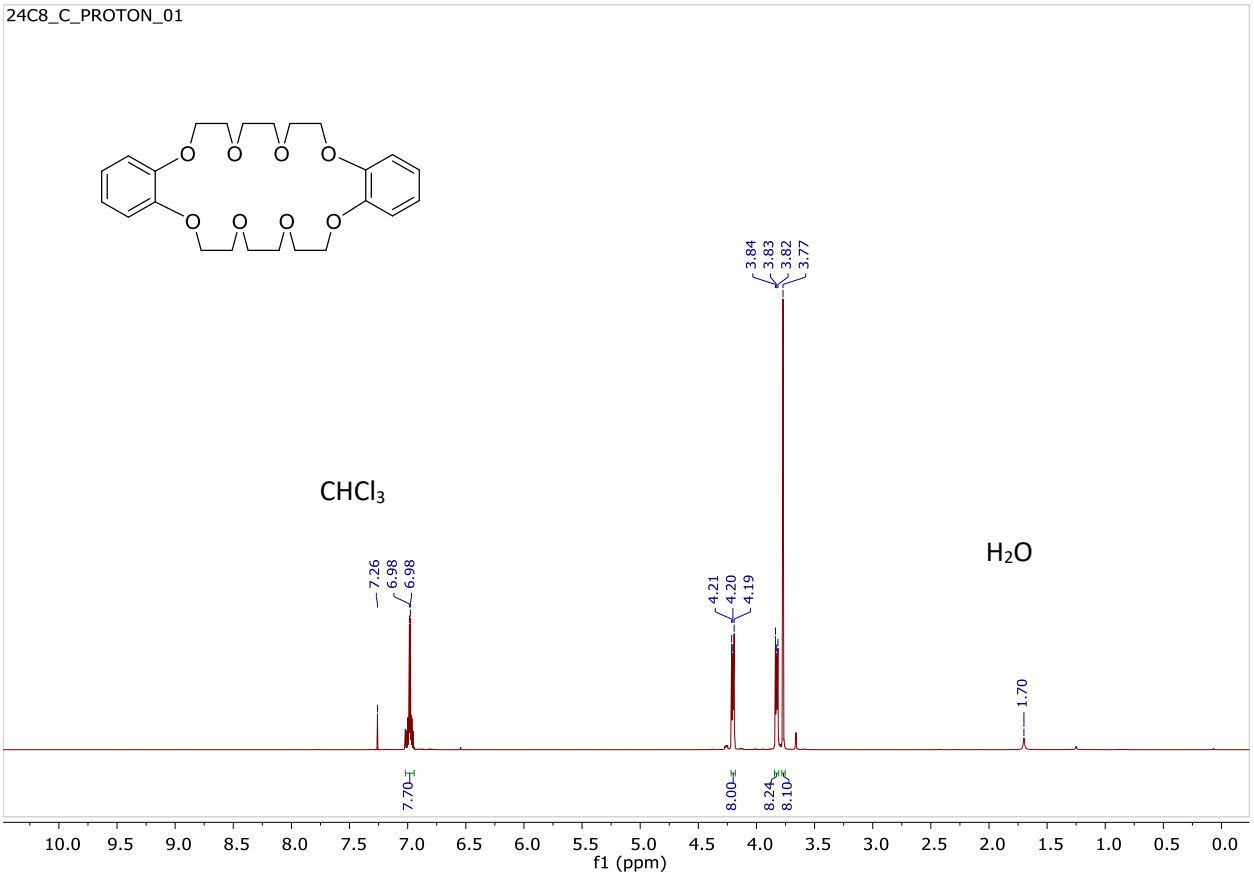

Figure 2.10. ^{1}H NMR spectrum of dibenzo-24-crown-8 (**1a**) in $CDCl_3$ at 400 MHz.

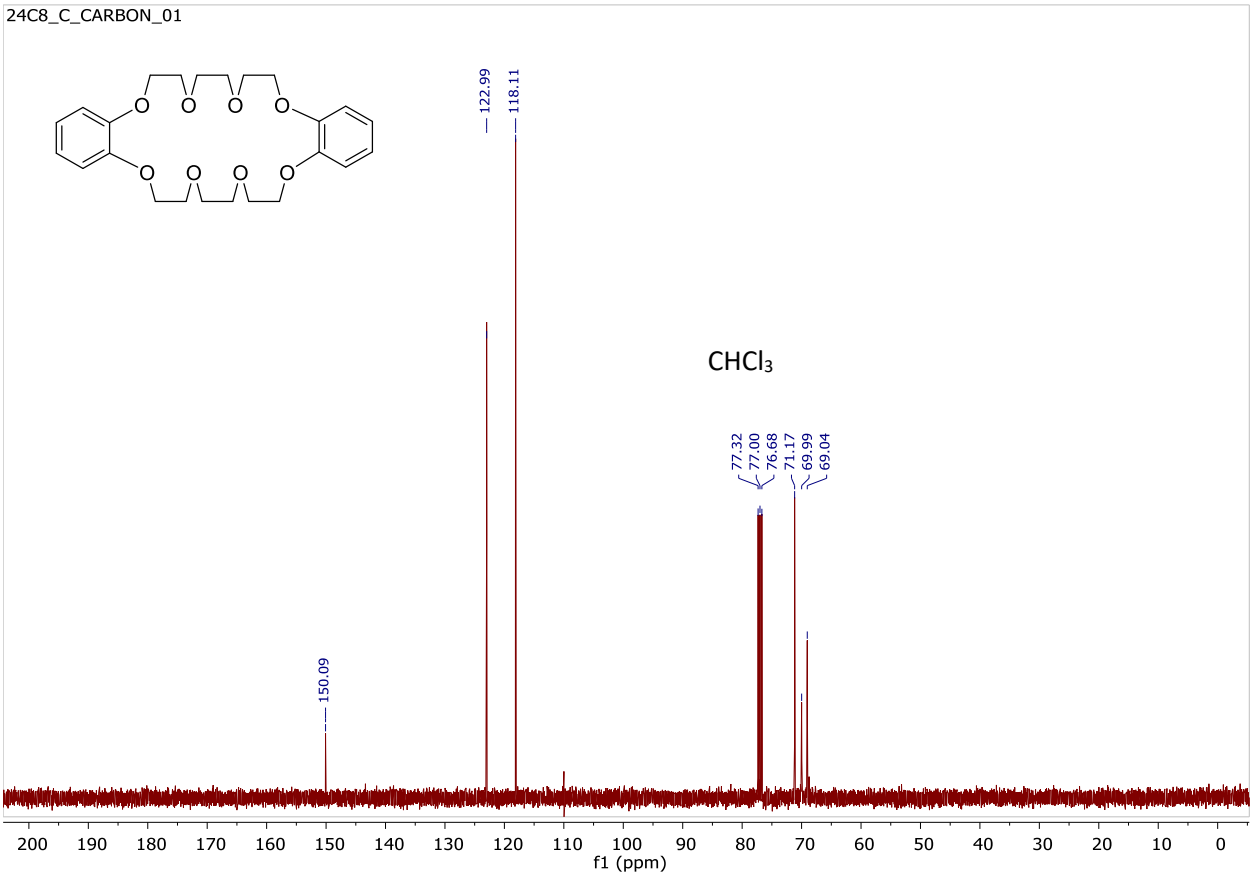

Figure 2.11. ^{13}C NMR spectrum of DB24C8 (**1a**) in $CDCl_3$ at 101 MHz.

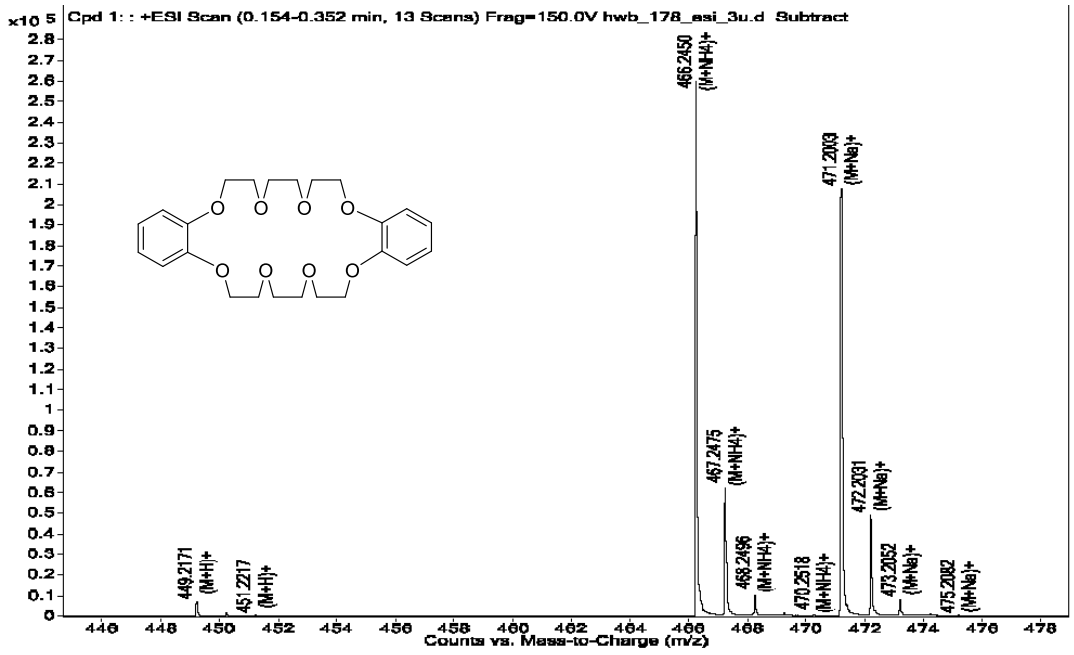

Figure 2.12. ESI-TOF HRMS of DB24C8 (**1a**).

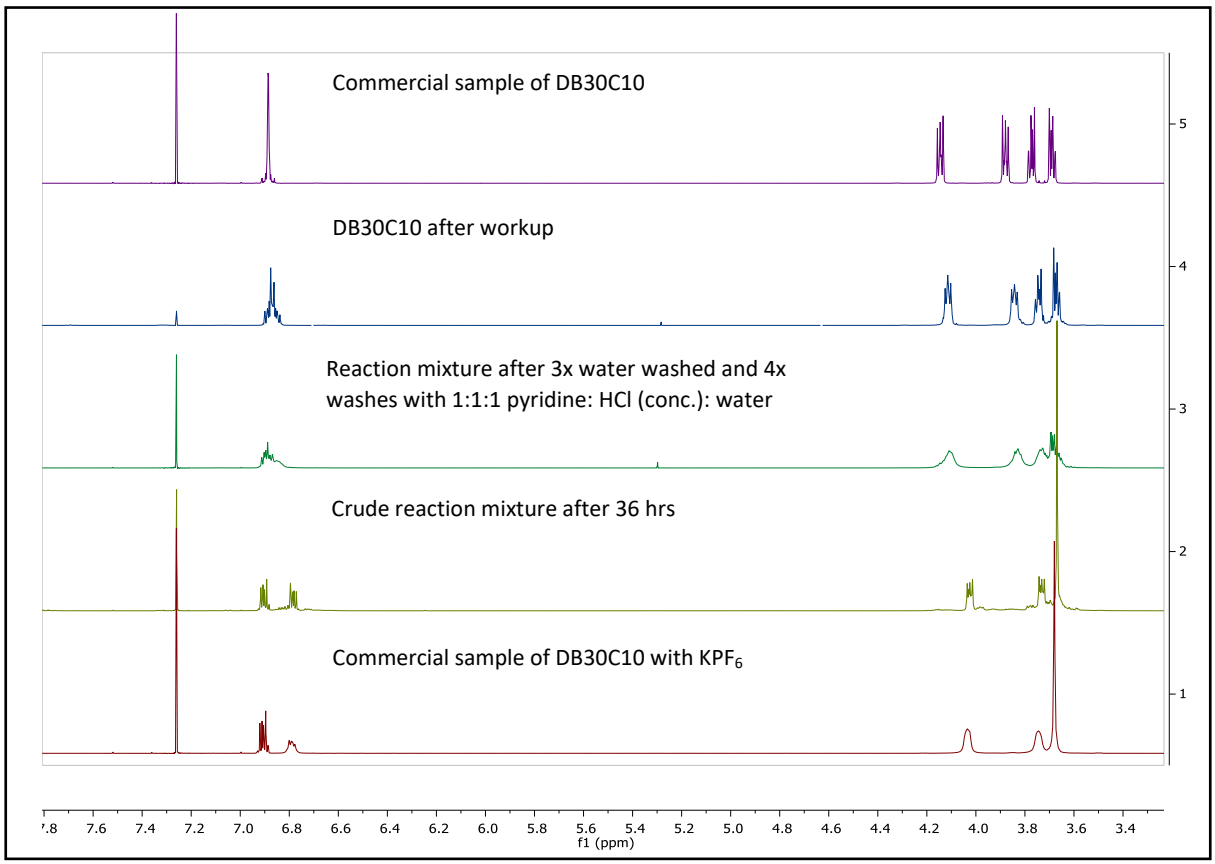

Figure 2.13. Partial ^{1}H NMR spectra at 400 MHz ($CDCl_3$) showing the removal of the K ions from DB30C10 during workup.

Chapter 3: Preparation of four new rotaxanes with DB30C10 as wheel components, demonstrating that the paraquats thread through the cavity of DB30C10

ABSTRACT

Three new [2]rotaxanes (**4**, **7** and **12**) and one new [3]rotaxane (**8**) based on dibenzo-30-crown-10/paraquat were synthesized. To the best of our knowledge, these are the first examples of rotaxanes using the dibenzo-30-crown-10/paraquat binding motif. The rotaxanes were all isolated, purified and characterized by ^{1}H NMR, ^{13}C NMR, and HRMS. An X-ray crystal structure of one of the rotaxanes (**7**) was obtained. This work demonstrates for the first time that dibenzo-30-crown-10 does form pseudorotaxane complexes with paraquats in solution.

Introduction

Crown ethers were the original macrocyclic hosts. Their discovery by C. J. Pedersen, the subsequent publication of the synthesis of 60 of these compounds [1] and the study of their properties, especially their complexation behavior with alkali metals led to his share in the 1987 Nobel Prize for Chemistry. Crown ethers played an important role in the study of alkali metal cations in biological membranes and supramolecular chemistry in general.[2]

Crown ethers are widely used as hosts in supramolecular chemistry. They are used as the wheel components in rotaxanes and other interlocked molecular structures with functionalities such as molecular shuttles,[3] molecular switches,[4-6] ionic sensors,[7] switchable catalysts,[8-10] molecular muscles,[11-12] simple mimics of ribosomes,[13-14] and others. A rotaxane which selectively complexes Ca^{2+} was reported to have potent anti-

cancer properties.[15] The selective shuttling, or switching, behavior of rotaxanes has led to investigation of their use in drug delivery.[16] These hosts have also been used to construct supramolecular polymers.[17-20] Supramolecular polymers can be formed by self-assembly, which makes more complex topologies and structures accessible,[21] and gives rise to interesting properties, self-healing[22-23] and optoelectronic properties,[24] for example. There have even been examples of polymers that completely change their topology (for example linear to cyclic,[25-26] and star to linear [27-28]), based on an external stimulus, a feat which would be impossible with conventional polymers.

In order for a host to be useful in the construction of supramolecular assemblies and polymers, it is imperative to determine the binding configuration with the intended guest molecule. The Gibson group has been especially interested in the construction of polymers that self-assemble through the formation of pseudorotaxane linkages.[18, 29-33] These types of materials would be switchable, or "smart", since the crown ether host/guest pairs respond to stimuli like heat, solvent polarity, addition and removal of K^+ ions, and pH.[34] Materials of this sort have been constructed using dibenzo-24-crown-8 (**DB24C8**),[29] bis(meta)phenylene-32-crown-10 (**BMP32C10**),[18, 30] and benzo crown ethers like benzo-21-crown-7 (**B21C7**).[35] Some dibenzo crown ether-based cryptands have been reported.[36] The cavity size of the crown ether limits the size of the guest molecule that can be accommodated (a guest molecular that is larger than the cavity of the crown ether simply will not fit). The association constant between the host and the guest also plays a crucial role in the degree of polymerization that can be reached by self-assembly. The association constant is therefore a crucial factor that contributes to the polymer properties. Our group has developed optimized syntheses for functionalized

(mono-[37] and di-fuctionalized[38]), and unfunctionalized[37] dibenzo-30-crown-10 (**DB30C10**). We can now make multiple grams of **DB30C10** in three steps from inexpensive and readily available starting materials. This is very helpful when multi-gram quantities of the materials are required, e. g., when you want to incorporate it into the backbone of the polymer. However, in order to use this crown ether for the synthesis of brush polymers, star-polymers,[39] graft-polymers[40] and for supramolecular chain extension, we need to know a bit more about the binding conformation of **DB30C10** with paraquat.

We discovered some time ago that bis(*m*-phenylene)-32-crown-10 (**BMP32C10**) has two possible binding conformations with paraquat and diquat hosts. The guest molecule can either thread through the cavity of the host, or the host can fold around the guest molecule, forming a so-called "taco-complex"[41] (Figure 3.1). In the case of bis(*p*-phenylene)-34-crown-10 (**BPP34C10**), only pseudorotaxanes have been found, due to the geometry of the crown ether. Examples of **BMP32C10** in both conformations are known.[42-43]

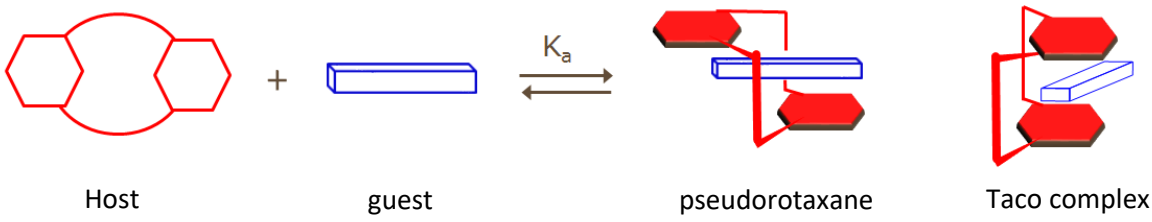

Figure 3.1. Cartoon representation of binding conformations of bis(m-phenylene) and dibenzo crown ethers with paraquat.

To our knowledge, direct evidence that **DB30C10** adopts the pseudorotaxane conformation has not been found. All X-ray crystal structures of the complexes between **DB30C10** and paraquats (*N,N'*-dialkyl-4,4'-bipyridinium salts) are in the taco

conformation. It is still possible that the pseudorotaxane conformation exists in solution, but this is difficult to observe directly. One way to obtain conclusive proof of the threaded structure is by synthesizing rotaxanes. The guest is trapped in the cavity by the presence of bulky stoppers and existence of rotaxanes means that the guest must have threaded through the cavity in solution.

We therefore set out to synthesize rotaxanes based on the paraquat/**DB30C10** biding motif. We successfully isolated and characterized three new [2]rotaxanes and one new [3]rotaxane, demonstrating conclusively that **DB30C10** does form pseudorotaxanes.

Results and discussion

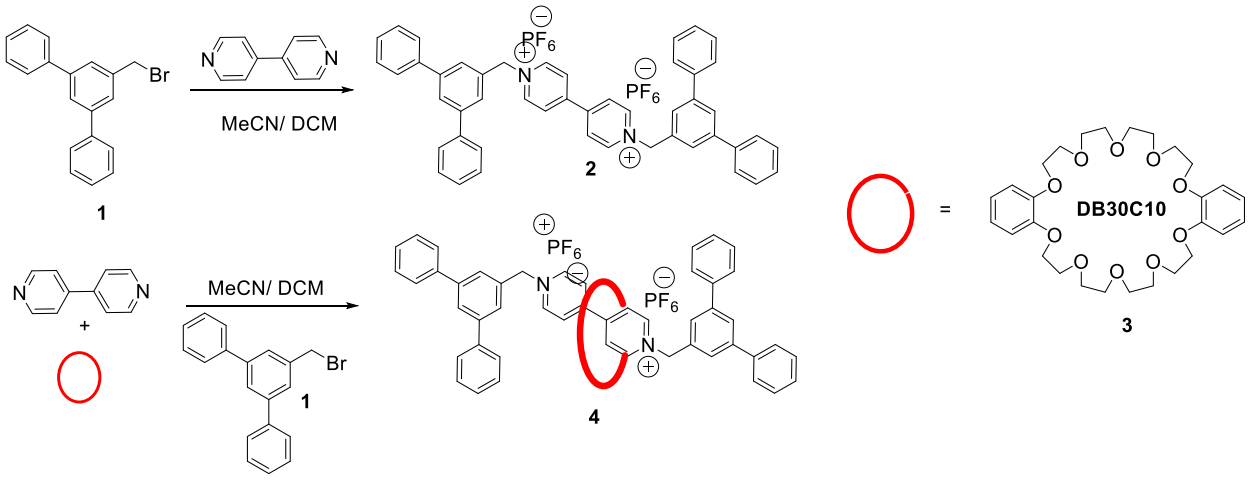

Scheme 3.1. Syntheses of new dumbbell **2** and rotaxane **4**.

Rotaxane **4** was synthesized by adding a solution of **DB30C10** to a solution of 4,4'-bipyridine in a minimum amount of MeCN followed by 3,5-diphenylbenzyl bromide (**1**). After four weeks of stirring at room temperature and an extensive workup and purification procedure, rotaxane **4** was isolated in 2.7% yield (Scheme 3.1). The low yield was anticipated due to the fact that **DB30C10** would have to complex with the half-quat (mono-

ammonium salt) before the second blocking group was added. The complexation between the half-quat and paraquat is very weak, which means that the **DB30C10** does not have a significant preference to associate with it.

Other systems were designed. In one, half-quat **3** was already formed. This provides more of a driving force for the complexation. Once the crown ether is complexed with half-quat **3**, the addition of a single blocking group yields the rotaxane. This two-step process increased the yield of rotaxane **4** to 13% (Scheme 3.2).

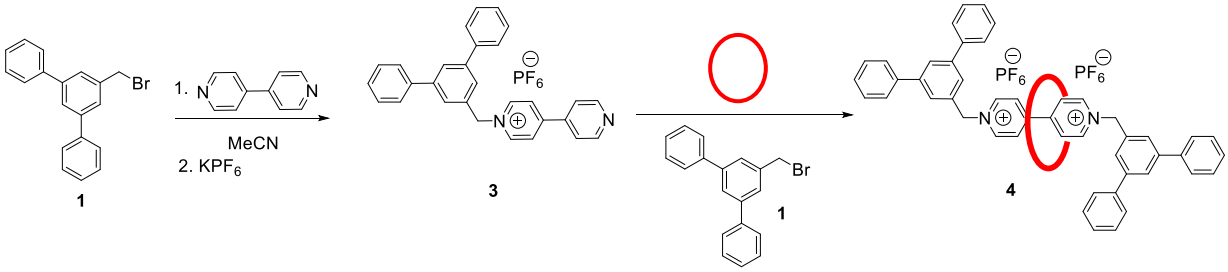

Scheme 3.2. Two-step synthesis of rotaxane **4**

Diazido paraquat **10** and three equivalents of **DB30C10** were combined in dry MeCN, under Ar(g). To the bright red solution was added a solution of 4-trityl-(3'-propynyloxy)benzene (**9**) in DCM (Scheme 3.3). Catalyst $Cu(CH_3CN)_4PF_6$ was added and DCM and MeCN were added dropwise until all solids were dissolved. $Cu(CH_3CN)_4PF_6$ and DCM/MeCN were chosen as the solvent system for the "click reaction", instead of $CuSO_4$ in water or MeOH, as the crown ether and blocking group are not soluble in water or MeOH. Even though the crown ether and blocking group are perfectly soluble in MeCN, we opted for the MeCN/DCM mixture to decrease solvent polarity as much as possible, because very polar solvents and solvents that form hydrogen bonds interfere with the

complexation. After several washing steps and chromatography the rotaxane **12** was isolated as a bright red solid in 6% yield.

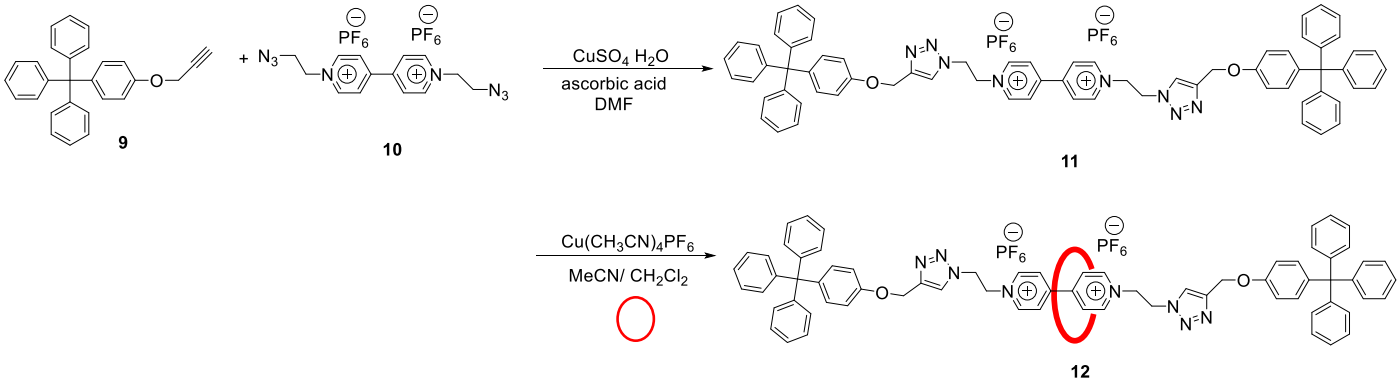

Scheme 3.3. Syntheses of dumbbell **11** and rotaxane **12**.

Rotaxanes **7** and **8** were synthesized by combining 4.6 equivalents of **DB30C10** and bis(half-quat) **5** in DCM/MeCN (Scheme 3.4). The blocking group, 3,5-diphenylbenzyl bromide (**1**), was added and the solution was allowed to stir at room temperature for four weeks. After washing, treatment with an ion exchange resin and chromatography, two orange bands were isolated. The first one contained the [3]rotaxane **8** in 4% yield and the second the [2]rotaxane **7** in 28% yield.

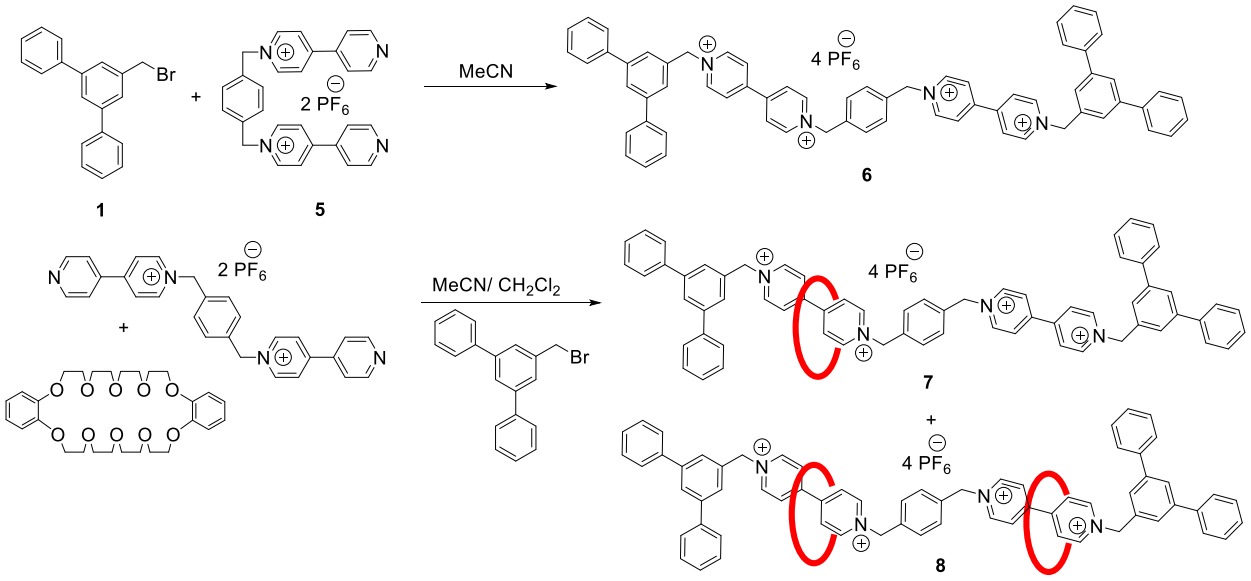

Scheme 3.4 Syntheses of dumbbell **6** and rotaxanes **7** and **8**

All rotaxanes were characterized by HRMS. For rotaxane **4** a peak at *m/z* 1323.5295 corresponds to M^+ and the peak at *m/z* 589.2831 $(M\text{-}2PF_6)^{2+}$. Rotaxane **7** displayed *m/z* 864.8138 corresponding to the loss of two PF_6^- counter ions $(M\text{-}2PF_6)^{2+}$ and *m/z* 528.2216 corresponding to the loss of three PF_6^- counter ions $(M\text{-}3PF_6)^{3+}$. Rotaxane **8** yielded *m/z* 1132.9465 corresponding to the loss of two PF_6^- counter ions $(M\text{-}2PF_6)^{2+}$, and *m/z* 706.9765 corresponding to the loss of three counter ions $(M\text{-}3PF_6)^{3+}$**.** Rotaxane **12** displayed *m/z* 1894.6626, 1725.8084, and 790.8737 corresponding to the molecular ion plus sodium $(M + Na)^+$, the loss of a PF_6^- counter ion $(M - PF_6)^+$, and the loss of two PF_6^- counter ions $(M\text{-}2PF_6)^{2+}$, respectively.

Aromatic crown ethers typically associate with paraquats through hydrogen-bonding, π-π stacking and charge transfer interactions.[5, 44] The charge transfer can be observed visually when aromatic crown ethers and paraquats are combined in solution. For example, during the synthesis of rotaxane **2**, the solution changed from clear to bright

yellow after a few minutes (presumably corresponding to the formation of the half-quat) and the solution gradually became dark orange. The solution of half-quat **5** and **DB30C10** (which is a colourless solid) was light yellow and became dark orange over time. The paraquat diazide **10** has a beige colour and the crown ether is colourless; the solution of the two went bright red as soon as the light yellow and clear solutions were combined. All the rotaxanes are bright orange or bright red (Figure 3.2). Equimolar solutions of the dumbbells (just the end-functionalized paraquats with no crown ether) and **DB30C10** in DMSO or MeCN were only slightly yellow.

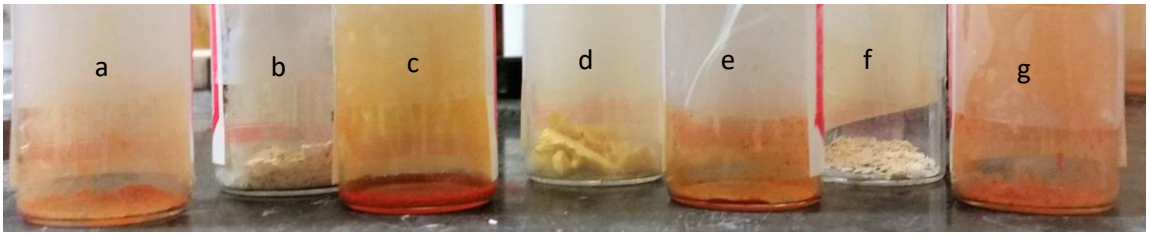

Figure 3.2. Photographs of rotaxanes and dumbbells a) rotaxane **8** b) dumbbell **6** c) rotaxane **8** d) dumbbell **2** e) rotaxane **4** f) dumbbell **11** g) rotaxane **12**

The complexations led to peak shifts in the ^{1}H NMR spectra. Because hydrogen bonding and dipole-dipole interactions contribute to the complexation, the solvent influences the extent of complexation between the host and the guest. In order to illustrate the effect of the solvent, we will examine the spectra of rotaxane **12** in DMSO-d_6 and MeCN-d_3. ^{1}H NMR spectra of dumbbell **11**, **DB30C10**, a 1:1 mixture of dumbbell **11** and **DB30C10**, and rotaxane **12** in DMSO-d_6 (Figure 3.3) are compared to those same spectra in MeCN-d_3 (Figure 3.4). DMSO is a highly polar solvent and competes with the complexation so much that it essentially eliminates complexation between the paraquat and the crown ether. Consequently, the 1:1 mixture of dumbbell **11** and **DB30C10** (Figure 3.3 c) shows no

peak shifts. The spectrum is an almost perfect superposition of the spectra of dumbbell **11** (Figure 3.3 a) and **DB30C10** (Figure 3.48, Table 3.1), indicating that there is no complexation between the crown ether and the dumbbell in solution. However, there are clear peaks shifts in the ^{1}H NMR spectrum of rotaxane **12.** The paraquat protons **j** and ethyleneoxy **k** are shifted upfield from 9.25 and 8.73 ppm to 9.05 and 8.34 ppm. The triazole peak (**g**) shifts downfield from 8.26 to 8.32 ppm. The aromatic peaks of the crown ether shift upfield from 6.95 and 6.87 to 6.56 and 6.40 ppm. The ethyleneoxy peaks shift upfield from 4.06, 3.73, 3.63 and 3.55 to 3.83, 3.61, 3.52 and 3.46 ppm.

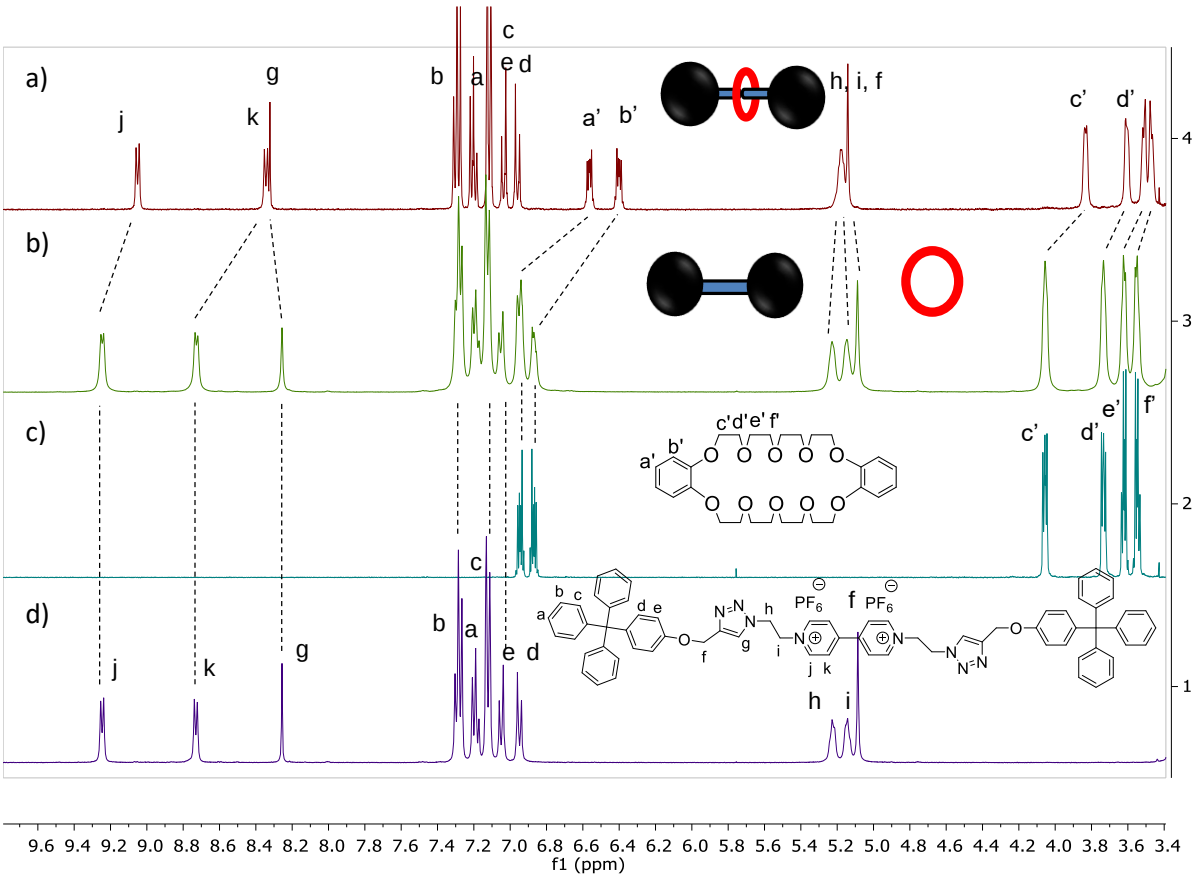

Figure 3.3. Stacked ^{1}H NMR spectra of a) rotaxane **12** b) 1:1 mixture of dumbbell **11** and **DB30C10** c) **DB30C10** and d) dumbbell **11** in DMSO-d_6 at 400 MHz

Table 3.1 Checmical shifts (ppm) of [2]rotaxane 12 and its components in DMSO-d_6				
Proton	**Dumbbell 11**	**DB30C10**	**11 + DB30C10**	**Rotaxane 12**
PQα (**j**)	9.25	---	9.25	9.05
Δ PQα	---	---	**+0.00**	**-0.20**
PQβ (**k**)	8.73	---	8.73	8.34
Δ PQβ	---	---	**-0.00**	**-0.39**
Crown a’	---	6.95	6.90	6.56
Δ a’	---	---	**-0.05**	**-0.39**
Crown b’	---	6.87	---	6.40
Δ b’	---	---	**---**	**-0.47**
OCH_2-1 (**c’**)	---	4.06	4.06	---
Δ OCH_2-1	---	---	**-0.00**	**---**
OCH_2-2 (**d’**)	---	3.73	3.73	3.83
Δ OCH_2-2	---	---	**-0.00**	**+0.10**
OCH_2-3 (**e’**)	---	3.62	3.63	3.61
Δ OCH_2-3	---	---	**+0.01**	**-0.01**
OCH_2-4 (**f’**)	---	3.55	3.55	3.49
Δ OCH_2-4	---	---	**+0.00**	**-0.06**

Figure 3.4 depicts the chemical shift changes in the proton NMR spectra of dumbbell **11** (Figure 3.4 d), **DB30C10** (Figure 3.4 c) a 1:1 solution of dumbbell **11** and **DB30C10** (Figure 3.4 b) and rotaxane **12** (Figure 3.4 a) in MeCN-d_3. MeCN is a less competitive solvent, and consequently we see a little bit of complexation between the dumbbell and **DB30C10** in the 1:1 solution; this is presumably the taco complex. The peaks shifts are much more pronounced in the rotaxane spectrum (Figure 3.4 a, table 3.2) as expected for the mechanically bonded structure.

Table 3.2 Chemical shifts (ppm) of [2]rotaxane 12 and its components in MeCN-d_3				
Proton	**Dumbbell 11**	**DB30C10**	**11 + DB30C10**	**Rotaxane 12**
PQα (**j**)	8.63	---	8.65	8.77
Δ PQα	---	---	**+0.02**	**+0.14**
PQβ (**k**)	8.12	---	8.11	7.87
Δ PQβ	---	---	**-0.01**	**-0.25**
Crown a'	---	6.91	6.86	6.54
Δ a'	---	---	**-0.05**	**-0.37**
Crown b'	---	6.91	---	6.45
Δ b'	---	---	**---**	**-0.46**
OCH_2-1 (**c'**)	---	4.09	4.01	---
Δ OCH_2-1	---	---	**-0.08**	**---**
OCH_2-2 (**d'**)	---	3.76	3.74	3.80
Δ OCH_2-2	---	---	**-0.02**	**-0.04**
OCH_2-3 (**e'**)	---	3.65	3.65	3.64
Δ OCH_2-3	---	---	**-0.00**	**-0.01**
OCH_2-4 (**f'**)	---	3.59	3.63	3.58
Δ OCH_2-4	---	---	**+0.04**	**-0.01**

Paraquat peak **j** moved 0.02 ppm downfield from 8.63 to 8.65 ppm. The proton on the triazole ring (**g**) moved downfield from 7.86 ppm in the dumbbell spectrum (Figure 3.4 d) to 7.89 ppm in the 1:1 solution (Figure 3.4 b). The aromatic peaks in the crown ether (**a'**, **b'**) moved upfield from 6.91 ppm in the **DB30C10** spectrum (Figure 3.4 c) to 6.86 ppm in the 1:1 solution (Figure 3.4 b). The ethyleneoxy peaks shifted from 4.09, 3.77, 3.65 and 3.60 ppm in the **DB30C10** spectrum to 4.01, 3.74, 3.65 and 3.63 ppm in the 1:1 solution. Further chemical shift changes are observed between the 1:1 solution and the rotaxane **12**. The paraquat peaks shift from 8.65 (**j**) and 8.11 ppm (**k**) to 8.77 and 7.87 ppm. Note that one of the paraquat peaks (**j**) moved downfield while the other one (**k**) moved upfield. The peak associated with the triazole ring (**g**) also moved downfield from 7.87 to 8.04 ppm. The changes between the rotaxane spectrum in DMSO and MeCN suggest that the crown ether occupies a slightly different position in each solvent. In DMSO the crown

ether seems to be associated with the paraquat. In MeCN one of the paraquat peaks move upfield, the other one moves downfield and the triazole peak moves downfield. This suggests that the crown ether is to one side of the paraquat unit, between the paraquat and the triazole. The aromatic peaks in the crown ether moved form 6.92 ppm in the **DB30C10** spectrum to 6.54 and 6.45 ppm. The linker protons **f** (between the ether oxygen and the triazole group) **h**, and **i** (between the triazole and the quaternary nitrogen of the paraquat unit) shifted downfield slightly from 5.13, 5.10 and 5.02 in the 1:1 solution to 5.16 and 5.11 in the rotaxane **12**. The ethyleneoxy peaks shifted from 4.01, 3.74, 3.65 and 3.63 ppm in the 1:1 solution to 3.80, 3.64 and 3.58 ppm in the rotaxane.

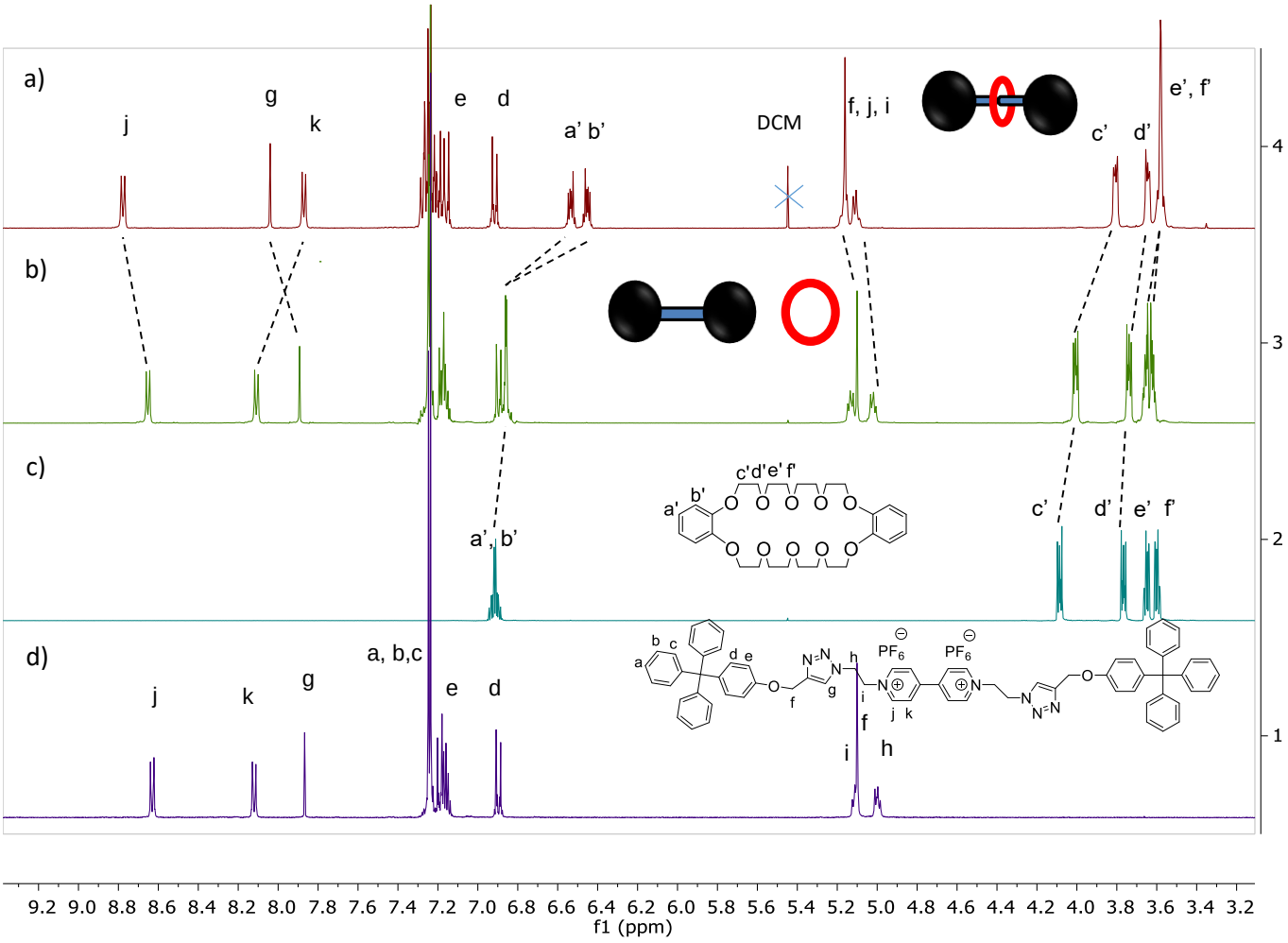

Figure 3.4. Partial ^{1}H NMR spectra of a) rotaxane **12** b) 1:1 solution of **DB30C10** and dumbbell **11** c) **DB30C10** and d) dumbbell **11** in MeCN-d_3 at 400 MHz

Figure 3.5 illustrates the peak shifts that were observed for rotaxane **7**. The peak shifts are summarized in Table 3.3. In MeCN-d_3, there are slight peak shifts (indicating some complexation, presumably taco formation) in a 1:1 solution of dumbbell to crown ether (Figure 3.5 b). Paraquat peaks **g, h,** and **i** shift upfield from 9.07 to 9.06 ppm, and 8.36 to 8.31 respectively, while **j** shifts downfield slightly from 8.92 to 8.94 ppm. The aromatic proton signal on the crown ether, **a'** and **b'**, at 6.91 ppm shifts upfield and splits into two multiplets at 6.78 and 6.64 ppm. The ethyleneoxy peaks on the crown ether shift upfield slightly and two of the peaks combine into one. However, there is a significant upfield shift

in all of the aforementioned peaks between the 1:1 solution of dumbbell and crown ether (Figure 3.5 b) versus the rotaxane (Figure 3.5 a). The rotaxane solution is also bright red as opposed to light yellow. In the spectrum of rotaxane **7**, paraquat peaks **h** and **i** move upfield another 0.18 ppm from 8.31 to 8.13 ppm. The aromatic proton peaks on the crown ether move upfield from 6.78 (**a'**) and 6.64 ppm (**b'**) to 6.45 to 6.24 ppm and the ethyleneoxy peaks move from 3.79 (**c'**) and 3.63 (**d'**-**f'**) to 3.76 (**c'**), 3.49 (**d'**), 3.40 (**e'**) and 3.33 (**f'**) ppm, an average shift of 0.27 ppm from the crown ether to the rotaxane.

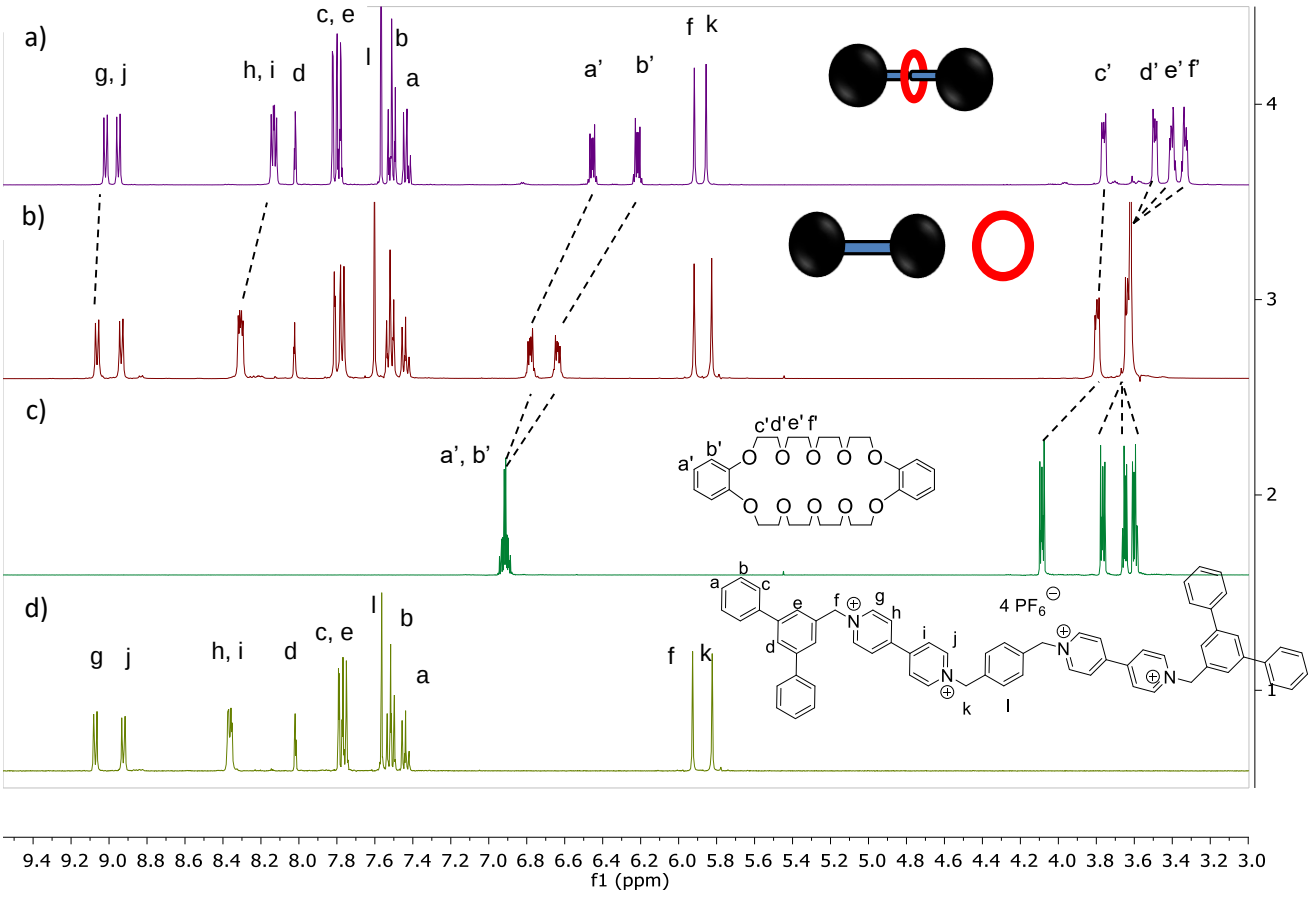

Figure 3.5. Partial ^{1}H NMR spectrum of a) dumbbell **6** b) **DB30C10**, c) a 1:1 solution of dumbbell **6** and **DB30C10** and d) rotaxane **7** in MeCN-d_3 at 400 MHz.

Table 3.3 Chemical shifts (ppm) of [2]rotaxane 7 and [3]totaxane 8 and their components in MeCN-d_3					
Proton	**Dumbbell 6**	**DB30C10**	**6 + DB30C10**	**Rotaxane 7**	**Rotaxane 8**
PQα (**g**)	9.07	---	9.06	9.02	9.02
Δ PQα	---	---	**-0.01**	**-0.05**	**-0.05**
PQβ	8.92	---	8.94	8.95	8.86
Δ PQβ	---	---	**+0.02**	**+0.03**	**-0.06**
PQα', PQβ'	8.36		8.31	8.13	7.95
Δ PQα', β'			**-0.05**	**-0.23**	**-0.41**
Crown a'	---	6.91	6.78	6.45	6.49
Δ a'	---	---	**-0.13**	**-0.46**	**-0.42**
Crown b'	---	6.91	6.64	6.22	6.33
Δ b'	---	---	**-0.27**	**-0.69**	**-0.58**
OCH_2-1	---	4.09	---	3.76	3.75
Δ OCH_2-1	---	---	---	**-0.33**	**-0.34**
OCH_2-2	---	3.76	3.79	3.49	3.48
Δ OCH_2-2	---	---	**+0.03**	**-0.27**	**-0.28**
OCH_2-3	---	3.65	3.63	3.40	3.40
Δ OCH_2-3	---	---	**-0.02**	**-0.25**	**-0.25**
OCH_2-4	---	3.59	---	3.33	3.36
Δ OCH_2-4	---	---	---	**-0.27**	**-0.17**

The [3]rotaxane **8** also showed changes in the chemical shifts in the ^{1}H NMR spectrum that were distinct from the 1:1 dumbbell:crown ether mixture as well as distinct from the [2]rotaxane **7** (Figure 3.5, Table 3.3). Notably the inner (β-) paraquat protons **h** and **i** shifted from 8.31 ppm in the dumbbell mixture (Figure 3.6 b) to 7.95 ppm in the [3]rotaxane (Figure 3.6 a), which is well upfield from where they are found in the [2]rotaxane **7** (Figure 3.5 a) as well (8.13 ppm). From this large upfield shift and the fact that there are four paraquat signals in both rotaxanes (9.02, 8.95, a signal that looks like overlapping doublets at 8.13 for rotaxane **7**, and 9.02, 8.86 and a signal that looks like overlapping doublets or a doublet of doublets at 7.95 ppm for rotaxane **8**), we can make some inferences about the position of the crown ether(s). If the crown ether is stationary on one of the paraquat sites as drawn in the scheme 3.1, we would expect to see eight paraquat signals; four for the paraquat complexed to the crown ether and four for the

uncomplexed paraquat, as the paraquat units are unsymmetrical. Instead we see only four signals indicating that the crown ether rapidly shuttles between the two paraquat sites. This is consistent with similar systems with two degenerate binding sites on an axle. At room temperature, the shuttling is fast enough that the two paraquat sites appear equivalent in the ^{1}H NMR spectrum. The fact that these same protons are 0.18 ppm upfield in [3]rotaxane **8** (relative to [2]rotaxane **7**) would indicate that the crown ethers spend all of their time on the paraquat binding sites. The two sets of aromatic protons (**a'** and **b'**) integrate to 8 H each and shifted upfield from 6.78 (**a'**) and 6.64 (**b'**) ppm to 6.49 and 6.33 ppm. This is slightly downfield from where they occur in [2]rotaxane **7**, again indicating that the crown ethers are donating more electron density to the paraquat site because the crown ethers are spending all of their time on the paraquat sites instead of shuttling between two sites. In the 3-4.5 ppm region, the ethyleneoxy peaks that appear in two groups in the 1:1 dumbbell mixture (Figure 3.6 b) are transformed to four peak groups in the [3]rotaxane **8** (Figure 3.6 a). The signals move upfield from 3.79 and 3.63 ppm to 3.75, 3.48, 3.40 and 3.36 ppm. The ethyleneoxy peaks integrate to a total of 64 H, consistent with the presence of two crown ether hosts.

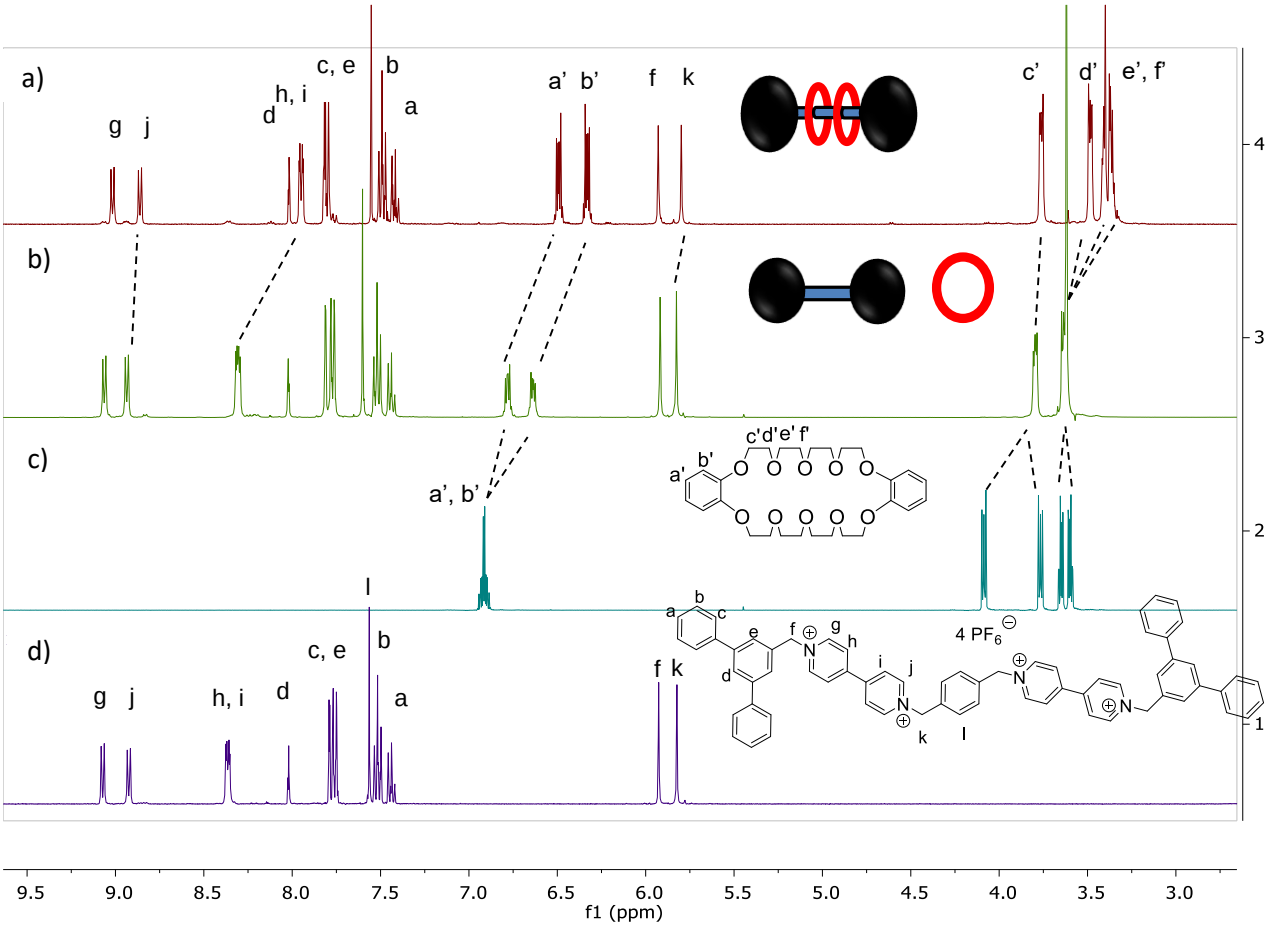

Figure 3.6. Stacked partial ^{1}H NMR spectra of a) rotaxane **8** b) 1:1 mixture of dumbbell **6** and **DB30C10** c) **DB30C10** and d) dumbbell **6** in MeCN-d_3 at 400 Mz.

Figure 3.7 shows the chemical shift changes between the proton NMR spectra of solutions of dumbbell **2** (Figure 3.7 d) and **DB30C10** (Figure 3.7 c) separately, a 1:1 solution of dumbbell **2** and **DB30C10** (Figure 3.7 b) and a solution of rotaxane **4** (Figure 3.7 a). The paraquat protons in dumbbell **2** (Figure 3.7 d) move upfield when **DB30C10** is added (the 1:1 solution, Figure 3.7 b) from 9.06 and 8.36 ppm to 9.05 and 8.27 ppm, signifying taco complexation. The aromatic protons in **DB30C10** (**a'** and **b'**) split from one multiplet at 6.91 ppm to two signals at 6.80 and 6.67 ppm in the 1:1 solution. There are four distinct ethyleneoxy signals in the **DB30C10** solution (Figure 3.7 c) at 4.09, 3.76,

3.65 and 3.59 ppm. In the 1:1 solution there are three signals at 3.83, 3.64 and 3.62 ppm. In the rotaxane solution (Figure 3.7 a), further upfield shifts are observed. The paraquat signals shift from 9.05 (**g**) and 8.27 ppm (**h**) in the 1:1 solution to 8.97 and 7.97 ppm. The aromatic groups in the crown ether shift from at 6.80 and 6.67 ppm in the 1:1 solution to 6.48 and 6.31 ppm in the rotaxane **4**. The ethyleneoxy peaks shift from 3.83, 3.64 and 3.62 ppm in the 1:1 solution to 3.73, 3.43 and 3.36 ppm. These chemical shits changes are summarized in (Table 3.4).

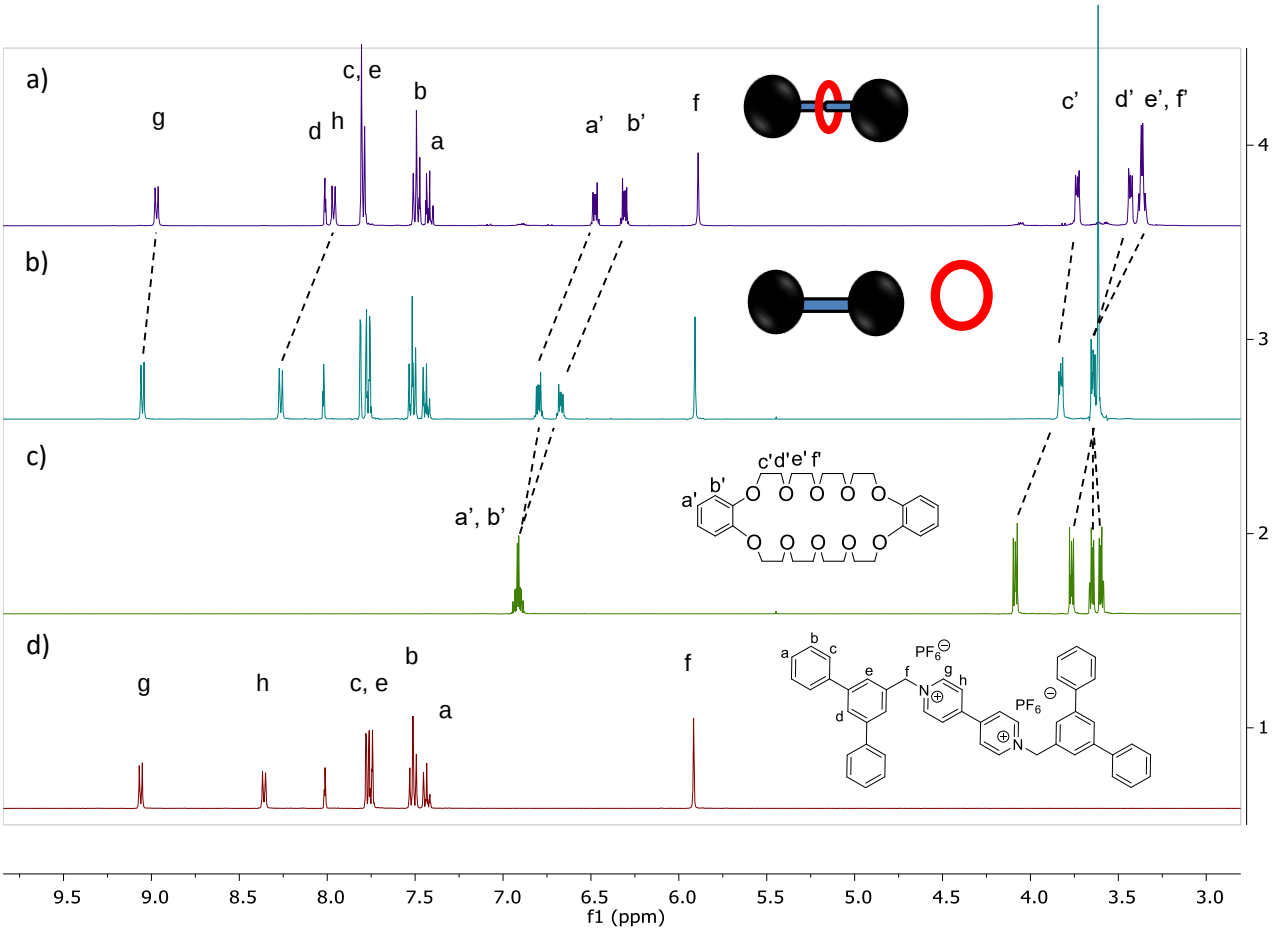

Figure 3.7. Partial ^{1}H NMR spectra of a) rotaxane **4** b) 1:1 mixture of dumbbell **2** and **DB30C10** c) **DB30C10** and d) dumbbell **2** in MeCN-d_3 at 400 MHz.

Table 3.4. Chemical shifts of [2]rotaxane 4 and its components in MeCN-d_3				
Proton	**Dumbbell 2**	**DB30C10**	**2 + DB30C10**	**Rotaxane 4**
PQα	9.06	---	9.05	8.97
Δ PQα	---	---	**-0.01**	**-0.09**
PQβ	8.36	---	8.27	7.97
Δ PQβ	---	---	**-0.09**	**-0.39**
Crown a’	---	6.91	6.80	6.48
Δ a’	---	---	**-0.11**	**-0.43**
Crown b’	---	6.91	6.67	6.31
Δ b’	---	---	**-0.24**	**-0.60**
OCH_2-1	---	4.09	---	---
Δ OCH_2-1	---	---	---	---
OCH_2-2	---	3.76	3.83	3.73
Δ OCH_2-2	---	---	**+0.07**	**-0.03**
OCH_2-3	---	3.65	3.64	3.43
Δ OCH_2-3	---	---	**-0.01**	**-0.22**
OCH_2-4	---	3.59	3.62	3.36
Δ OCH_2-4	---	---	**+0.03**	**-0.23**

2D NOESY spectra were obtained for each of the rotaxanes. Figure 3.8 shows a partial 2D NOESY spectrum of rotaxane **4**. The spectrum shows a few cross-peaks between the dumbbell part and the crown ether. Peaks **d** and **h**, which correspond to a pair of paraquat protons and one of the protons on the blocking group, show cross peaks with **d’** and **e’**, which are protons in the ethyleneoxy arms of the crown ether. Additionally, there is a small cross peak between proton **f** (the methylene group next to the pyridinium group) and protons **d’** and **e’** of the ethyleneoxy protons in the crown ether.

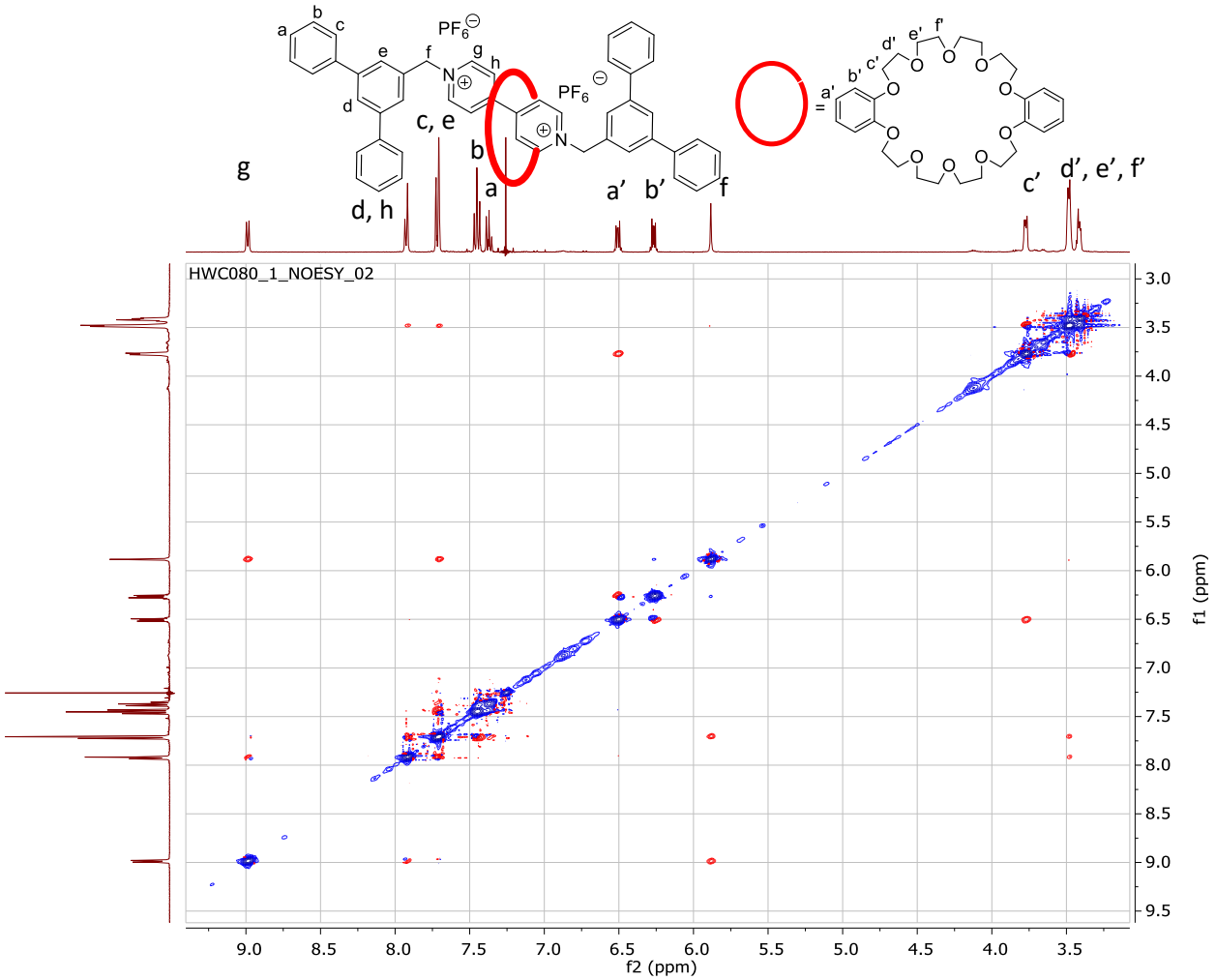

Figure 3.8. Partial 2D NOESY spectrum of rotaxane **4** in $CDCl_3$ at 400 MHz.

Figure 3.9 shows part of the 2D NOESY spectrum of rotaxane **7**. The cross-peaks between the dumbbell section and the crown ether are; between a set of paraquat protons **g**, blocking group protons **c** and **d**, and the aromatic protons of the crown ether **a’**, and between paraquat protons **j**, linking group protons **l** and **f**, and aromatic protons of the crown ether **b’**.

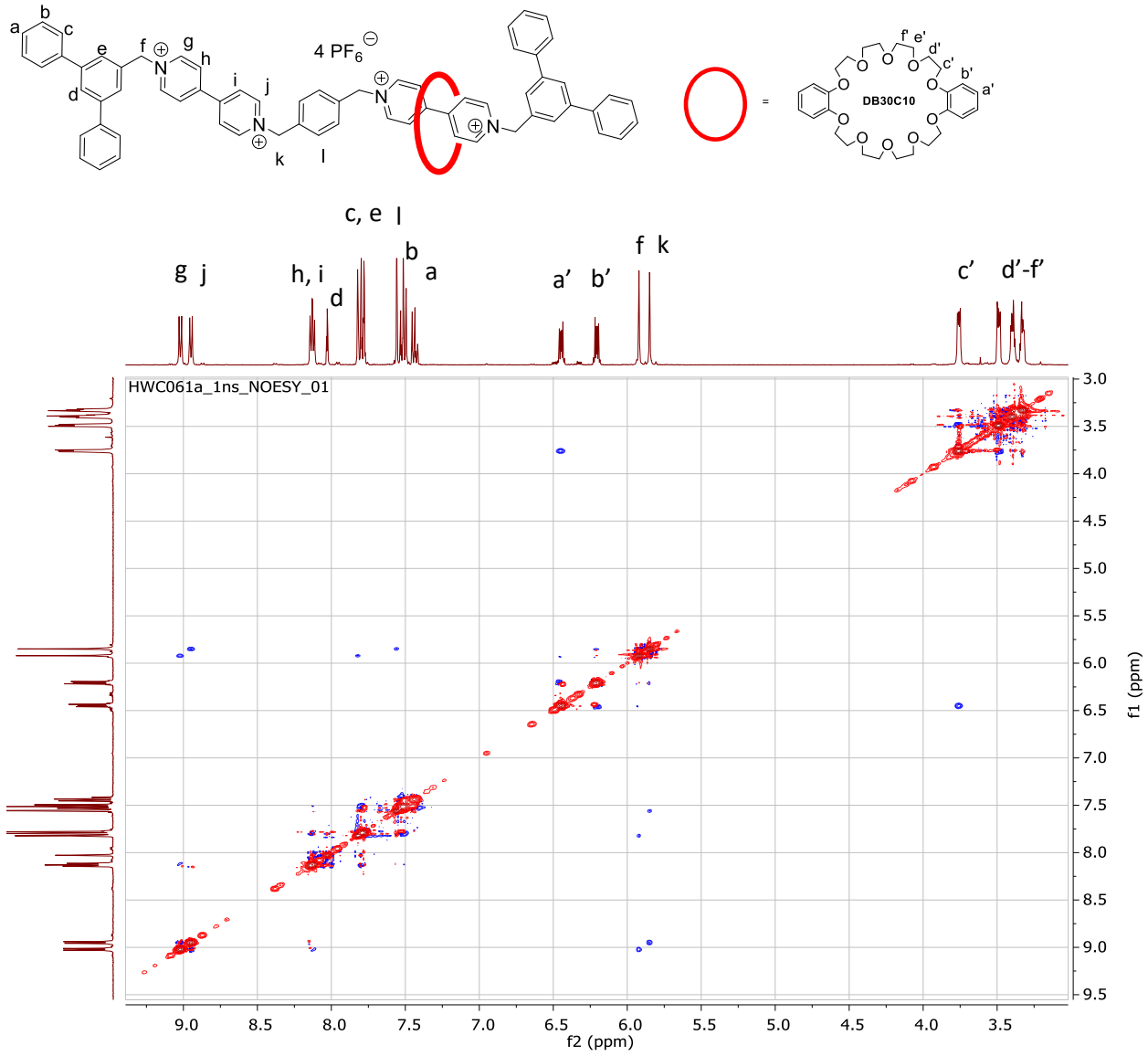

Figure 3.9. Partial 2D NOESY spectrum of [2]rotaxane **7** in MeCN-d_3 at 400 MHz.

Rotaxane **8** shows cross-peaks in the 2D NOESY spectrum (Figure 3.10). Similar to the NOESY of rotaxane **7**, paraquat protons **g** show correlates with blocking group protons **e** and the aromatic peaks on the crown ether **a’,** and paraquat protons **g’** show cross peaks with the linking aromatic groups **j** and the methylene linker **i**.

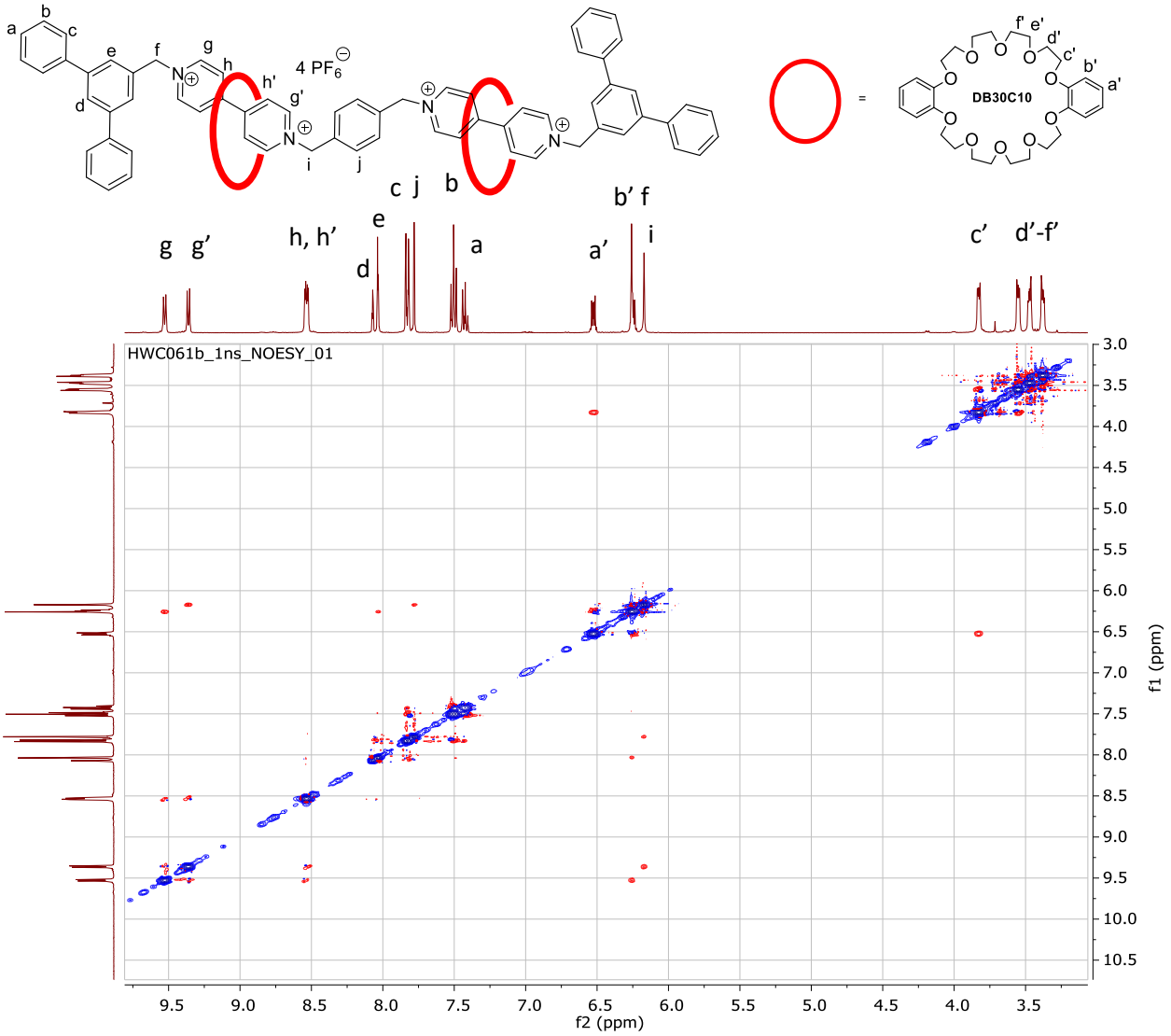

Figure 3.10. Partial 2D-NOESY spectrum of [3]rotaxane **8** in MeCN-d_3 at 400 MHz

A cross-peak is observed for rotaxane **12** between the ethylene linker between the paraquat and the triazole ring, and the ethyleneoxy protons in the crown ether (protons designated **h**, **f’** and **e’** in Figure 3.11).

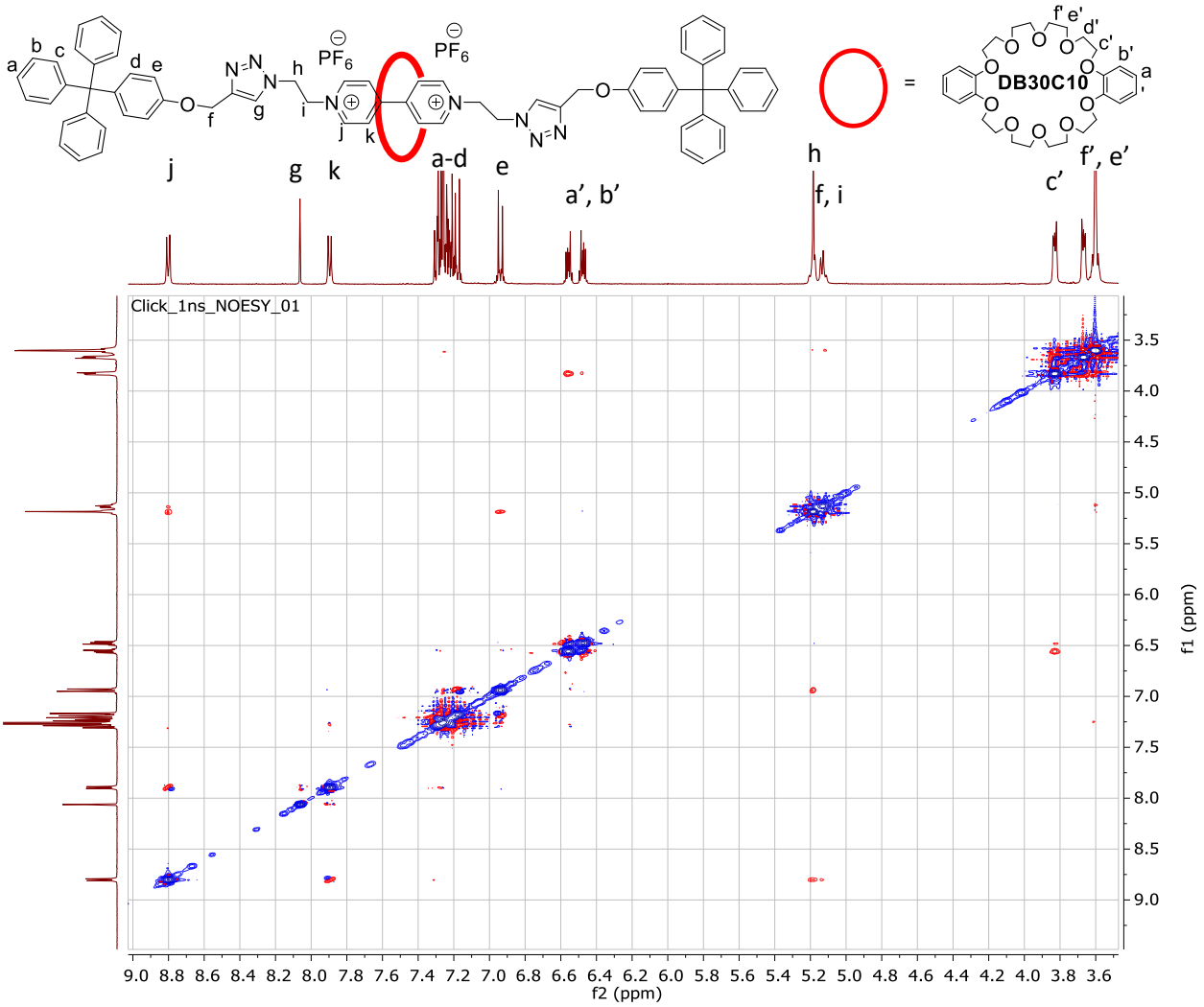

Figure 3.11. Partial 2D NOESY of rotaxane **12** in MeCN-d_3 at 400 MHz

Several attempts were made to grow crystals of suitable quality for single crystal X-ray diffraction. A suitable crystal of rotaxane **7** was obtained by slow vapour diffusion of pentane into MeCN/MeOH (Figure 3.12). The crystal structure clearly shows that the guest molecule is threaded through the host cavity. The host adopted a folded conformation rather than an S-shaped or step conformation that has been observed for some rotaxanes.[45-46] However, the guest did not thread in the manner depicted in Figure 3.1 wherein the guest is positioned “parallel” to the back (the ethyleneoxy groups) of the

host (which is frequently observed in pseudorotaxanes [47-48] and cryptands [41, 49] based on **BMP32C10**) the guest is positioned so that the guest "sticks out" of the crown ether. A similar conformation has been reported for a [2]catenane.[50] The centroid to centroid distance between the benzo groups of the host is 6.98 Å. Thus the centroid to centroid distance between the benzo groups of the host and the bipyridinium moiety on the guest is approximately 3.5 Å. The bipyridyl twist is 13.1 º.

The N-benzylic groups are engaged in hydrogen bonding with C-H···O distances of 2.81 and 2.56 Å and bond angles of 147 and 128 º for the back hydrogens and 2.76 and 2.55 Å with bond angles of 146 and 122 º for the back hydrogens (Figure 3.12 b). The α-H's of

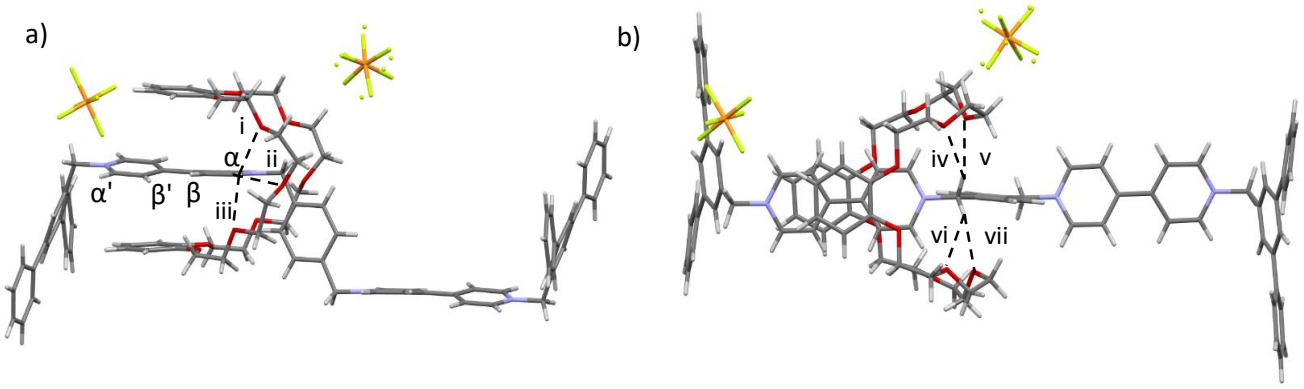

Figure 3.12. Two views of X-ray crystal structure of rotaxane **7.** Side view **(a)** and top view **(b)**. Carbon atoms are grey, oxygen atoms are read, hydrogen atoms are white, nitrogen atoms are blue, phosphorous atoms are orange and fluorine atoms are green. Centroid to centroid distance between phenyl groups of host 6.98 Å. Centroid to centroid between host and guest 3.5 Å. Bipyridyl twist, 13.1 º. CH-O, H-bond distances in Å and bond angles in degrees: i = 2.64, 122 º; ii = 2.52, 147 º; iii = 6.64, 113 º; iv =2.81, 147 º; v =2.56, 128 º; vi = 2.76, 146 º; vii = 2.55, 122 º

the bipyridyl units are engaged in H-bonding with the ethyleneoxy oxygen atoms with H···O distances of 2.67, 2.72 and 2.47 Å for the back H's and 2.64, 2.52 and 2.69 Å for the front H's respectively. The β-hydrogens of the bipyridyl units are not engaged in H-bonding at all. This absence of H-bonding involvement of one pair of paraquat protons (which is also observed by the lack of significant upfield shift of one pair of paraqat protons

as depicted in Figure 3.2) could mean that the association constant in solution is lower than expected, resulting in the relatively low rotaxane yields.

Conclusions

In conclusion we have prepared and isolated three new [2]rotaxanes and one new [3]rotaxane with **DB30C10** as the host and paraquats as the guest species. These are the first examples of rotaxanes using the **DB30C10**/paraquat binding motif. The new rotaxanes where all purified, isolated and fully characterized by ^{1}H NMR, ^{13}C NMR, and HRMS. An X-ray crystal structure of rotaxane **3** was obtained, which clearly shows that the guest is threaded through the cavity. These findings demonstrate that **DB30C10** does indeed form pseudorotaxane complexes with paraquats in solution.

Experimental

General: The two blocking groups 3,5-diphenylbenzyl bromide[51] and 4-trityl-(3'-propynyloxy)benzene[52] as well as the half-quat **2** [53] were synthesized according to literature procedures.

Melting points were measured with a Mel-Temp II device in capillary tubes and are uncorrected. ^{1}H and ^{13}C NMR spectra were obtained at ambient temperatures on JOEL Eclipse Plus 500 MHz, Varian Unity Plus or Varian MR 400 MHz spectrometers. ^{1}H NMR and ^{13}C spectra are corrected relative to residual solvent peaks. High-resolution mass spectra were obtained with an Agilent 6220 LCMS ESI-TOF spectrometer using acetonitrile as solvent. Ion exchange was performed with Amberlite GC-120, strongly acid sulfonated cation exchange resin (RSO_3^- Na^+) 100-200 mesh. Column chromatography

was performed with silica gel, 40-63 μm, 60 Å from Sorbent Technologies, or Flash Alumina-N from Agela Technologies.

N,N'-Bis(2''-azidoethyl)-4,4'-bipyridium Hexafluorophosphate (10): 2-Azidoethyl 4-methylbenzenesulfonate (7.25 g, 30 mmol) and 4,4'-bipyridine (1.57 g, 10 mmol) were combined in $MeNO_2$ (30 mL) and the mixture was brought to reflux. After 10 days, the solution was allowed to cool to room temperature. The solution was very dark, almost black. The solvent was removed by rotary evaporation to yield a black tar-like substance. The solid was washed with DCM and acetone and dissolved in water and MeOH. The solution was treated with decolorizing carbon, which had no visible effect. A saturated solution was KPF_6 was added. The black solution turned brown with a precipitate. The light brown solid was collected by vacuum filtration, dissolved in boiling water and treated with decolorizing carbon. The hot solution was filtered through a pad of *Celite*®. The volume of water was reduced and the boiling solution was allowed to cool to room temperature. The solid was collected by vacuum filtration to yield off-white crystals (1.95 g, 33%), mp 206 ºC (dec.). ^{1}H NMR (400 MHz, DMSO-d_6) δ 9.33 (d, J = 7 Hz, 4H), 8.77 (d, J = 7 Hz, 4H), 4.87 – 4.81 (m, 4H), 4.10 – 4.03 (m, 4H). ^{13}C NMR (101 MHz, DMSO-d_6) δ 149.1, 146.2, 126.5, 59.7, 50.2. HRMS (ESI-TOF) $C_{14}H_{16}F_{12}N_8NaP_2$ $(M+Na)^+$, *m/z* 609.0695 (found), 609.0674 (calc.), δ 3.4 ppm; $C_{14}H_{20}F_{12}N_9P_2$ $(M+NH_4)^+$, *m/z* 604.1123 (found), 604.1120 (calc.), δ 0.5 ppm; $C_{14}H_{16}N_8$ $(M^{\bullet})^+$, *m/z* 296.1530 (found), 296.1496 (calc.), δ 3.6 ppm.

N-([1,1':3',1''-Terphenyl]-5'-ylmethyl)-[4,4'-bipyridin]-1-ium hexafluorophosphate (3): 4,4'-Bipyridine (0.64 g, 3.9 mmol) and 3,4-diphenylbenzyl bromide (0.32 g, 0.9 mmol) were combined in acetone (20 mL) and heated at reflux for 7 h. The solution went from

light yellow to light green with a precipitate. The solution was cooled to room temperature and the solid was collected by vacuum filtration, washed well with DCM and acetone and allowed to air dry. The light green material was dissolved in water/acetone and KPF_6 (sat.) was added. The solution was boiled to remove the acetone. An orange precipitate was collected by vacuum filtration, washed several times with H_2O and dried to yield a light orange powder (0.22 g, 43%), mp 155 ºC (dec.). ^{1}H NMR (400 MHz, CD_3CN) δ 8.94 (d, *J* = 7 Hz, 2H), 8.85 – 8.81 (m, 2H), 8.32 (d, *J* = 7 Hz, 2H), 8.00 (t, *J* = 2 Hz, 1H), 7.80 – 7.73 (m, 8H), 7.52 (t, *J* = 7 Hz, 4H), 7.43 (t, *J* = 7 Hz, 2H), 5.85 (s, 2H). ^{13}C NMR (101 MHz, DMSO-d_6) δ 153.2, 151.4, 145.7, 142.3, 141.4, 139.8, 135.9, 129.4, 128.5, 127.5, 127.2, 126.5, 126.6, 122.4, 63.6. HRMS: ESI-TOF $C_{29}H_{23}F_6N_2P$ $(M\text{-}PF_6)^+$, *m/z* 399.1855 (found), 399.1861 (calc.), δ -1 ppm.

N,N'-Di(3'',5''-diphenylbenzyl)-4,4'-bipyridinium Bishexafluorophosphate, Dumbbell 2: 3,5-Diphenylbenzyl bromide (**1**, 0.3583 g, 1.1 mmol) and 4,4'-bipyridine (0.06923, 0.4 mmol) were suspended in MeCN (10 mL) and was heated at reflux for 5 days, allowed to cool to room temperature and vacuum filtered. The yellow solid was washed with acetone and DCM, and allowed to air dry. The yellow solid (0.28 g) was dissolved in boiling water and a saturated solution of KPF_6 was added. The volume was reduced from 500 mL to 50 mL. The yellow solid was collected by vacuum filtration, washed with water and allowed to air dry, 0.3825 g (93 %), mp 244 °C (dec.). ^{1}H NMR (400 MHz, DMSO-d_6) δ 9.62 (d, *J* = 7 Hz, 4H), 8.69 (d, *J* = 7 Hz, 4H), 8.00 – 7.96 (m, 6H), 7.79 (d, *J* = 8 Hz, 8H), 7.51 (t, *J* = 7 Hz, 8H), 7.46 – 7.40 (m, 4H), 6.01 (s, 4H). ^{13}C NMR (101 MHz, DMSO-d_6) δ 149.3, 145.6, 141.9, 139.2, 135.3, 129.0, 128.1, 127.3, 127.1, 126.7, 126.1, 63.7. ^{1}H NMR (400 MHz, CD_3CN) δ 9.06 (d, *J* = 7 Hz, 4H), 8.36 (d, *J* = 7

Hz, 4H), 8.01 (t, *J* = 2 Hz, 2H), 7.79 – 7.73 (m, 12H), 7.51 (t, *J* = 7 Hz, 8H), 7.43 (t, *J* = 7 Hz, 4H), 5.92 (s, 4H). ^{13}C NMR (101 MHz, CD_3CN) δ 151.33, 146.69, 143.87, 140.62, 134.85, 130.07, 129.2, 128.5, 128.2, 128.1, 128.0, 65.7. HRMS (ESI-TOF) $C_{48}H_{38}F_{12}N_2P_2$ $(M\text{-}PF_6)^+$, *m/z* 787.2671 (calc.), 787.2689 (found), δ 2.2 ppm; $C_{48}H_{38}F_6N_2P$ $(M\text{-}PF_6\text{+}K^+)^{2+}$, 826.2249 (found), 826.2303 (calc.), δ -6.5 ppm

Dumbbell 6: Bis(half-quat) **5** (0.3136 g, 0.4 mmol) and 3,5-diphenylbenzyl bromide (**1**, 0.3588 g, 1.1 mmol) were dissolved in MeCN (60 mL) and the solution was heated at reflux under N_2 (g) for 40 h. The yellow solid was collected by vacuum filtration, washed with DCM x 3, allowed to dry on the frit and dissolved in acetone/water; KPF_6 was added. The solution was allowed to reflux over-night. The beige solid was collected by vacuum filtration, allowed to dry and recrystallized from water/acetone to yield yellow crystals, 0.5066 g (77%), mp 216.1-219.9 °C (dec.). ^{1}H NMR (400 MHz, DMSO-d_6) δ 9.64 (d, *J* = 7 Hz, 4H), 9.44 (d, *J* = 7 Hz, 4H), 8.70 (t, *J* = 7 Hz, 8H), 8.00 (dd, *J* = 7, 2 Hz, 6H), 7.80 (d, *J* = 9 Hz, 8H), 7.66 (s, 4H), 7.52 (t, *J* = 7 Hz, 8H), 7.44 (t, *J* = 7 Hz, 4H), 6.03 (s, 4H), 5.91 (s, 4H). ^{13}C NMR (101 MHz, DMSO-d_6) δ 149.4, 149.1, 145.7, 141.9, 139.2, 135.4, 135.2, 129.7, 129.0, 128.1, 127.3, 127.2, 127.1, 126.7, 126.1, 63.7, 62.9. ^{1}H NMR (400 MHz, CD_3CN) δ 9.07 (d, *J* = 7 Hz, 4H), 8.93 (d, *J* = 7 Hz, 4H), 8.37 (overlapping d, *J* = 7, 2 Hz, 8H), 8.02 (t, *J* = 2 Hz, 2H), 7.81 – 7.74 (m, 12H), 7.57 (s, 4H), 7.52 (t, *J* = 7 Hz, 8H), 7.44 (t, *J* = 7 Hz, 4H), 5.93 (s, 4H), 5.83 (s, 4H). ^{13}C NMR (101 MHz, CD_3CN) δ 151.5, 151.2, 146.6, 146.59, 143.8, 140.6, 135.2, 134.8, 131.3, 130.0, 129.2, 128.5, 128.48, 128.1, 128.1, 128.0, 65.7, 64.9. ESI-TOF HRMS of $C_{66}H_{54}F_{24}N_4P_4$ $(M\text{+}NH_4)^+$, *m/z* 1500.3278 (found), 1500.3254 (calc.), δ 1.6 ppm; $C_{66}H_{54}F_{24}N_4NaP_4$ $(M\text{+}Na)^+$, *m/z*

1505.2842 (found), 1505.2808 (calc.), δ 2.3 ppm; $C_{66}H_{54}F_{12}N_4P_2^{2+}$ $(M\text{-}2PF_6)^{2+}$, *m/z* 596.1824 (found), 596.1811 (calc.), δ 2.2 ppm.

Dumbbell 11: 4-Trityl-(3'-propynyloxy)benzene (**9**, 0.38 g, 1.0 mmol) was dissolved in a minimal amount of DMF. Paraquat diazide (**10**, 0.2831 g, 0.5 mmol) was added and the solution turned a dark red-brown colour. $CuSO_4 \cdot 5H_2O$ (0.0360 g, 0.1 mmol) and ascorbic acid (0.0857 g, 0.4 mmol) were added in rapid succession. The dark brown solution was allowed to stir at room temperature. After 2 months, the brown solid was collected by vacuum filtration. The solid was washed well with DCM, acetone and water and recrystallized from acetone and water, beige solid, 0.1686 g (26%), mp 226.5 – 227.2 °C (dec.). ^{1}H NMR (400 MHz, DMSO-d_6) δ 9.25 (d, *J* = 7 Hz, 4H), 8.73 (d, *J* = 7 Hz, 4H), 8.26 (s, 2H), 7.28 (t, *J* = 7 Hz, 12H), 7.19 (t, *J* = 7 Hz, 6H), 7.12 (d, *J* = 7 Hz, 12H), 7.05 (d, *J* = 9 Hz, 4H), 6.95 (d, *J* = 9.0 Hz, 4H), 5.28 – 5.11 (m, 9H), 5.09 (s, 4H). ^{13}C NMR (101 MHz, DMSO-d_6) δ 155.9, 148.8, 146.5, 146.3, 143.0, 138.8, 131.6, 130.4, 127.7, 126.4, 125.9, 125.4, 113.6, 63.7, 60.9, 59.8, 42.9. ^{1}H NMR (400 MHz, Acetonitrile-d_3) δ 8.63 (d, *J* = 7 Hz, 4H), 8.12 (d, *J* = 7 Hz, 4H), 7.87 (s, 2H), 7.24 (d, *J* = 4 Hz, 24H), 7.21 – 7.13 (m, 10H), 6.90 (d, *J* = 9 Hz, 4H), 5.12-2.10 (m, 8H), 5.02 – 4.98 (m, 4H). HRMS (ESI-TOF) $C_{70}H_{60}F_{12}N_8NaO_2P_2^+$ $(M+Na)^+$, *m/z* 1357.3997 (found), 1357.4015 (calc.), δ -1.3 ppm; $C_{70}H_{60}F_{12}N_8O_2P_2$ $(M\text{-}PF_6)^+$, *m/z* 1189.4484 (found), 1189.4476 (calc.), δ 0.7 ppm.; $C_{70}H_{60}N_8O_2^{2+}$ $(M\text{-}2PF_6)^{2+}$, *m/z* 522.2401 (found), 522.2414 (calc.), δ -2.5 ppm.

Rotaxane 4:

Method 1: Half-quat **3** (0.22 g, 0.4 mmol), and **DB30C10** (0.65 g, 1.2 mmol) were combined in acetone. The solvent was removed. 3,5-diphenylbenzyl bromide (**1**, 0.14 g, 0.4 mmol) was added and the mixture was dissolved in DCM (9 mL) and MeCN (1 mL)

and stirred at room temperature. The solution went from yellow to dark orange over the course of several days. After a month of stirring at room temperature, the solid precipitate was collected by vacuum filtration and washed with DCM. The filtrate was collected, concentrated to dryness and the resulting solid was washed with ethyl acetate. The filtrate was concentrated and washed with toluene. The toluene filtrate was collected. Some crystals formed (crown ether) and they were filtered. The resulting bright orange residue was dissolved in DCM to load onto a column. However, some yellow solid would not dissolve. This solid was filtered and the resulting filtrate was concentrated by rotary evaporation. The orange solid was dissolved in a minimum amount of DCM and purified by column chromatography (silica gel; DCM: MeOH 10:1). The orange fractions were contaminated with unreacted dumbbell and crown ether. The orange fractions were collected, concentrated and subjected to another round of chromatography (neutral alumina; EA -> 5% MeOH in EA). The orange fractions were combined and concentrated to give a red solid, 0.08 g (13%).

Method 2: 4,4'-Bipyridyl (0.13 g, 0.8 mmol) was dissolved in MeCN (10 mL) and filtered into a round bottomed flask. **DB30C10** (1.42 g, 2.6 mmol) was added and enough DCM was added to dissolve the solids. 3,5-Diphenylbenzyl bromide (**1**, 0.60 g, 1.9 mmol) was added and the solution was allowed to stir at room temperature. The solution went from orange to yellow with precipitate. After 4 weeks, the solid was filtered and washed well with MeCN. The filtrate was concentrated and DCM was added. The solid material was filtered and the filtrate was concentrated to give an orange solid. The solid was purified by column chromatography (DCM – 10% MeOH in DCM – 12:2:1 MeOH:2M NH_4Cl: $MeNO_2$). The orange fractions were collected and purified twice more (silica gel; 20:1

MeOH: 2M NH_4Cl and silica 30:1 MeOH: 2M NH_4Cl). The orange solid was dissolved in MeOH and water. A saturated solution of KPF_6 was added. The organic solvent was removed by rotary evaporation and the red solid was collected, washed with water and allowed to dry on the frit and then under vacuum to yield a dark orange solid, 0.0328 g (2.7%), mp 80.5 – 105 ºC. ^{1}H NMR (400 MHz, $CDCl_3$) δ 8.99 (d, *J* = 7 Hz, 4H), 7.91 (d, *J* = 7 Hz, 6H), 7.73-7.71 (m, 12H), 7.44 (t, *J* = 7 Hz, 8H), 7.36 (t, *J* = 7 Hz, 4H), 6.49 (dd, *J* = 6, 4 Hz, 4H), 6.26 (dd, *J* = 6, 4 Hz, 4H), 5.90 (s, 4H), 3.76 (d, *J* = 5 Hz, 8H), 3.47 (d, *J* = 5 Hz, 16H), 3.40-3.39 (m, 8H). ^{13}C NMR (101 MHz, $CDCl_3$) δ 147.8, 147.1, 145.4, 143.1, 139.5, 133.5, 129.0, 128.1, 127.2, 126.5, 125.8, 121.6, 114.0, 70.2, 70.0, 68.6, 64.6. ^{1}H NMR (400 MHz, Acetonitrile-d_3) δ 8.94 (d, *J* = 7 Hz, 4H), 8.85 – 8.82 (m, 3H), 8.32 (d, *J* = 7 Hz, 4H), 8.00 (t, *J* = 2 Hz, 2H), 7.79 – 7.73 (m, 15H), 7.52 (t, *J* = 7 Hz, 7H), 7.43 (t, *J* = 7 Hz, 4H), 5.85 (s, 4H). ^{1}H NMR (400 MHz, DMSO-d_6) δ 9.49 (d, *J* = 6 Hz, 4H), 8.86 (d, *J* = 6 Hz, 4H), 8.65 – 8.60 (m, 4H), 8.03 – 7.95 (m, 11H), 7.80 (d, *J* = 7 Hz, 8H), 7.52 (t, *J* = 7 Hz, 8H), 7.43 (t, *J* = 7 Hz, 4H), 5.97 (s, 4H). ^{13}C NMR (101 MHz, DMSO-d_6) δ 152.7, 150.9, 145.3, 141.91, 140.95, 139.3, 135.4, 129.0, 128.0, 127.1, 126.7, 125.9, 122.0, 63.1. HRMS (ESI-TOF) $C_{76}H_{78}F_6N_2O_{10}P$ (M^+), *m/z* 1323.5293 (calc.), 1323.5295 (found), δ 0.1 ppm; $C_{76}H_{78}N_2O_{10}$ $(M\text{-}2PF_6)^{2+}$, *m/z* 589.2823 (calc.), 589.2831 (found), δ 1.4 ppm.

Rotaxanes 7 and 8: DB30C10 (2.23 g, 4.2 mmol) and bis(half-quat) **5** (0.6145 g, 0.9 mmol) were dissolved in MeCN/DCM. The blocking group **1** (0.6093 g, 1.9 mmol) was added and the solution was allowed to stir at room temperature. The solution went from clear yellow to orange with precipitate to murky over the course of two days. After 4 weeks, the yellow solid was collected by vacuum filtration and washed with acetone. The red filtrate was concentrated to dryness and re-dissolved in DCM. Ion exchange resin

(Amberlite IRA 400 Cl^-) was added and the solution was stirred at room temperature for 30 min. The ion exchange resin was filtered and the solvent was removed. The resulting residue was purified by column chromatography (silica gel; DCM:MeOH 20:4 -> MeOH -> MeOH:NH_4Cl 10:1 -> MeOH:NH_4Cl:$MeNO_2$ 11:2:1). A red band started to move in MeOH and moved more in MeOH:NH_4Cl. Two orange bands were collected and concentrated.

First band, orange solid, **[3]Rotaxane 8**, 0.0907 g (4 %), mp 110 – 115 ºC. ^{1}H NMR (400 MHz, CD_3CN) δ 9.02 (d, *J* = 7 Hz, 4H), 8.86 (d, *J* = 7 Hz, 4H), 8.02 (t, *J* = 2 Hz, 2H), 7.96-7.94 (m, 8H), 7.83 – 7.78 (m, 13H), 7.55 (s, 4H), 7.50 (t, *J* = 7 Hz, 8H), 7.42 (t, *J* = 7 Hz, 4H), 6.50 (dd, *J* = 6, 4 Hz, 8H), 6.33 (dd, *J* = 6, 4 Hz, 8H), 5.93 (s, 4H), 5.80 (s, 4H), 3.83 – 3.72 (m, 16H), 3.54 – 3.47 (m, 16H), 3.43 – 3.32 (m, 32H). ^{13}C NMR (101 MHz, CD_3CN) δ 149.8, 148.7, 146.8, 146.4, 143.8, 140.6, 135.6, 135.2, 130.6, 130.0, 129.1, 128.2, 127.9, 127.7, 127.4, 122.2, 114.4, 71.0, 70.9, 70.6, 69.5, 65.5, 64.6. HRMS (ESI-TOF) $C_{122}H_{134}F_{12}N_4O_{20}P_2$ $(M\text{-}2PF_6)^{2+}$, *m/z* 1132.9449 (calc.), 1132.9465 (found), δ 1.4 ppm; $C_{122}H_{134}F_6N_4O_{20}P$ $(M\text{-}3PF_6)^{3+}$, *m/z* 706.9750 (calc.), 706.9765 (found) δ 2.1 ppm.

Second band, orange solid, **[2]Rotaxane 7**, 0.4841 g (28 %), mp 137.5-144.8 ºC. ^{1}H NMR (400 MHz, DMSO-d_6) δ 9.44 (d, *J* = 7 Hz, 4H), 9.24 (d, *J* = 7 Hz, 4H), 8.43 (dd, *J* = 16, 7 Hz, 8H), 8.00-7.99 (m, 6H), 7.82 – 7.77 (m, 8H), 7.57 (s, 4H), 7.48 (t, *J* = 7 Hz, 8H), 7.40 (t, *J* = 7 Hz, 4H), 6.34 (dd, *J* = 6, 4 Hz, 4H), 5.95 (s, 4H), 5.90 (dd, *J* = 6, 4 Hz, 4H), 5.86 (s, 4H), 3.73-3.71 (m, 8H), 3.41-3.41 (m, 8H), 3.23-3.22 (m, 8H), 3.15-3.14 (m, 8H). ^{1}H NMR (400 MHz, CD_3CN) δ 9.02 (d, *J* = 7 Hz, 4H), 8.86 (d, *J* = 7 Hz, 4H), 8.02 (t, *J* = 2 Hz, 2H), 7.95 (dd, *J* = 7, 2 Hz, 8H), 7.82 – 7.79 (m, 12H), 7.55 (s, 4H), 7.51 – 7.47 (m, 8H), 7.44 – 7.39 (m, 4H), 6.49 (dd, *J* = 6, 4 Hz, 8H), 6.33 (dd, J = 6, 4 Hz , 8H), 5.93 (s,

4H), 5.80 (s, 4H), 3.79 – 3.74 (m, 16H), 3.51 – 3.46 (m, 16H), 3.42-3.40 (m, 16H), 3.36 (m 16H).^{13}C NMR (101 MHz, CD_3CN) δ 148.8, 148.7, 148.1, 146.5, 146.4, 143.69, 140.63, 135.59, 135.53, 130.3, 129.9, 129.0, 128.2, 127.7, 127.6, 126.9, 126.8, 122.2, 114.5, 71.0, 70.9, 70.5, 69.5. HRMS (ESI-TOF) $C_{94}H_{94}F_{12}N_4O_{10}P_2$ $(M\text{-}2PF_6)^{2+}$, *m/z* 864.8138 (calc.), 864.8138 (found), δ 0.0 ppm; $C_{95}H_{95}F_6N_4O_{10}P$ $(M\text{-}3PF_6)^{3+}$, *m/z* 528.2210 (calc.), 528.2216 (found), δ 1.1 ppm.

Rotaxane 12: Paraquat diazide **10** (0.61 g, 1 mmol) and **DB30C10** (1.65 g, 3 mmol) were combined in a minimum amount of dry MeCN. The solution turned bright red. The alkyne blocking group **9** (0.81 g, 2 mmol) and dry DCM were added until all the solid was dissolved. The solution was degassed by bubbling Ar (g) through it for several minutes. $Cu(CH_3CN)_4PF_6$ (0.38 g, 1 mmol) was added and DCM and MeCN were added until all solids were just dissolved. The solution was degassed with Ar (g) and allowed to stir at room temperature under positive pressure of Ar (g). After 20 days, the solution was opened to atmosphere. The solution went from red to brown and a precipitate formed. The solution was filtered through pad of a *Celite*®. The filtrate was concentrated and the resultant orange solid was washed with EA. The white solid was filtered and the filtrate was collected and the solvent removed by rotary evaporation. This process was repeated with DCM and acetone. The red tacky solid was washed with toluene. The red compound did not dissolve in toluene. A red and a white solid were collected on the frit. The solid was dissolved in MeOH/acetone/DCM and Amberlite IRA-400 (Cl) ion exchange resin was added. The solution was allowed to stir for several hours. The solution went from orange and clear to cloudy with lots of white precipitate. The solids were removed by filtration and the filtrate was concentrated and purified by column chromatography (silica

gel; MeOH:2M NH_4Cl 50:1 – 20:1 – 10:1). The orange band was collected, and the solvent removed. The solid was dissolved in water with a little bit of MeOH to dissolve residual solids and a saturated solution KPF_6 was added. The red sticky solid was collected, washed with water and air dried, 0.1105 g (6%), mp 126.1-145.1 °C. ^{1}H NMR (400 MHz, CD_3CN) δ 8.78 (d, *J* = 7 Hz, 4H), 8.04 (s, 2H), 7.87 (d, *J* = 7 Hz, 4H), 7.31 – 7.18 (m, 30H), 7.16 (d, *J* = 9 Hz, 4H), 6.92 (d, *J* = 9 Hz, 4H), 6.53 (dd, *J* = 6, 4 Hz, 4H), 6.45 (dd, *J* = 6, 4 Hz, 4H), 5.16-5.11 (m, 12H), 3.82-3.80 (m, 8H), 3.65-3.64 (m, 8H), 3.58 (s, 16H). ^{13}C NMR (101 MHz, CD_3CN) δ 157.2, 148.8, 148.1, 146.7, 145.0, 140.6, 132.9, 131.6, 128.6, 126.9, 126.6, 125.8, 122.7, 115.0, 114.6, 71.0, 70.7, 69.6, 62.1, 60.5, 49.8. ^{1}H NMR (400 MHz, DMSO-d_6) δ 9.05 (d, J = 7 Hz, 4H), 8.39 – 8.30 (m, 6H), 7.29 (t, J = 7 Hz, 12H), 7.20 (t, J = 7 Hz, 6H), 7.14 – 7.10 (m, 12H), 7.04 (d, J = 9 Hz, 4H), 6.96 (d, J = 9 Hz, 4H), 6.56 (dd, J = 6, 4 Hz, 4H), 6.40 (dd, J = 6, 4 Hz, 4H), 5.23 – 5.11 (m, 12H), 3.84-3.83 (m, 8H), 3.61-3.60 (m, 9H), 3.52-3.46 (m, 16H). ^{13}C NMR (101 MHz, DMSO-d_6) δ 156.3, 149.3, 147.0, 146.7, 143.4, 139.2, 132.0, 130.8, 128.1, 126.8, 126.3, 125.8, 114.0, 64.2, 61.3, 60.3, 49.6. HRMS (ESI-TOF) $C_{98}H_{100}F_{12}N_8NaO_{10}P_2$ $(M + Na)^+$, *m/z* 1894.6670 (calc.), 1894.6626 (found), δ -2.3 ppm; $C_{98}H_{100}F_{12}N_8O_{10}P_2$ $(M – PF_6)^+$, *m/z* 1725.9097 (calc.), 1725.8084 (found), δ -0.76 ppm; $C_{98}H_{100}N_8O_{10}$ $(M\text{-}2PF_6)^{2+}$, *m/z* 790.8742 (calc.), 790.8737 (found), δ -0.6 ppm.

Crystal Structure of Roaxane 7: An orange parallelepiped (0.13 x 0.29 x 0.37 mm^3) was centered on the goniometer of a Rigaku Oxford Diffraction Gemini E Ultra diffractometer operating with CuKα radiation. The data collection routine, unit cell refinement, and data processing were carried out with the program CrysAlisPro.[54] The Laue symmetry and systematic absences were consistent with the monoclinic space

group P21/n. The structure was solved using SHELXS-2014 [55] and refined using SHELXL-2014 [55] via Olex2.[56] A 2-position disorder model was used for one PF_6 anion, with relative occupancies that refined to 0.578(5) and 0.422(5). The crystals also contain a substantial amount of disordered solvent. A crude attempt to identify the solvent suggested 2 CH_3CN and 5 CH_3OH/asymmetric unit, but the disorder was substantial and the solvent model did not refine well. Therefore, the solvent mask feature of OLEX2 was used to subtract the solvent contribution to the electron density map. A total of 637 electrons was subtracted from a volume of 1688.6 Å3/unit cell. The final refinement model involved anisotropic displacement parameters for non-hydrogen atoms and a riding model for all hydrogen atoms. Olex2 was used for molecular graphics generation. Crystal structure obtained and solved by Dr. Carla Slebodnick.

References

1. Pedersen, C. J., Cyclic Polyethers and Their Complexes with Metal Salts. *J. Am. Chem. Soc.* **1967,** *89*, 7017-7036.
2. Izatt, R. M., Charles J. Pedersen: Innovator in macrocyclic chemistry and co-recipient of the 1987 Nobel Prize in chemistry. *Chem. Soc. Rev.* **2007,** *36*, 143-147.
3. Ashton, P. R.; Ballardini, R.; Balzani, V.; Baxter, I.; Credi, A.; Fyfe, M. C. T.; Gandolfi, M. T.; Gómez-López, M.; Martinez-Diaz, M. V.; Perisanti, A.; Specer, N.; Stoddart, J. F.; Venturi, M.; White, A. J. P.; Williams, D. J., Acid-Base Controllable Molecualr Shuttles. *J. Am. Chem. Soc.* **1998,** *120*, 1132-11942.
4. Jia, C.; Li, H.; Jiang, J.; Wang, J.; Chen, H.; Cao, D.; Stoddart, J. F.; Guo, X., Interface-Engineered Bistable [2]Rotaxane-Graphene Hybrids with Logic Capabilities. *Adv. Mater.* **2013,** *25*, 6752-6759.
5. Martinez-Diaz, M. V.; Specer, N.; Stoddart, J. F., The Self-Assembly of a Switchable [2]Rotaxane. *Angew. Chem. Int. Ed. Engl* **1997,** *36*, 1904-1907.
6. Zhu, N.; Nakazono, K.; Takata, T., Solid-State Rotaxane Switch: Synthesis of Thermoresponsive Rotaxane Shuttle Utilizing a Thermally Decomposable Acid. *Chem. Lett.* **2016,** *45*, 445-447.

7. Lehr, J.; Lang, T.; Blackburn, O. A.; Barendt, T. A.; Faulkner, S.; Davis, J. J.; Beer, P. D., Anion Sensing by Solution- and Surface-Assembled Osmium(II) Bipyridyl Rotaxanes. *Chem. Eur. J.* **2013,** *19*, 15898-15906.
8. Leigh, D. A.; Marcos, V.; Wilson, M. R., Rotaxane Catalysts. *ACS Catal.* **2014,** *4*, 4490-4497.
9. Blanco, V.; Leigh, D. A.; Marcos, V., Artificial switchable catalysts. *Chem. Soc. Rev.* **2015,** *44*, 5341-5370.
10. Hoekman, S.; Kitching, M. O.; Leigh, D. A.; Papmeyer, M.; Roke, D., Goldberg Active Template Syntehsis of a [2]Rotaxane Ligand for Asymmetric Transition-Metal Catalysis. *J. Am. Chem. Soc.* **2015,** *137*, 7656-7659.
11. Bruns, C. J.; Stoddart, J. F., Rotaxane-Based Molecular Muscles. *Acc. Chem. Res.* **2014,** *47*, 2186-2199.
12. Du, G.; Moulin, E.; Jouault, N.; Buhler, E.; Giuseppone, N., Muscle-like Supramolecular Polymers: Integrated Motion from Thousands of Molecular Machines. *Angew. Chem. Int. Ed.* **2012,** *51*, 12504-12508.
13. McGonigal, P. R.; Stoddart, J. F., A Molecular porduction line. *Nat. Chem.* **2013,** *5*, 260-262.
14. Lewandowski, B.; De Bo, G.; Ward, J. W.; Papmeyer, M.; Kuschel, S.; Aldegunde, M. J.; Gramlich, P. M. E.; Heckmann, D.; Goldup, S. M.; D'Souza, D. M.; Fernandes, A. E.; Leigh, D. A., Sequence-Specific Peptide Synthesis by an Artificial Small-Moleucule Machine. *Science* **2013,** *339*, 189-193.
15. Smithrud, D. B.; Powers, L.; Lunn, J.; Abernathy, S.; Peschka, M.; Ho, S.-M.; Tarapore, P., A Ca2+ Selective Host Rotaxane is Highly Toxic Against Prostate Cancer Cells. *ACS Med. Chem. Lett.* **2017**.
16. Barat, R.; Legigan, T.; Tranoy-Opalinski, I.; Renoux, B.; Peraudeau, E.; Clarhaut, J.; Poinot, P.; Fernandes, A. E.; Aucagne, V.; Leigh, D. A.; Papot, S., A mechanically interlocked molecular system programmed for the delivery of an anticancer drug. *Chem. Sci.* **2015,** *6*, 2608-2613.
17. Zheng, B.; Wang, F.; Dong, S.; Huang, F., Supramolecular polymers constructed by crown ether-based molecular recognition. *Chem. Soc. Rev.* **2012,** *41*, 1621-1636.
18. Huang, F.; Nagvekar, D. S.; Zhou, X.; Gibson, H. W., Formation of a Linear Supramolecular Polymer by Self-Assembly of Two Homoditopic Monomers Based on the Bis(m-phenylene)-32-crown-10/Paraquat Recognition Motif. *Macromolecules* **2007,** *40*, 3561-3567.
19. Wang, X.-Q.; Wang, W.; Wang, Y.-X.; Yang, H.-B., Supramoleuclar Polymers Constructed through Self-sorting Host-Guest Interactions. *Chem. Lett.* **2015,** *44*, 1040-1046.
20. Arunachalam, M.; Gibson, H. W., Recent Developments in polypseudorotaxanes and polyrotaxanes. *Prog. Polym. Sci.* **2014,** *39*, 1043-1073.

21. Li, S.-L.; Xiao, T.; Lin, C.; Wang, L., Advanced supramolecular polymers constructed by orthoganol self-assembly. *Chem. Soc. Rev.* **2012,** *41*.

22. Zhang, M.; Xu, D.; Yan, X.; Chen, J.; Dong, S.; Zheng, B.; Huang, F., Self-Healing Supramoleulcar Gels Formed by Crown Ether Based Host-Guest Interactions. *Angew. Chem. Int. Ed.* **2012,** *51*, 7011-7015.

23. Zhan, J.; Zhang, M.; Zhou, M.; Liu, B.; Chen, D.; Liu, Y.; Chen, Q.; Qiu, H.; Yin, S., A Multiple-Responsive Self-Healing Supramolecular Polymer Gel Network Based on Multiple Orthoganal Interactions. *Macromol. Rapid Commun.* **2014,** *35*.

24. Lipeng, H.; Liang, J.; Cong, Y.; Chen, X.; Bu, W., Concentration and acid-base controllable fluorescence of a metallosupramoleuclar polymer. *Chem. Commun.* **2014,** *50*.

25. Ogawa, T.; Nakazono, K.; Aoki, D.; Uchida, S.; Takata, T., Effective Approach to Cyclic Polymer from Linear Polymer: Synthesis and Transformation of Macromolecular [1]Rotaxane. *ACS Macro Lett.* **2015,** *4*.

26. Valentina, S.; Ogawa, T.; Nakazono, K.; Aoki, D.; Takata, T., Efficient Synthesis of Cyclic Block Copolymers by Rotaxane Protocal by Linear/ Cyclic Topology Transformation. *Chem. Eur. J.* **2016,** *22*, 8759-8762.

27. Aoki, D.; Uchida, S.; Takata, T., Star/Linear Polymer Topology Transformation Facilitated by Mechanical Linking of Polymer Chains. *Angew. Chem. Int. Ed.* **2015,** *54*, 6770-6774.

28. Sato, H.; Aoki, D.; Takata, T., Synthesis and Star/Linear Topology Transformation of a Mechanically Linked ABC Terpolymer. *ACS Macro Lett.* **2016,** *5*, 699-703.

29. Yamaguchi, N.; Gibson, H. W., Formation of Supramolecular Polymers from Homoditopic Molecules Containing Secondary Ammonium Ions and Crown Ether Moieties. *Angew. Chem. Int. Ed.* **1999,** *38*, 143-147.

30. Yamaguchi, N.; Nagvekar, D. S.; Gibson, H. W., Self-Organization of a Heteroditopic Molecule to Linear Polymolecular Arrays in Solution. *Angew. Chem. Int. Ed.* **1998,** *37*, 2361-2364.

31. Lee, M.; Schoonover, D. V.; Gies, A. P.; Hercules, D. M.; Gibson, H. W., Synthesis of Complementary Host- and Guest-Functionalized Polymeric Building Blocks and Their Self-Assembling Behavior. *Macromolecules* **2009,** *42*, 6483-6494.

32. Gibson, H. W.; Ge, Z.; Huang, F.; Jones, J. W.; Lefebvre, H.; Vergne, M. J.; Hercules, D. M., Syntheses and Model Complexation Studies of Well-Defined Crown Terminated Polymers. *Macromolecules* **2005,** *38*, 2626-2637.

33. Gibson, H. W.; Yamaguchi, N.; Jones, J. W., Supramolecular Pseudorotaxane Polymers from Complementary Pairs of Homoditopic Molecules. *J. Am. Chem. Soc.* **2002,** *125*, 3522-3533.

34. Ji, X.; Yao, Y.; Li, J.; Yan, X.; Huang, F., A Supramolecular Cross-Linked Conjugated Polymer Network for Multiple Fluorescent Sensing. *J. Am. Chem. Soc.* **2013,** *135*, 74-77.

35. Wang, P.; Gao, Z.; Yuan, M.; Zhu, J.; Wang, F., Mechanically linked poly[2]rotaxanes constructed from the benzo-21-crown-7/secondary ammonium salt recognition motif. *Polym. Chem.* **2016,** *7*, 3664-3668.

36. Wang, F.; Zhang, J.; Ding, X.; Dong, S.; Liu, M.; Zheng, B.; Li, S.; Wu, L.; Yu, Y.; Gibson, H. W.; Huang, F., Metal Coordination Mediated Reversible Conversion between Linear and Cross-Linked Supramolecular Polymers. *Angew. Chem. Int. Ed.* **2010,** *49*, 1090-1094.

37. Wessels, H. R.; Gibson, H. W., Multi-gram syntheses of four crown ethers using K+ as templating agent. *Tetrahedron* **2016,** *72*, 396-399.

38. Pederson, A. M. P.; Ward, E. M.; Schoonover, D. V.; Slebodnick, C.; Gibson, H. W., High-Yielding, Regiospecific Synthesis of cis(4,4')-Di(carbomethoxybenzo)-30-crown-10, Its Conversion to a Pyridyl Cryptand and Strong Complexation of 2,2'- and 4,4'-Bipyridinium Derivatives. *J. Org. Chem.* **2008,** *73*, 9094-9101.

39. Huang, F.; Nagvekar, D. S.; Slebodnick, C.; Gibson, H. W., A Supramolecular Triarm Star Polymer from a Homotritopic Tris(Crown Ether) Host and a Complementary Monotopic Paraquat-Terminated Polystyrene Guest by a Supramolecular Coupling Method. *J. Am. Chem. Soc.* **2005,** *127*, 484-485.

40. Lee, M.; Moore, R. B.; Gibson, H. W., Supramolecular Pseudorotaxane Graft Copolymer from a Crown Ether Polyester and a Complementary Paraquat-Terminated Polystyrene Guest. *Macromolecules* **2011,** *44*, 5987-5993.

41. Bryant, W. S.; Jones, J. W.; Mason, P. E.; Guzei, I.; Rheingold, A. L.; Fronczek, F. R.; Nagvekar, D. S.; Gibson, H. W., A New Cryptand: Synthesis and Complexation with Paraquat. *Org. Lett.* **1999,** *1*, 1001-1004.

42. Huang, F.; Fronczek, F. R.; Gibson, H. W., First supramolecular poly(taco complex). *Chem. Commun.* **2003**, 1480-1481.

43. Li, S.; Zhu, K.; Zheng, B.; Wen, X.; Li, N.; Huang, F., A Bis(m-phenylene)-32-crown-10/Paraquat [2]Rotaxane. *Eur. J. Org. Chem* **2009**, 1053-1057.

44. Allwood, B. L.; Specer, N.; Shahriari-Zavareh; Stoddart, J. F.; Williams, D. J., Complexation of Paraquat by a bisparaphenylene-34-crown-10 derivative. *J. Chem. Soc., Chem. Commun.* **1987**, 1064-1066.

45. Niu, Z.; Slebodnick, C.; Bonrad, K.; Huang, F.; Gibson, H. W., The First [2]Pseudorotaxane and the First Pseudocryptand-Type Poly[2]pseudorotaxaen Based on Bis(*meta*-phenylene)-32-Crown-10 and Paraquat Derivatives. *Org. Lett.* **2011,** *13*, 2872-2875.

46. Suhan, N. D.; Allen, L.; Gharib, M. T.; Viljoen, E.; Vella, S. J.; Loeb, S. J., Color coding the co-conformations of a [2]rotaxane flip-switch. *Chem. Commun.* **2011,** *47*, 5991-5993.

47. Bryant, W. S.; Guzei, I. A.; Rheingold, A. L.; Gibson, H. W., Unique "Cradled Barbell" Complex between a Secondary Diammonium Ion and Bis(m-phenylene)-32-crown-10. *Org. Lett.* **1999,** *1*, 47-50.

48. Huang, F.; Lam, M.; Mahan, E. J.; Rheingold, A. L.; Gibson, H. W., Promotion of host folding during the formation of a taco complex. *Chem. Commun.* **2005**.

49. Huang, F.; Switek, K. A.; Zakharov, L. N.; Fronczek, F. R.; Slebodnick, C.; Lam, M.; Golen, J. A.; Bryant, W. S.; Mason, P. E.; Rheingold, A. L.; Ashraf-Khorassani, M.; Gibson, H. W., Bis(*m*-phenylene)-32-crown-10-Based Cryptands, Powerful Hosts for Paraquat Derivatives. *J. Org. Chem.* **2005,** *70*, 3231-3241.

50. Zhang, M.; Luo, Y.; Zhen, B.; Yan, X.; Fronczek, F. R.; Huang, F., Improved Pseudorotaxane and Catenane Formation from a Derivative of Bis(m-phenylene)-32-crown-10. *Eur. J. Org. Chem* **2010**, 6798-6803.

51. Dotz, F.; Brand, J. D.; Ito, S.; Gherghel, L.; Mullen, K., Synthesis of Large Polycyclic Aromatic Hydrocarbons: Variation of Size and Periphery. *J. Am. Chem. Soc.* **2000,** *122*, 7707-7717.

52. Skorobogatyi, M. V.; Pchelintseva, A. A.; Petrunina, A. L.; Stepanova, I. A.; Andronova, V.; Galegov, G. A.; Malakhov, A. D.; Kroshun, V. A., 5-Alkynyl-20-deoxyuridines, containing bulky aryl groups: evaluation of structure–anti-HSV-1 activity relationship. *Tetrahedron* **2006,** *62*, 1279-1287.

53. Geuder, W.; Hunig, S.; Suchy, A., SINGLE AND DOUBLE BRIDGED VIOLOGENES AND INTRAMOLECULAR PIMERIZATION OF THEIR CATION RADICALS. *Tetrahedron* **1986,** *42*, 1665-1677.

54. CrysAlisPro Software System *Rigaku Oxford Diffraction*, v1.171.37.35; Rigaku Corporation: Oxford, UK, 2015.

55. Sheldrick, G. M., A short history of SHELX. *Acta Cryst.* **2008,** *A64*, 112-122.

56. Dolomanov, O. V.; Bourhis, L. J.; Gildea, R. J.; Howard, J. A.; Puschmann, H., *J. Appl. Cryst.* **2009,** *42*, 339-341.

Table of contents graphic

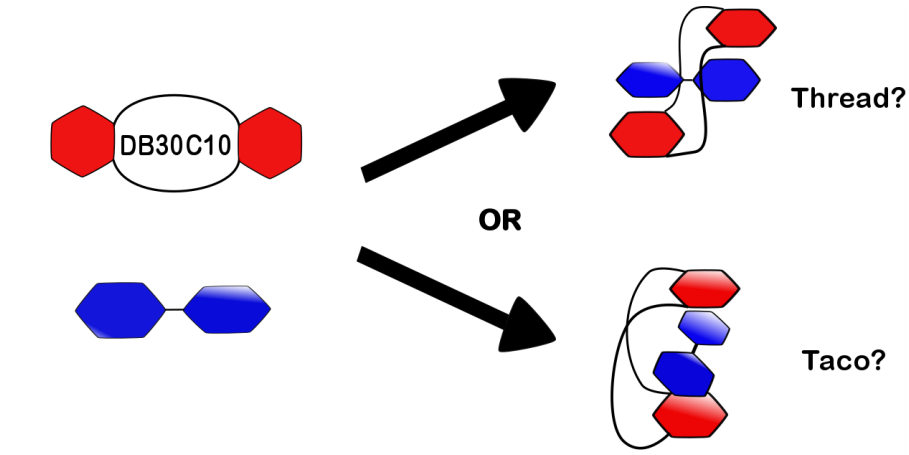

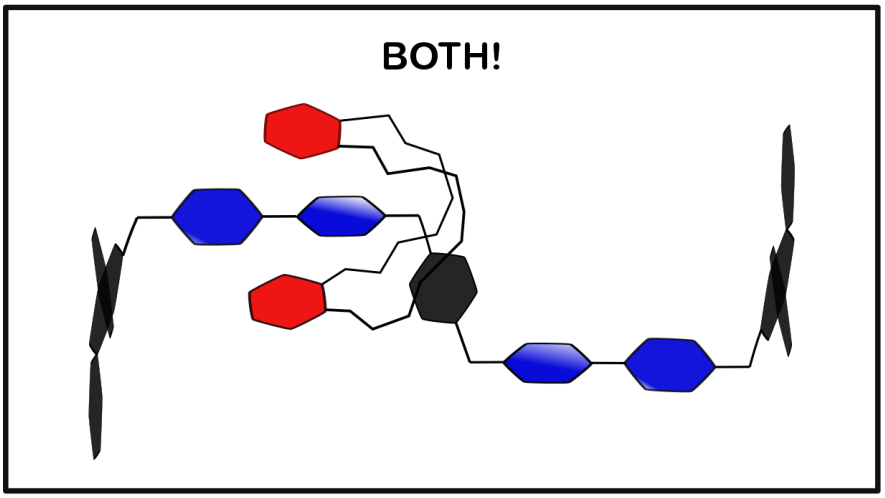

Characterization data of compounds (^{1}H NMR, ^{13}C NMR, HRMS)

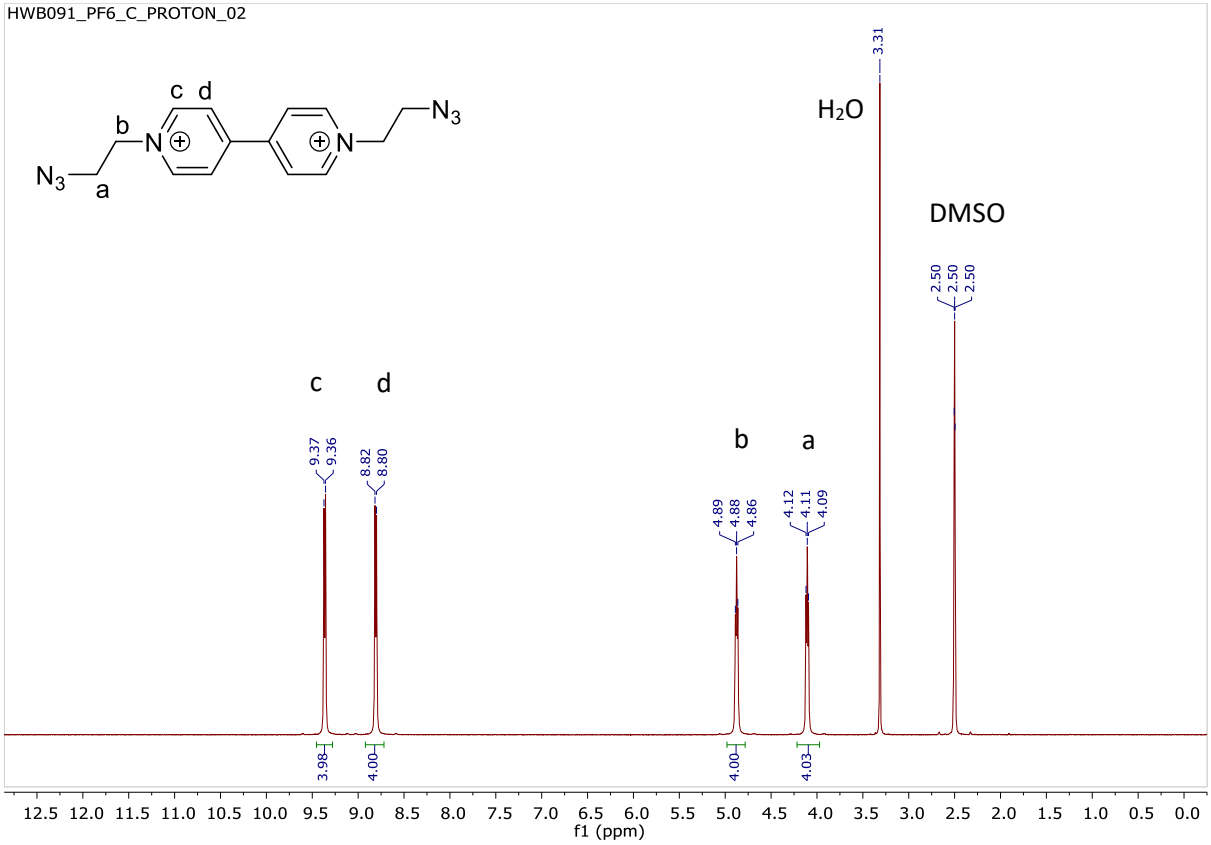

Figure 3.13. ^{1}H NMR spectrum of paraquat azide **10** in DMSO-d_6 at 400 MHz

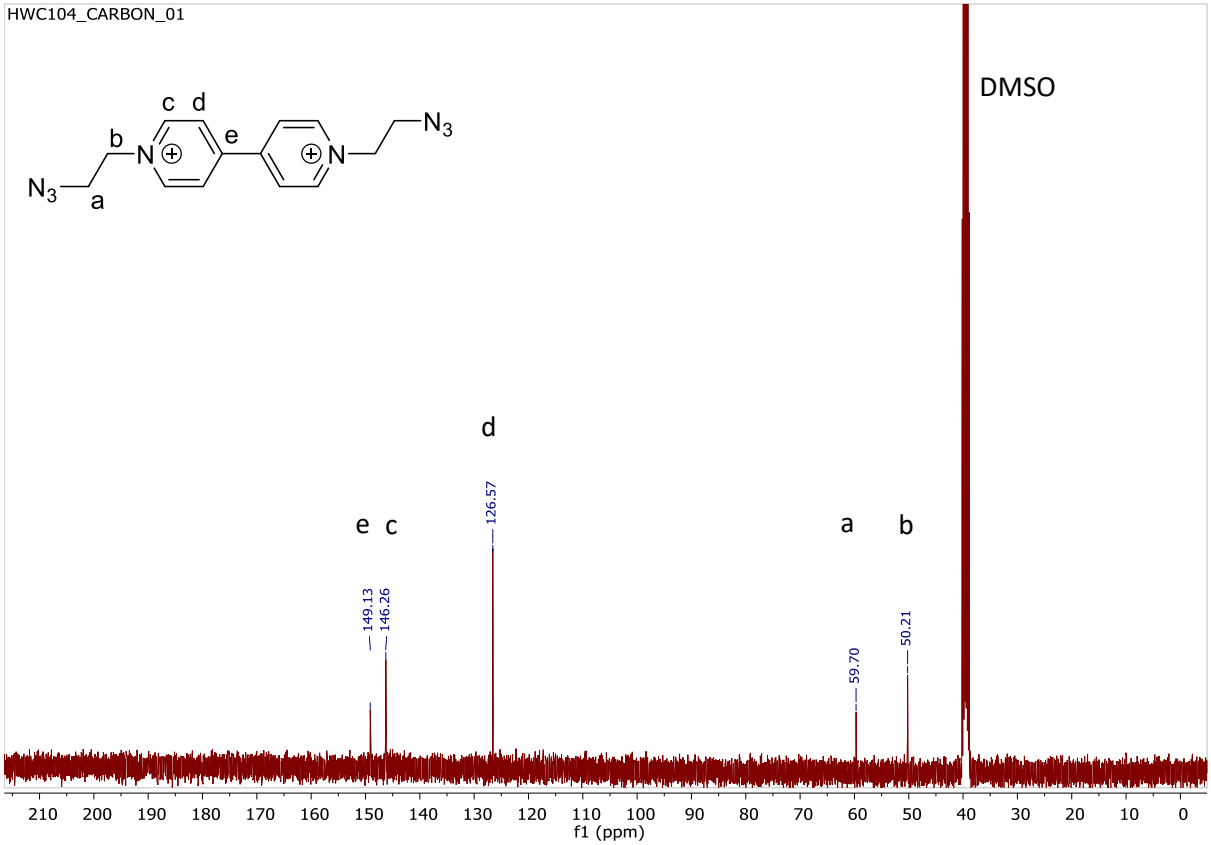

Figure 3.14.^{13}C NMR spectrum of paraquat azide **10** in DMSO-d_6 at 101 MHz

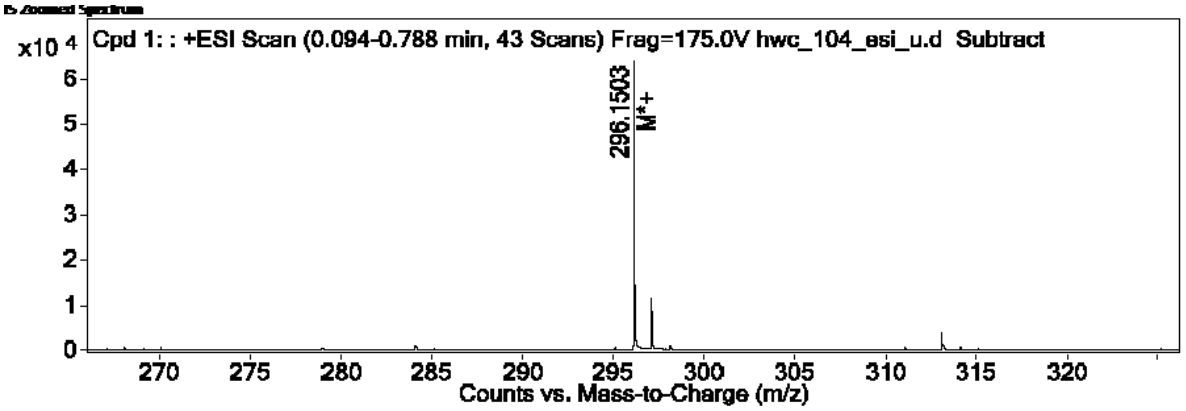

Figure 3.15. ESI-TOF HRMS of *N,N'*-bis(2''-azidoethyl)-[4,4'-bipyridium] Hexafluorophosphate

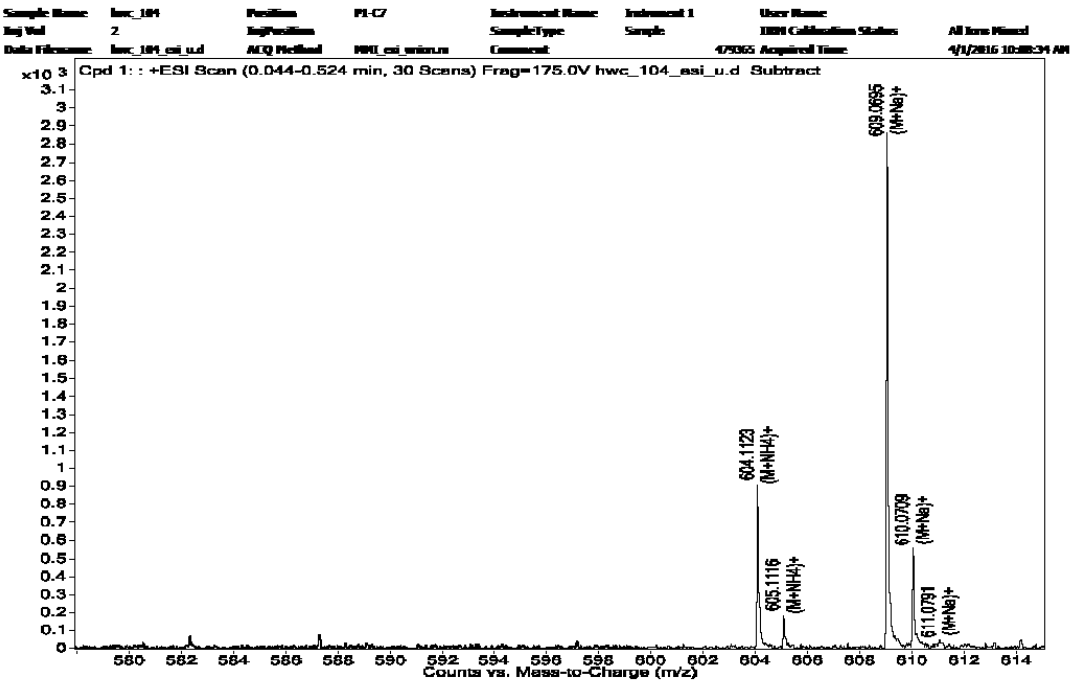

Figure 3.16. ESI-TOF HRMS of *N,N'*-bis(2''-azidoethyl)-[4,4'-bipyridium] Hexafluorophosphate

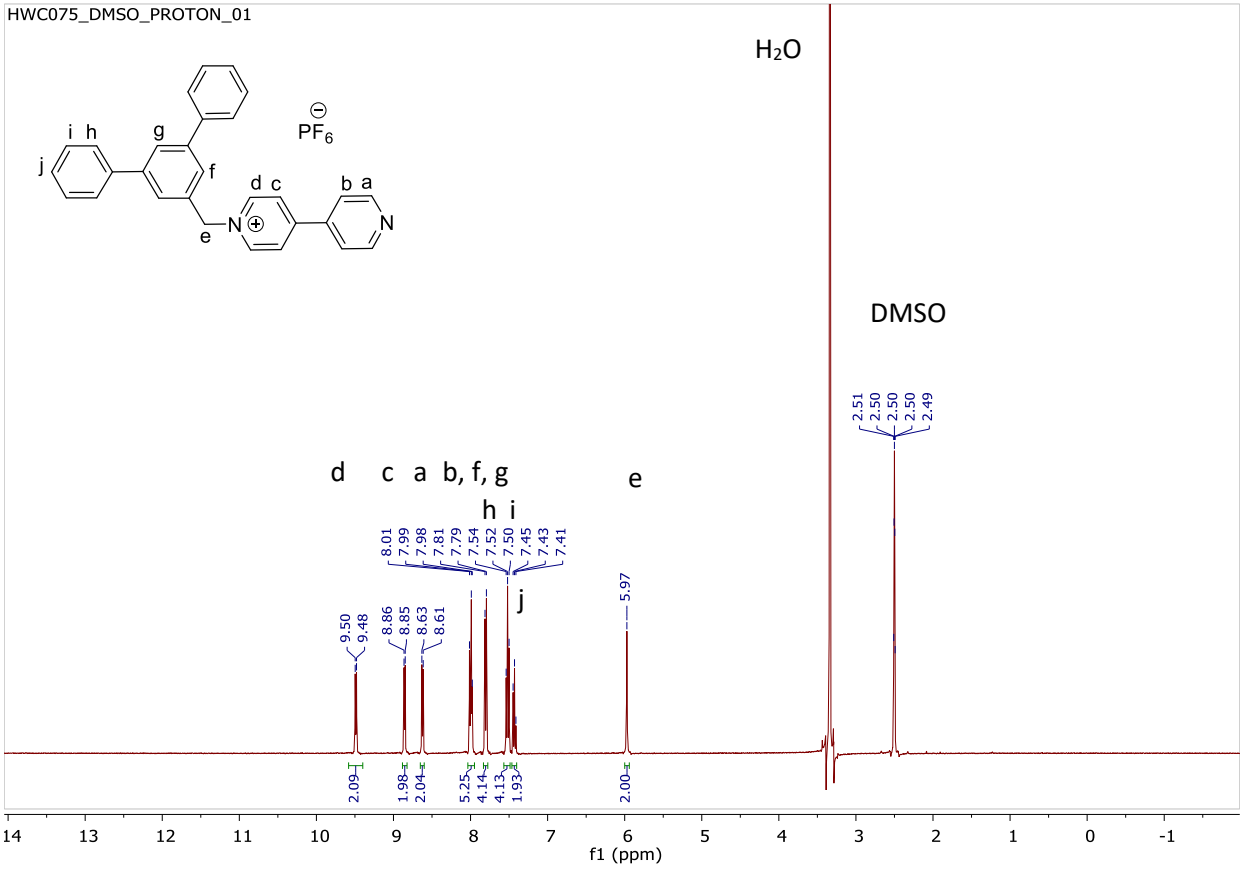

Figure 3.17. ^{1}H NMR spectrum of halfquat **3** in DMSO-d_6 at 400 MHz

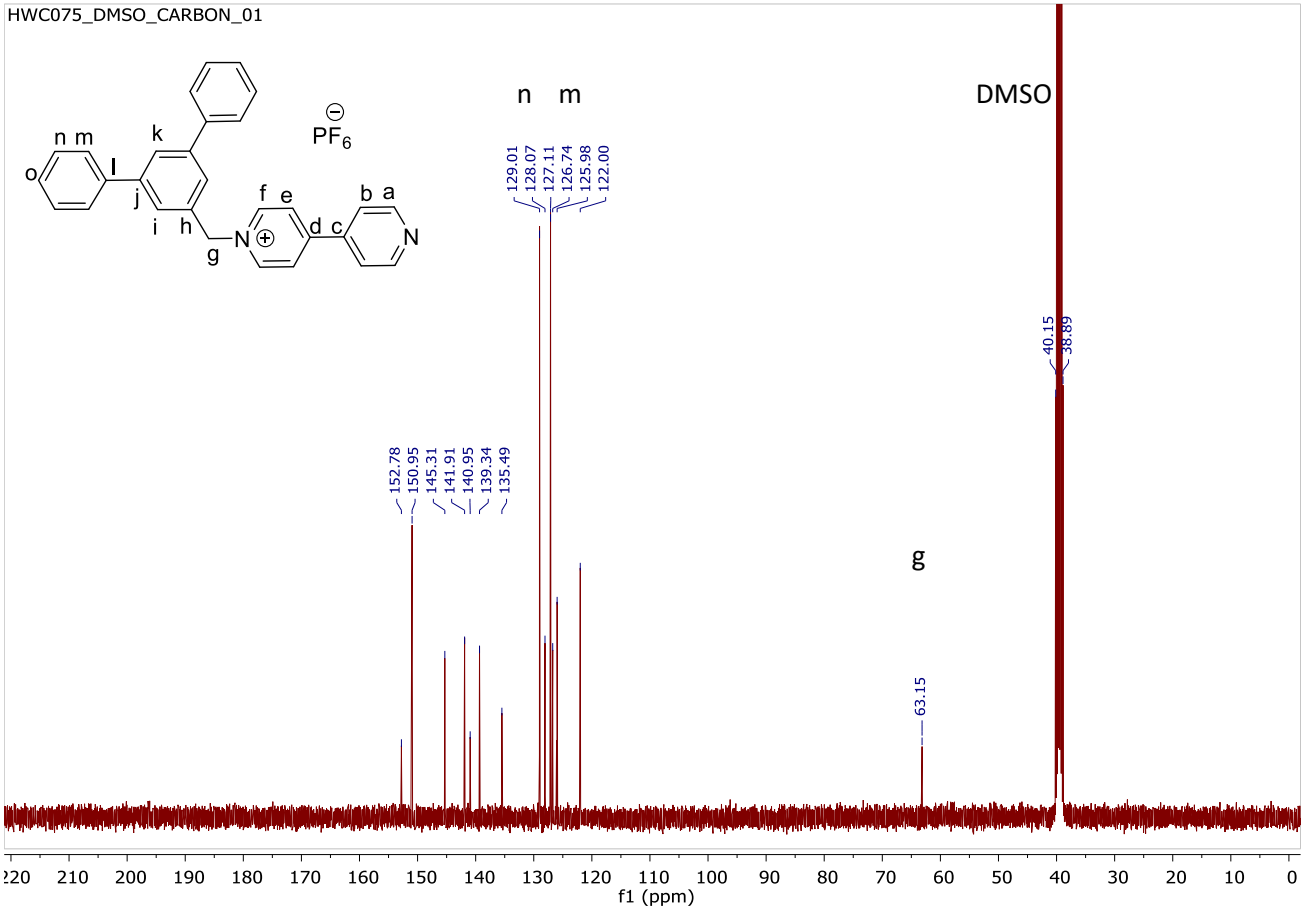

Figure 3.18. ^{13}C NMR spectrum of halfquat **3** in DMSO-d_6 at 101 MHz

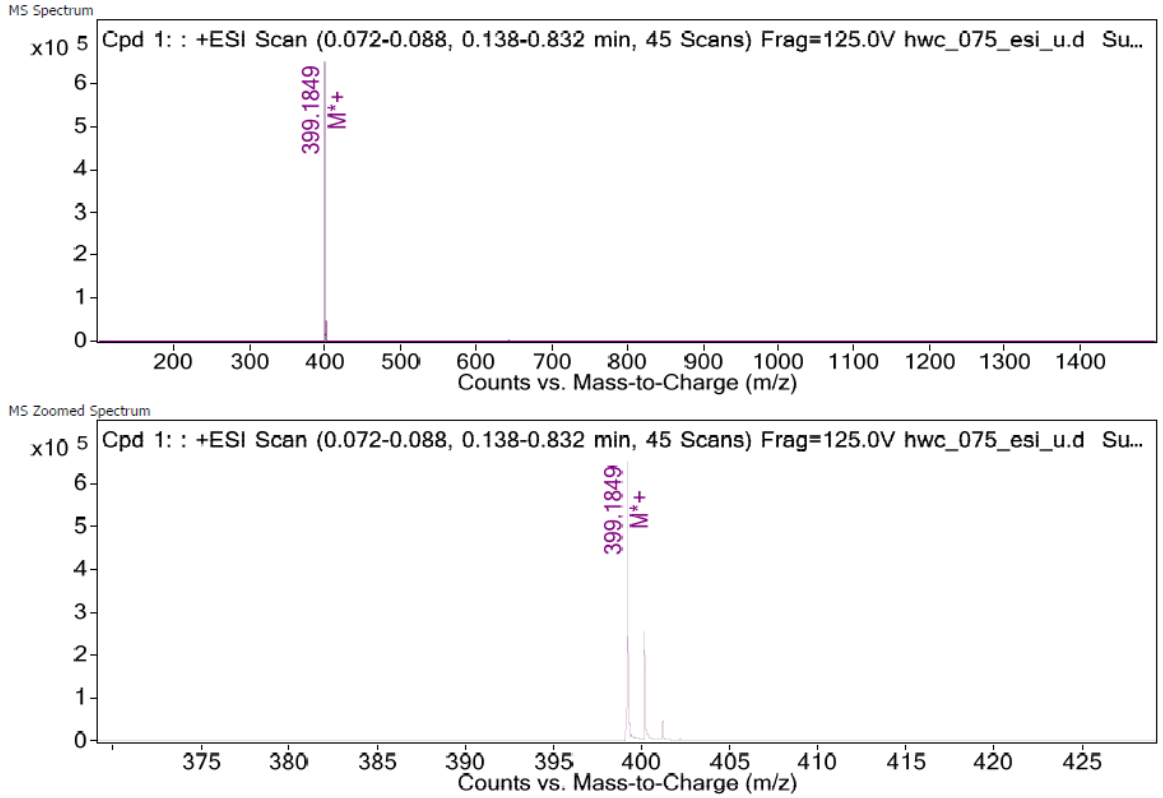

Figure 3.19. ESI-TOF HRMS of half-quat **3**

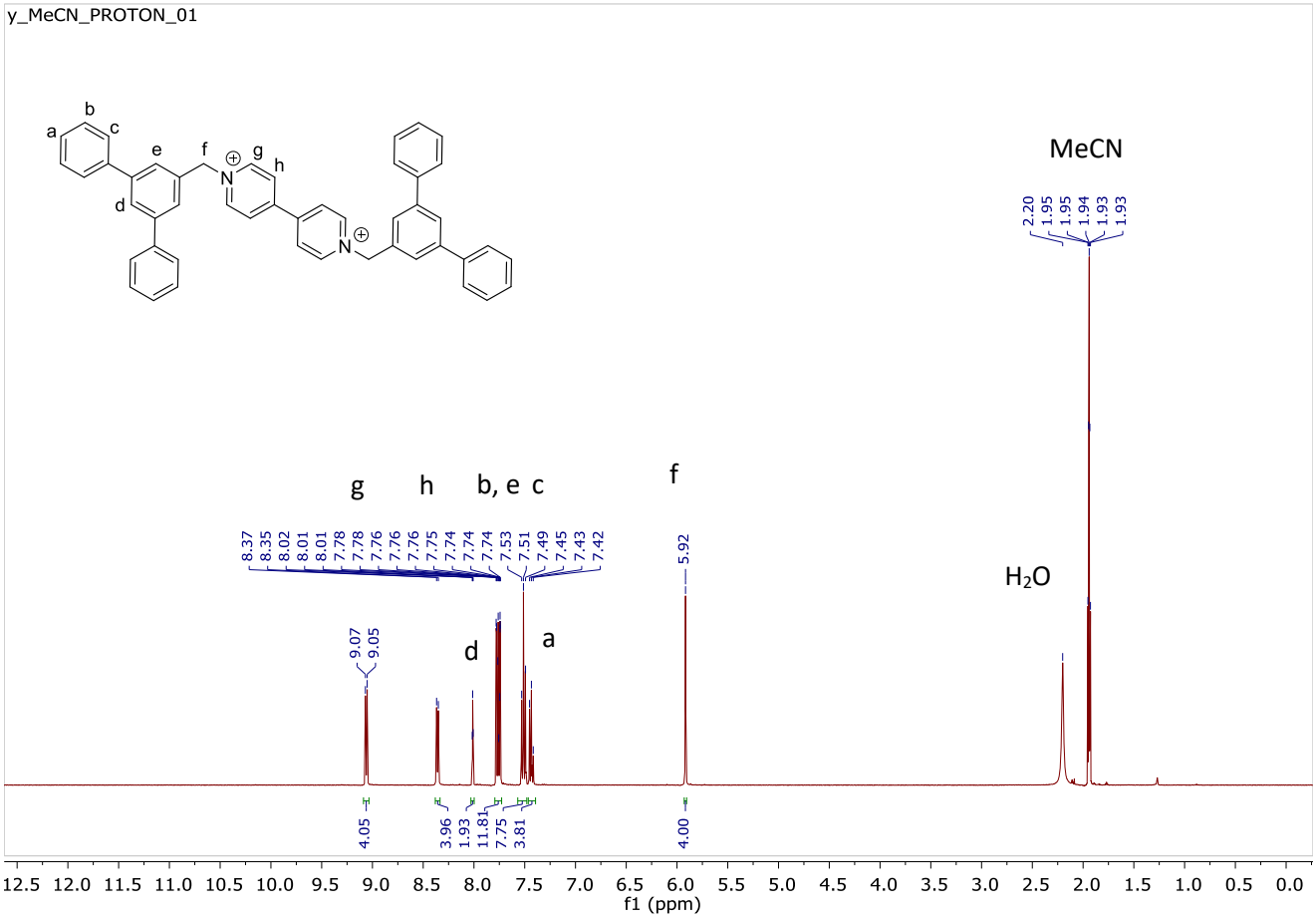

Figure 3.20. ^{1}H NMR spectrum of dumbbell **2** in MeCN-d_3 at 400 MHz

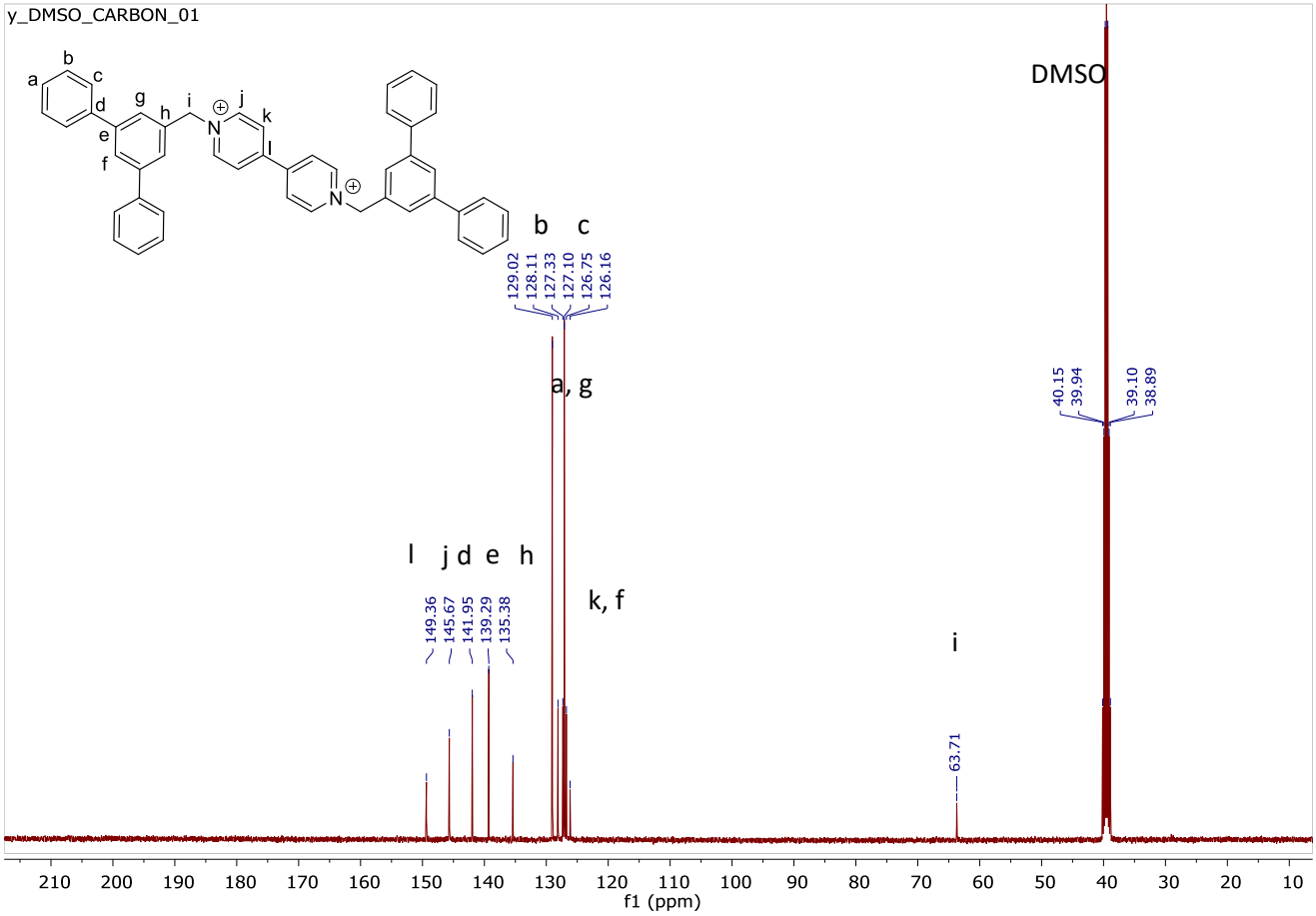

Figure 3.21. ^{13}C NMR spectrum of dumbbell **2** in DMSO-d_6 at 101 MHz

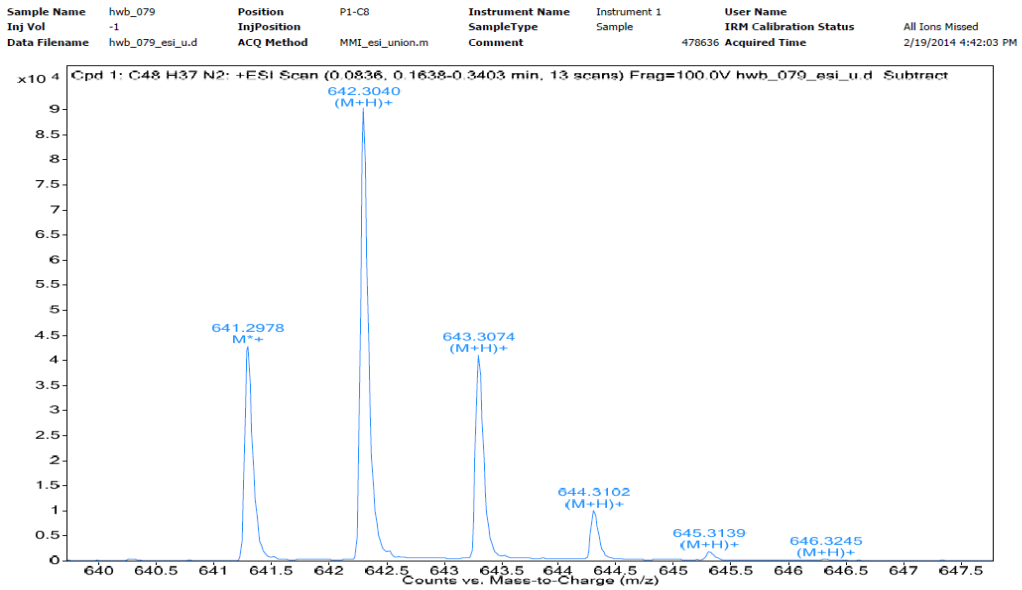

Figure 3.22. ESI-TOF HRMS of dumbbell **2**

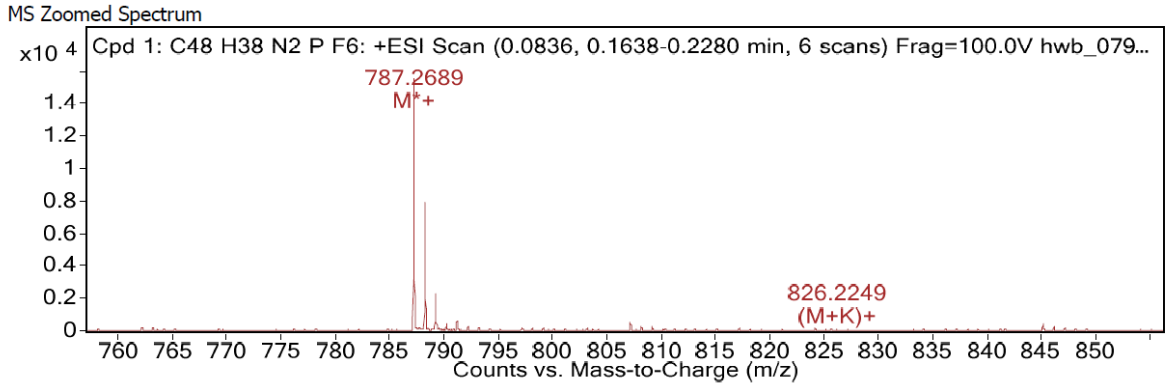

Figure 3.23. ESI-TOF HRMS of dumbbell **2**

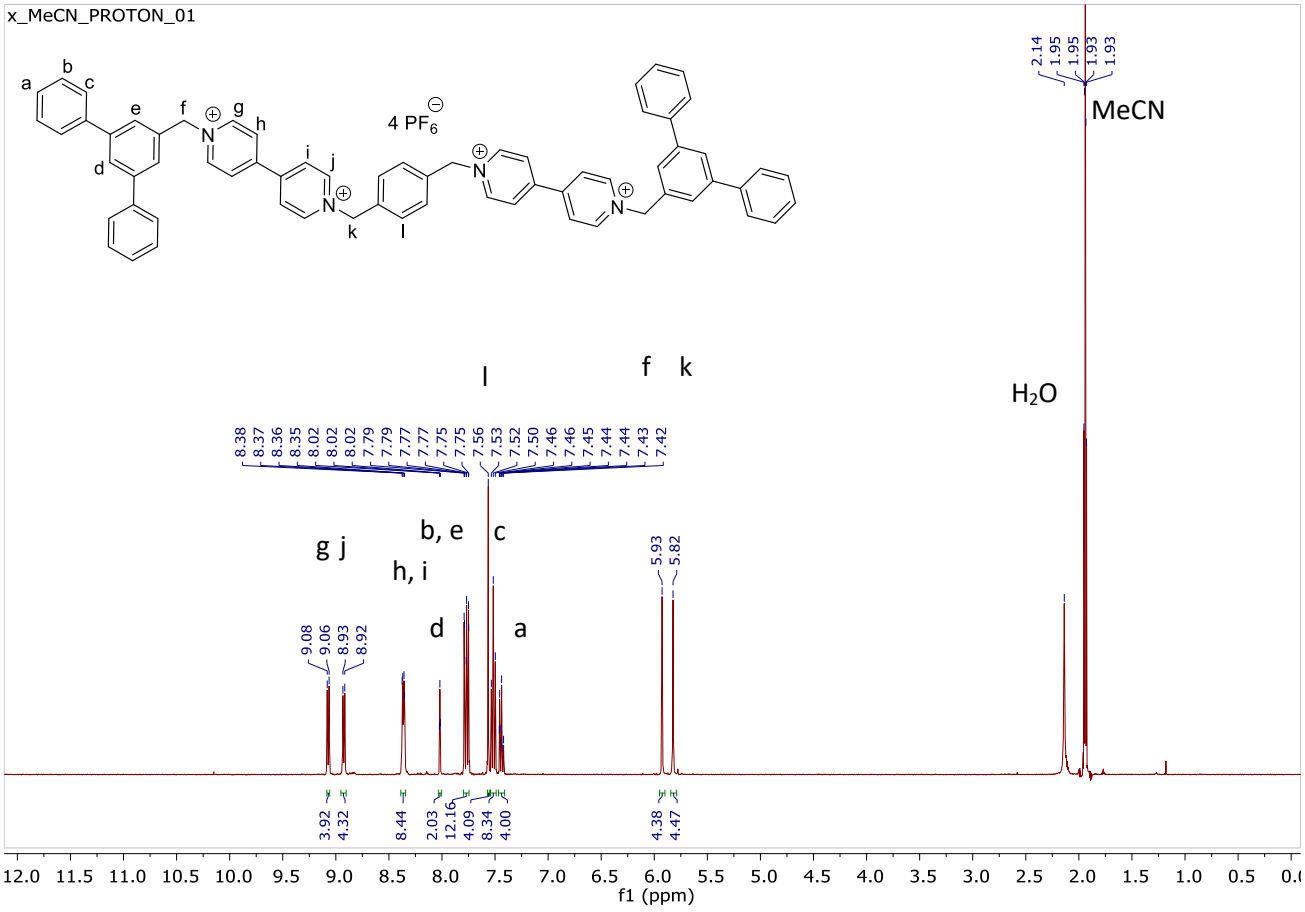

Figure 3.24. ^{1}H NMR spectrum of dumbbell **6** in MeCN-d_3 at 400 MHz

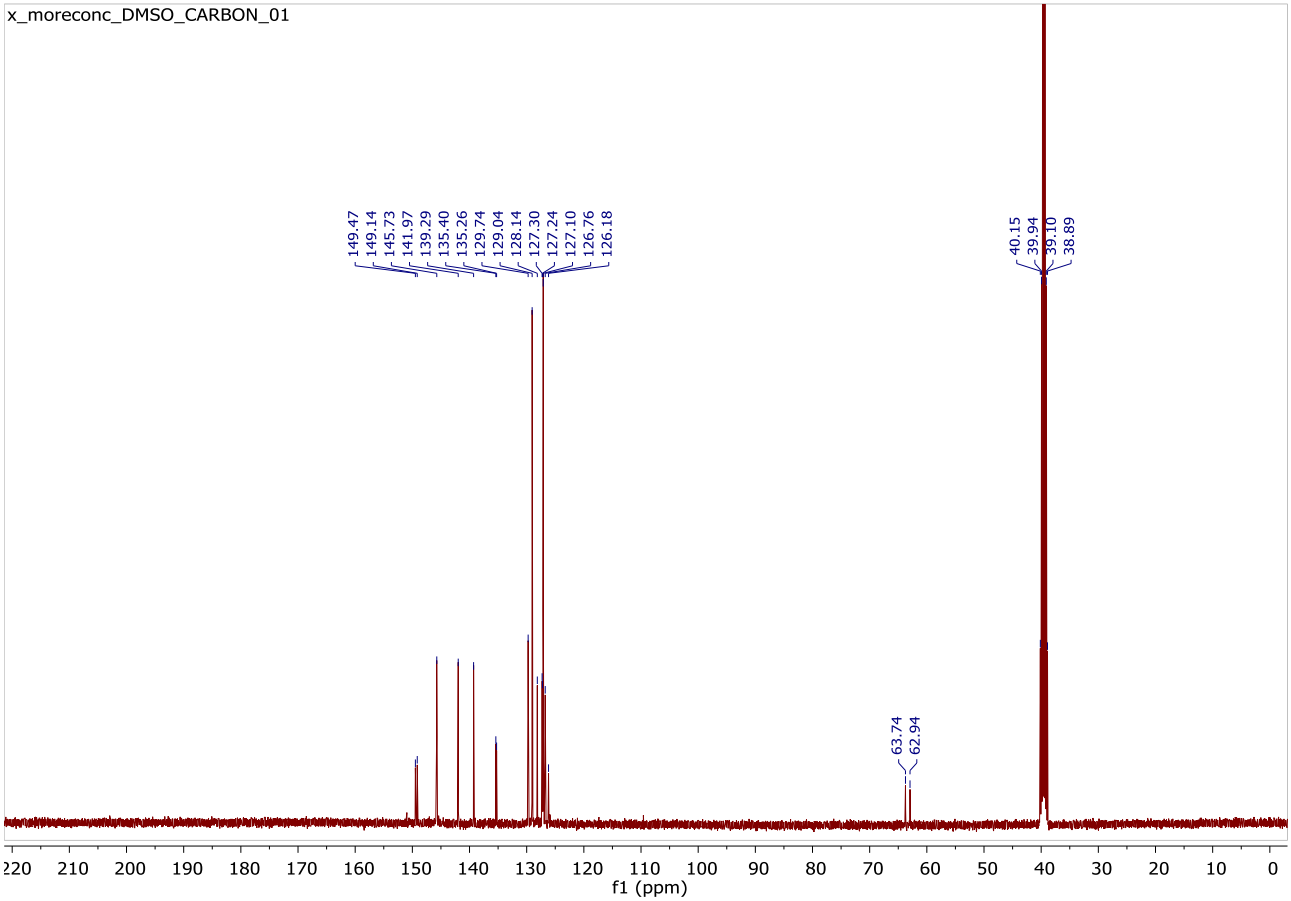

Figure 3.25. ^{13}C NMR spectrum of dumbbell **6** in DMSO-d_3 at 101 MHz

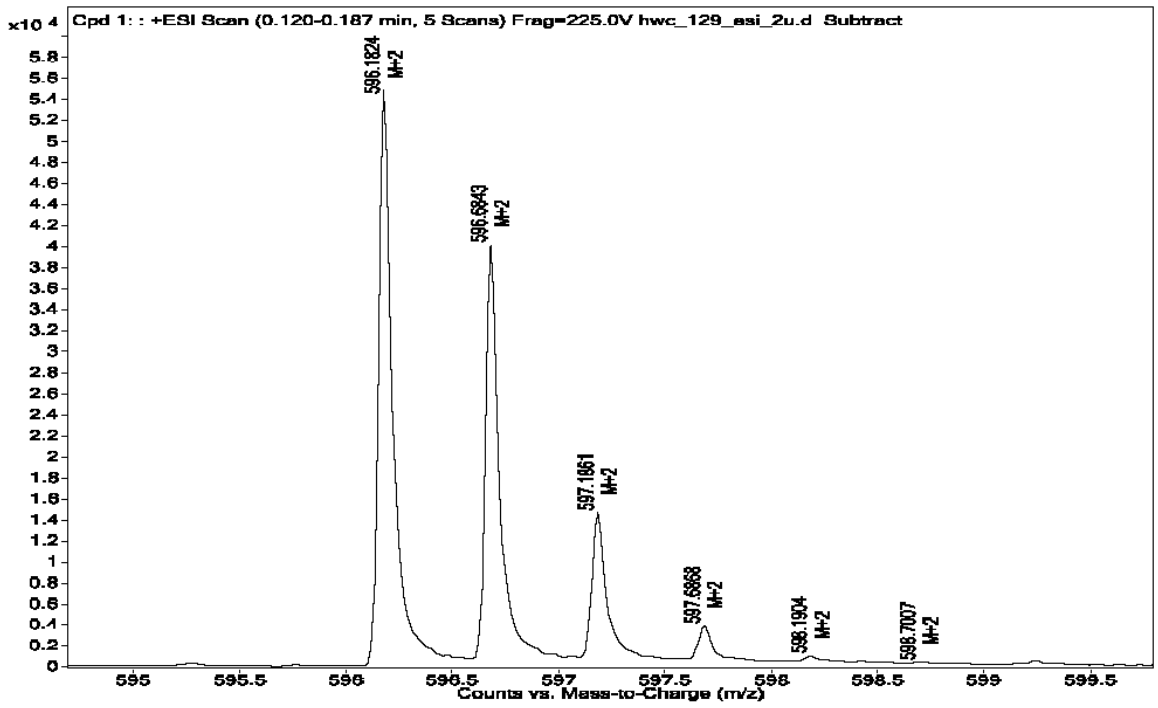

Figure 3.26. ESI-TOF HRMS of dumbbell **6**

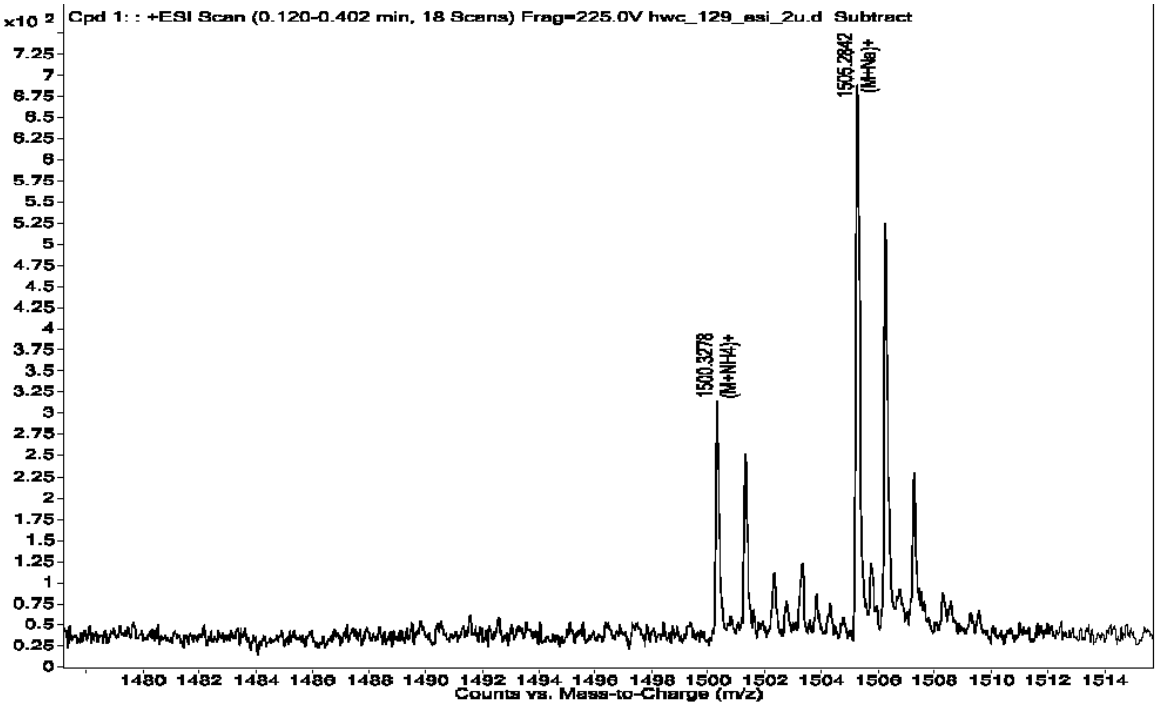

Figure 3.27. ESI-TOF HRMS of dumbbell **6**

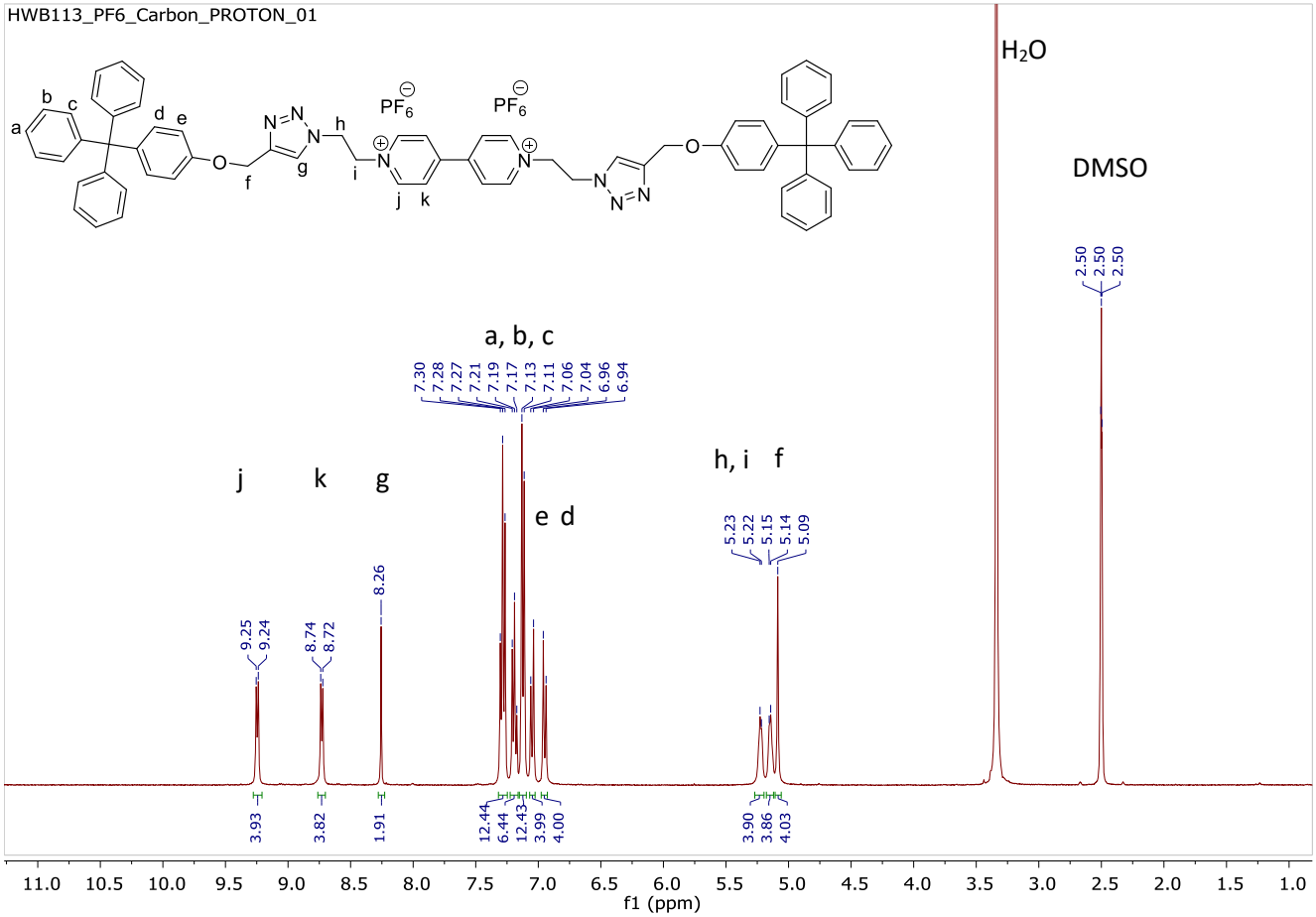

Figure 3.28. ^{1}H NMR spectrum of click dumbbell **11** in DMSO-d_6 at 400 MHz

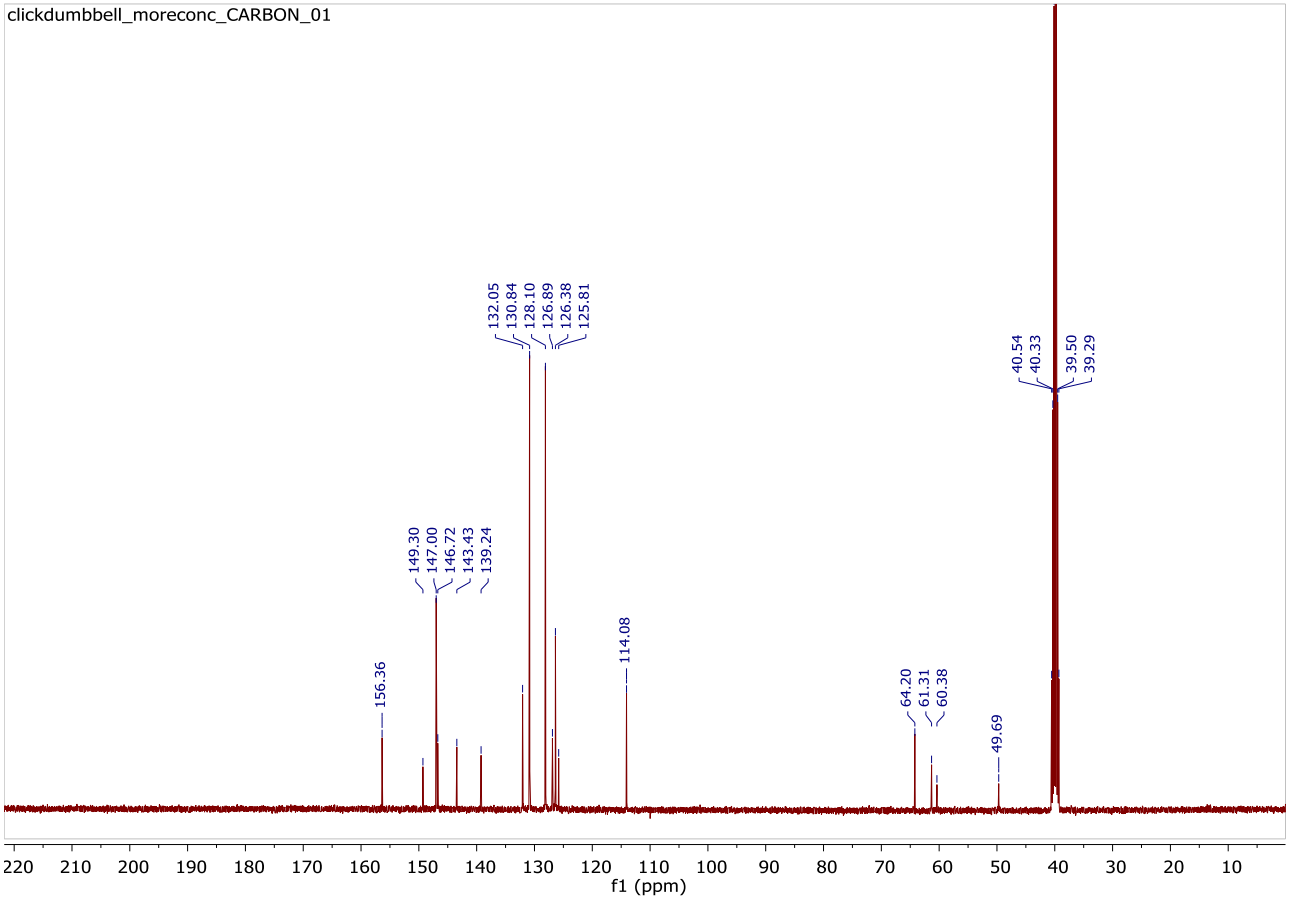

Figure 3.29. ^{13}C NMR spectrum of click dumbbell **11** in DMSO-d_6 at 101 MHz

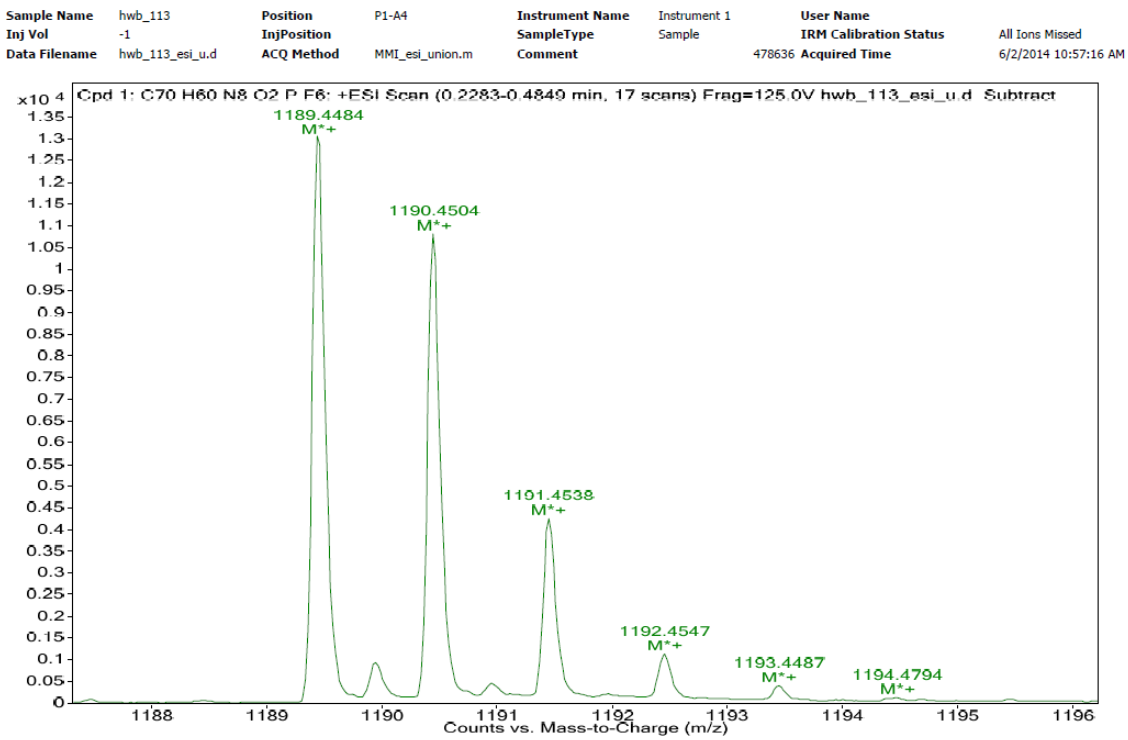

Figure 3.30. ESI-TOF HRMS of click dumbbell **11** M^{*+}

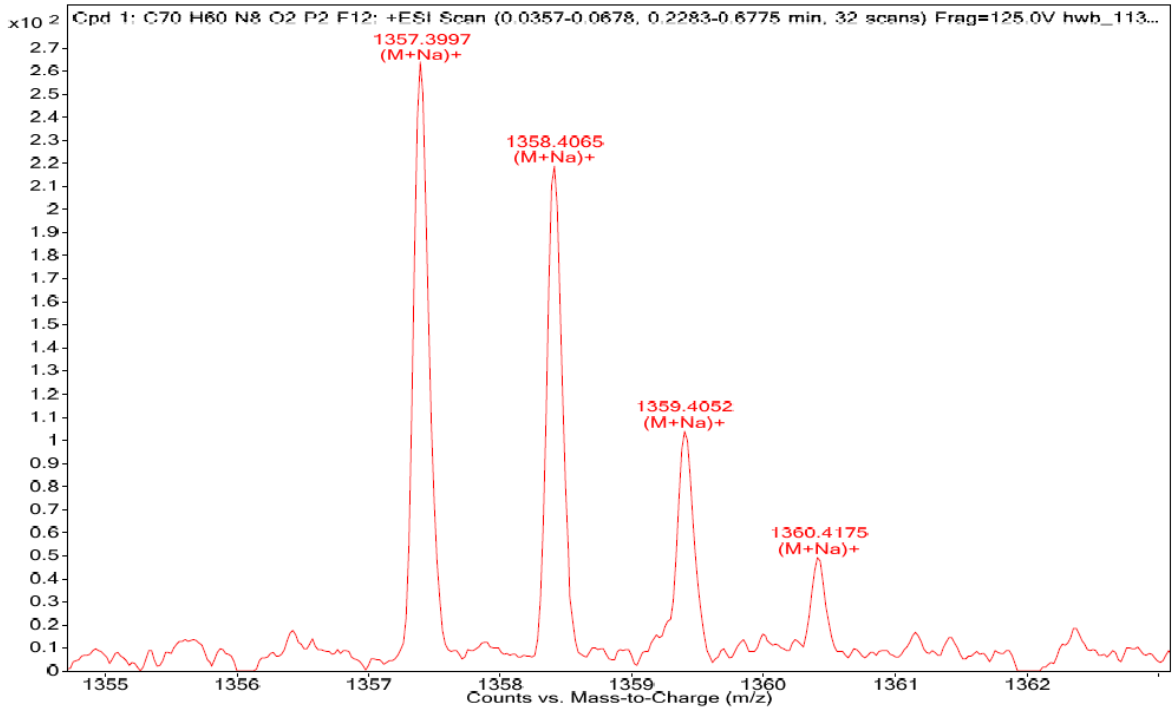

Figure 3.31. ESI-TOF HRMS of dumbbell **11** $(M+Na)^+$

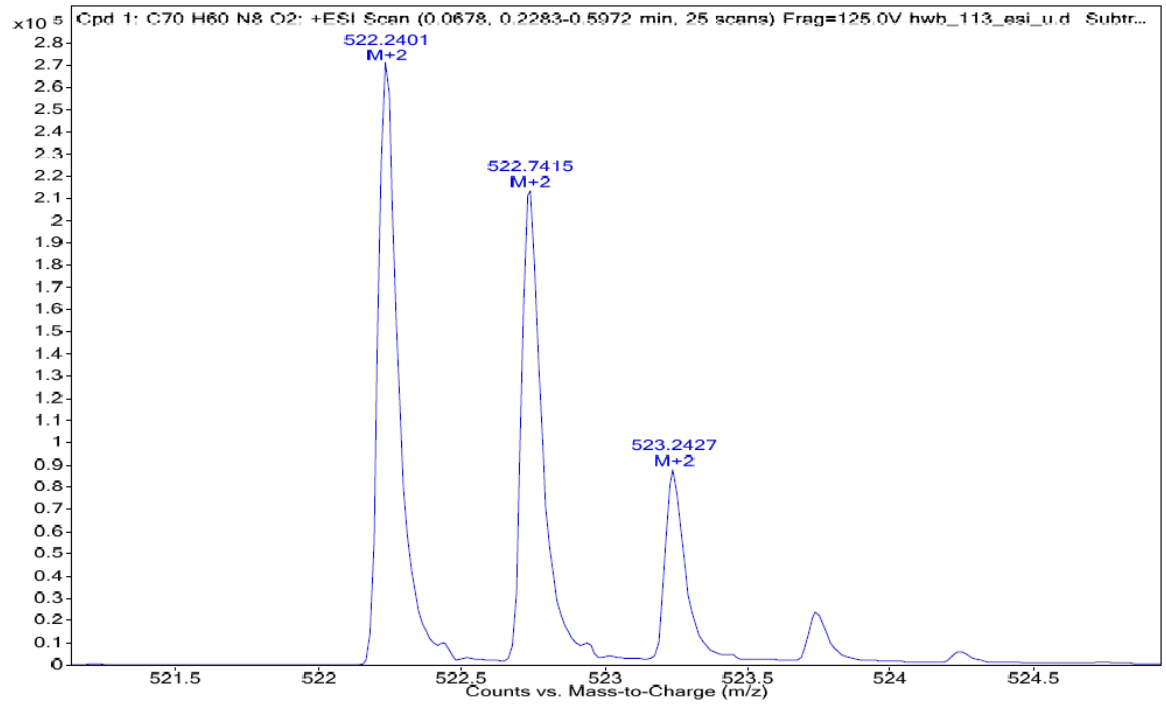

Figure 3.32. ESI-TOF HRMS of dumbbell **11** $(M-2PF_6)^{2+}$

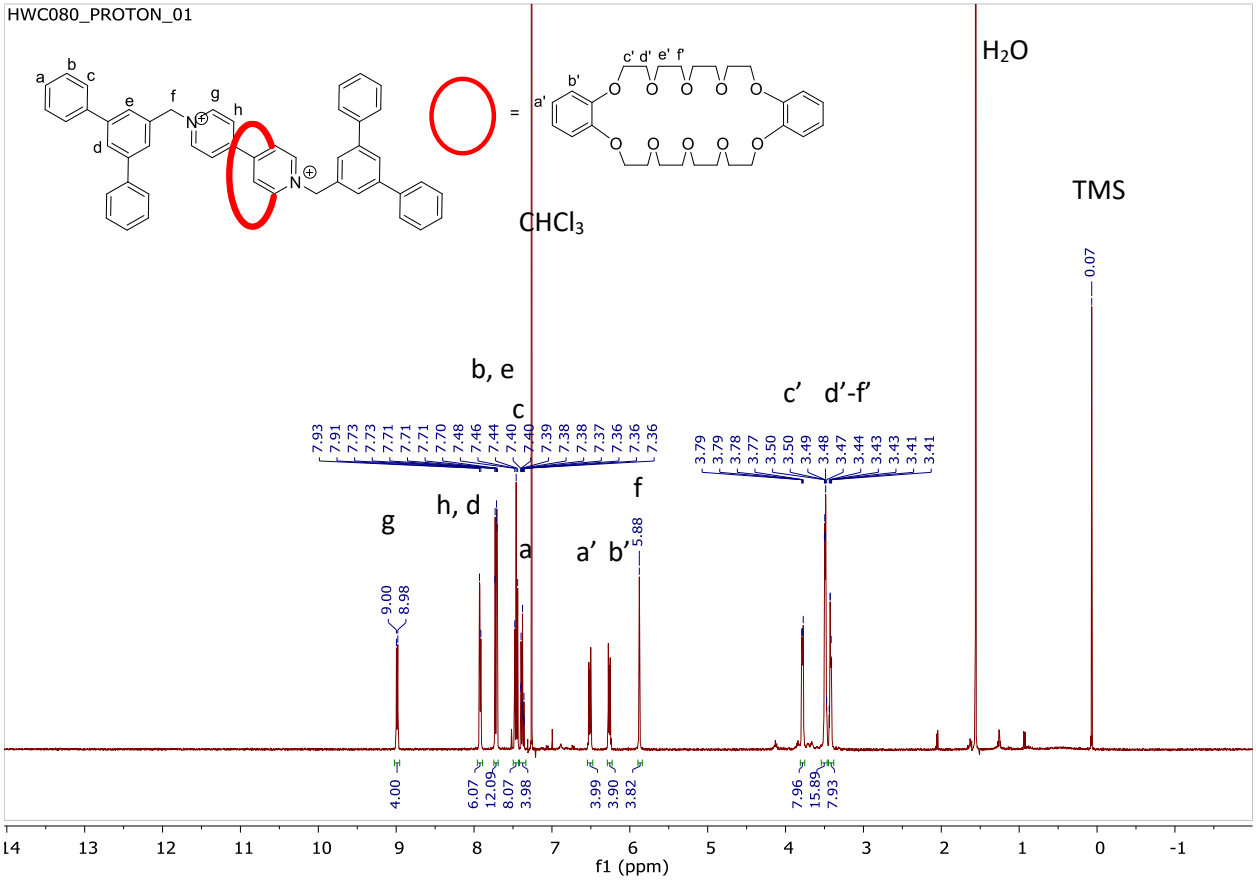

Figure 3.34. ^{1}H NMR of rotaxane **4** in $CDCl_3$ at 400 MHz

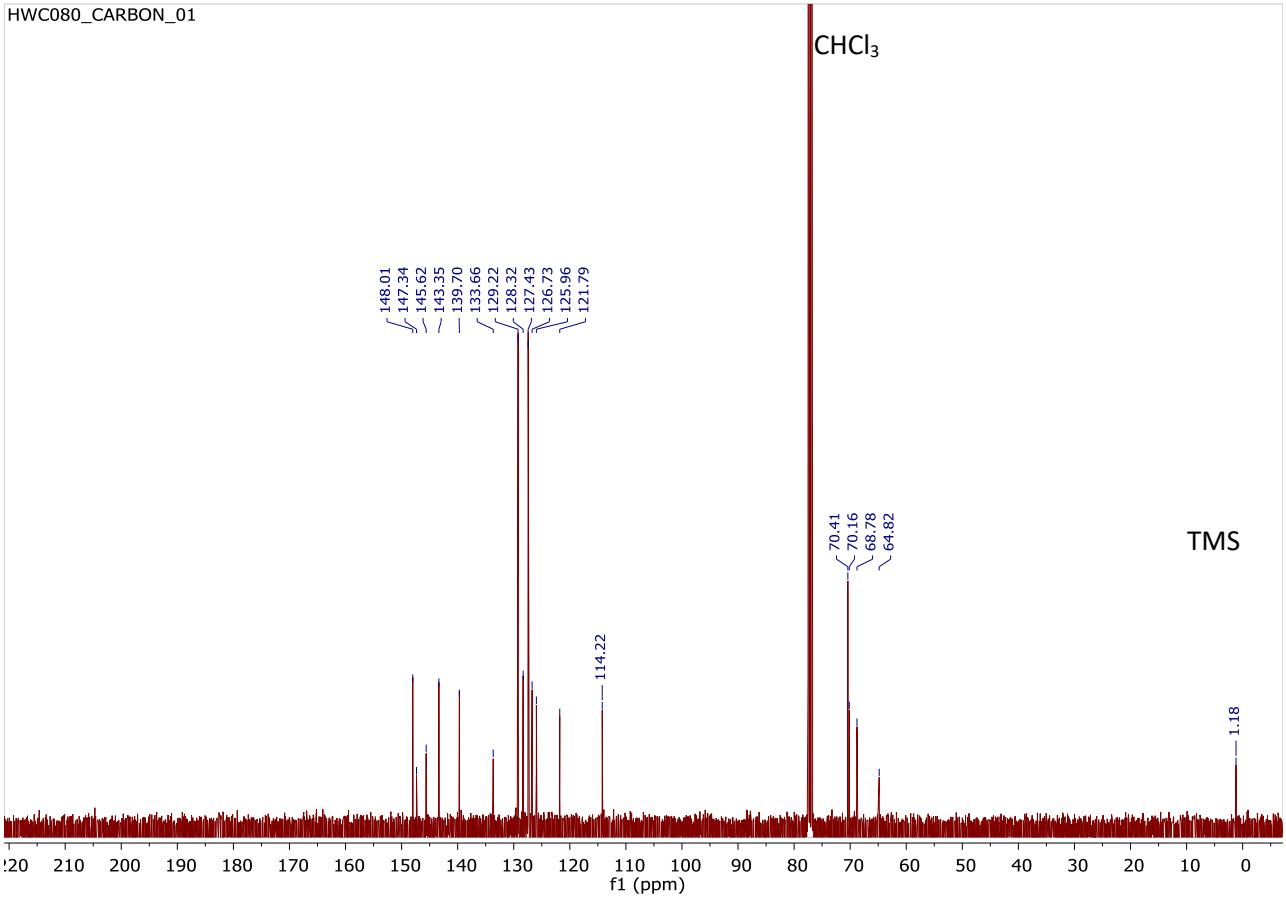

Figure 3.35. ^{13}C NMR spectrum of rotaxane **4** in $CDCl_3$ at 101 MHz

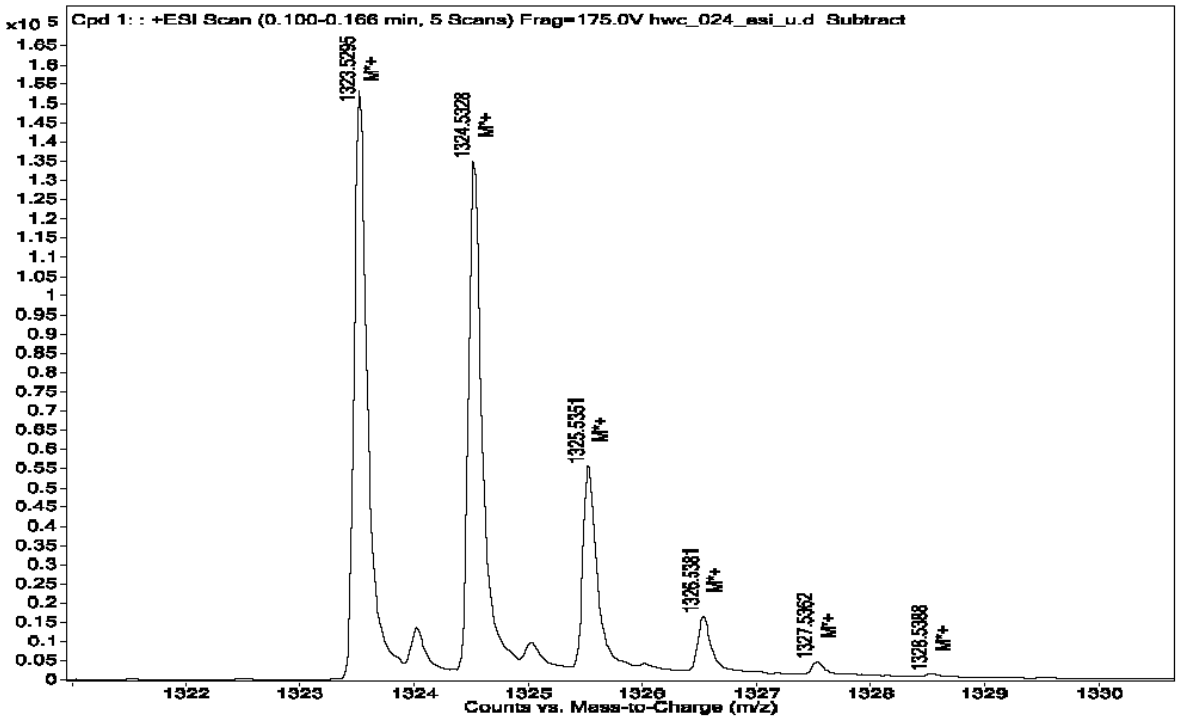

Figure 3.36. HRMS (ESI-TOF) of rotaxane **4** $(M\text{-}PF_6)^-$

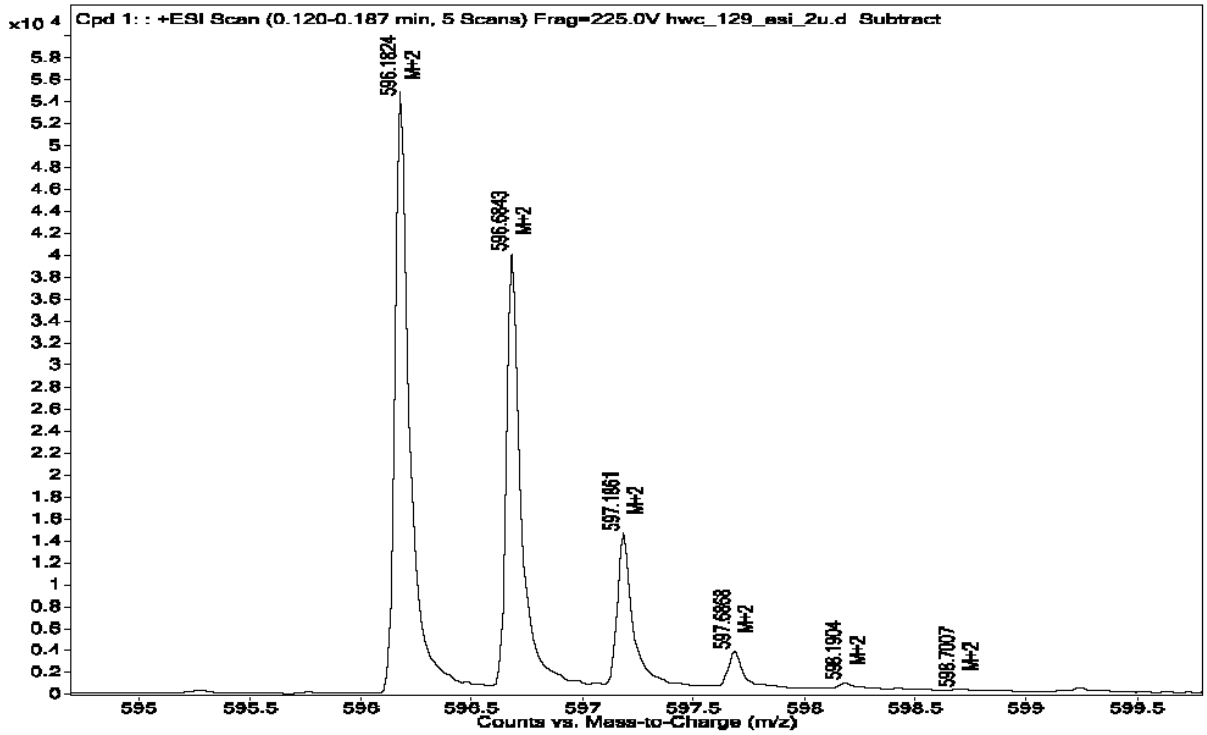

Figure 3.37. ESI-TOF HRMS of rotaxane **4** $(M\text{-}2PF_6)^+$

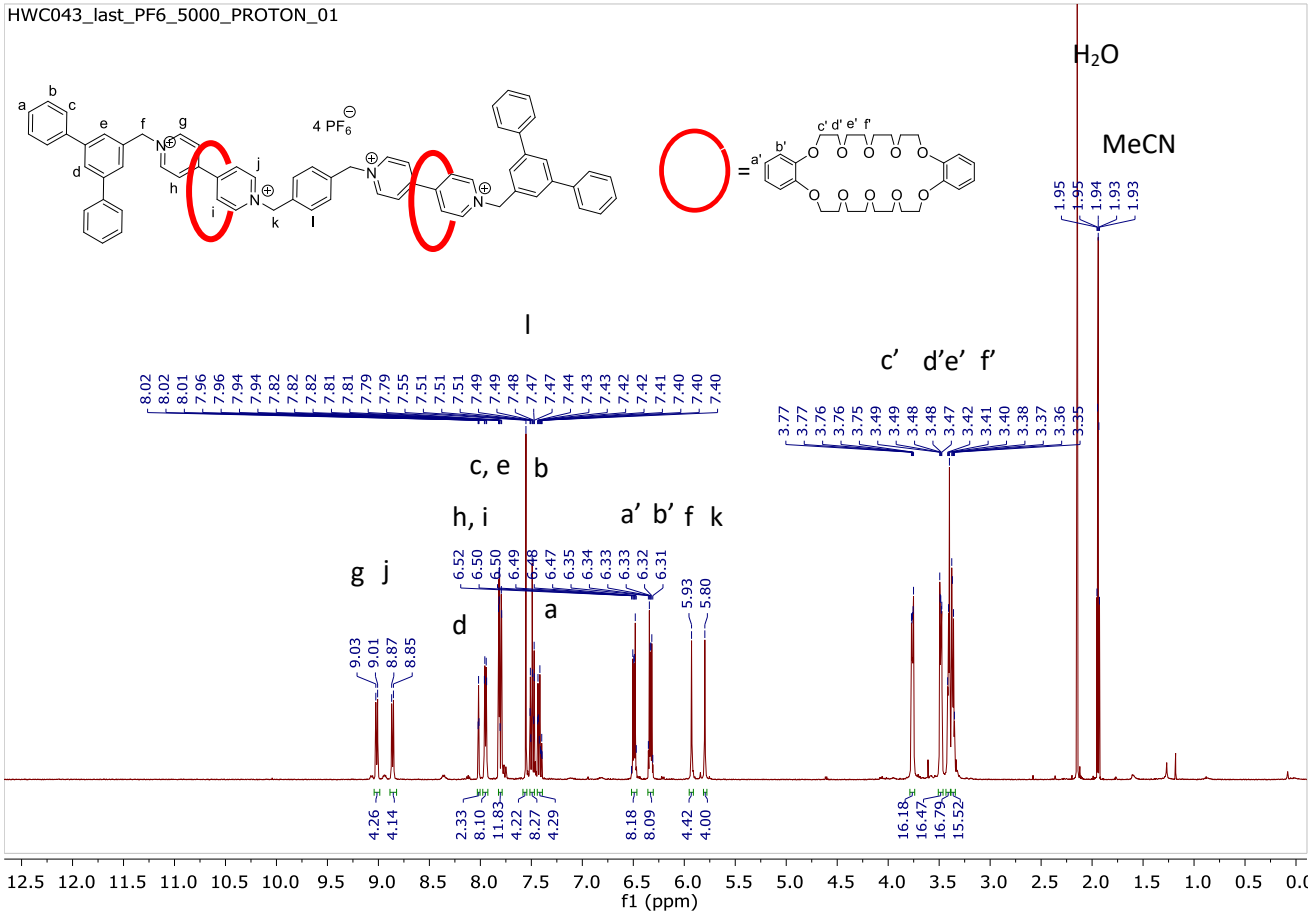

Figure 3.38. ^{1}H NMR spectrum of rotaxane **8** in MeCN-d_3 at 400 MHz

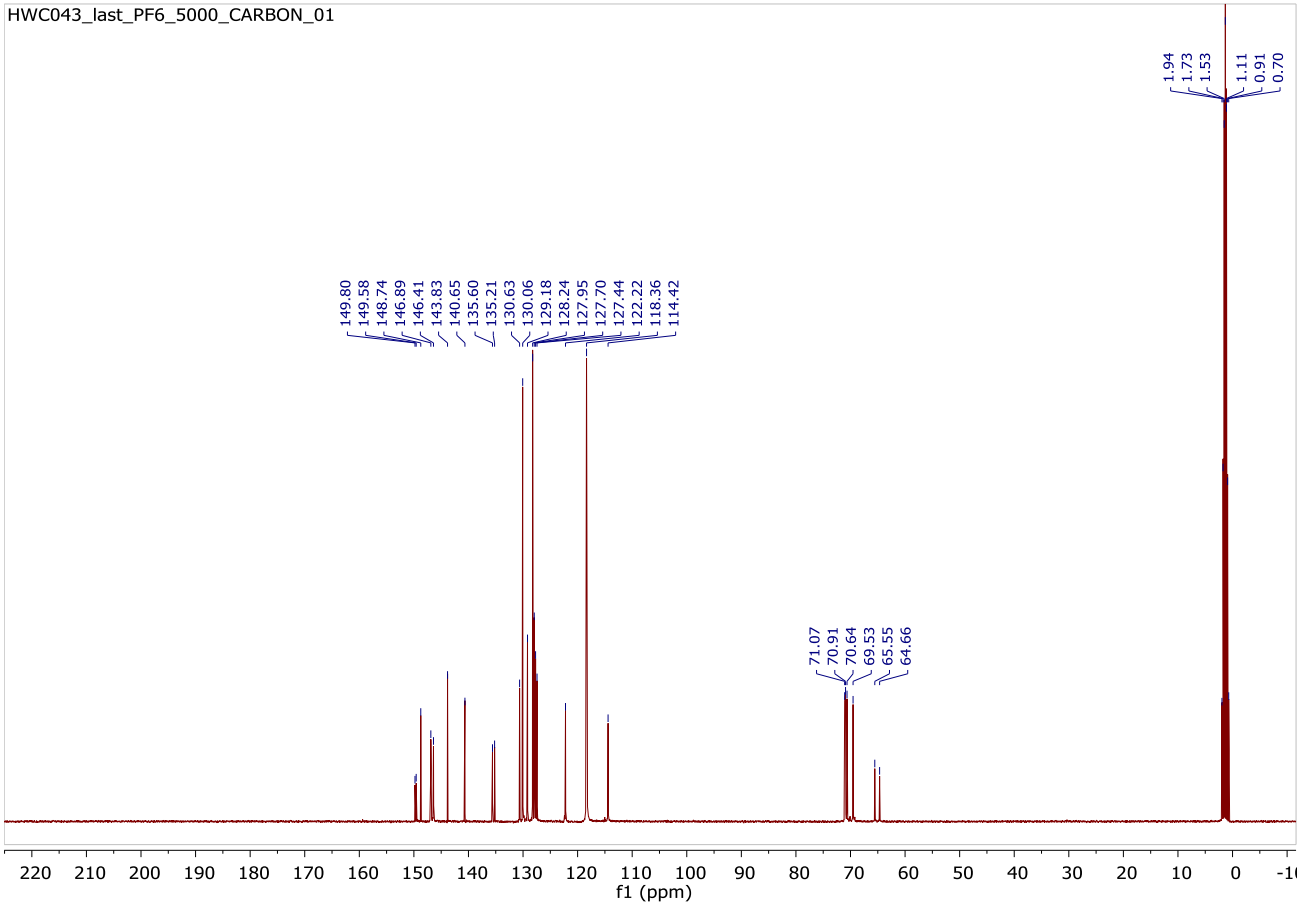

Figure 3.39. ^{13}C NMR spectrum of rotaxane **8** in MeCN-d_3 at 101 MHz

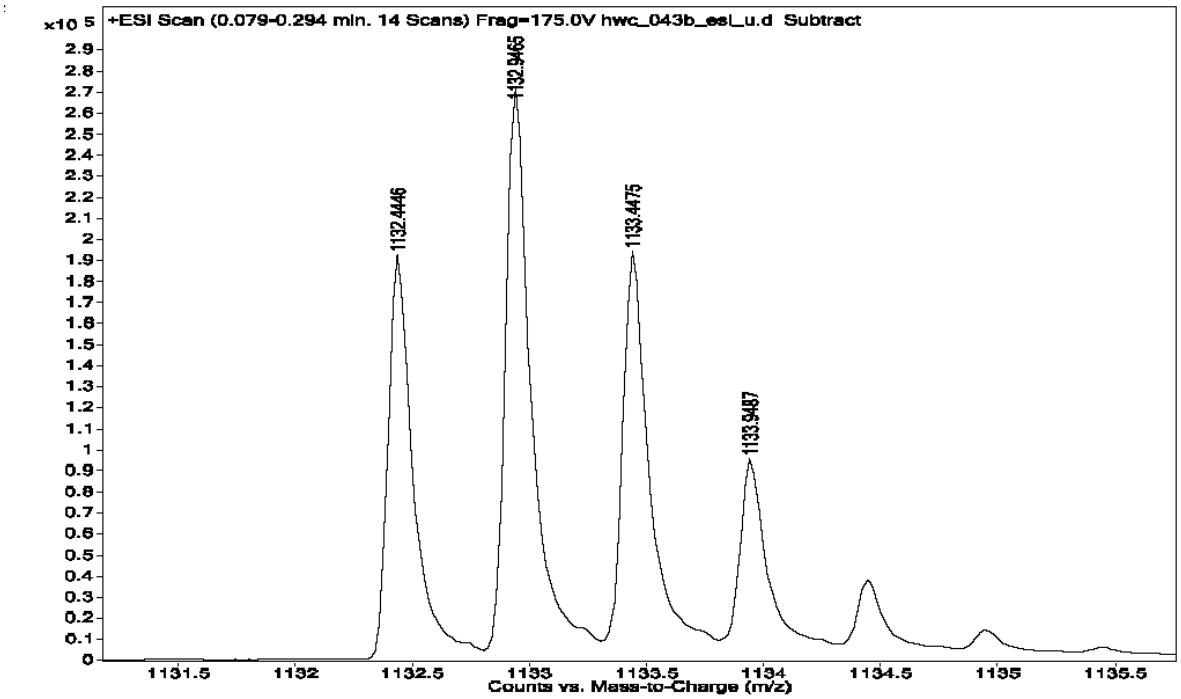

Figure 3.40. ESI-FOR HRMS $(M\text{-}2PF_6)^{2+}$ (rotaxane **8**)

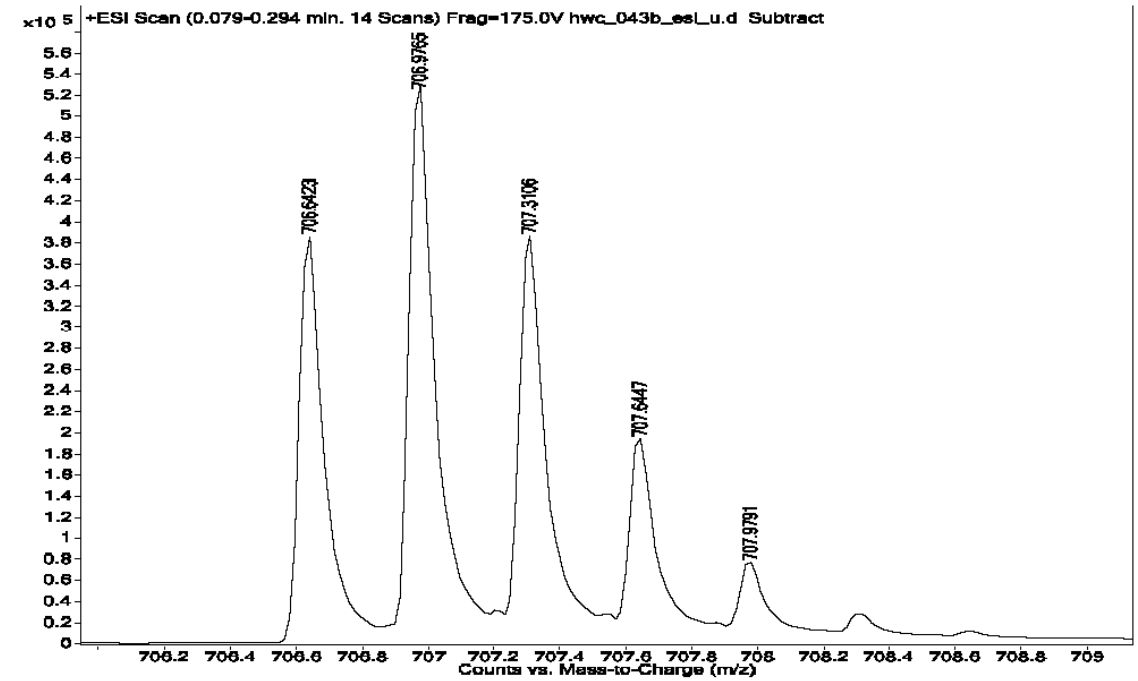

Figure 3.41. ESI-TOF HRMS of rotaxne **8** $(M - 3PF_6)^{3+}$

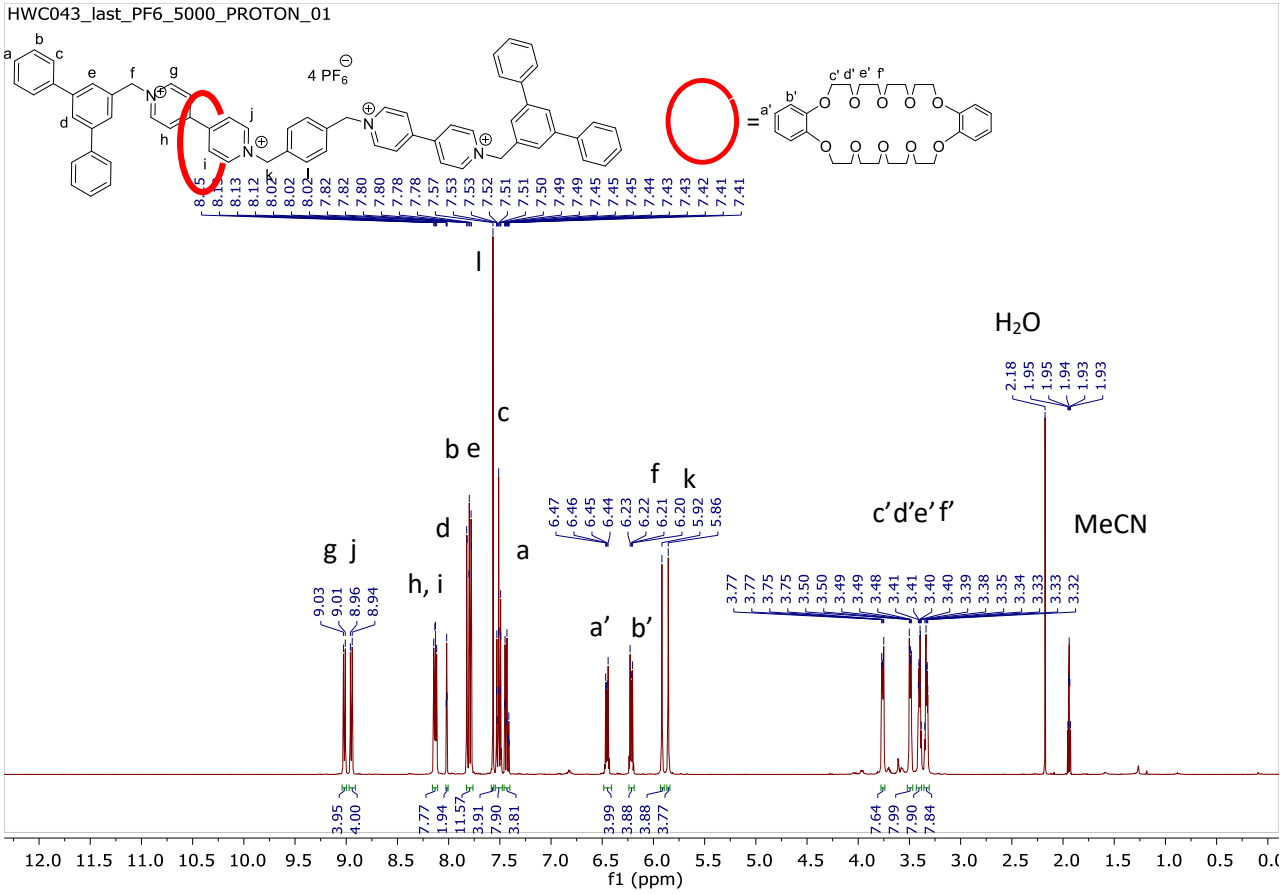

Figure 3.42. ^{1}H NMR spectrum of [2]rotaxane **7** in MeCN-d_3 at 400 MHz

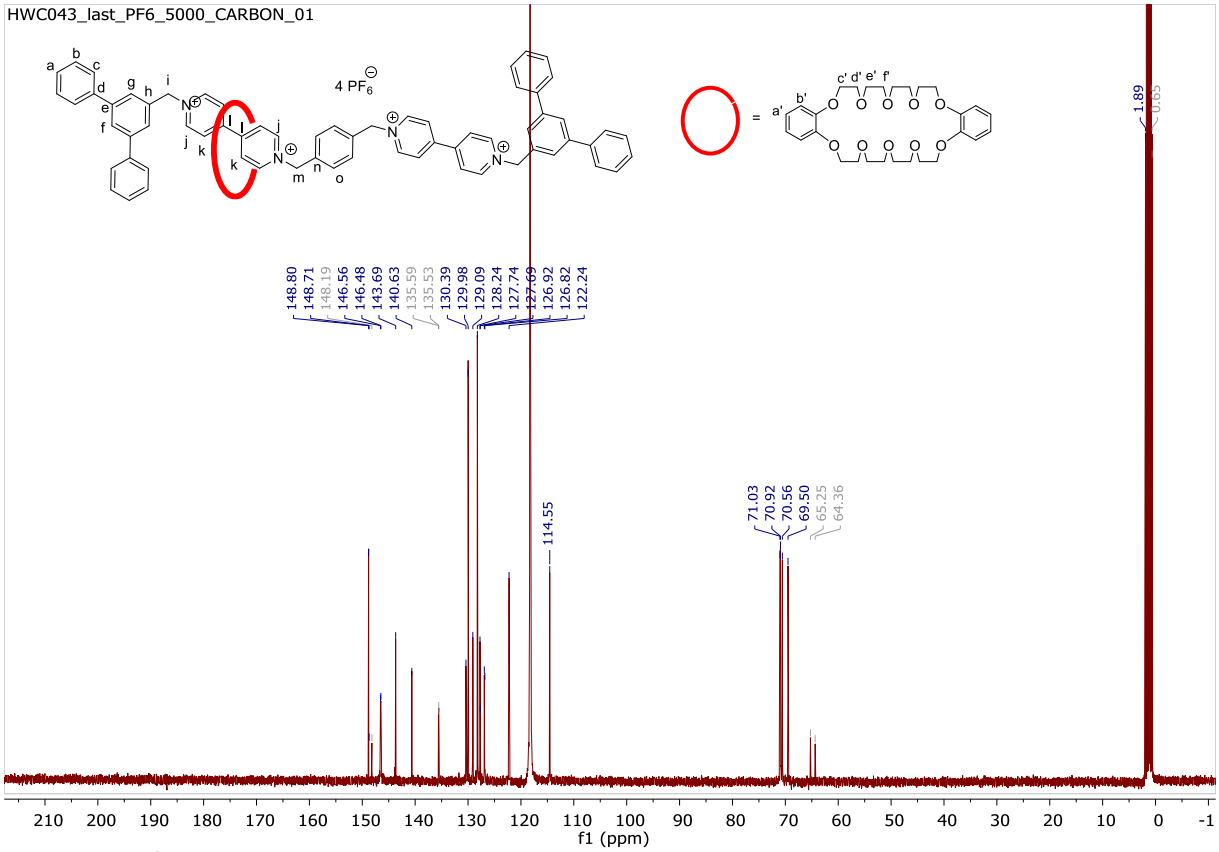

Figure 3.43. ^{13}C NMR spectrum of [2]rotaxane **7** in MeCN-d_3 at 101 MHz

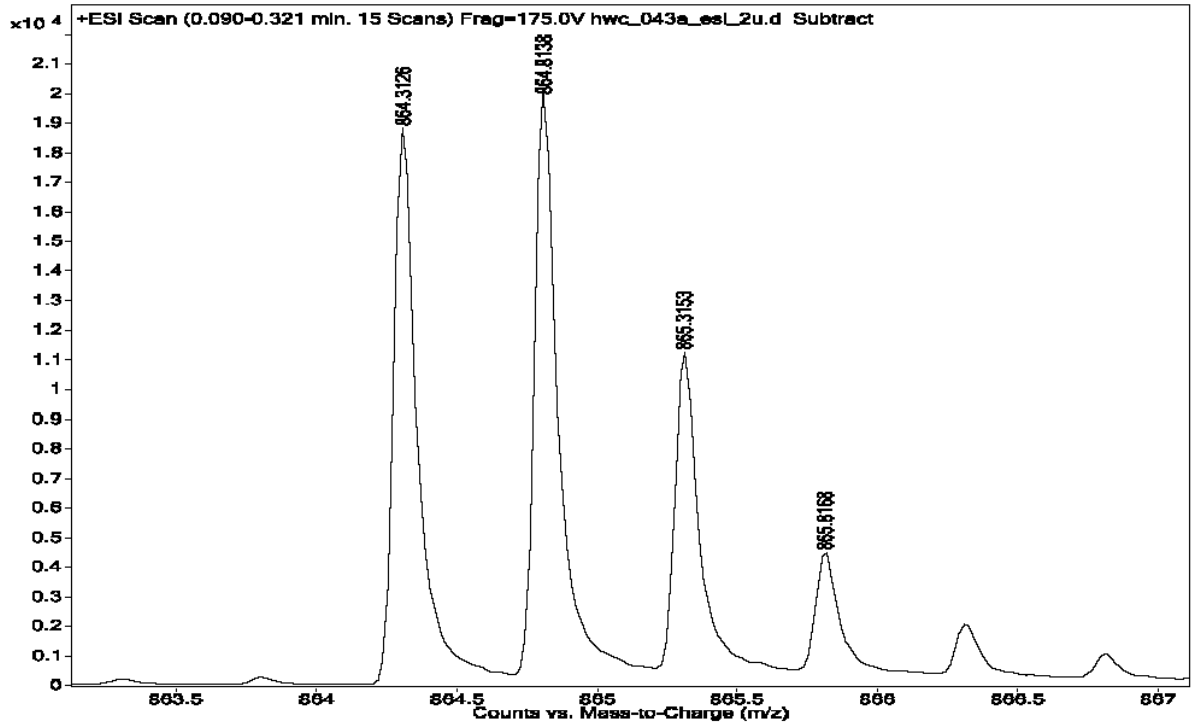

Figure 3.44. ESI-TOF HRMS $(M-2PF_6)^{2+}$ (rotaxane **7**)

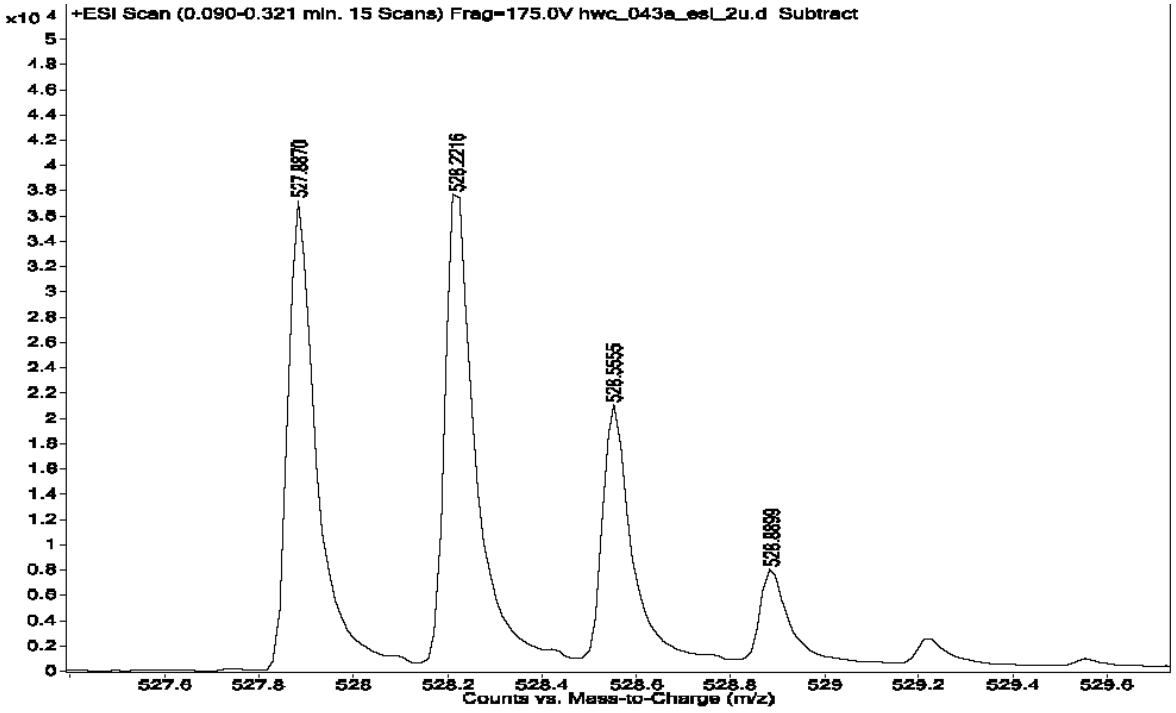

Figure 3.45. ESI-TOF HRMS of rotaxane **7** $(M - 3PF_6)^{3+}$

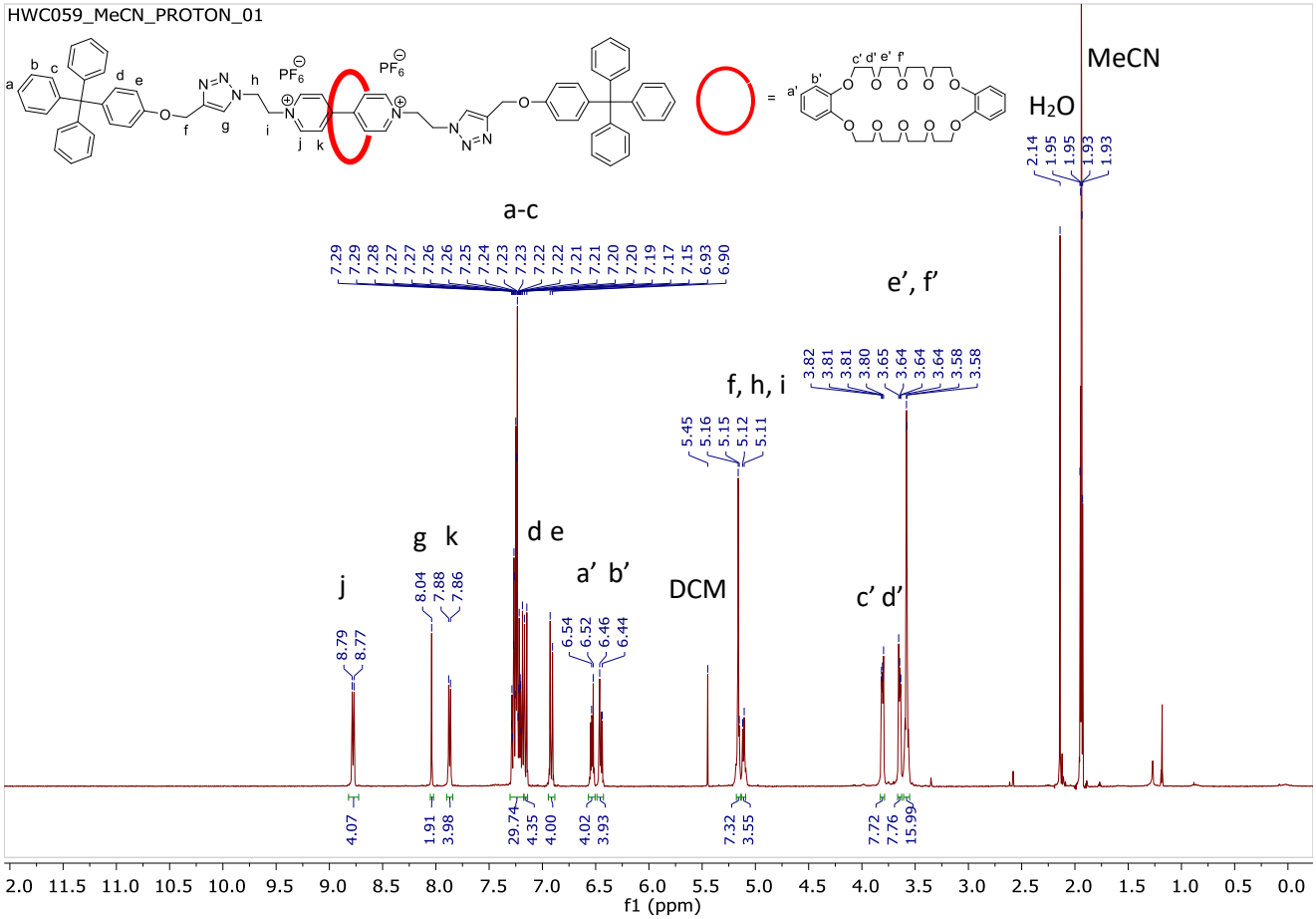

Figure 3.46. ^{1}H NMR spectrum of rotaxane **12** in MeCN-d_3 at 400 MHz

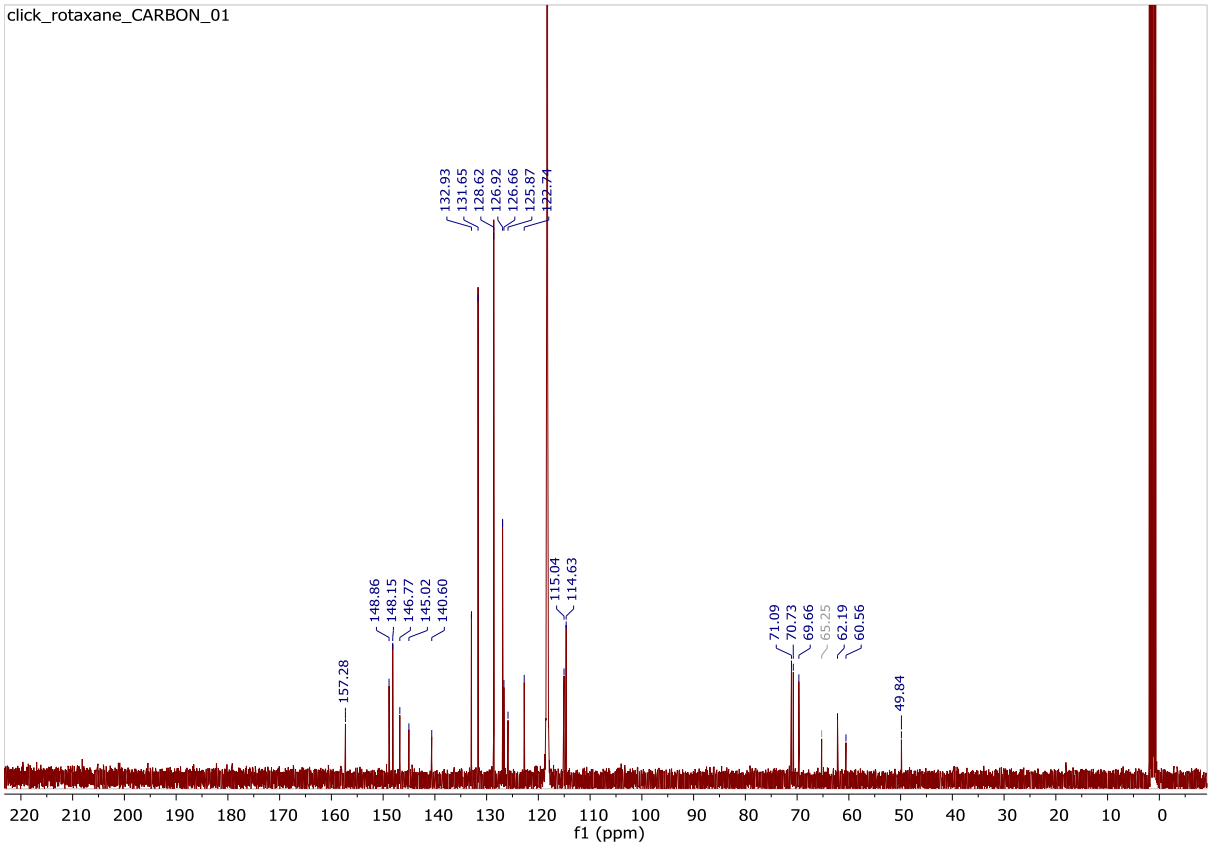

Figure 3.47. ^{13}C NMR of rotaxane **12** in MeCN-d_6 at 101 MHz

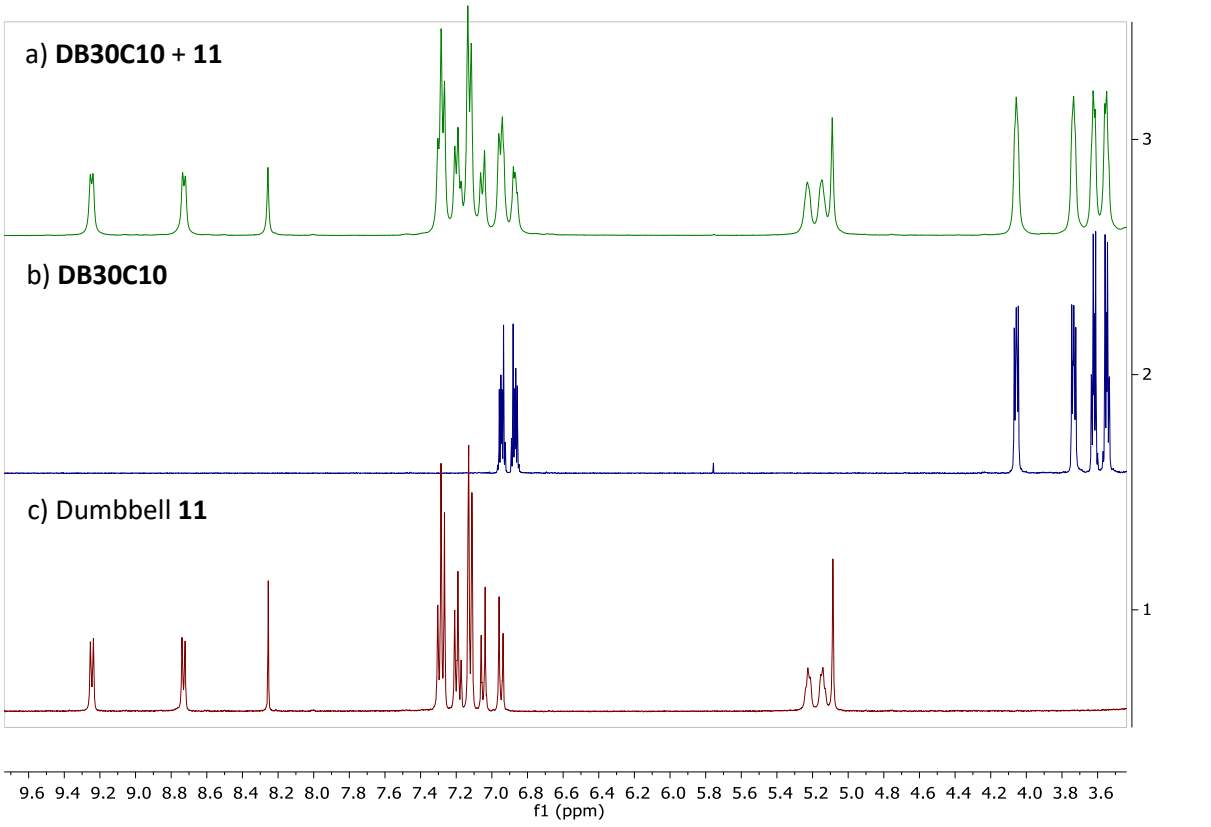

Figure 3.48. Partial ^{1}H NMR spectra of c) dumbbell **11** (bottom) b) **DB30C10** (middel), and a) a mixture of **DB30C10** and dumbbell **11** in DMSO-d_6 at 400 MHz

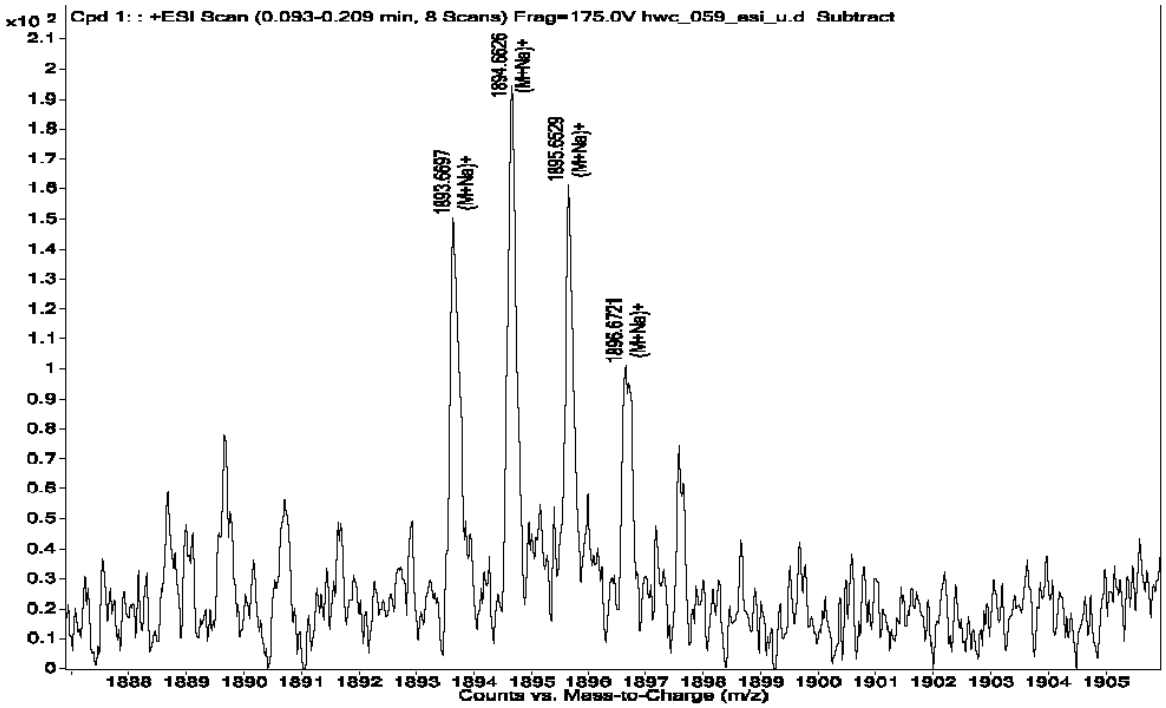

Figure 3.49. HRMS of rotaxane 12 $(M + Na)^+$

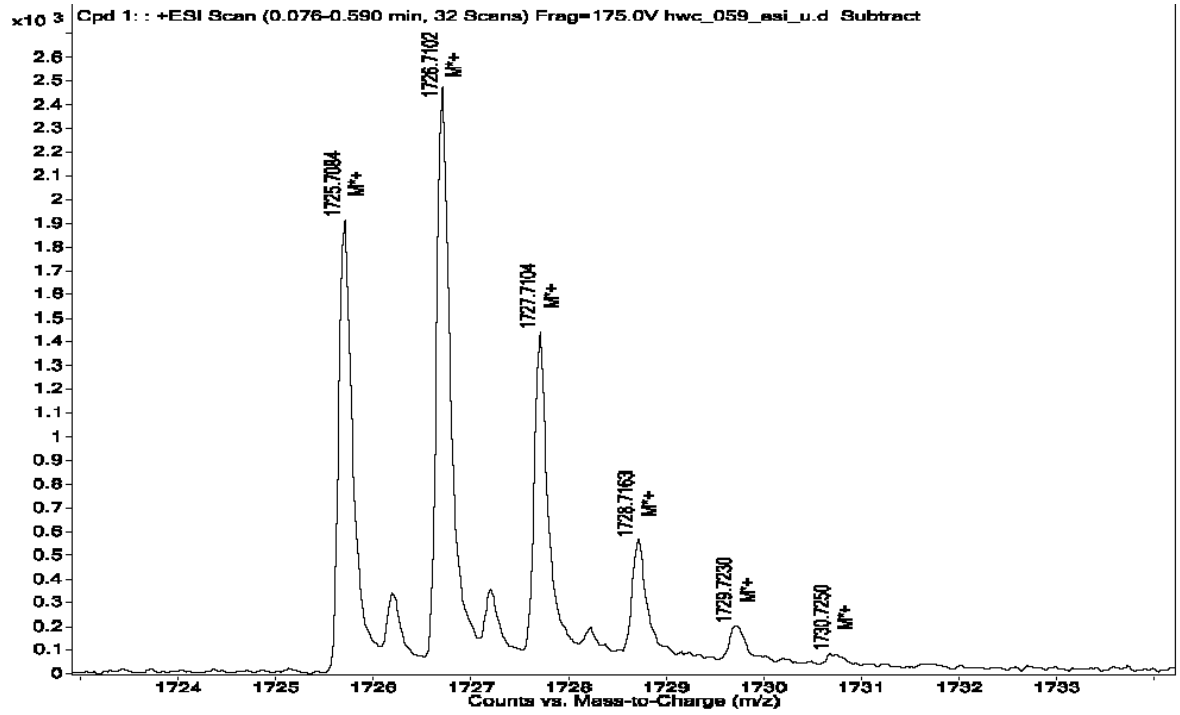

Figure 3.50. HRMS (ESI-TOF) of rotaxane **12** M^+

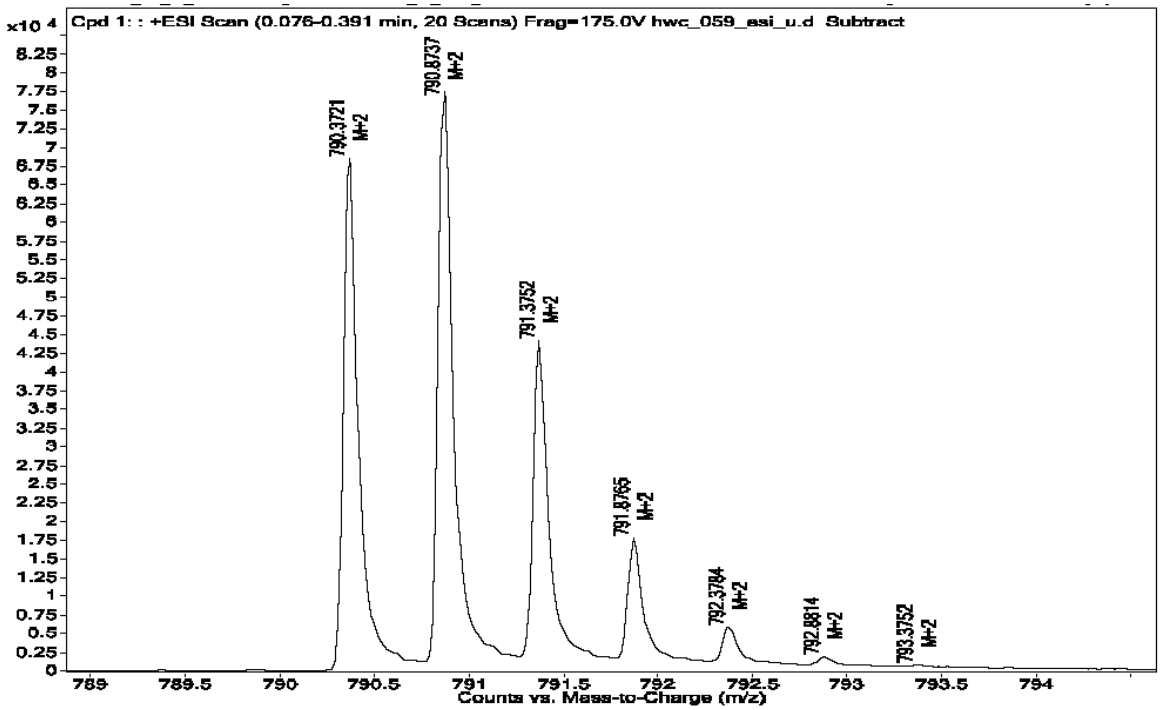

Figure 3.51. HRMS of rotaxane **12** $(M - 2PF_6)^{2+}$

2-D NOESY spectra of the rotaxanes

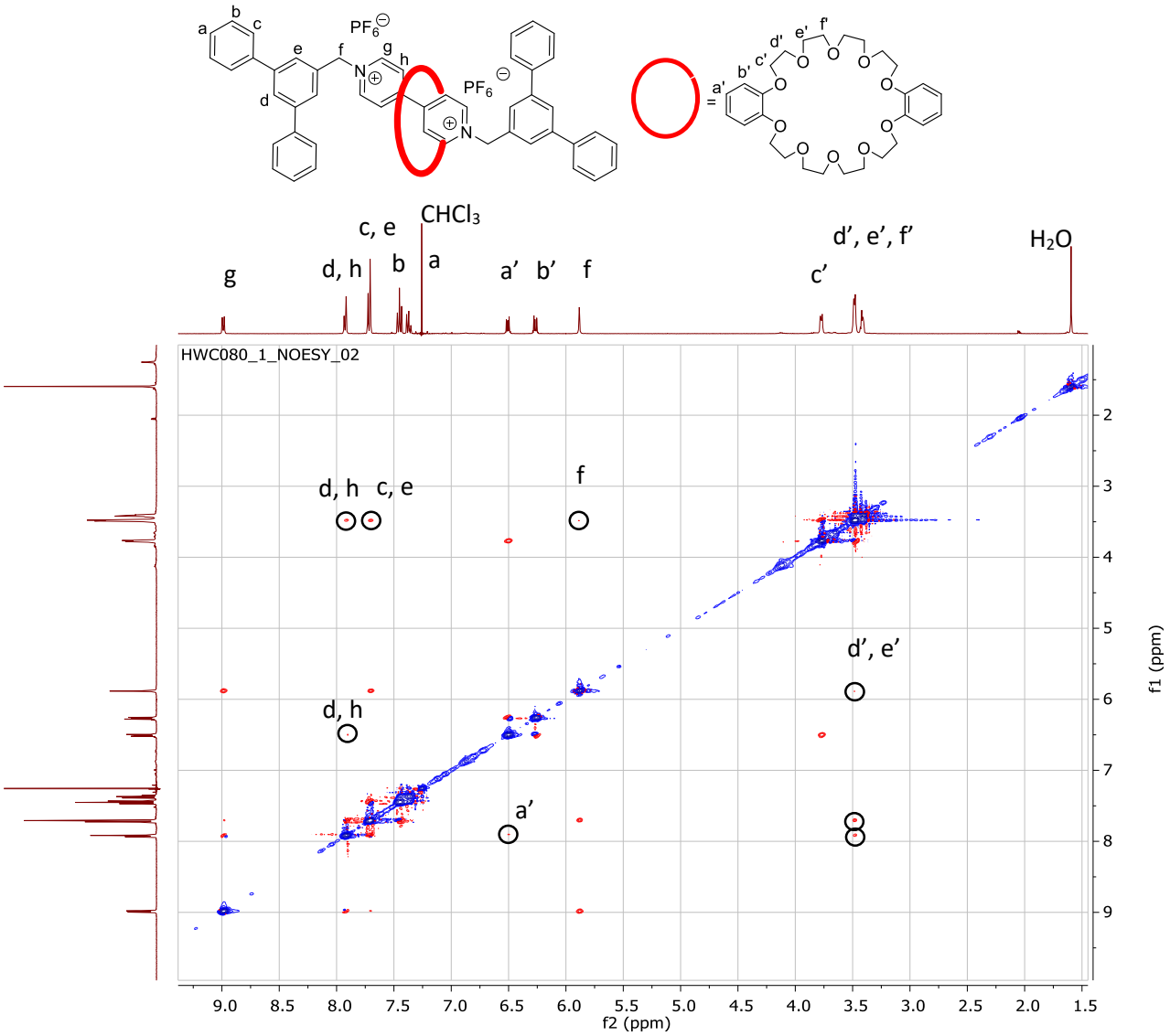

Figure 3.52. 2D NOESY spectrum of rotaxane **4** in $CDCl_3$ at 400 MHz

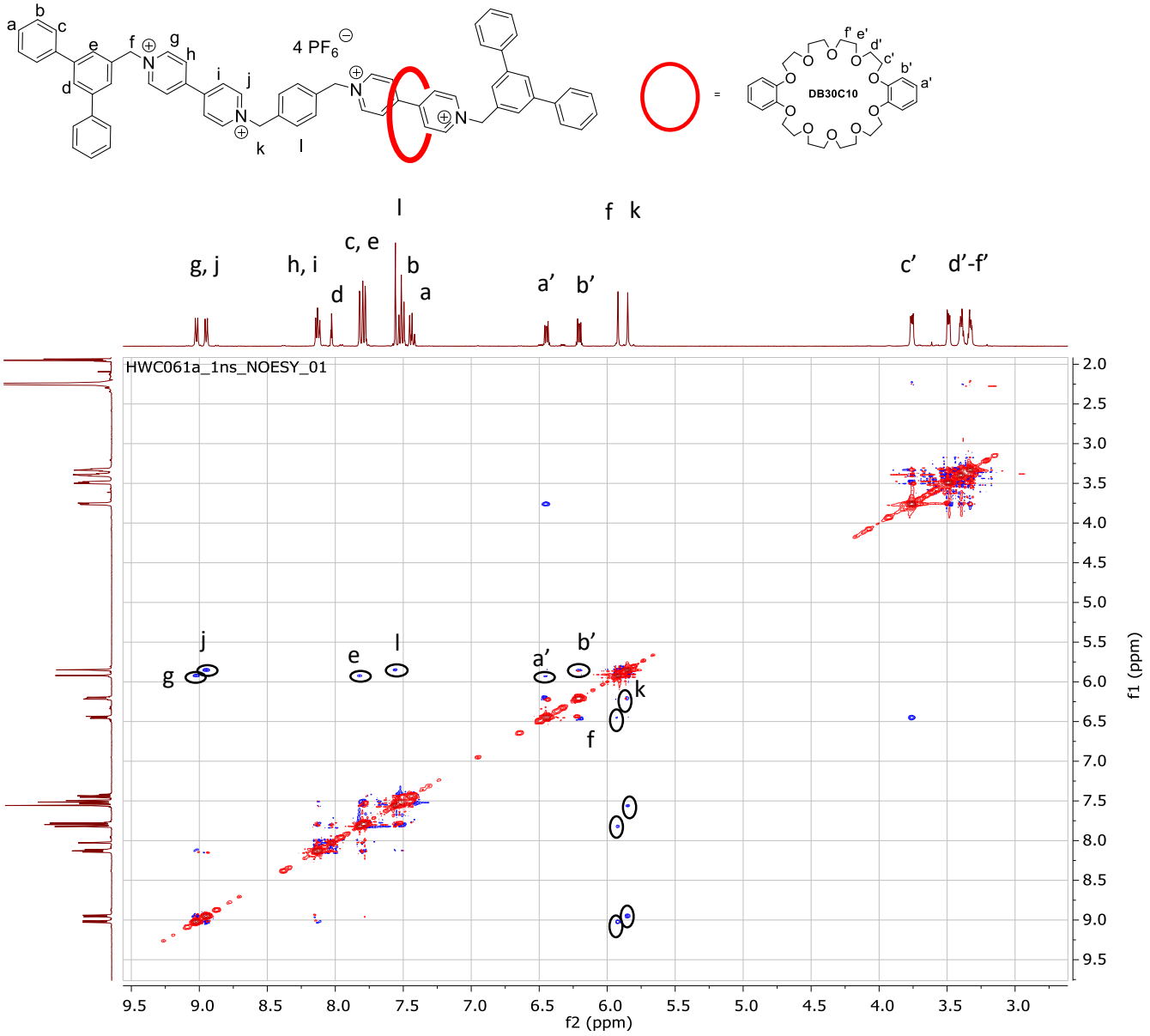

Figure 3.53. 2D NOESY NMR of [2]rotaxane **7** in MeCN-d_3 at 400 MHz

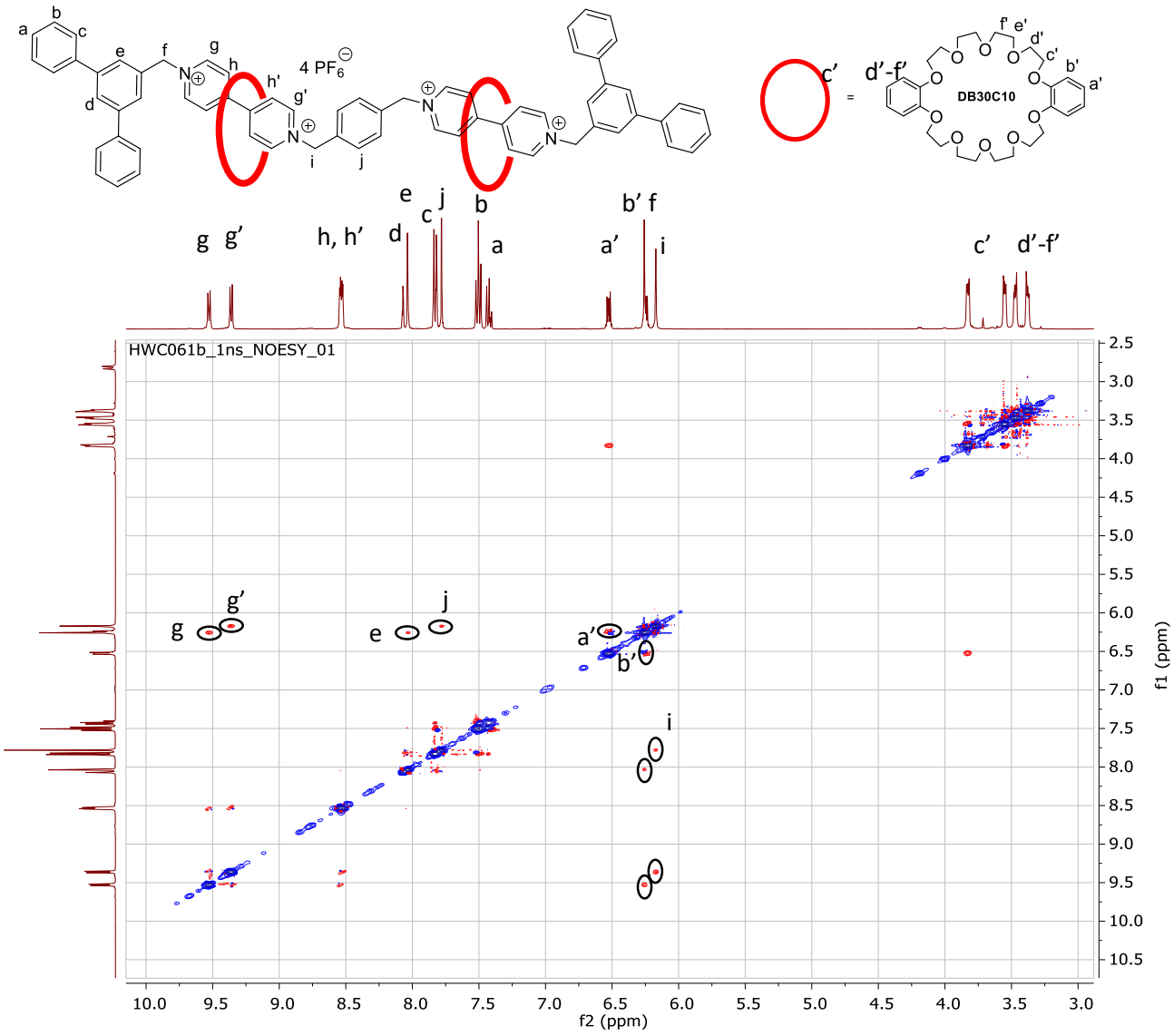

Figure 3.54. 2D NOESY spectrum of [3]rotaxane **8** MeCN-d_3 at 400 MHz

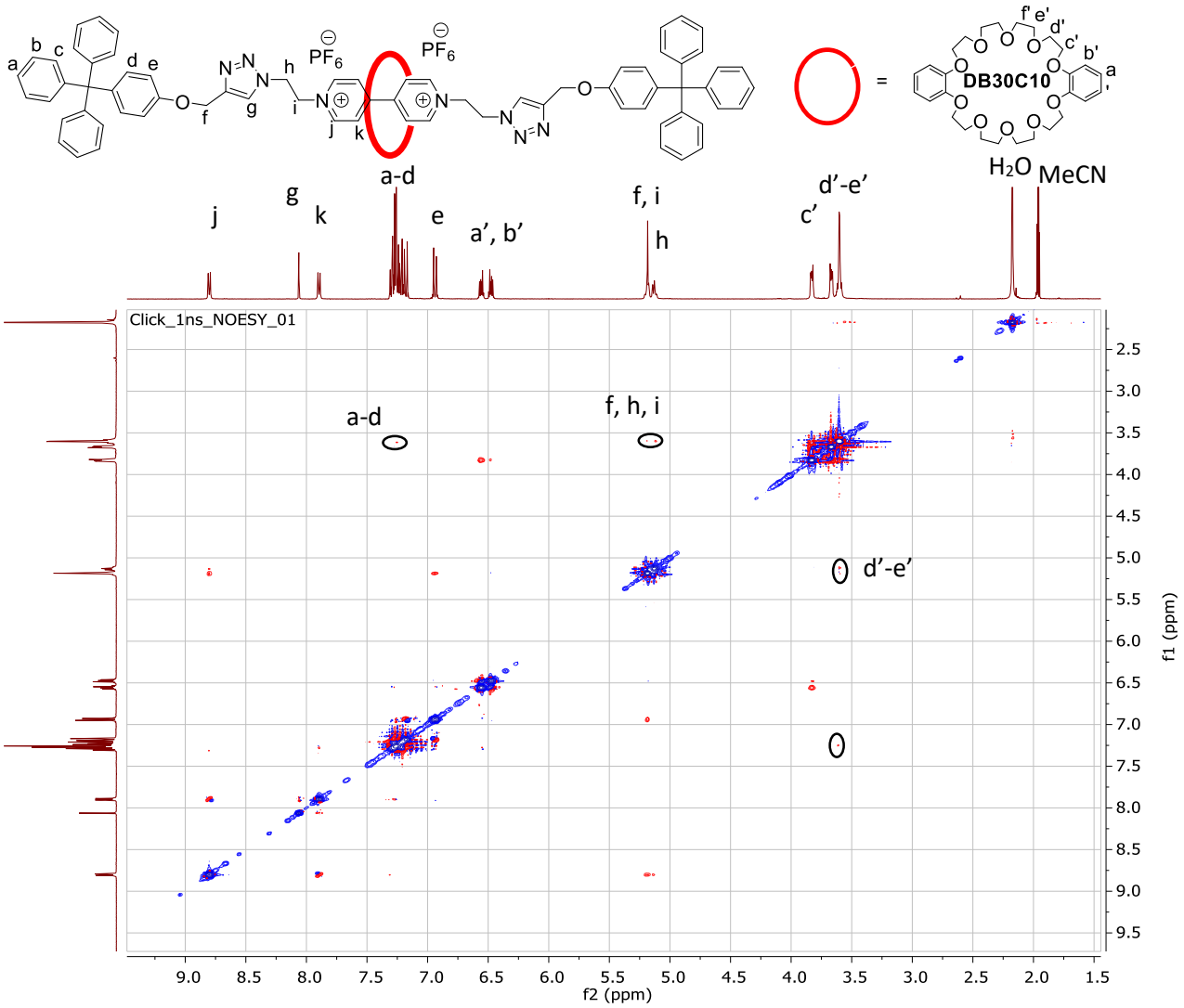

Figure 3.55. 2D NOESY spectrum of rotaxane **12** in MeCN-d_3 at 400 MHz

Chapter 4: Determining the threading efficiency of crown ethers by the formation of segmented poly(pseudorotaxane) polyurethanes

ABSTRACT

Six segmented polyurethanes containing a central PTMO (poly(tetramethylene ether) glycol or poly(tetrahydrofuran)) unit and terminal paraquat units in the backbone were synthesized. In addition to the backbone polymer, five polymers were made in the presence of crown ether or cryptand hosts. The crown ethers used were bis-(*para*-phenylene)-34-crown-10 (**BPP34C10)**, bis-(*meta*-phenylene)-32-crown-10 (**BMP32C10)**, dibenzo-30-crown-10 (**DB30C10)**, dibenzo-24-crown-8 (**DB24C8**) and a pyridyl cryptand based on **DB30C10**. The threading efficiency was determined by taking the integration ratio between the aromatic protons belonging to the host and the paraquat protons in the ^{1}H NMR spectra. **BPP34C10** was the most efficient with 50% threading efficiency, followed by **DB30C10** with 17.5%, the pyridyl cryptand with 16%, **DB24C8** with 9.5% and **BMP32C10** with < 1%. We also report a 3 step method for the synthesis of **BMP32C10**.

Introduction

Crown ethers are a class of macrocycles used as host molecules in supramolecular chemistry. They were discovered in 1961 when C.J. Pedersen isolated a crystalline compound from an “unattractive goo”. He quickly realized that this molecule that he isolated (dibenzo-18-crown-6) was able to render sodium ions soluble in organic solvents and postulated that the ion had “fallen into the hole in the centre of the molecule”.[1] In 1967 he published his seminal paper describing the synthesis of 33 crown ethers and their complexes with metal salts.[2] His discovery garnered a lot of interest in the scientific community and was instrumental in launching the field of

supramolecular chemistry. Pedersen received the 1987 Nobel Prize for chemistry along with Jean-Marie Lehn and Donald J. Cram. (The 2016 Nobel Prize was also awarded in the field of supramolecular chemistry, specifically for molecular machines).

A major point of interest in the study of crown ethers is their ability to associate, or bind, with various guest molecules. Many of the early studies on crown ethers were focused on binding with specific metal cations. It was discovered that altering the cavity size of the crown ether led to higher affinities for specific metal cations within limits. For example: The size of Li^+ ions matches the cavity size of [12]crown-4 best, [15]crown-5's cavity is complementary to the size of Na^+ ions, and K^+ ions fit very well into the cavity of [18]crown-6.[3] [12]Crown-4 is shows selective binding for Li^+, [15]crown-5 binds about equally well with Na^+ and K^+. [18]Crown-6 has highest binding constant with all three these cations, but it is selective for K^+ over Na^+ or Li^+.[4-5] The ability of crown ethers to bind to metal ions has led to a great number of applications such as treating wastewater and radioactive waste,[6] sensors for particular metal ions,[5, 7-8] separating metal ions, antimicrobial agents [9-11] and artificial ion channels.[12-13]

Metal cations are not the only species that can act as guests for crown ethers. They can also serve as hosts for several organic cations: polyatomic species like ammonium ions, dialkyl ammonium salts,[14] imidazolium,[14] benzimidazolium,[15] *N*-benzylanilinium,[16] bis(pyridinium)ethane, triazolium,[17] *N,N'*-dialkyl-4,4'-bipyridinium (paraquat or viologen) salts[14] as well as neutral guests such as naphthalene diimide (NpI) units.[18] Fullerenes and various carbon nanostructures such as carbon nanotubes, nanohorns and graphene can form supramolecular complexes with crown ethers.[19]

Construction of a system with two guest sites led to the discovery that the host molecule moved back and forth between the two degenerate sites. This molecule was dubbed a “molecular shuttle”.[20] The incorporation of multiple guest sites, with which the host has different binding affinities, allows one to direct or bias the motion of the machine by chemical, electronic, or photophysical means. The ability to modulate the binding affinity of a guest site by, for example protonating and deprotonating an ammonium ion, coupled with the concept of a molecular shuttle has been the basis for the design of a wide variety of systems with different functions.[21] Examples of systems that depend on, or incorporate, this design are a “molecular elevator”,[22-23] various drug delivery systems, molecular “muscles”,[24-26] switchable catalysts,[27-28] molecular sensors,[29] and molecular switches.[30-31] Naturally, polymer systems incorporating host-guest motifs have been developed, in order to develop stimuli responsive materials. Some very interesting examples have been developed both in terms of topology and function.

In order to use a crown ether as a host for interlocked systems, some knowledge of the system’s complexation behaviour is required. In particular, it is necessary to know how the host and guest form complexes, their binding geometry, and some measure of how strong the complexation is. Obtaining an accurate idea of the extent of binding in a polymeric system is not necessarily straightforward. Association constants are usually measured in small molecule systems and can vary greatly with parameters such as temperature and solvent polarity.[32-33] Presumably, threading several hosts onto a polymer that contains several guest sites will introduce a threading “mechanism”. Multiple binding sites can also influence the binding constants as the sites can act in a cooperative fashion, an anti-cooperative fashion or not affect the binding behaviour of neighbouring sites at all.[34] In addition, our group is not so much

interested in the binding constant for its own sake, but more as a way to calculate how many binding sites are occupied in a particular polymer sample. Given these considerations and the difficulty in characterizing polyelectrolytes in general, we opted for a more direct measurement.

Previously, the amounts of threading of between bis(*para*-phenylene)-34-crown-10 (**BPP34C10**) and polyurethanes with paraquat incorporated into the backbone were measured directly by ^{1}H NMR.[35] The aromatic protons in the crown ether show a pronounced downfield shift when they are complexed with paraquat, due to the donor-acceptor behaviour of the system. The ratio between the signals for complexed ether and the total paraquat sites was used to determine the number of complexed versus uncomplexed sites. In the case of **BPP34C10** the extent of the threading was nearly 100%.[35] This result cannot be extended to other crown ether systems, as X-ray crystal structures of the complexes formed between other larger crowns like bis(*meta*-phenylene)-32-crown-10 (**BMP32C10**)[36] and dibenzo-30-crown-10 (**DB30C10**)[37] show that the crown ether cavities are not as open as is the case in **BPP34C10**.[38] Crown ethers are fairly flexible and the **BMP32C10** and **DB30C10** can adopt a variety of conformations, for example, a conformation in which the crown is folded around the guest, forming a taco complex or a stair step shape (Figure 4.1).

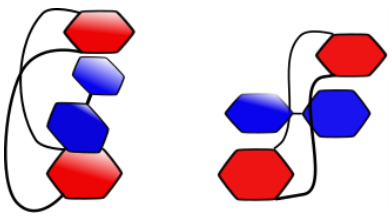

Figure 4.1. Cartoon showing a complex between paraquat and DB30C10 in the taco conformation (left) and the stair step conformation (right)

We have recently shown that **DB30C10** does form psuedorotaxane complexes with paraquat by making rotaxanes with **DB30C10** as the wheel component. Since we

streamlined procedures for making **DB24C8**,[39] **DB30C10,**[39] and the pyridyl cryptand derived from **DB30C10**,[40] we would like to know whether these hosts could be used to make polymers with interesting topologies (such as star, brush, H-shaped, hyperbranched, etc.), as well as poly(rotaxanes) and main chain poly(pseudorotaxanes), wherein the polymers form by self-assembly of host, and guest terminated macromonomers. Such polymers have been made in the past, but usually using **DB24C8**[41] or **B21C7**/ammonium complexes[42] or **BMP32C10**[43-44] or **BPP34C10**,[45] or the pyridyl cryptand based on **BMP32C10**.[46] We decided to use the previous methodology to measure the threading efficiency of **BPP34C10** and directly compare the threading efficiency with **DB30C10, DB24C8**, **BMP32C10** and **DB30C10** pyridyl cryptand and **BPP34C10** in order to determine which host(s) would be most appropriate for future supramolecular polymer development.

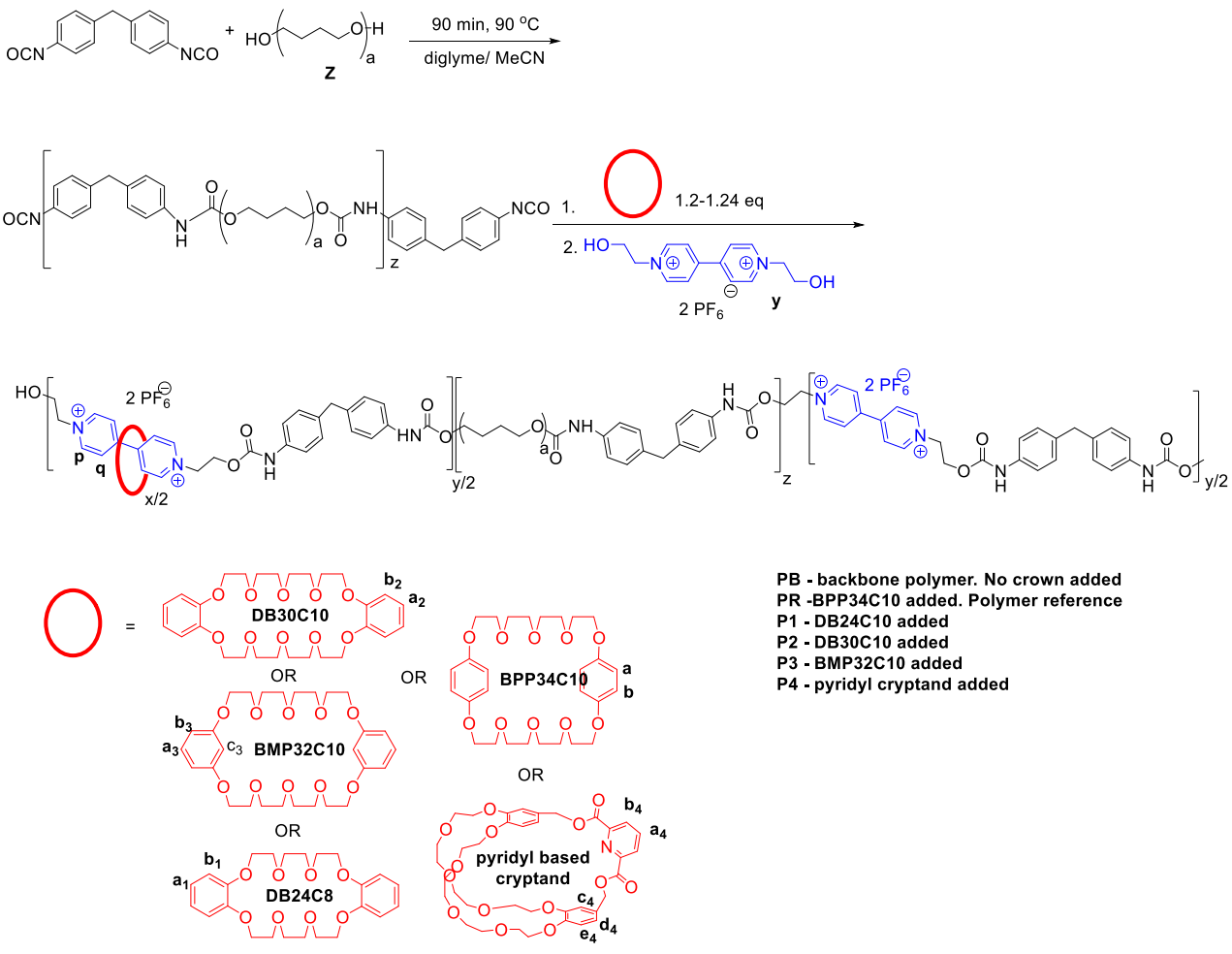

Scheme 4.1. Preparation of the polyurethane poly(pseudorotaxane)s.

Results and Discussion

In order to be able to draw direct comparisons between the complexation behaviour of the set of crown ethers under study (**DB30C10**, **DB24C10**, **BMP32C10** and pyridyl cryptand), the procedure used in the previous study with **BPP34C10** was duplicated.[35] The backbone polyurethane (PB) and the polymer with **BPP34C10** (PR) were prepared as references.

The segmented backbone polyurethane (PB) was prepared as follows: 4,4'-methylenediphenyl diisocyanate was dissolved in a mixture of diglyme and MeCN (1:2) and the mixture was lowered into an oil bath that had been pre-heated to 90 ºC. Poly(THF) with an average molecular weight of 1000 g/mol was added and the

reaction mixture was allowed to stir under argon. After 90 min, paraquat diol was added and the solution was allowed to stir at 90 ºC under argon for 36 hours. The solution was allowed to cool to room temperature and precipitated into rapidly stirring methanol. The polymer was purified by precipitation from acetone into methanol 2-3 times.

The crown ether containing polymers were prepared in a similar fashion, except the crown ether was added to the solution after the initial 90 min heating period and 1,1'-bis(2-hydroxyethyl)-[4,4'-bipyridine]-1,1'-diium hexafluorophosphate was added 10-15 min after the addition of the crown ether. The ratio of crown ether to paraquat untis was 1.2-1.24 to 1.

The crown ether containing polymers (PB and P1-P4) were all purified by repeated precipitations from acetone into methanol. ^{1}H NMR spectra in acetone-d_6 were obtained after each precipitation. Precipitations were continued until two consecutive spectra yielded similar integration ratios, that is, until all of the excess crown ether had been removed. This was generally achieved between the second and third precipitation, which is consistent with our previous findings.[47-48] The threading efficiency was obtained by integration of paraquat protons (4 H) versus the aromatic protons of the host. An example of the procedure is illustrated below in the case of the polymer with **BPP34C10** (PR).

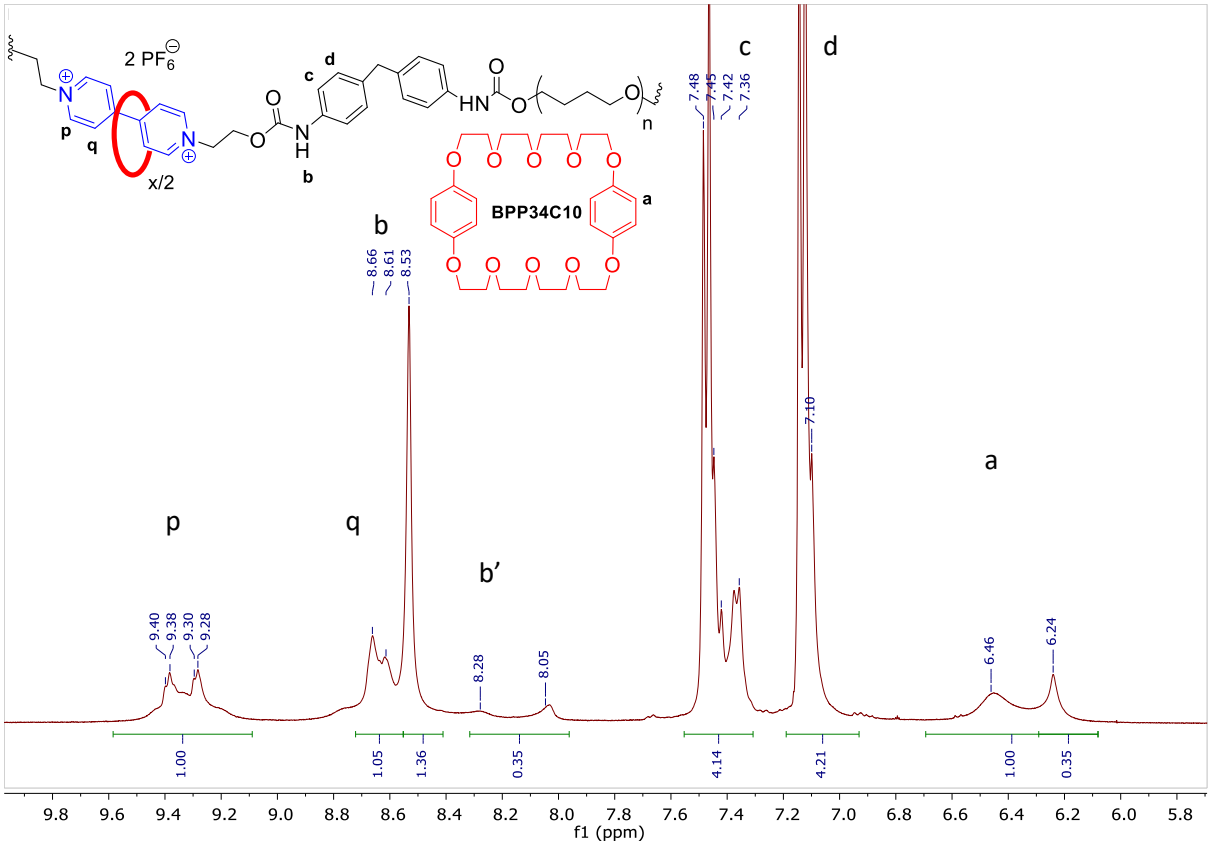

Figure 4.2. Partial ^{1}H NMR spectrum of **PR** in Acetone-d_6 at 400 MHz

PR (the control polymer with **BPP34C10** added), was a red substance. Further indication that threading had taken place was the shifts in the paraquat protons, and the aromatic protons of the crown ether. The paraquat protons shifted upfield from 9.40 ppm and 8.81 ppm in the backbone polymer to 9.34 and 8.64 ppm in PR. The aromatic protons of the crown ether shifted from a single peak at 6.78 ppm in the uncomplexed crown ether to two broad peaks at 6.46 and 6.24 ppm in PR. The peak groups at 9.40 ppm (**p**) and 8.81 (**q**) were assigned as the one set of paraquat protons (which integrate to 4 H) each. The two broad peaks at 6.46 and 6.24 ppm (**a**) were attributed to the aromatic protons on the crown ether, which would be 8 hydrogens in total. The presence of two peaks, instead of the expected one, is attributed to the fact that the crown ether can interact with the N-H group (**b**) of the urethane linkage (through hydrogen boding) as well as with the paraquat. The small, broad singlets **b'**

have the same integration as the smaller of the **a** peaks. This could indicate that **h'** is the signal for the complexed urethane linkage. Using **p** + **q** and **a**, the integration ratio is 2:1, so the number of incorporated rings per paraquat unit is 0.5, i.e. the threading efficiency is 50 %. This difference (50% vs the 100% reported previously[35]) could be attributed to the fact that that the polymer was allowed to stir in MeOH for several hours instead of 30 min. This would allow the system to establish an equilibrium by dethreading. When equilibrium experiments were conducted allowing a solution of backbone polymer and crown ether to establish equilibrium they also found a threading efficiency of 50%.[35]

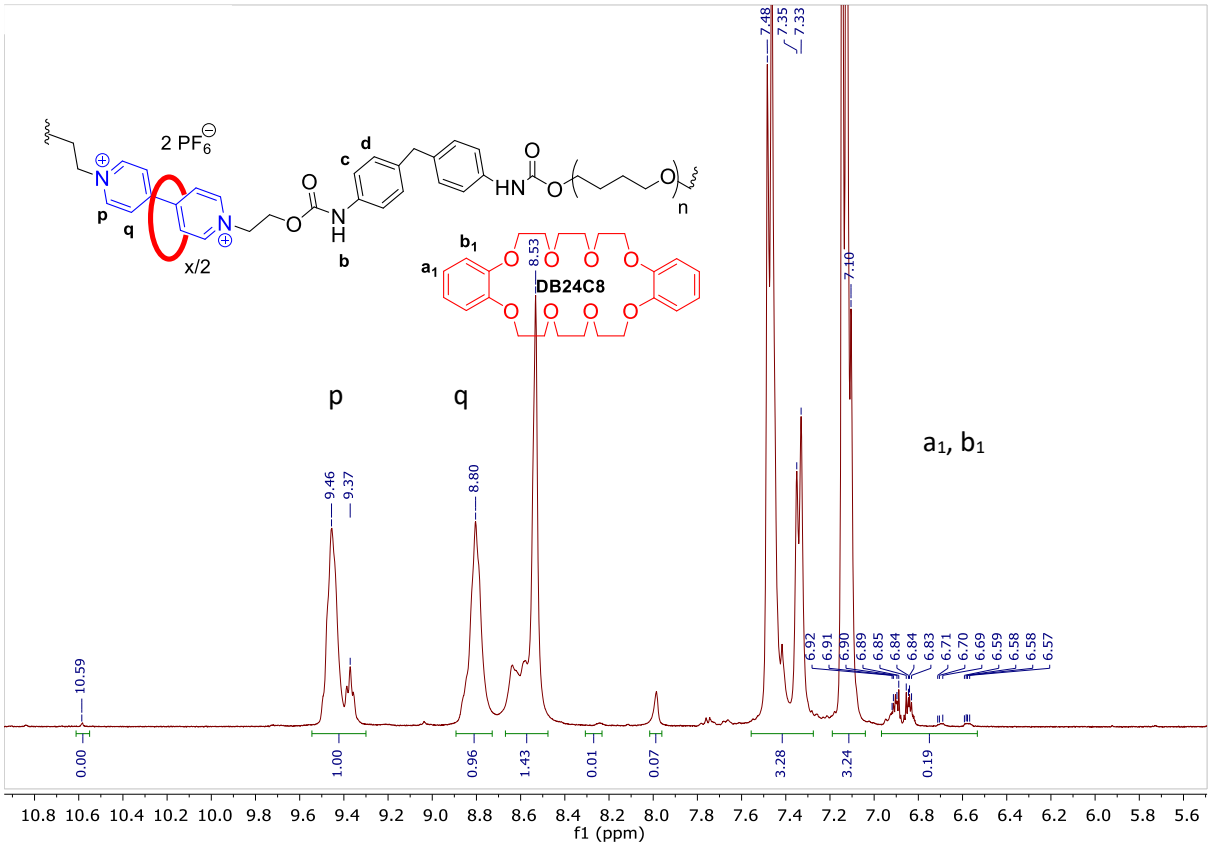

Figure 4.3. Partial NMR spectrum of **DB24C8** containing polymer P1 in acetone-d_6

For P1, the **DB24C8** containing polymer, there is a barely perceptible upfield shift in one of the paraquat protons (**q**) from 8.81 ppm in the backbone polymer to 8.80 ppm

in the complexed polymer (Figure 4.3). The aromatic protons of the crown ether go from 2 multiplets in the crown ether spectrum (Figure 4.19) to 4 multiplets in the polymer spectrum (designated a_1 and b_1 in the above spectrum). The multiplets shift upfield from 6.94 and 6.87 to 6.90, 6.84, 6.70 and 6.58 ppm. Using the peaks at 9.46 and 9.37 (**p**) as four paraquat protons and both sets of multiplets (**a_1** + **b_1**) as the 8 aromatic protons of the crown ether, the relative integration ratio is 1: 0.19. The threading efficiency is 9.5%.

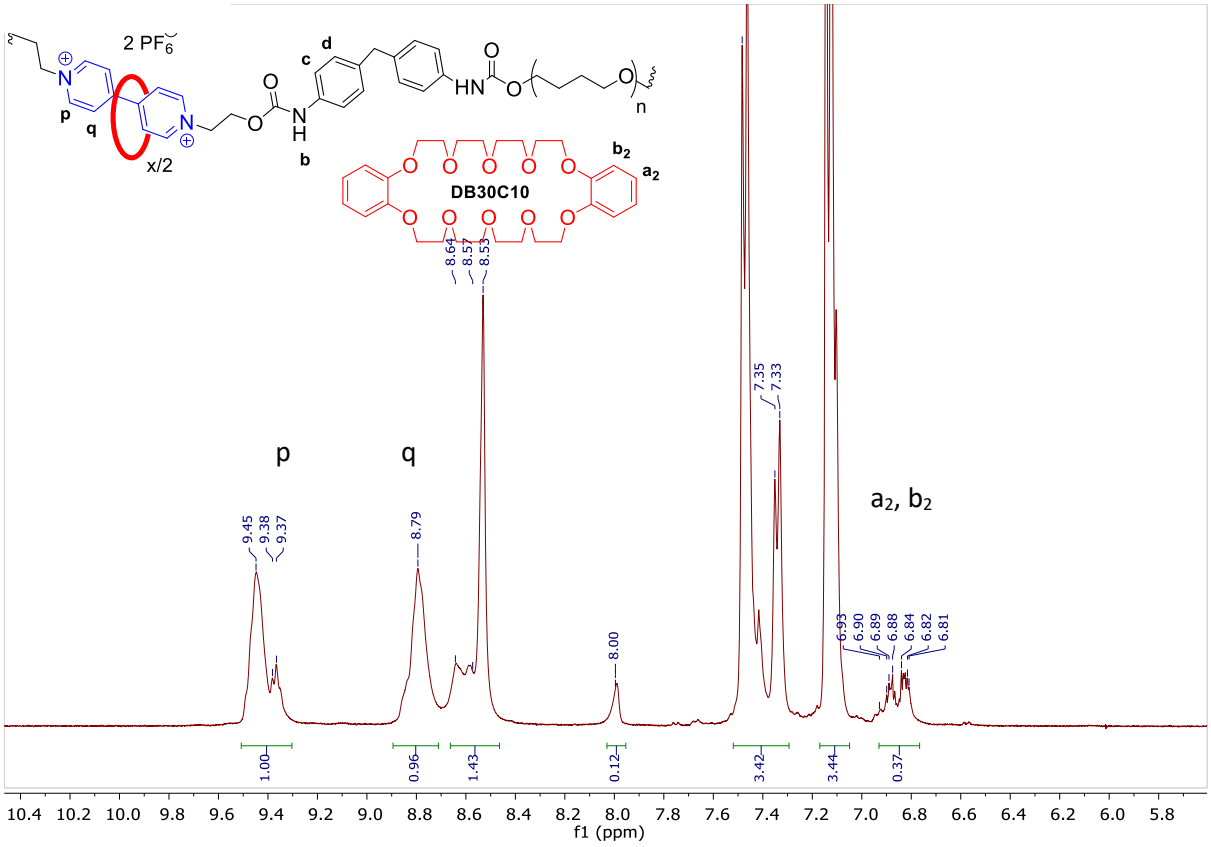

Figure 4.4. Partial NMR spectrum of **DB30C10** containing polymer P2 in acetone-d_6

When **DB30C10** was added to the polymerization mixture (P2), the resulting polymer again did not show have any perceptible change in the chemical shifts of the paraquat protons (**p**, **q**). The aromatic protons of the crown ether shift upfield from two multiplets at 6.96 and 6.89 ppm to two multiplets at 6.97 and 6.85 ppm (**a_2** and **b_2** respectively).

Using the aforementioned method to determine threading efficiency,17.5% of the paraquat units are encircled. As expected, the threading efficiency varies with the concentration. Over three runs the threading efficiency varied from 11-17.5%. The lowest threading yield was obtained when the concentration was lowest (0.28 M) and highest with the highest concentration (0.53 M).

In the course of synthesizing **BMP32C10** to perform the polymerization on a sufficiently large scale, we used our previously reported 3 step method of synthesizing crown ethers. 1,3-Dihydroxybenzene was reacted with tetra(ethylene glycol) monotosylate in the presence of K_2CO_3. The resulting diol was tosylated and purified by column chromatography. A mixture of the resulting ditosylate product and resorcinol (1:1) were added to a refluxing mixture of solvent and K_2CO_3 dropwise. This crown ether did not undergo templation reactions with K^+, Cs^+ or any other cation as yet identified, but pseudo-high dilution techniques (aprox. 3-5 mM) allow one to obtain an isolated yield of 40-45 % consistently. This method differs from others in the literature in that it does not employ a protection step,[36] does not use DMF as solvent, and does not make use of a large excess of tetra(ethylene glycol) ditosylate[49] or dichloride.[50]

Pseudorotaxane formation seemed to be very limited when **BMP32C10** was added to the reaction mixture (P3). In one reaction attempt, no evidence of threading was found. In another, the threading efficiency was 1% or less. It should be noted in this attempt there was a rather long delay between lowering the MDI into the oil bath and adding the poly(THF), which seems to have resulted in the formation of a significant number of urea linkages (as determined by the presence of the singlet at 10.83 ppm). The material became very viscous and was difficult to dissolve in acetone or THF. The fraction that could be dissolved was re-precipitated and showed very little evidence of threading, although the material was orange.

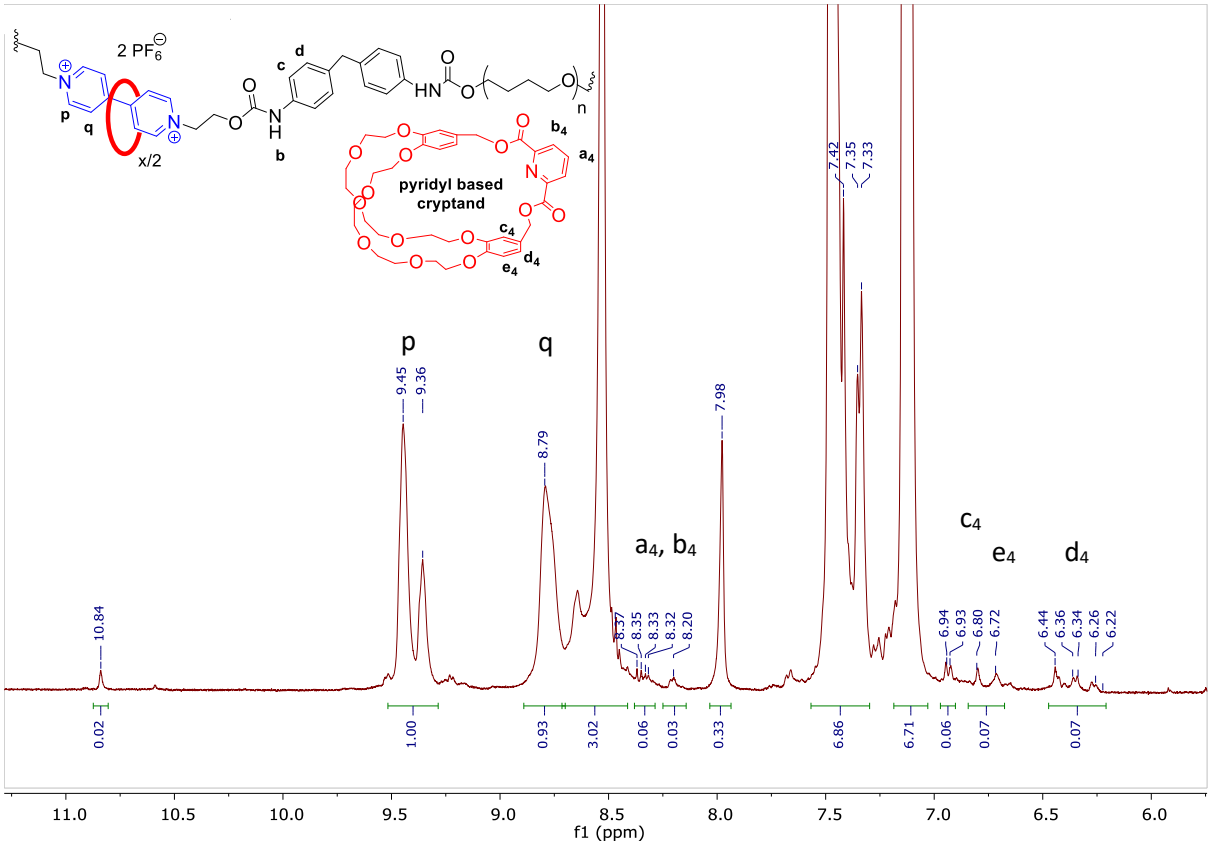

Figure 4.5. Partial NMR spectrum of pyridyl cryptand and acetone-d_6 at 400 MHz

The pyridyl cryptand containing polymer (P4) showed surprising results. There was evidence of threading, but the threading efficiency was much less than expected. The pyridyl cryptand's binding constant with paraquat in acetone is about two orders of magnitude higher than that of the crown ether in the same solvent.[51-52] Thus, we naturally supposed that the threading would be almost quantitative. Instead, the signals that comprise paraquat proton **p** in P4 only moved about 0.01 ppm upfield in comparison to the backbone polymer (9.45. 9.36 vs. 9.46, 9.37 and 9.36 ppm for the respective polymers)(Figure 4.5). Proton **q** shifted form 8.81 ppm in the backbone polymer to 8.79 ppm in P4. The lack of upfield shift in the paraquat protons seems to correlate with low threading efficiency. The equilibrium is fast on the NMR time scale, which means that the signals are time averaged. Taking the signals between 6.94 and 6.22 ppm as $\mathbf{c_4}$, $\mathbf{d_4}$ and $\mathbf{e_4}$ of the cryptand (6H), and comparing it to the paraquat

protons **p** (4H) gives a threading efficiency of only 16%. The protons of the pyridyl group, $\mathbf{a_4}$ and $\mathbf{b_4}$, do not shift upfield, only broaden. The peaks for $\mathbf{c_4}$-$\mathbf{e_4}$ show a significant upfield shift (as well as broadening). The doublets at 7.08 ($\mathbf{c_4}$) and 6.85 ($\mathbf{e_4}$) and the doublet of doublets at 6.98 ppm ($\mathbf{d_4}$) shift upfield and become doublets at 6.93 and 6.76 and a multiplet at 6.38 ppm; an average upfield shift of 0.28 ppm. The material is more soluble compared to the other polymers and a very bright orange. This result may mean that the shape of the binding cavity might be more important than the binding constant in the preparation of poly(pseudorotaxanes) by this method (*in situ* formation of the pseudorotaxane while the paraquat diol is being incorporated into the backbone). Another possible interpretation is that the formation of the pseudorotaxane hinders the incorporation of the paraquat unit into the backbone.

Conclusion

In conclusion, we synthesized six polyurethanes, four of which were novel and two synthesized as controls. The polypseudorotaxanes synthesized with **BMP32C10**, **DB30C10**, **DB24C8** and the pyridyl cryptand based on **DB30C10** showed threading efficiencies of < 1%, 17.5%, 9.5% and 16% respectively. These results run contrary to our expectation that the pyridyl cryptand would show nearly quantitative threading. We also expected to find evidence of **BMP32C10** threading in solution. This could suggest that the shape and size of the cavity is more important to threading efficiency in solution than previously thought. However, these data do support our supposition that **DB30C10** and the pyridyl cryptand can be used as hosts in cases where pseudorotaxane formation is crucial.

Experimental

DB30C10 and **DB24C10** were made according to the published procedure.[39] The pyridyl cryptand was synthesized according to our reported templation procedure.[40] 4,4'-MDI was distilled under vacuum at 200 ºC at 1 Torr. Poly(THF) 1000 was dissolved in DCM and washed with NaOH (10 %) 3x and water 3x. The organic layer was dried over $MgSO_4$. The DCM was removed by rotary evaporation. The crown ethers, the cryptands, the paraquat diol and the poly(THF) was dried over P_2O_5 under vacuum for at least 24 hours before use. The glassware and stir bars were dried in the oven for at least 12 hours before use. Anhydrous diglyme and MeCN were purchased and used without further purification. Melting points were measured with a Mel-Temp II device or Büchi Melting Point B-540 in capillary tubes and are uncorrected. The heating rate was 2 º/ min. Melting points are recorded as the average of three measurements (collapse point – fully liquid). ^{1}H and ^{13}C NMR spectra were obtained at ambient temperatures on Varian Unity Plus or Varian MR 400 MHz spectrometers. ^{1}H NMR and ^{13}C spectra are corrected relative to residual solvent peaks: 2.05 ppm for acetone-d_6, 2.50 ppm for DMSO-d_6,1.940 ppm for MeCN-d_3 and 7.26 ppm for chloroform-*d*. High-resolution mass s pectra were obtained with an Agilent 6220 LCMS ESI-TOF spectrometer using acetonitrile as solvent. Column chromatography was performed with silica gel, 40-63 μm, 60 Å from Sorbent Technologies, or Flash Alumina-N from Agela Technologies.

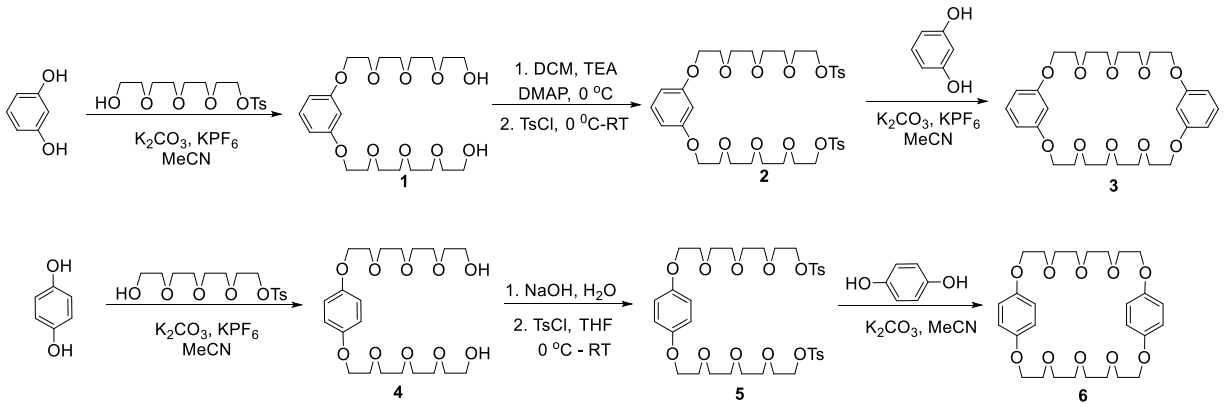

Scheme 4.2. Synthesis of **BMP32C10** and **BPP34C10**

1,1'-Bis(2-hydroxyethyl)-[4,4'-bipyridine]-1,1'-diium hexafluorophosphate. 4,4'-Bipyridine (5.04 g, 32 mmol) and 2-chloroethanol (25.0 mL, 373 mmol) were combined with MeCN (70 mL). The contents dissolved to give a clear yellow solution. The solution was heated to reflux. After 4 days the mixture was white and completely opaque. After 7 more days the mixture was cooled to room temperature. The white solid was collected by vacuum filtration. The solid was washed with acetone 5 x and DCM 2 x. The solid was allowed to dry on the frit. The solid was dissolved in water and a solution of KPF_6 (sat.) was added. The solid that precipitated was collected by vacuum filtration and recrystallized from water 4 times to give a clear crystalline solid (7.26 g, 41 %). Mp 204.7-205.4 ºC decomp. (Lit mp 215-220 ºC).[53] ^{1}H NMR (400 MHz, DMSO-d_6) δ 9.30 (d, J = 7 Hz, 4H), 8.77 (d, J = 7 Hz, 4H), 5.34 (t, J = 5 Hz, 2H), 4.80 – 4.72 (m, 4H), 3.93 (q, J = 5 Hz, 4H).

1,3-Bis-[2-[2'-[2''-(2'''-hydroxyethoxy)ethoxy]ethoxy]ethoxy]benzene[54] (1) Resorcinol (2.27 g, 20.7 mmol) and tetra(ethyleneglycol) monotosylate (15.16 g, 43.4 mmol) were dissolved in MeCN (200 mL) and Ar (g) was bubbled through the solution for about 15 min. K_2CO_3 (28.74 g, 207 mmol) was added and the reaction vessel was wrapped in aluminium foil to exclude light. The solution was brought to reflux under Ar

(g). After 5 days the solution was pink with a precipitate. The heat was removed and after the solution had cooled it turned brown. The solvent was removed by rotary evaporation. The residue was dissolved in DCM/ water and transferred to a separatory funnel. The organic layer was removed and the aqueous layer was extracted with DCM 3x. The combined organic layers were washed with 1:1 brine: 10% NaOH (3x) and with water (2x). The organic layer was dried over $MgSO_4$, filtered and the solvent was removed to yield a brown oil (7.87 g, 83%). ^{1}H NMR (400 MHz, chloroform-*d*) δ 7.14 (t, *J* = 8 Hz, 1H), 6.53 – 6.48 (m, 3H), 4.13 – 4.08 (m, 4H), 3.85 – 3.82 (m, 4H), 3.75 – 3.63 (m, 24H), 3.61 – 3.58 (m, 4H), 2.75 – 2.64 (m, 2H). ^{13}C NMR (101 MHz, chloroform-*d*) δ 160.0, 129.9, 107.2, 101.9, 72.7, 70.9, 70.8, 70.7, 70.4, 69.8, 67.5, 61.8.

1,3-Bis[2'-[2''-[2'''-(2''''-hydroxyethoxy)ethoxy]ethoxy]ethoxy]benzene bis(*p*-methylbenzenesulfonate) (2) Diol **1** (7.63 g, 16.5 mmol) was dissolved in DCM (40 mL). Triethylamine (5.5 mL, 40 mmol) and DMAP (0.30 g, 0.2 mmol) were added. The solution was cooled to 2 ºC in an ice bath. TsCl (9.40 g, 49.3 mmol) was dissolved in DCM and added to the solution drop-wise over the course of 3 h. The solution was left in the ice bath over-night. The reaction mixture was washed with water, 10% NaOH (3x), and water again. The organic layer was dried over $MgSO_4$, filtered and the solvent removed to yield a brown oil (12.33 g). The brown oil was purified by column chromatography (silica gel: EtOAc). Fractions containing the product were combined to yield a light yellow oil (8.36 g, 66%). ^{1}H NMR (400 MHz, chloroform-*d*) δ 7.79 (d, *J* = 8 Hz, 4H), 7.33 (d, *J* = 8 Hz, 4H), 7.14 (t, *J* = 8 Hz, 1H), 6.51 (d, *J* = 2 Hz, 1H), 6.49-6.47 (m, 2H), 4.16 – 4.12 (m, 4H), 4.11 – 4.07 (m, 4H), 3.85 – 3.81 (m, 4H), 3.71 – 3.62 (m, 13H), 3.58 (s, 8H), 2.43 (s, 6H). ^{13}C NMR (101 MHz, chloroform-*d*) δ 160.0, 144.9, 133.1, 129.9, 128.1, 107.1, 101.8, 70.9, 70.8, 70.7, 70.6, 69.8, 69.3, 68.8, 67.5,

21.7. HRMS ESI-TOF $C_{36}H_{51}O_{14}S_2$ $(M+H)^+$ m/z 771.2698 (found) 771.2715 (calc.) δ -2.2 ppm, $C_{36}H_{54}NO_{14}S_2$ $(M+NH_4)^+$ m/z 788.2987 (found) 788.2980 (calc.) δ 0.9 ppm. $C_{36}H_{50}NaO_{14}S_2$ $(M+Na)^+$ m/z 793.2531 (found) 793.2534 (calc.) δ -0.37.

BMP32C10 (3) Resorcinol (0.99 g, 8.79 mmol) and K_2CO_3 (5.03 g, 36.4 mmol) were combined in MeCN (500 mL) and the solution was degassed with Ar (g). A separate solution of ditosylate (6.78 g, 8.79 mmol) in MeCN (150 mL) was prepared and degassed with Ar (g). The resorcinol solution was heated to reflux under Ar (g) and the ditosylate solution was added to it drop-wise *via* an addition funnel over the course of 3 h. The solution was allowed to heat at reflux for two weeks. The solution was cooled to room temperature and the solvent was removed *in vacuo*. The brown residue was dissolved in DCM/ water. The layers were separated and the water layer was extracted with DCM 3x. The organic layers were combined and washed with water (4x). The organic layer was dried over $MgSO_4$, filtered and the solvent was removed to give a viscous brown oil. The brown oil was purified by column chromatography (silica gel with EtOAc as eluent). The first fraction was concentrated to give a white solid (1.94 g, 41%). Mp 72.3-73.2 ºC, methanol. (Lit mp 72-74 ºC, methanol).[36] ^{1}H NMR (400 MHz, chloroform-*d*) δ 7.15 – 7.08 (m, 2H), 6.51 – 6.46 (m, 6H), 4.09 – 4.03 (m, 8H), 3.85 – 3.80 (m, 8H), 3.73 – 3.65 (m, 16H). ^{13}C NMR (101 MHz, chloroform-*d*) δ 160.1, 129.9, 107.2, 101.8, 71.0, 70.9, 69.8, 67.6.

1,4-Bis-[2-[2'-[2''-(2'''-hydroxyethoxy)ethoxy]ethoxy]ethoxy]benzene (4) [55]

Hydroquinone (4.31 g, 39.1 mmol) and tetra(ethylene glycol) monotosylate (30.00 g, 86.1 mmol) were dissolved in MeCN (500 mL). The solution was degassed by bubbling Ar (g) through it for several minutes. K_2CO_3 (32.45 g, 234 mmol) was added, the flask was wrapped in foil and the reaction was heated to reflux under Ar (g). After 5 days

the reaction flask was cooled to room temperature and the solvent was removed by rotary evaporation. The residue was re-dissolved in DCM/ water and transferred to a separatory funnel. The layers were separated and the organic layer was washed 4 x with 1:1 NaOH (10 % w/v): NaCl (sat.). The organic layer was dried over $MgSO_4$, filtered and the solvent was removed under reduced pressure to yield a brown oil (12.89 g, 71 %). ^{1}H NMR (400 MHz, chloroform-*d*) δ 6.84 (s, 4H), 4.11 – 4.04 (m, 4H), 3.85 – 3.80 (m, 4H), 3.73 – 3.66 (m, 16H), 3.62 – 3.58 (m, 4H), 2.13 (s, 2H). ^{13}C NMR (101 MHz, chloroform-*d*) δ 153.1, 115.6, 72.6, 70.8, 70.7, 70.6, 70.4, 69.9, 68.1, 61.8.

1,4-Bis[2'-[2''-[2'''-(2''''-hydroxyethoxy)ethoxy]ethoxy]ethoxy]benzene bis(*p*-methylbenzenesulfonate (5).[56]

Diol **4** (12.89 g, 27.9 mmol) and THF (40 mL) were combined and the flask was submerged in an ice bath. A solution of NaOH (2.68 g, 66.9 mmol) in water (10 mL) was added. The solution went from colourless to light yellow. When the solution reached an internal temperature of 3 ºC, a solution of TsCl (15.95 g, 83.6 mmol) in THF (130 mL) was added drop-wise. After the addition was complete, the ice in the ice bath was left to melt and the solution was left to stir over-night. The solution was poured into ice. The ice melted and the solution was transferred to a separatory funnel and extracted with DCM (4 x). The combined organic layers were washed with NaOH (10 % w/v) (2 x), and water (2 x). Triethylamine (10 mL) was added to the organic layer as well as 2x 30 mm filter papers torn into small pieces. The solution was allowed to stir over-night.[58] The filter paper was filtered out and the organic layer was washed with 10 % (v/v) HCl 3 x and water 2 x. The organic layer was dried over $MgSO_4$, filtered and the solvent removed to yield a brown oil. The brown oil was purified by column chromatography (silica gel; ethyl acetate). The fractions containing product were collected and concentrated to yield a yellow oil (12.06 g, 56%). ^{1}H NMR (400 MHz,

chloroform-*d*) δ 7.79 (d, *J* = 8 Hz, 4H), 7.33 (d, *J* = 8 Hz, 4H), 6.83 (s, 4H), 4.17 – 4.13 (m, 4H), 4.08 – 4.05 (m, 4H), 3.83 – 3.79 (m, 4H), 3.70 – 3.67 (m, 8H), 3.65 – 3.63 (m, 4H), 3.58 (s, 8H), 2.43 (s, 6H).

BPP34C10 K_2CO_3 (13.38 g, 96 mmol) was suspended in MeCN (1 L). The solvent was degassed by bubbling Ar(g) through it for several minutes. Hydroquinone (1.72 g, 15.6 mmol) and ditosylate **(5)** (12.06 g, 15.6 mmol) were dissolved in MeCN and the solution was degassed by bubbling Ar (g) through it before being transferred to an addition funnel. The reaction flask was heated to reflux under Ar (g). The flask was then wrapped in aluminum foil to exclude light and the hydroquinone and ditosylate solution was added drop-wise. The resulting solution was allowed to reflux under Ar (g) for three weeks. The solution was cooled to room temperature. The solvent was removed from the brown, murky solution to yield a brown residue. The residue was re-dissolved in DCM/ water and transferred to a separatory funnel and the layers were separated. The layers were separated and the organic layer was washed with water, a solution of NaOH (10% w/v): NaCl (sat.) 1:1 twice, followed by another water wash. The organic layer was dried over $MgSO_4$, filtered and the solvent removed to yield a brown solid (5.21 g). The brown solid was purified by column chromatography (silica; 4:1 ethyl acetate: DCM). The third fraction was collected and concentrated to yield a white solid (1.81 g, 21 %). Mp 86.1-87.8 ºC Lit mp 93-94 ºC,[57] 87-89 ºC,[38] 95-96.8. ºC[35]. ^{1}H NMR (400 MHz, chloroform-*d*) δ 6.75 (s, 8H), 4.00-3.97 (m, 8H), 3.85-3.82 (m, 8H), 3.73-3.68 (m, 16H). ^{13}C NMR (101 MHz, chloroform-*d*) δ 153.0, 115.4, 70.8, 70.6, 69.7, 68.1.

Backbone poly(urethane) (PB) 4,4'-Methylenediphenyl diisocyanate (0.7881 g, 3.1491 mmol) was dissolved in dry MeCN (2 mL) and diglyme (1 mL) and lowered into an oil bath that had been pre-heated to 90 ºC. After a few minutes, poly(THF), with an average molecular weight 1000 g/mol, (1.8154 g, 1.8154 mmol) was added in MeCN (2 mL) and dioxane (1 mL). The solution was allowed to stir at 90 ºC under Ar (g) for 1.5 h. After this time paraquat diol (0.7553 g, 1.4085 mmol) was added. Some solid residue was observed and 1 mL of dioxane was added to dissolve the solid. The solution was allowed to stir at reflux for 3 days (around 40 h). The solution was removed from the oil bath and allowed to cool to room temperature. The viscous, light yellow material was precipitated into rapidly stirring MeOH (400 mL). The solid was collected and precipitated from MeOH three more times.

Poly(urethane) with BPP34C10 added (PR) 4,4'-Methylenediphenyl diisocyanate (0.7689 g, 3.072 mmol) was dissolved in MeCN (2 mL) and diglyme (1 mL) and lowered into an oil bath that had been pre-heated to 90 ºC. Poly(THF) 1000 (1.8270 g, 1.8270 mmol) was added along with MeCN (2 mL). The solution was allowed to heat under Ar (g). After 1.5 hours **BPP34C10** (0.8024 g, 1.4952 mmol) was added in diglyme (0.5 mL). Paraquat diol (0.6677 g, 1.2451 mmol) was added after 10 min. The solution turned dark red immediately. The solution was allowed to stir under Ar (g) for 46 h. During this time the oil bath was kept between 80 and 110 ºC. The flask was removed from the oil bath. When the flask was cool the viscous blood red oil was precipitated in rapidly stirring MeOH (400 mL). The red solid was collected and precipitated from acetone into MeOH three more times. During one of the precipitations, the polymer was allowed to stir in MeOH for 24 h.

Poly(urethane) with DB30C10 added (P2) 4,4'-Methylenediphenyl diisocyanate (0.7266 g, 2.9034 mmol) was dissolved in MeCN (2 mL) and diglyme (1 mL) and lowered into an oil bath pre-heated to 90 ºC. Poly(THF) 1000 (1.7265 g, 1.7265 mmol) was added. The poly(THF) was cooled in the freezer to facilitate transfer and 1.5 mL MeCN was used to complete transfer. The solution was allowed to reflux in the oil bath under Ar (g). After 1.5 h, **DB30C10** (0.7584 g, 1.4133 mmol) was added and the solution was allowed to stir for 12 min under Ar (g). Paraquat diol (0.6315 g, 1.178 mmol) was added. The solution went from very light yellow to orange. The solution was kept in the oil bath between 85 and 110 ºC under Ar (g) for 46 h. The viscous orange solution was cooled to room temperature and precipitated into rapidly stirring MeOH (400 mL). The orange gooey material was collected, dissolved and precipitated three times from acetone into MeOH. The polymer was allowed to stir in MeOH for 24 hours after the third precipitation.

Poly(urethane) with DB24C8 added (P1) 4,4'-MDI (0.7705 g, 3.079 mmol) was dissolved in MeCN (1 mL) and diglyme (1 mL). The solution was lowered into an oil bath pre-heated to 90 ºC. After a few minutes, poly(THF) 1000 (1.7304 g, 1.7304 mmol) was added and with MeCN (2 mL) to fully transfer the polymer. The solution was allowed to stir at 90 ºC under Ar (g) for 2 h. **DB24C8** (0.6631 g, 1.478 mmol) was added and the solution was allowed to stir for 20 min before paraquat diol (0.6629 g, 1.2362 mmol) was added. The solution went from light yellow to orange and murky. More diglyme (1 mL), and a little more MeCN were added to dissolve the solids. The solution was allowed to stir in the heat bath for 3 days before it was cooled to room temperature. The orange, viscous solution was precipitated into rapidly stirring MeOH (400 mL). The orange solid was collected and precipitated from acetone into MeOH twice more.

Poly(urethane) with BMP32C10 added (P3) 4,4'-MDI (0.7822 g, 3.126 mmol) was dissolved in MeCN (1 mL) and diglyme (0.8 mL) and lowered into an oil bath pre-heated to 90 ºC. After 15 min, poly(THF) 1000 (1.8119 g, 0.1811 mmol) was added with MeCN (2 mL) and diglyme (0.6 mL). The solution was allowed to heat under Ar (g) for 90 min. **BMP32C10** (0.8032 g, 1.496 mmol) was added. The solution was very viscous and murky. The stir bar had almost entirely stopped. MeCN (1 mL) and diglyme (2 mL) were added. After 10 min., paraquat diol (06523 g, 1.216 mmol) was added. The stir bar had resumed stirring and the solution was orange and murky. After 14 h. stirring at 90 ºC under Ar (g), the contents of the flask were bright orange and appeared to be a solid block of gel. The flask was removed from the heating bath and the acetone was added. What could be dissolved was precipitated into rapidly stirring MeOH. The procedure was repeated twice. The end product was a light yellow solid.

Poly(urethane) with pyridyl cryptand added (P4) 4,4'-MDI (0.7829 g, 3.128 mmol) was dissolved in MeCN (1 mL) and diglyme (1 mL). The solution was lowered into an oil bath pre-heated to 100 ºC. The solution was allowed to stir a few minutes under Ar (g) before poly(THF) 1000 (1.0895 g, 1.0895 mmol) was added with MeCN (3 mL) to facilitate transfer of the sticky solid. After 85 min, cryptand (1.0895 g, 1.497 mmol) was added. The cryptand took a few minutes to dissolve. Paraquat diol (0.6632 g, 1.237 mmol) was added with diglyme (1 mL). The solution went from light yellow to bright red. The solution was allowed to stir in the oil bath under Ar (g) for 47 h. The solution was taken out of the oil bath and allowed to cool to room temperature. The sticky viscous solution was precipitated into rapidly stirring MeOH (400 mL). The sticky, bright orange polymer was collected and precipitated from acetone into MeOH three more times.

References

1. Izatt, R. M., Charles J. Pedersen's legacy to chemistry. *Chem. Soc. Rev.* **2017,** *46*, 2380-2384.
2. Pedersen, C. J., Cyclic Polyethers and Their Complexes with Metal Salts. *J. Am. Chem. Soc.* **1967,** *89*, 7017-7036.
3. Liu, Z.; Nalluri, S. K. M.; Stoddart, J. F., Surveying macrocyclic chemistry: from flexible crown ethers to rigid cyclophanes. *Chem. Soc. Rev.* **2017,** *46*, 2367-2650.
4. Steed, J. W.; Atwood, J. L., *Supramolecular chemistry*. second ed.; John Wiley & Sons: 2009.
5. Gokel, G. W.; Leevy, W. M.; Weber, M. E., Crown Ethers: Sensors for Ions and Molecular Scaffolds for Materials and Biological Models. *Chem. Rev.* **2004**, 2723-2750.
6. Awual, M. R., Ring size dependant crown ether based mesoporous adsorbent for high cesium adsorption from wastewater. *Chem. Eng. J.* **2016,** *303*, 539-546.
7. Liu, Y.; Xue, Y.; Tang, H.; Want, M.; Qin, Y., Click-immobalized K^+-selective ionophore for potentiometric and optical sensors. *Sens. Actuators, B* **2012,** *171-172*, 556-562.
8. Esteves, C. I. C.; Batista, R. M. F.; Raposo, M. M. M.; Costa, S. P. G., Novel functionalised imidazo-benzocrown ethers bearing a thiophene spacer as fluorimetric chemosensors for metal ion detection. *Dyes and Pigments* **2016,** *135*, 134-142.
9. Leevy, W. M.; Donato, G. M.; Ferdani, R.; Goldman, W. E.; Schlesinger, P. H.; Gokel, G. W., Synthetic Hydrophile Channels of Appropriate Length Kill *Escherichia coli*. *J. Am. Chem. Soc.* **2002,** *124*, 9022-9023.
10. De Rosa, M.; Vigliotta, G.; Soriente, A.; Capaccio, V.; Gorrasi, G.; Adami, R.; Reverchon, E.; Mella, M.; Izzo, L., "Leaching or not leaching": an alternative approach to antimicrobial materials *via* copolymers containing crown ethers as active groups. *Biomater. Sci.* **2017,** *5*, 741-751.
11. Febles, M.; Montalvão, S.; Crespín, G. D.; Norte, M.; Padrón, J. M.; Tammela, P.; J., F. J.; Daranas, A. H., Synthesis and biological evaluation of crown ether acyl drivatives. *Bioorg. Med. Chem* **2016,** *26*, 5591-5593.
12. Schneider, S.; Licsandru, E.-D.; Kocsis, I.; Gilles, A.; Dumitru, F.; Moulin, E.; Tan, J.; Lehn, J.-M.; Giuseppone, N.; Barboiu, M., Columnar Self-Assemblies of Triarylamines as Scoffolds for Artificial Biomimetic Channels for Ion and for Water Transport. *J. Am. Chem. Soc.* **2017,** *139*.
13. Feng, W.-X.; Sun, Z.; Zhang, Y.; Legrand, Y.-M.; Petit, E.; Su, C.-Y.; Barboiu, M., Bis-15-crown-5-ether-pillar[5]arene K^+-Responsive Channels. *Org. Lett.* **2017,** *19*, 1438-1441.
14. Ghosh, S.; Mukhopadhyay, C., Interpenetrated molecules: crown-ether and linear organic molecule supramolecular architechtures. *J. Incl. Phenom. Chem.* **2017,** *88*, 105-128.

15. Zhu, K.; Vukotic, N.; Noujeim, N.; Loeb, S. J., Bis(benzimidazolium) axles and crown ether wheels: a versatile templating pair for the formation of [2]rotaxane molecular shuttles. *Chem. Sci.* **2012,** *3*, 3265-3271.
16. Loeb, S. J.; Tiburcio, J.; Vella, S. J., [2]Pseudorotaxane Formation with *N*-Benzylanilinium Axles and 24-Crown-8 Ether Wheels. *Org. Lett.* **2005,** *7*, 4923-4926.
17. Busseron, E.; Coutrot, F., N-Benzyltriazolium as Both Molecular Station and Barrier in [2]Rotaxane Molecular Machines. *J. Org. Chem.* **2013,** *78*, 4099-4106.
18. Jacquot de Rouville, H.-P.; Lehl, J.; Bruns, C. J.; McGrier, P. L.; Frasconi, M.; Sarjeant, A. A.; Stoddart, J. F., A Neutral Naphthalene Diimide [2]Rotaxane. *Org. Lett.* **2012,** *14*, 5188-5191.
19. Moreira, L.; Illescas, B. M.; Nazario, M., Supramolecular Complexation of Carbon Nanostructures by Crown Ethers. *J. Org. Chem.* **2017,** *82*, 3347-3358.
20. Anelli, P. L.; Spencer, N.; Stoddart, J. F., A Molecular Shuttle. *J. Am. Chem. Soc.* **1991,** *113*, 5131-5133.
21. Xue, M.; Yang, Y.; Chi, X.; Yan, X.; Huang, F., Development of Pseudorotaxanes and Rotaxanes: From Synthesis to Stimuli-Responsive Motions to Applications. *Chem. Rev.* **2015,** *115*, 7398-7501.
22. Badjic, J. D.; Raconi, C. M.; Stoddart, J. F.; Balzani, V.; Silvi, S.; Credi, A., Operating Molecular Elevators. *J. Am. Chem. Soc.* **2006,** *128*, 1489-1499.
23. Badjic, J. D.; Balzani, V.; Credi, A.; Silvi, S.; Stoddart, J. F., A Molecular Elevator. *Science* **2004,** *303*, 1845-1849.
24. Bruns, C. J.; Stoddart, J. F., Rotaxane-Based Molecular Muscles. *Acc. Chem. Res.* **2014,** *47*, 2186-2199.
25. Du, G.; Moulin, E.; Jouault, N.; Buhler, E.; Giuseppone, N., Muscle-like Supramolecular Polymers: Integrated Motion from Thousands of Molecular Machines. *Angew. Chem. Int. Ed.* **2012,** *51*, 12504-12508.
26. Goujon, A.; Mariani, G.; Lang, T.; Moulin, E.; Rawiso, M.; Buhler, E.; Giuseppone, N., Controlled Sol-Gel Transitions by Actuating Molecular Machine Based Supramolecular Polymers. **2017,** *139*, 4923-4928.
27. Blanco, V.; Leigh, D. A.; Marcos, V., Artificial switchable catalysts. *Chem. Soc. Rev.* **2015,** *44*, 5341-5370.
28. Leigh, D. A.; Marcos, V.; Wilson, M. R., Rotaxane Catalysts. *ACS Catal.* **2014,** *4*, 4490-4497.
29. Ji, X.; Yao, Y.; Li, J.; Yan, X.; Huang, F., A Supramolecular Cross-Linked Conjugated Polymer Network for Multiple Fluorescent Sensing. *J. Am. Chem. Soc.* **2013,** *135*, 74-77.

30. Sun, J.; Wu, Y.; Wang, Y.; Liu, Z.; Cheng, C.; Hartlieb, K. J.; Wasielewski, M. R.; Stoddart, J. F., An Electrochromic Tristable Molecular Switch. *J. Am. Chem. Soc.* **2015,** *137*, 13484-13487.
31. Jiang, L.; Okano, J.; Orita, A.; Otera, J., Intermittent Molecular Shuttle as a Binary Switch. *Angew. Chem. Int. Ed.* **2004,** *43*, 2121-2124.
32. Thordarson, P., Determining association constants from titration experiments in supramolecular chemistry. *Chem. Soc. Rev.* **2011,** *40*, 1305-1323.
33. Hirose, K., A Practical Guide for the Determination of Binding Constants. *J. Incl. Phenom. Chem.* **2001,** *39*, 193-209.
34. Burnsveld, L.; Folmer, B. J. B.; Meijer, E. W.; Sijbesma, R. P., Supramolecular Polymers. *Chem. Rev.* **2001,** *101*, 4071-4097.
35. Gibson, H. W.; Shen, Y. X.; Bheda, M. C.; Gong, C., Polymeric molecular shuttles: Polypseudorotaxanes & polyrotaxanes based on viologen (paraquat) urethane backbones & bis(p-phenylene)-34-crown-10. *Polymer* **2014,** *55*, 3202-3211.
36. Allwood, B. L.; Shahriari-Zavareh, H.; Stoddart, J. F.; Williams, D. J., Complexation of Paraquat and Diquat by a Bismetaphenylene-32-crown-10 Derivative *J. Chem. Soc., Chem. Commun.* **1987**, 1058-1061.
37. Bush, M. A.; Truter, M. R., Crystal Structures of Complexes between Alkali-metal Salts and Cyclic Polyethers. Part IV. The Crystal Structures of Dibenzo-30-crown-I0 (2,3: 17,18-di benzo-I ,4,7,10,13,16,19,22,25,28-decaoxacyclotriaconta-2,17-diene) and of its Complex with Potassium Iodide. *J. Chem. Soc., Perkin Trans. 2* **1972,** *0*, 345-350.
38. Allwood, B. L.; Specer, N.; Shahriari-Zavareh, H.; Stoddart, J. F.; Williams, D. J., Complexation of Diquat by a bisparaphenylene-34-crown-10 derivative. *J. Chem. Soc., Chem. Commun.* **1987**, 1061-1064.
39. Wessels, H. R.; Gibson, H. W., Multi-gram syntheses of four crown ethers using K+ as templating agent. *Tetrahedron* **2016,** *72*, 396-399.
40. Price, T. L. J.; Wessels, H. R.; Slebodnick, C.; Gibson, H. W., High-Yielding Syntheses of Crown Ether-Based Pyridyl Cryptands. *J. Org. Chem.* **2017,** *82*, 8117-8122.
41. Yamaguchi, N.; Gibson, H. W., Formation of Supramolecular Polymers from Homoditopic Molecules Containing Secondary Ammonium Ions and Crown Ether Moieties. *Angew. Chem. Int. Ed.* **1999,** *38*, 143-147.
42. Wang, P.; Gao, Z.; Yuan, M.; Zhu, J.; Wang, F., Mechanically linked poly[2]rotaxanes constructed from the benzo-21-crown-7/secondary ammonium salt recognition motif. *Polym. Chem.* **2016,** *7*, 3664-3668.

43. Huang, F.; Nagvekar, D. S.; Slebodnick, C.; Gibson, H. W., A Supramolecular Triarm Star Polymer from a Homotritopic Tris(Crown Ether) Host and a Complementary Monotopic Paraquat-Terminated Polystyrene Guest by a Supramolecular Coupling Method. *J. Am. Chem. Soc.* **2005,** *127*, 484-485.
44. Gibson, H. W.; Ge, Z.; Huang, F.; Jones, J. W.; Lefebvre, H.; Vergne, M. J.; Hercules, D. M., Syntheses and Model Complexation Studies of Well-Defined Crown Terminated Polymers. *Macromolecules* **2005,** *38*, 2626-2637.
45. Gibson, H. W.; Liu, S.; Lacavalier, P.; Wu, C.; Shen, Y. X., Synthesis and Preliminary Characterization of Some Polyester Rotaxanes. *J. Am. Chem. Soc.* **1995,** *117*, 852-874.
46. Wang, F.; Zhang, J.; Ding, X.; Dong, S.; Liu, M.; Zheng, B.; Li, S.; Wu, L.; Yu, Y.; Gibson, H. W.; Huang, F., Metal Coordination Mediated Reversible Conversion between Linear and Cross-Linked Supramolecular Polymers. *Angew. Chem. Int. Ed.* **2010,** *49*, 1090-1094.
47. Gong, C. Linear, Branched and Crosslinked Polyesters, Polyurethanes and Polymethacrylates Derived From Rotaxane Formation: Synthesis and Properties. Virginia Polytechnic Institute and State University, Blacksburg, Virginia, 1997.
48. Xi-Shen, Y. New Polymer Architectures: Synthesis and Characterization of Polyurethane-Crown Ether Based Polyrotaxanes. Virginia Polytechnic and State University, Blacksburg, Virginia, 1992.
49. Amabilino, D. B.; Anelli, P. L.; Ashton, P. R.; Brown, G. R.; Córdova, E.; Godínez, L. A.; Hayes, W.; Kaifer, A. E.; Philp, D.; Slawin, A. M. Z.; Spencer, N.; Stoddart, J. F.; Tolley, M. S.; Williams, D. J., Molecular Meccano. 3. Constitutional and Translational Isomerism in [2]Catenanes and [*n*]Pseudorotaxanes. *J. Am. Chem. Soc.* **1995,** *117*, 11142-11170.
50. Nagvekar, D. S.; Gibson, H. W., IMPROVED SYNTHESES OF 20- AND 26-MEMBERED bis(5-CARBOMETHOXY-1,3-PHENYLENE) CROWN ETHERS. *Org. Prep. Proced. Int.* **1997,** *29*, 237-240.
51. Pederson, A. M. P.; Ward, E. M.; Schoonover, D. V.; Slebodnick, C.; Gibson, H. W., High-Yielding, Regiospecific Synthesis of cis(4,4')-Di(carbomethoxybenzo)-30-crown-10, Its Conversion to a Pyridyl Cryptand and Strong Complexation of 2,2'- and 4,4'-Bipyridinium Derivatives. *J. Org. Chem.* **2008,** *73*, 9094-9101.
52. He, C.; Shi, Z.; Zhou, Q.; Li, S.; Li, N.; Huang, F., Syntheses of *cis*- and *trans*-Dibenzo-30-Crown-10 Derivatives *via* Regioselective Routes and Their Complexations with Paraquat and Diquat. *J. Org. Chem.* **2008,** *75*, 5872-5880.

53. Ashton, P. R.; Philp, D.; Reddington, M. V.; Slawin, A. M. Z.; Specer, N.; Stoddart, J. F.; Williams, D. J., The Self-assembly of Complexes with [2]Pseudorotaxane Superstructures. *J. Chem. Soc. Chem. Commun.* **1991**, 1680-1683.

54. Lari, J.; Moradgholi, F.; Vahedi, H.; Massoudi, A., Synthesis of Novel di Benzo Spiro Bis-Crown-Ether. *Lett. Org. Chem.* **2015,** *12*, 668-673.

55. Zhao, Y.-L.; Liu, L.; Zhang, W.; Sue, C.-H.; Li, Q.; Miljanić, O. Š.; Yaghi, O. M.; Stoddart, J. F., Rigid-Strut-Containing Crown Ethers and [2]Catenanes for Incorporation into Metal-Organic Frameworks. *Chem. Eur. J.* **2009,** *15*, 13356-13380.

56. Ashton, P. R.; Huff, J.; Menzer, S.; Parsons, I. W.; Preece, J. A.; Stoddart, J. F.; Tolley, M. S.; White, A. J. P.; Williams, D. J., Bis[2]catenanes and a Bis[2]rotaxane-Model Compounds for Polymers with Mechanically Interlocked Components. *Chem. Eng. J.* **1996,** *2*, 31-44.

57. Helgeson, R. C.; Timko, J. M.; Cram, D. J., The [2.2]Paracyclophanyl Group as a Structural Unit in Host Compounds. *J. Am. Chem. Soc.* **1974,** *96*, 7380-7382.

58. Schoonover, D. V.; Gibson, H. W., Facile removal of tosyl chloride from tosylates using cellulosic materials, e. g., filter paper. *Tetrahedron Lett.* **2017,** *58*, 242-244.

^{1}H NMR and ^{13}C NMR spectra for crown ethers and their precursors

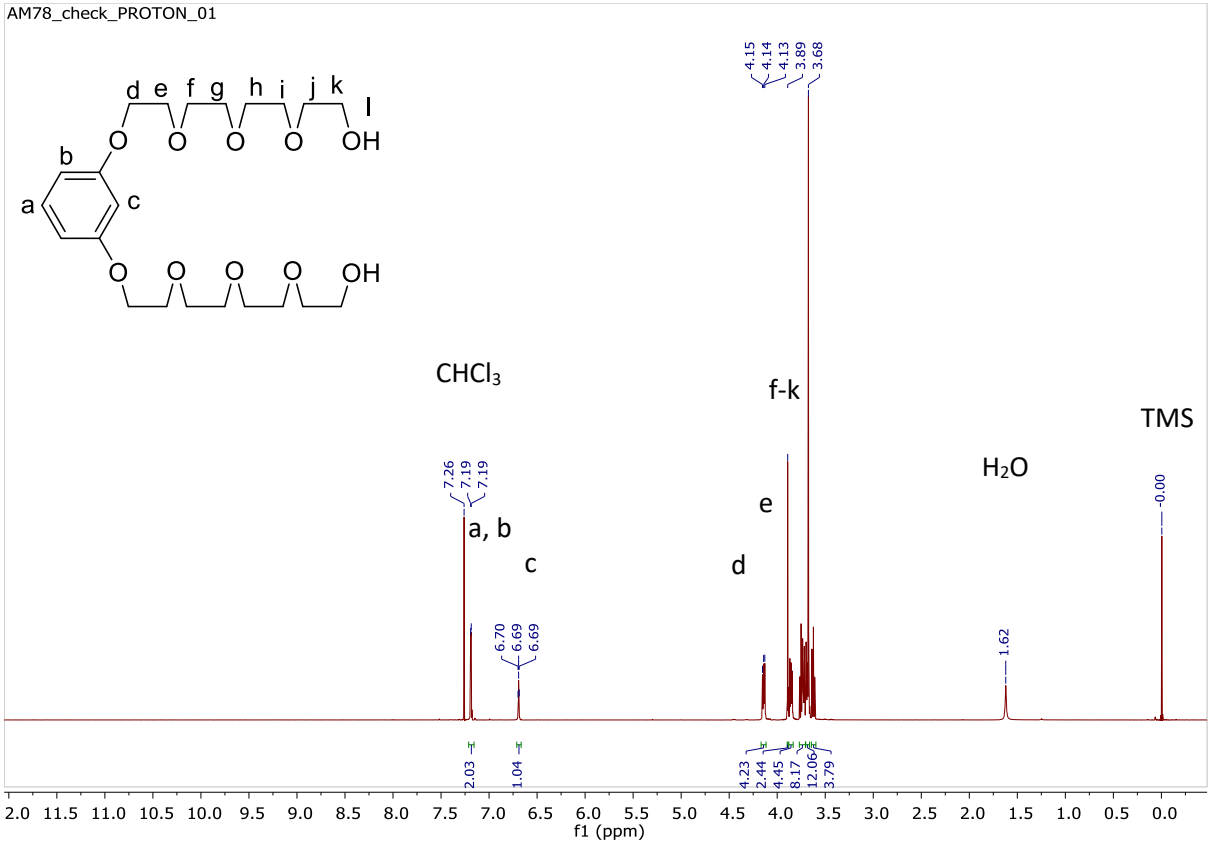

Figure 4.6. ^{1}H NMR spectrum of diol **1** in $CDCl_3$ at 400 HMz

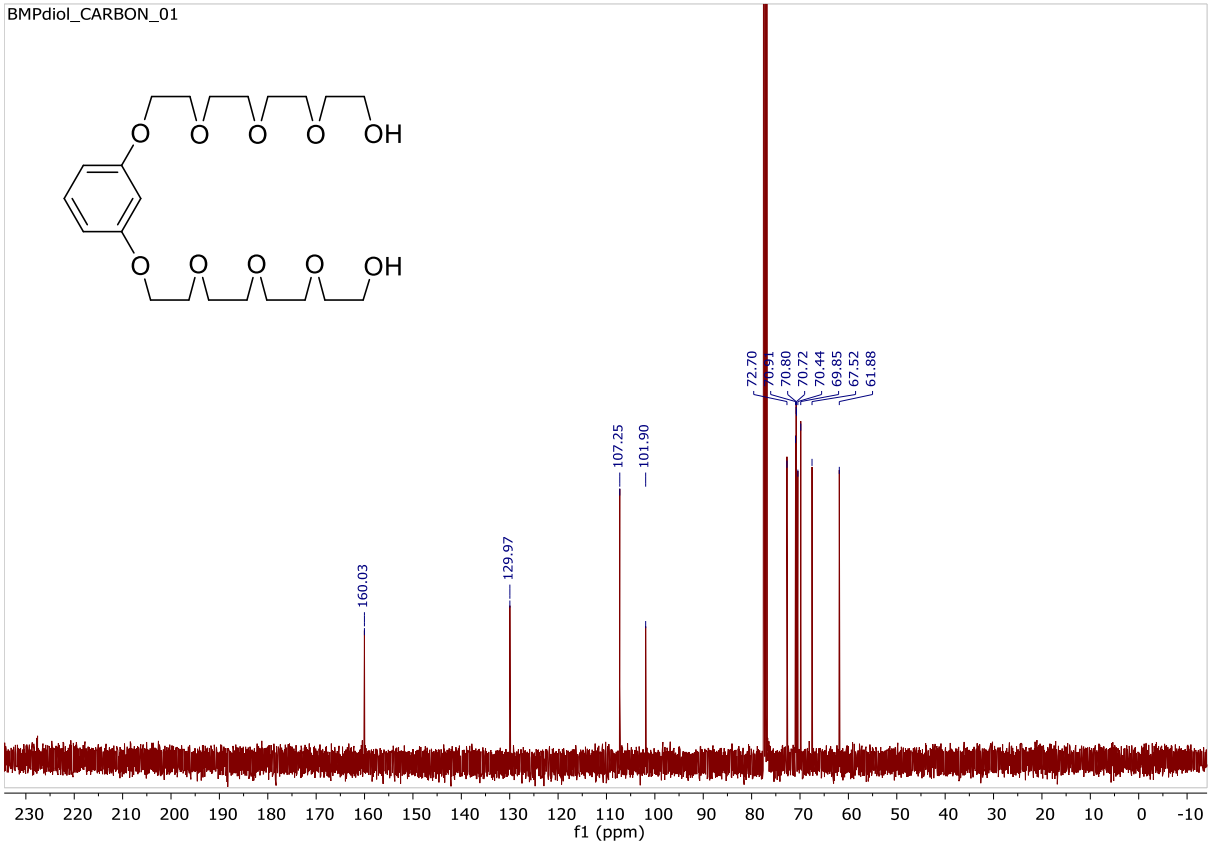

Figure 4.7. ^{13}C NMR spectrum of diol **1** in $CDCl_3$ at 101 MHz

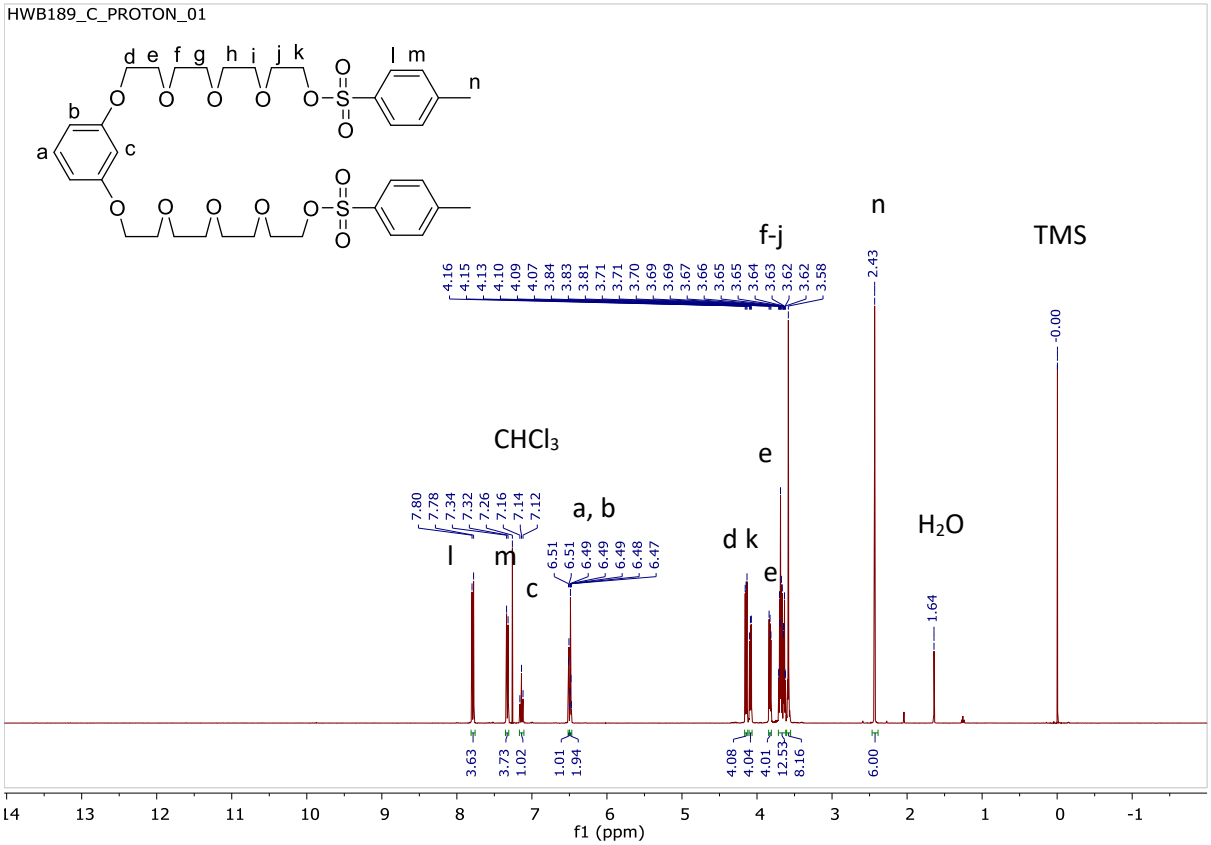

Figure 4.8. ^{1}H NMR spectrum of ditosylate **2** in $CDCl_3$ at 400 MHz

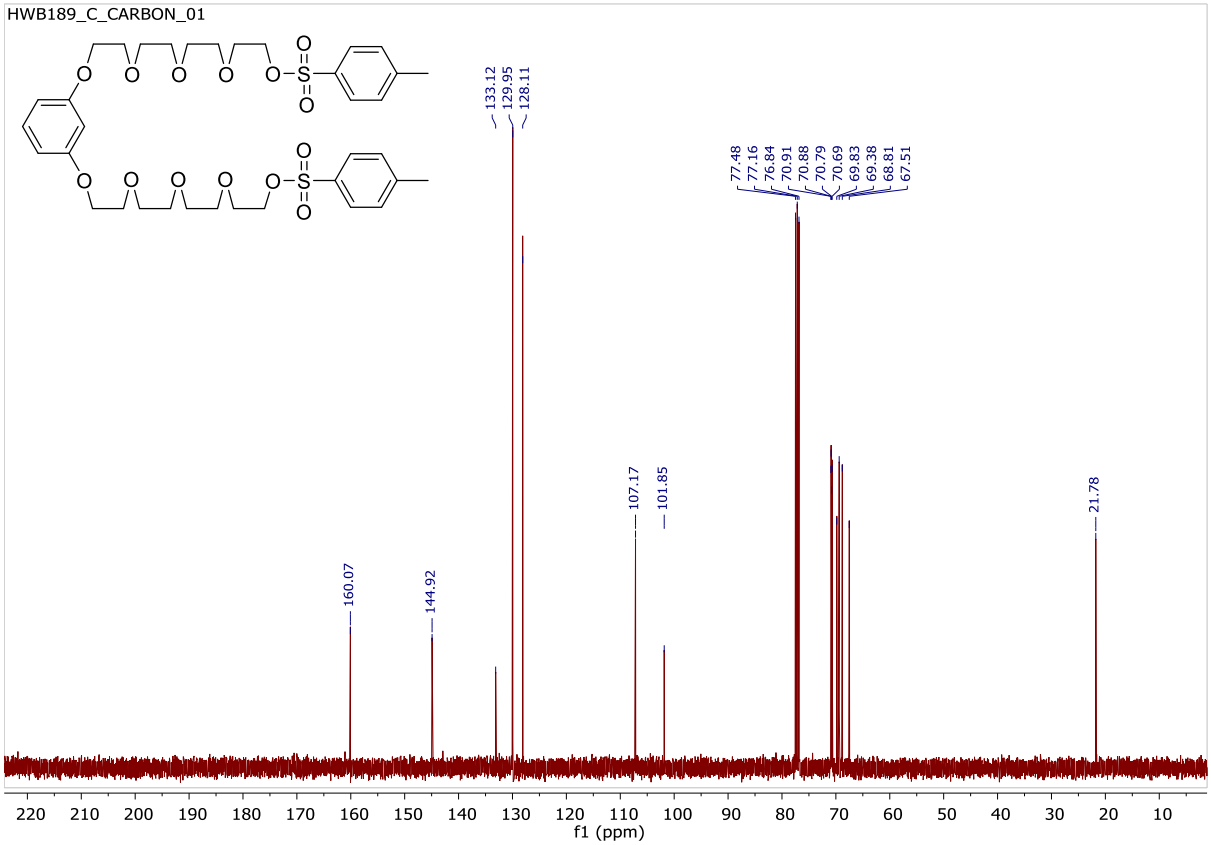

Figure 4.9. ^{13}C NMR of ditosylate **2** in $CDCl_3$ at 101 MHz

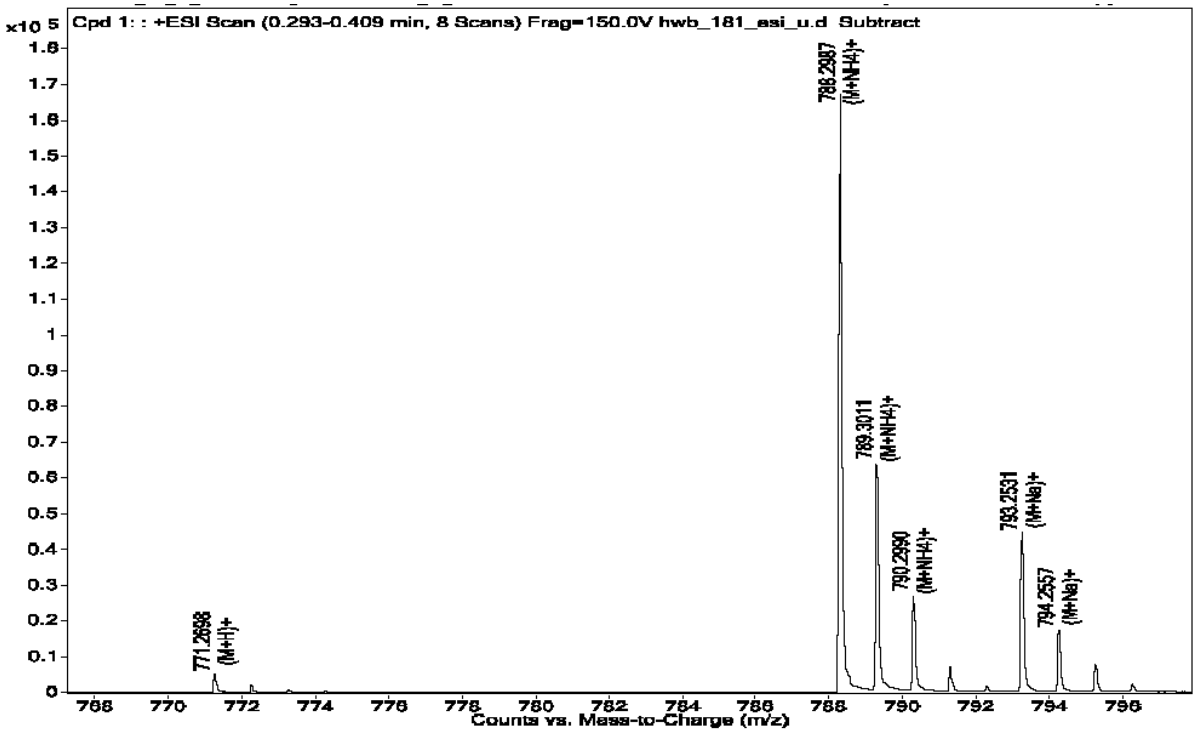

Figure 4.10 HRMS (ESI-TOF) of ditosylate **2**

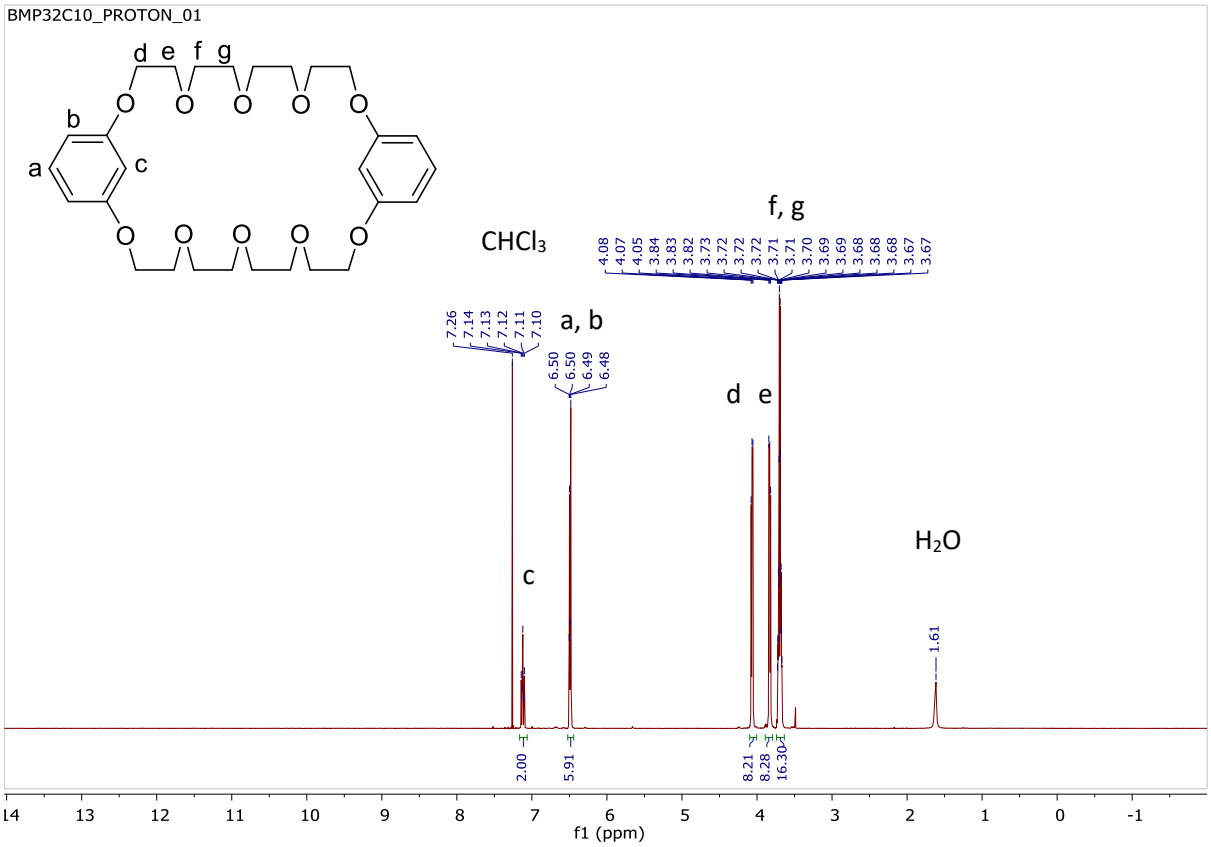

Figure 4.11. ^{1}H NMR spectrum of **BMP32C10** in $CDCl_3$ at 400 MHz

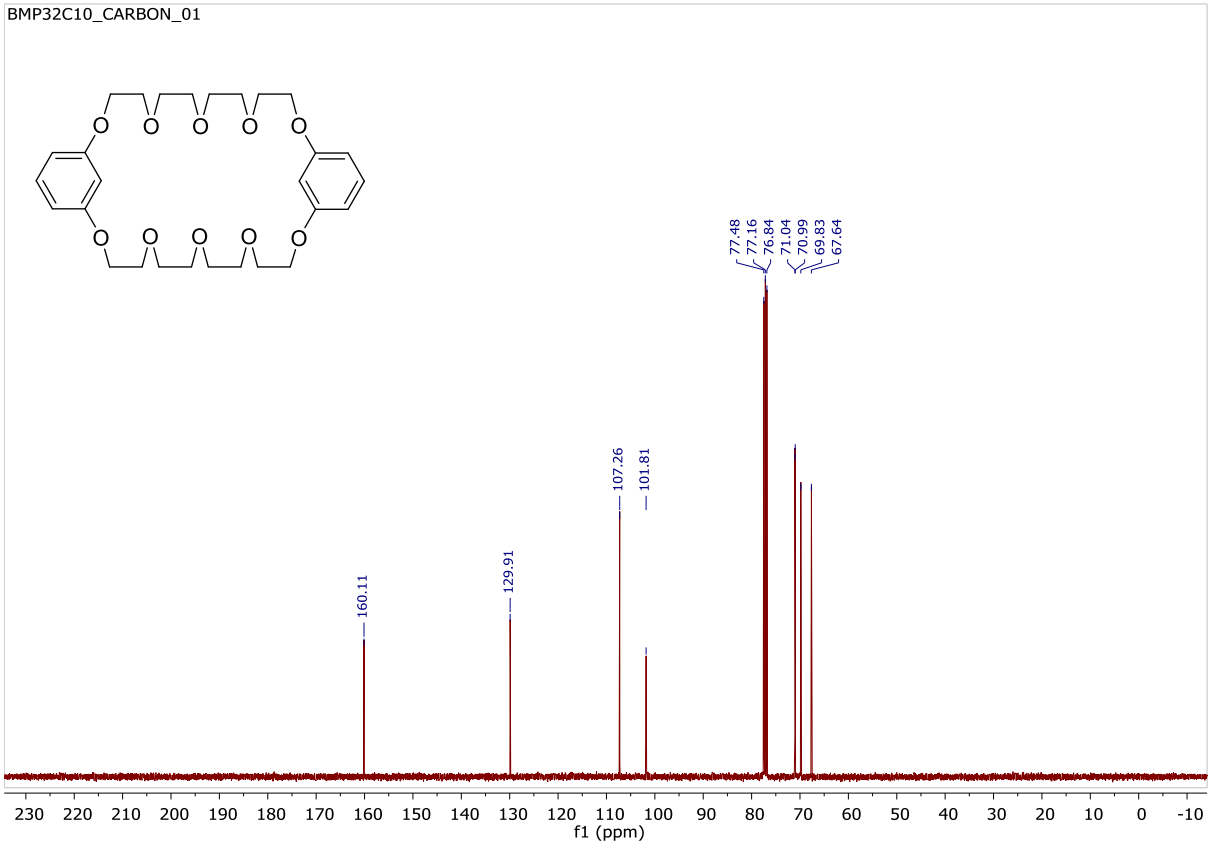

Figure 4.12. ^{13}C NMR of **BMP32C10** in $CDCl_3$ at 101 MHz

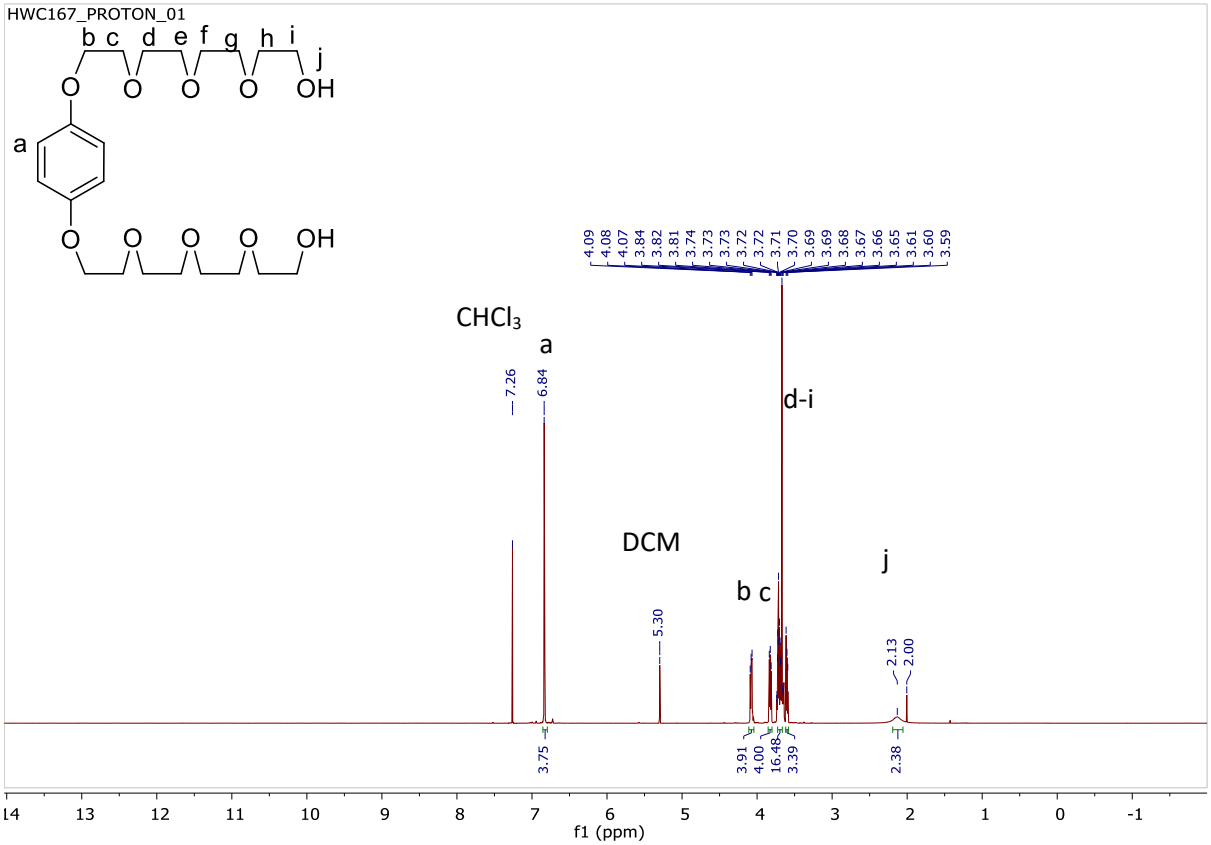

Figure 4.13. ^{1}H NMR spectrum of diol **4** in $CDCl_3$ at 400 MHz

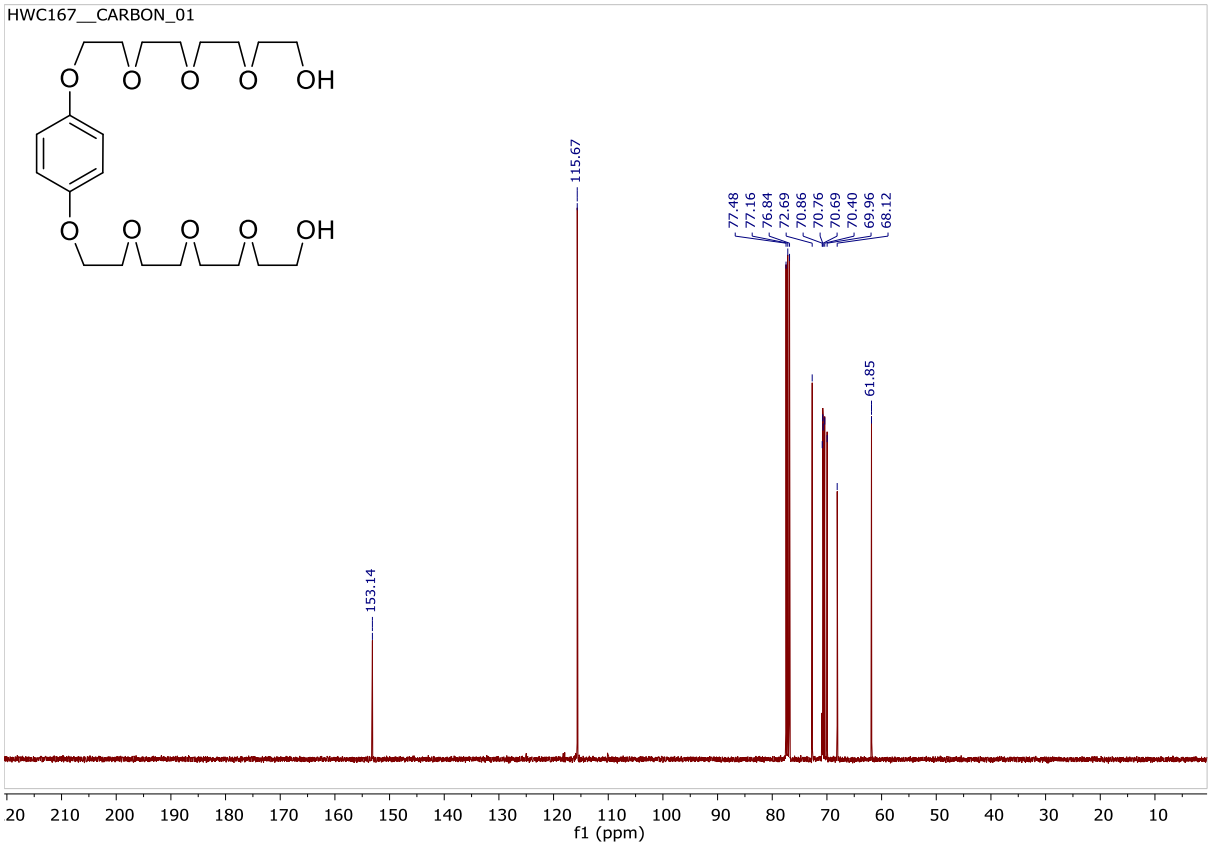

Figure 4.14. ^{13}C NMR spectrum of diol **4** in $CDCl_3$ at 101 MHz

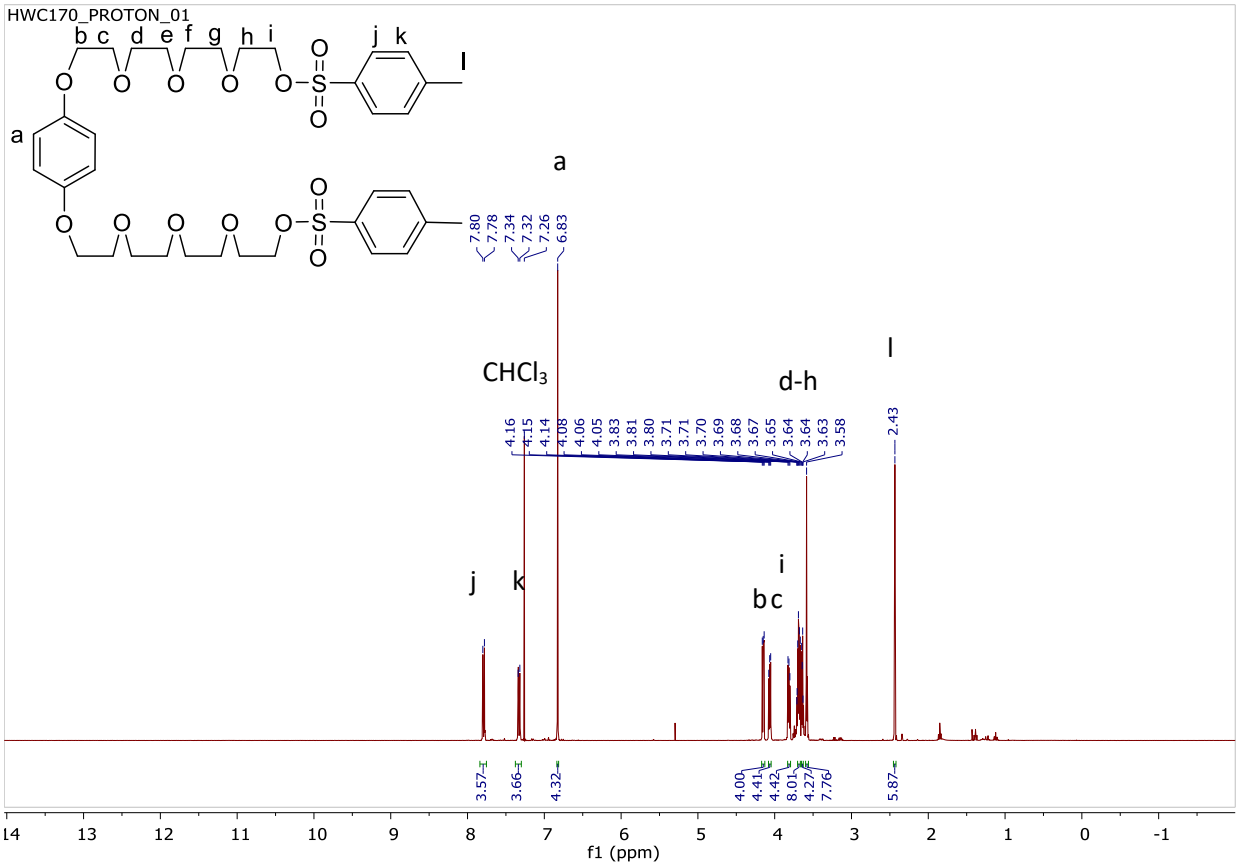

Figure 4.15. ^{1}H NMR spectrum of ditosylate **5** in $CDCl_3$ in 400 MHz

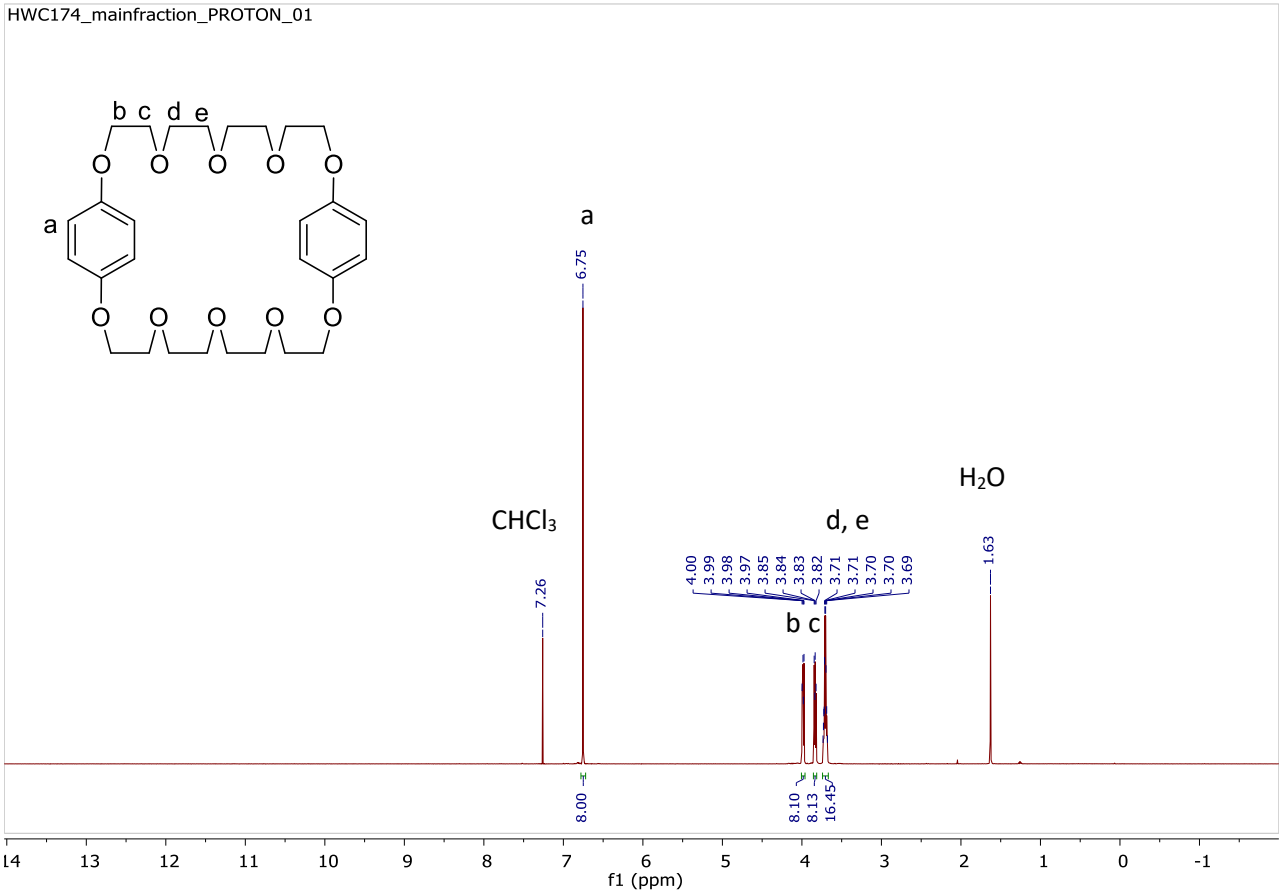

Figure 4.16. ^{1}H NMR spectrum of **BPP34C10** in $CDCl_3$ at 400 MHz

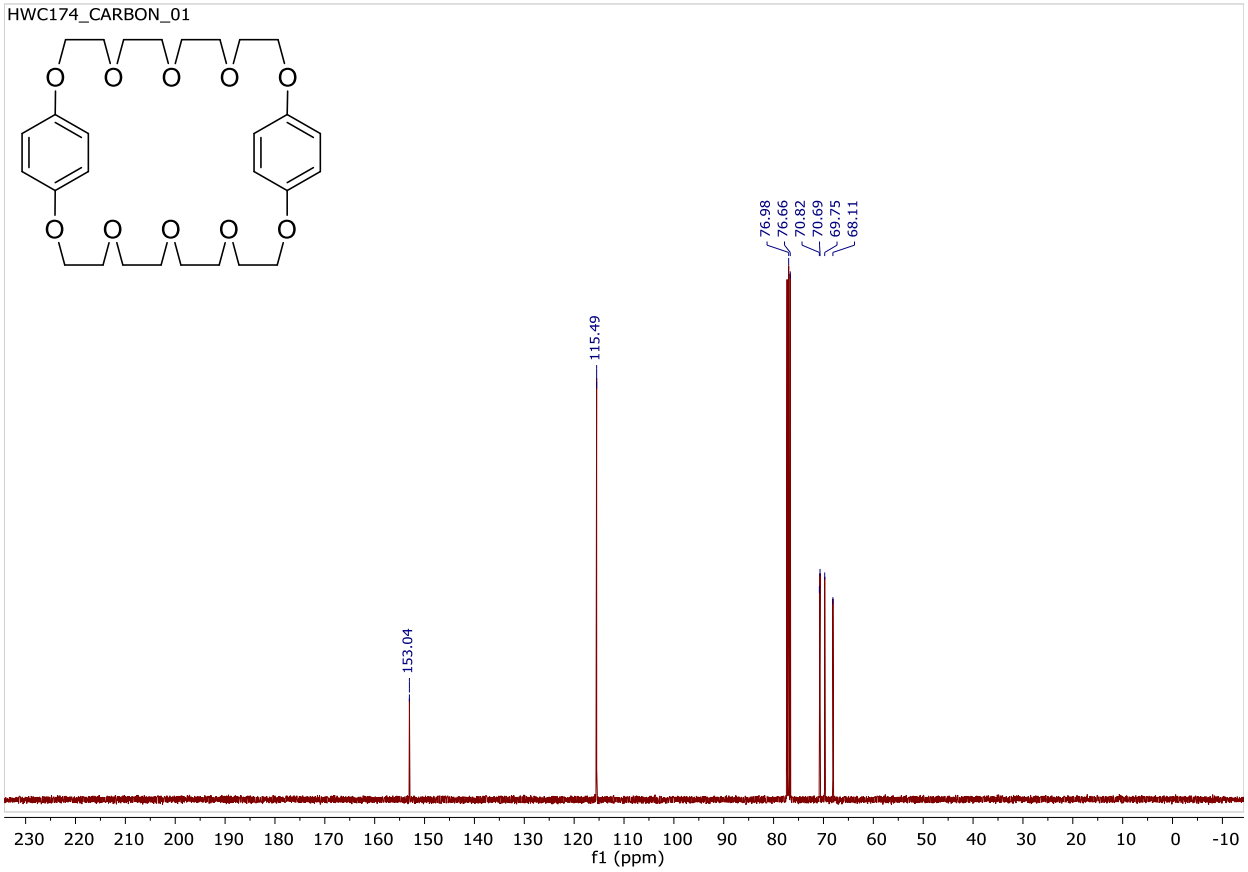

Figure 4.17. ^{13}C NMR of **BPP43C10** in $CDCl_3$ at 101 MHz

Spectra of hosts (BPP34C10, DB24C8, DB30C10, BMP32C10 and pyridyl cryptand) in acetone-d_6

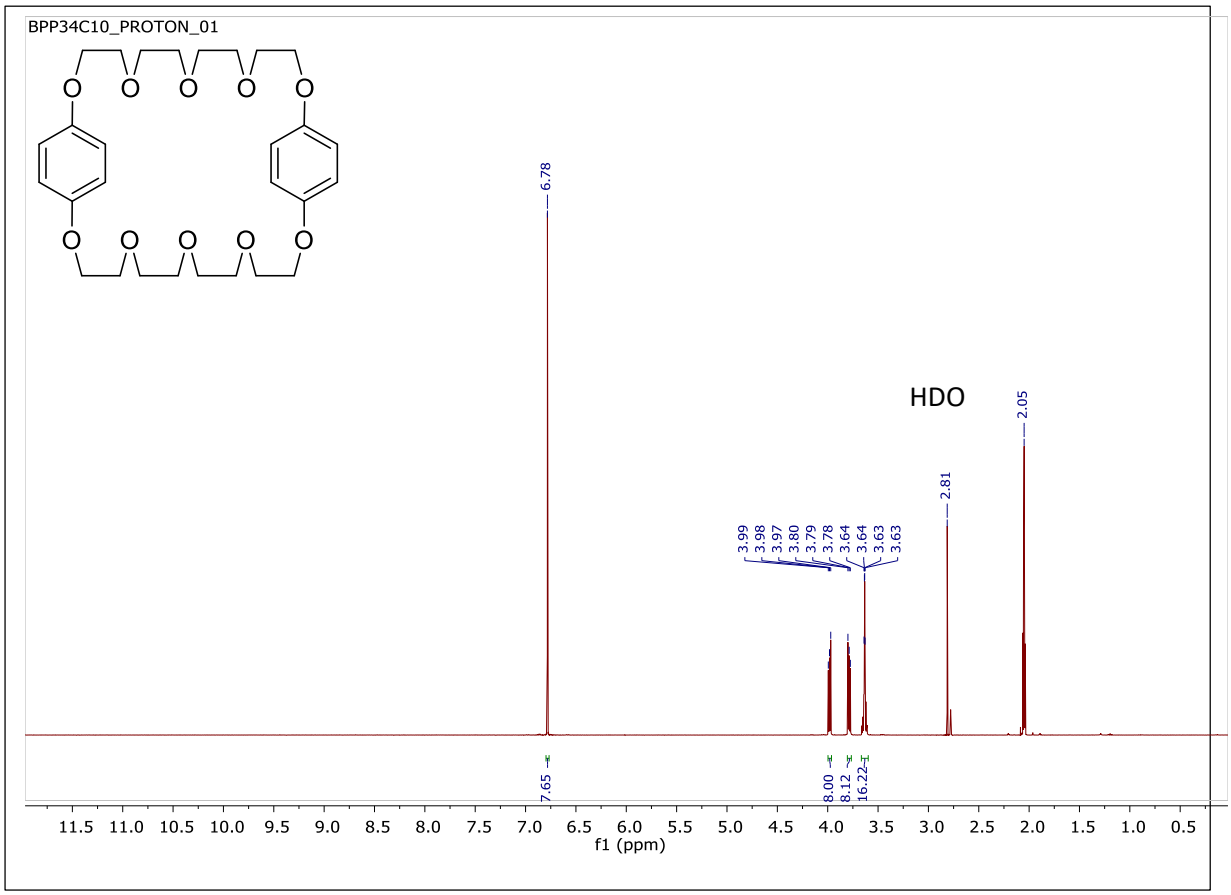

Figure 4.18. ^{1}H NMR spectrum of **BPP34C10** in acetone-d_6 at 400 MHz

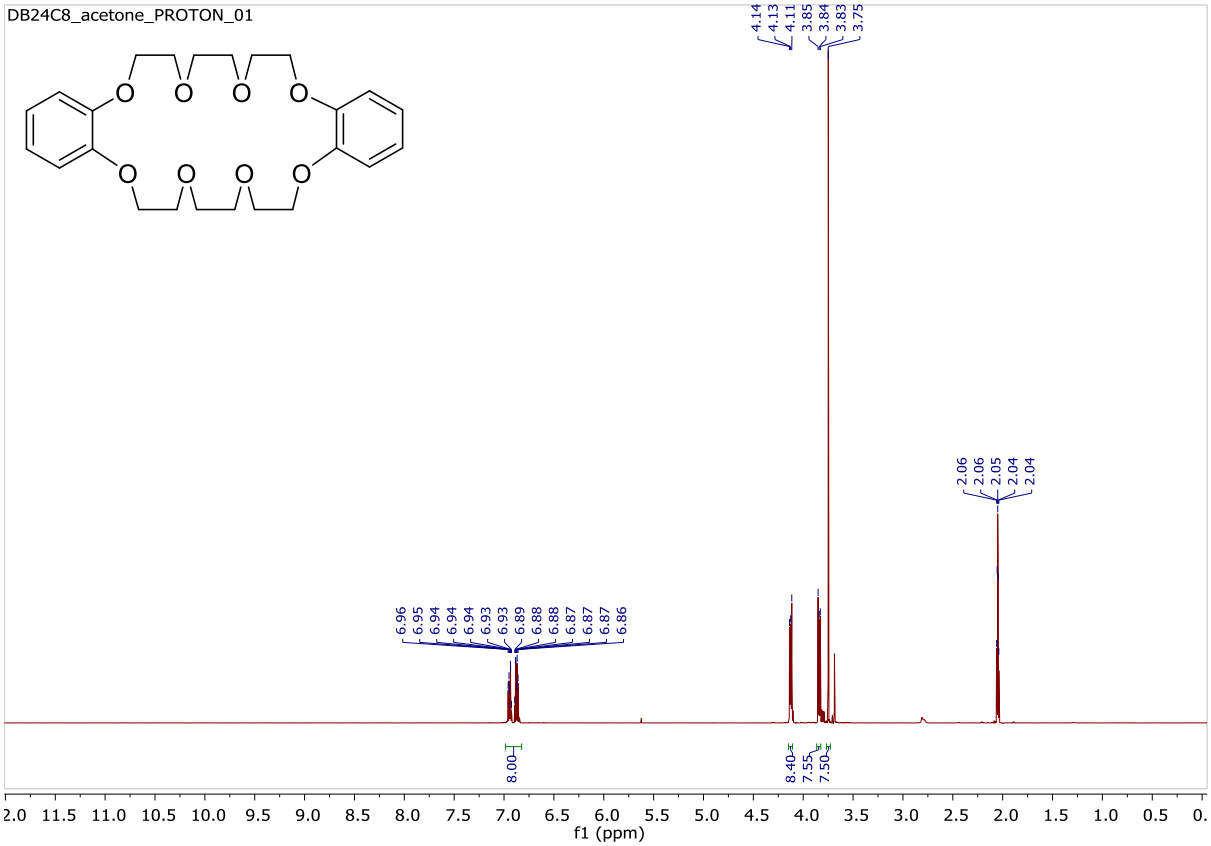

Figure 4.19. ^{1}H NMR spectrum of **DB24C8** in acetone-d_6 at 400 MHz

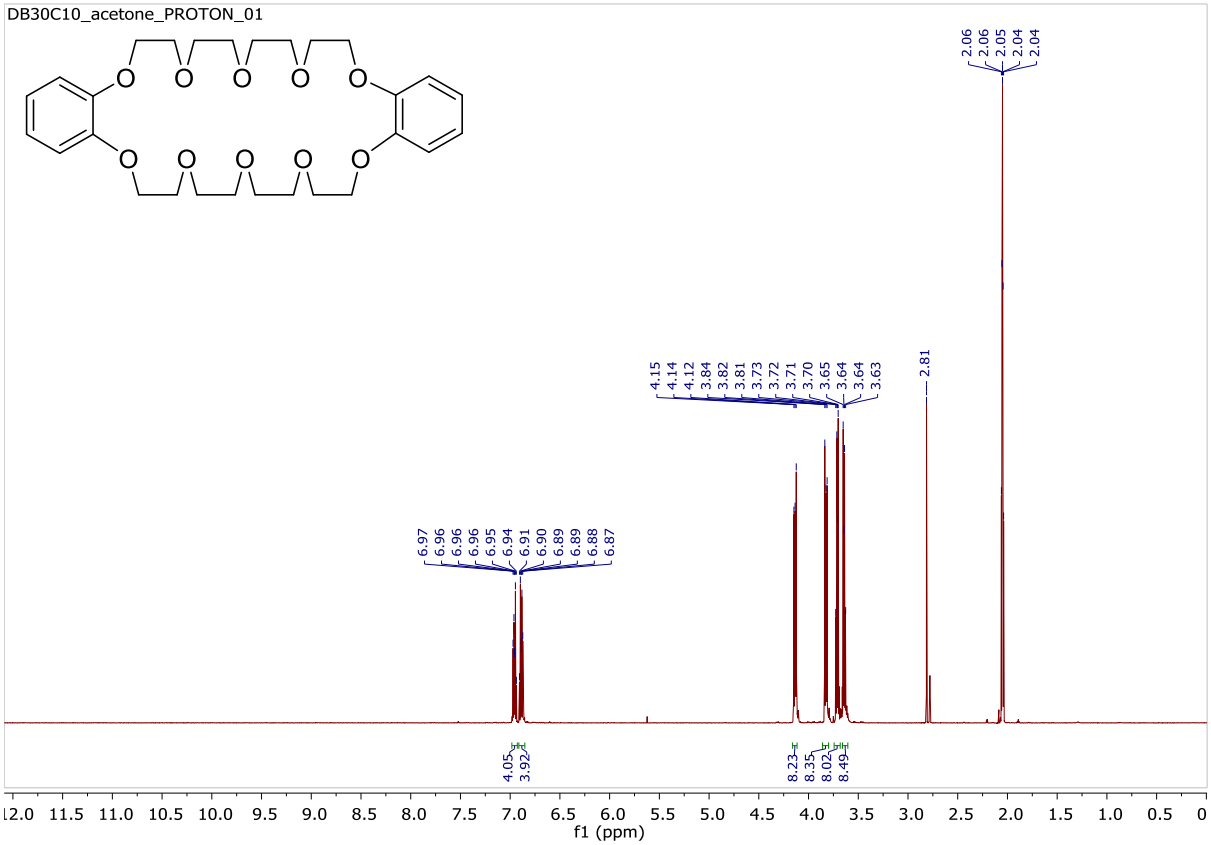

Figure 4.20. ^{1}H NMR spectrum of **DB30C10** in acetone-d_6 at 400 MHz

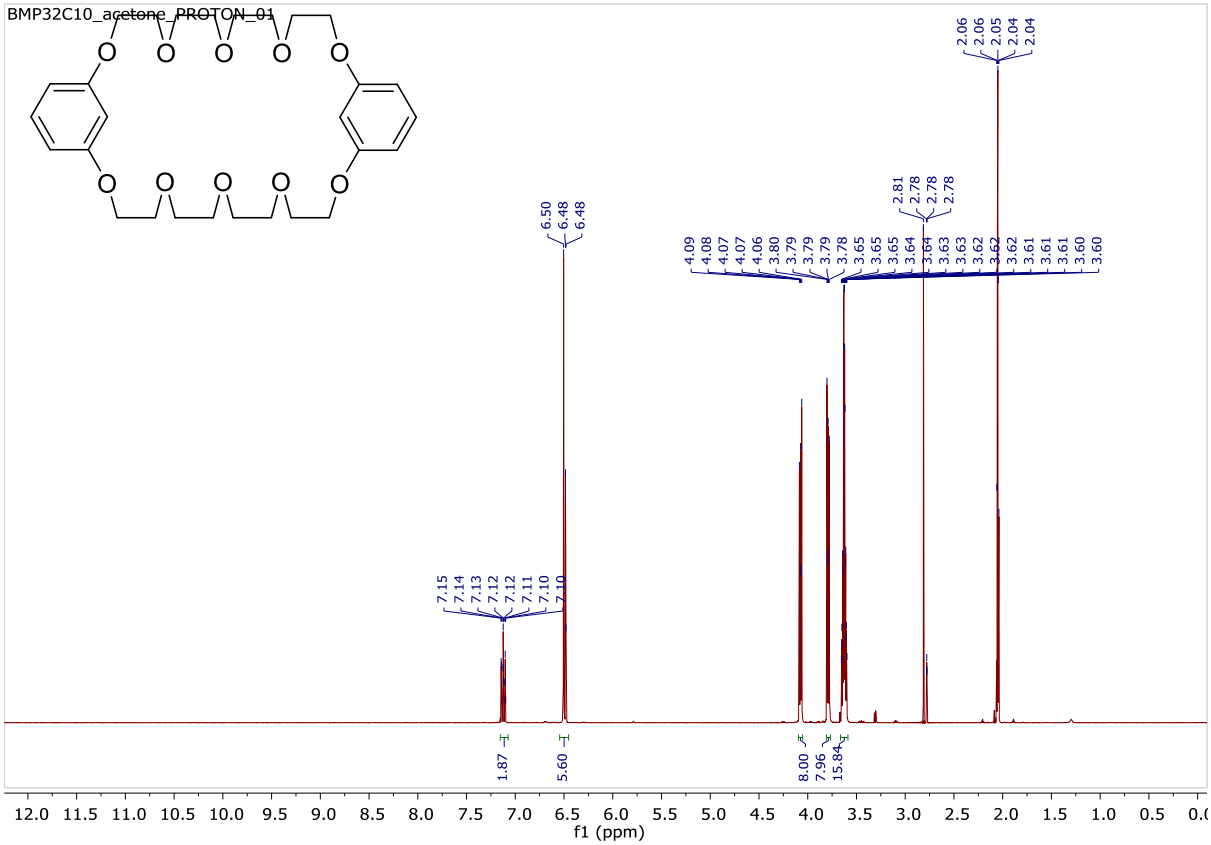

Figure 4.21. ^{1}H NMR spectrum of **BMP32C10** in acetone-d_6 at 400 MHz

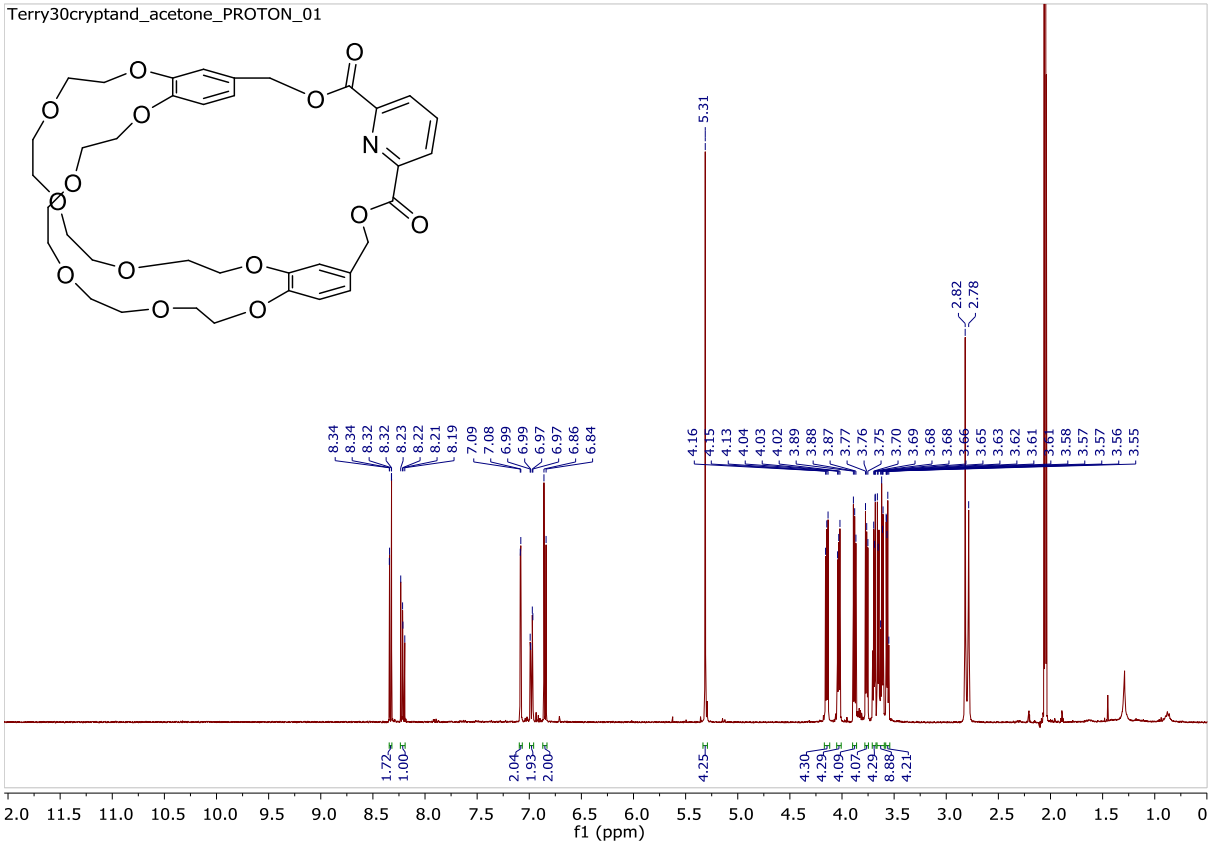

Figure 4.22. ^{1}H NMR spectrum of pyridyl cryptand in acetone-d_6 at 400 MHz

^{1}H NMR spectra of poly(pseudorotaxanes)

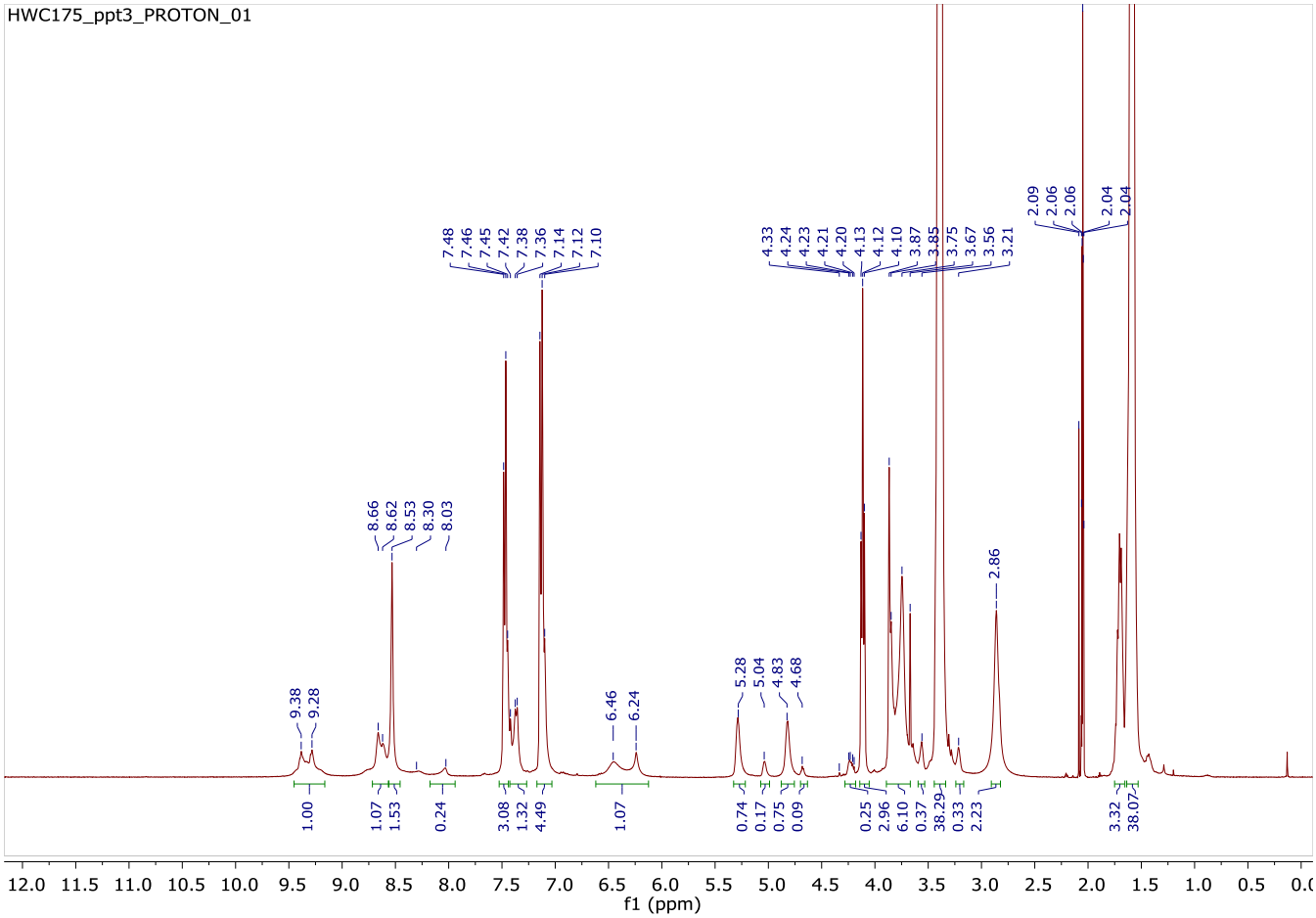

Figure 4.23. ^{1}H NMR spectrum of polyurethane formed in the presence **BPP34C10** after three precipitations into MeOH in acetone-d_6, 400 MHz.

*using the one pair of paraquat protons at 9.38 and 9.28 ppm as 4 H and the two broad singlets at 6.46 and 6.24 ppm as all the aromatic protons in the crown ether (8 H). The treading efficiency is 50 %

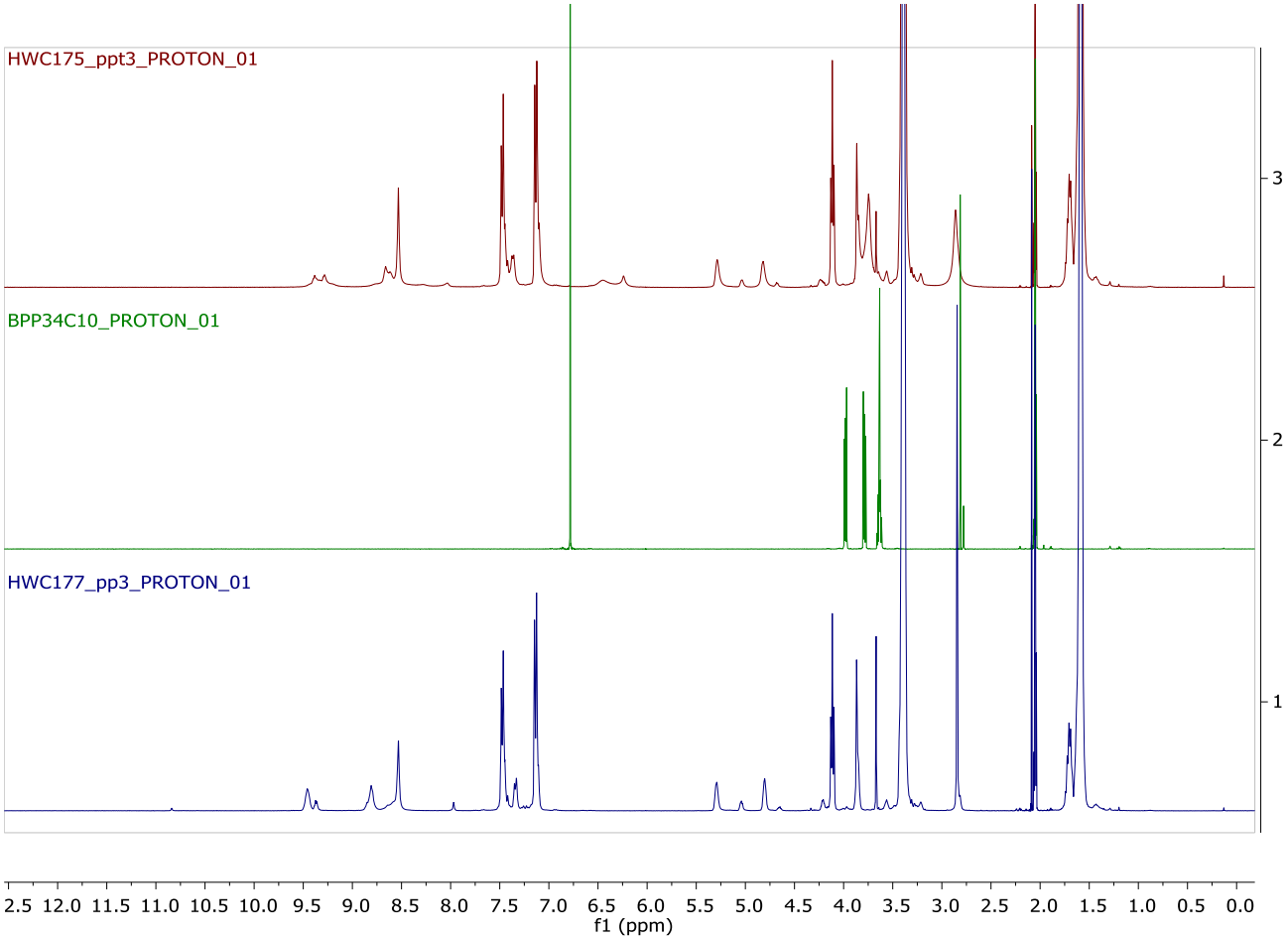

Figure 4.24. ^{1}H NMR spectra of a) polyurethane formed in the presence of **BPP34C10** (top) b) **BPP34C10** (middle) and c) polyurethane without any crown ether, the backbone polymer (bottom). All spectra were obtained in acetone-d_6 at 400 MHz

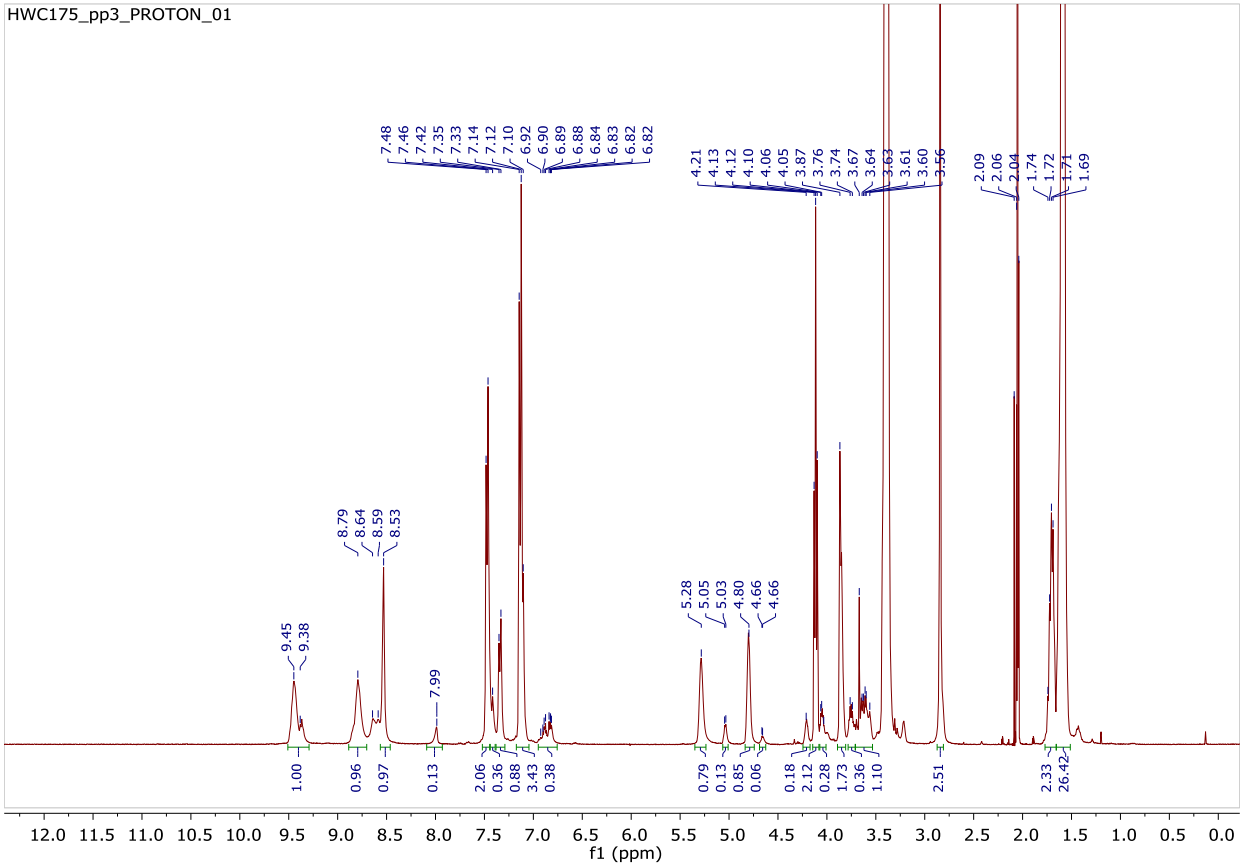

Figure 4.25. ^{1}H NMR spectrum of polyurethane formed in the presence of **DB30C10** after 3 precipitations into MeOH in acetone-d_6 at 400 MHz

*using the peaks at 9.45 and 9.38 as one set of paraquat peaks (4 H) and the aromatic protons at 6.93-6.84 ppm as all the aromatic peaks in the crown ether (8 H), the threading efficiency is (0.38/2)*100 = 19%

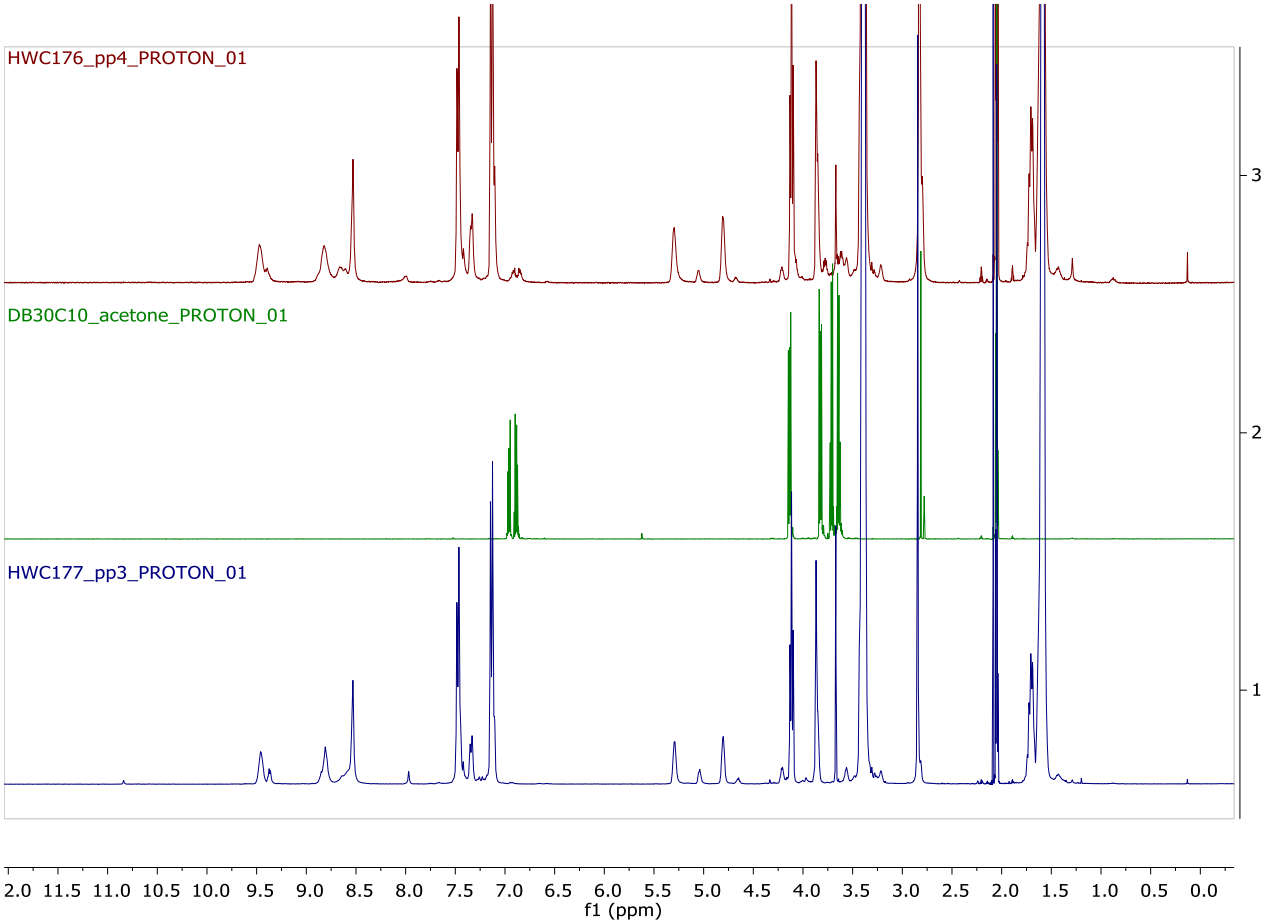

Figure 4.26. ^{1}H NMR spectra of a) polyurethane formed in the presence of **DB30C10** after 4 precipitations in MeOH (top) b) DB30C10 (middle) and c) polyurethane formed without any crown ether, the backbone polymer (bottom). All spectra were taken in acetone-d_6 at 400 MHz

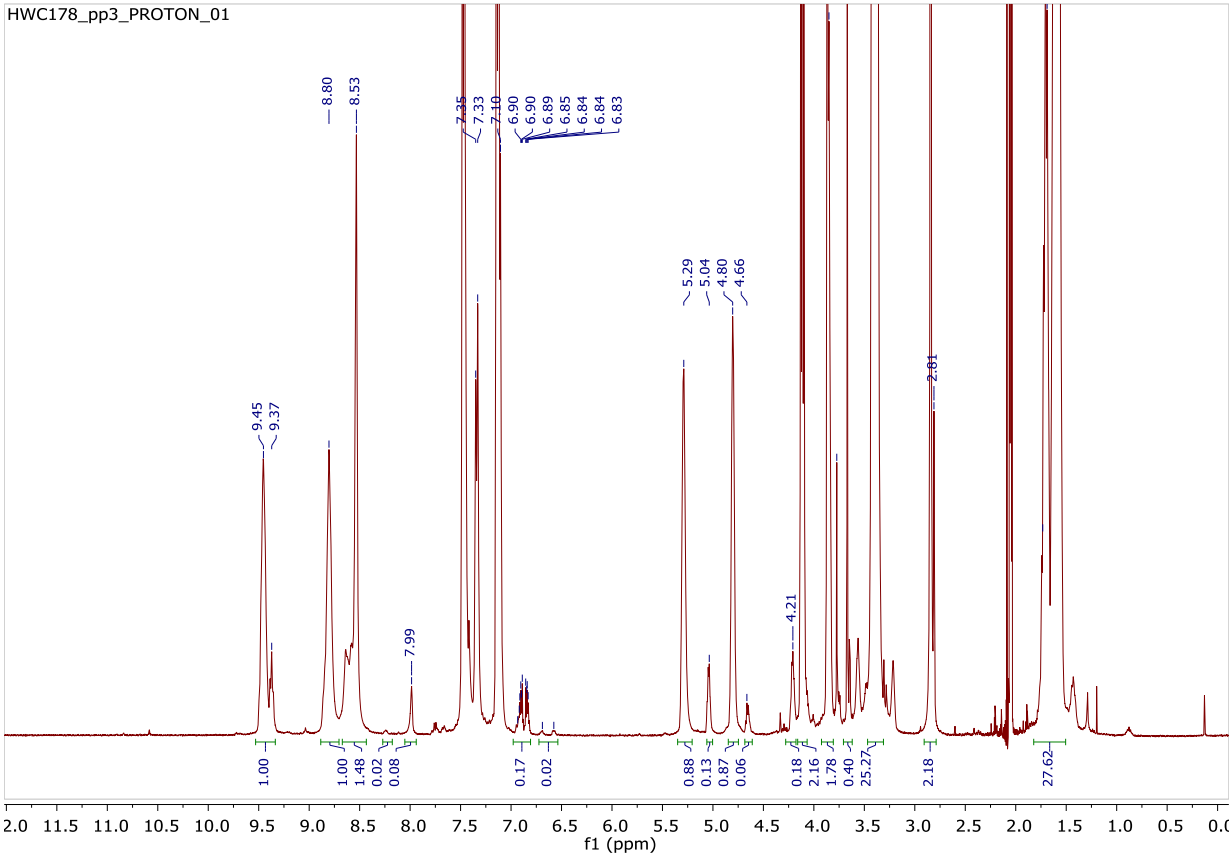

Figure 4.27. ^{1}H NMR spectrum of polyurethane formed in the presence of **DB24C8** after 3 precipitations into MeOH in acetone-d_6 at 400 MHz

*if the peaks at 9.45 and 9.37 ppm are one set of paraquat protons (4 H) and the two sets of peaks at 6.93-6.83 ppm and 6.69 and 6.58 are the aromatic peaks in DB24C8 bound to two different binding sites (8 H), the threading efficiency is ((0.17 + 0.02)/2)*100 = 9.5%

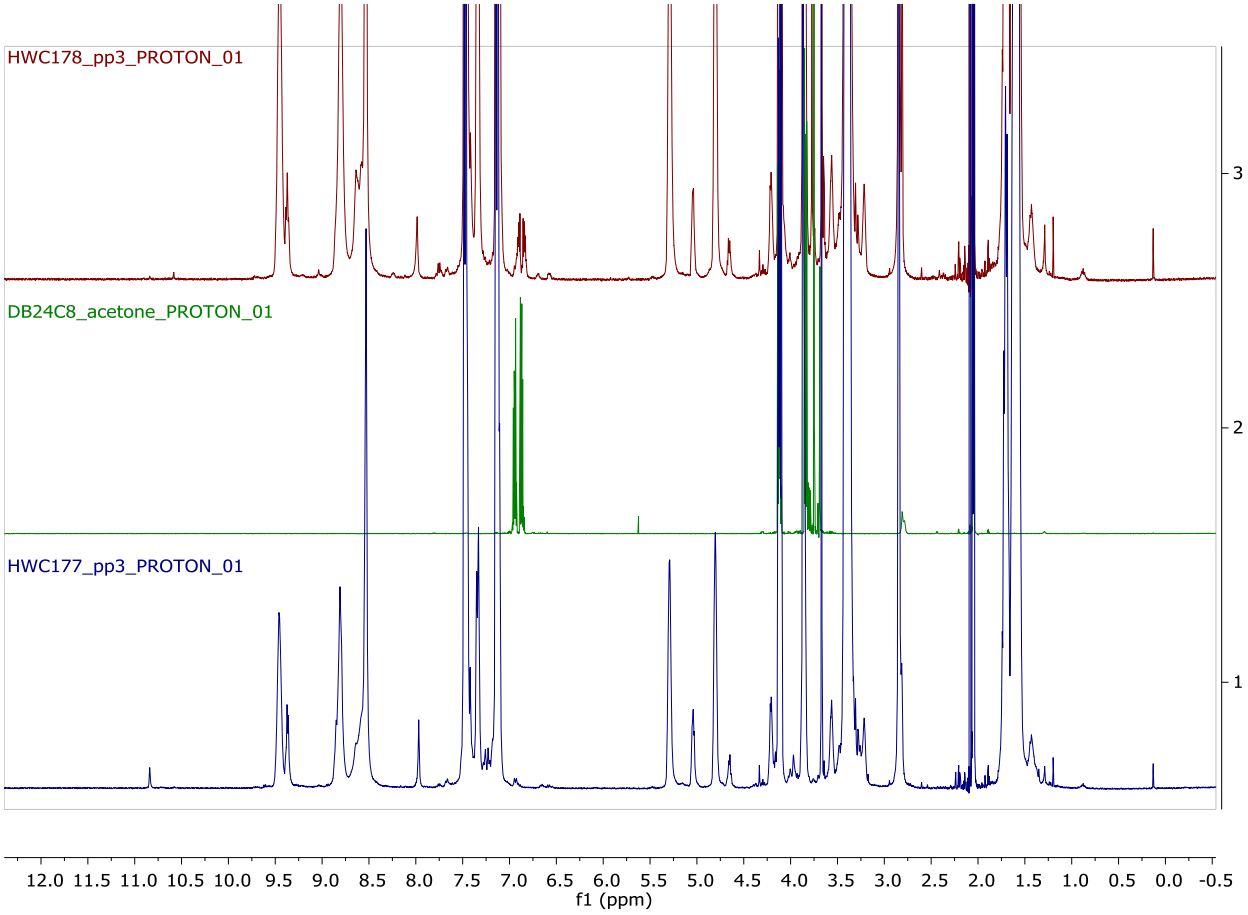

Figure 4.28. ^{1}H NMR spectra of a) polyurethane formed in the presence of **DB24C8** after 3 precipitations into MeOH (top) b) **DB24C8** (middle) and c) polyurethane backbone with no crown ether (bottom). All spectra were obtained in acetone-d_6 at 400 MHz

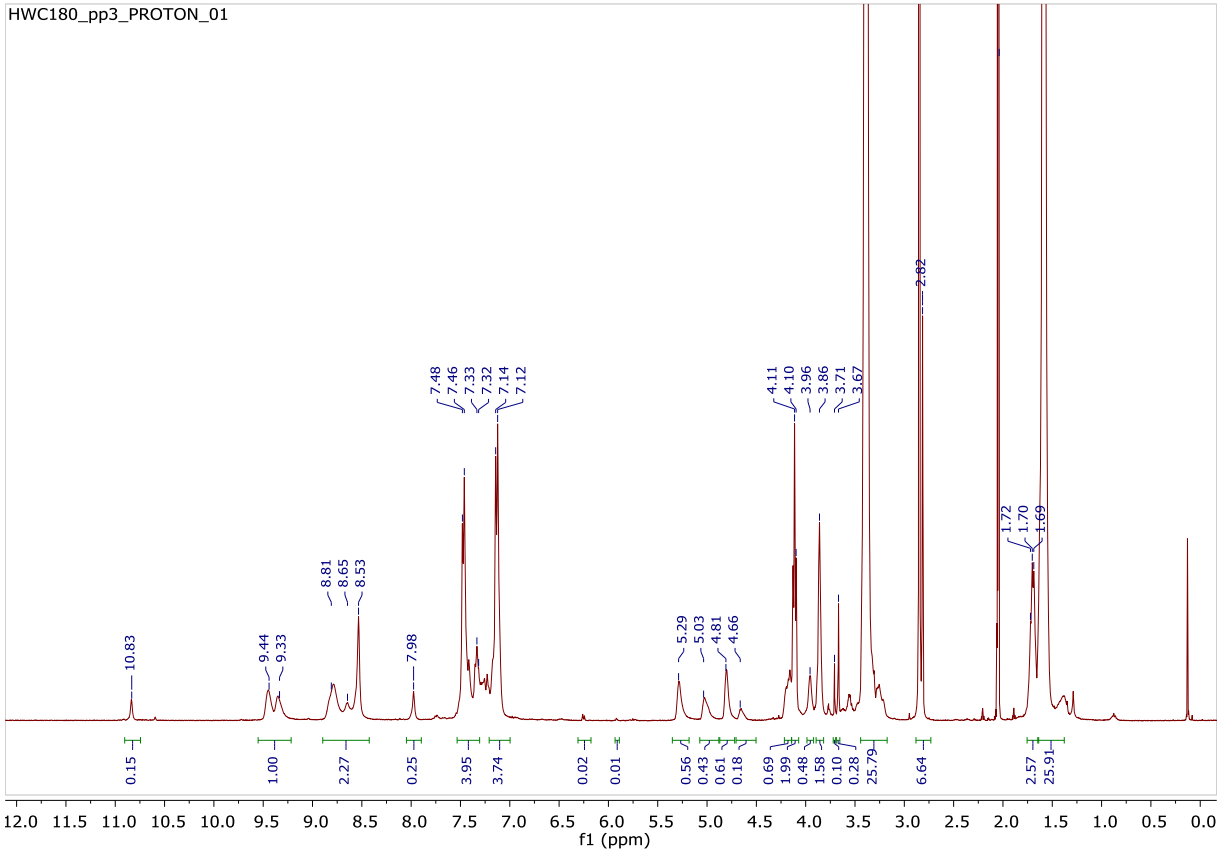

Figure 4.29. [1] HMR spectrum of polyurethane formed in the presence of **BMP32C10** in acetone-d_6 at 400 MHz

*In this reaction the MDI was heated too long before the poly(THF) was added and resulted in a gel that only dissolved with extreme difficulty. This spectrum was from everything that dissolved in acetone that was precipitated twice. The gel is bright orange.

Using the peaks at 9.47 and 9.36 ppm as one set of paraquat protons (4 H) and the peak at 6.25 ppm as the 6 aromatic protons on the crown ether, the threading efficiency is ((0.02)/6)*100 = 0.3%

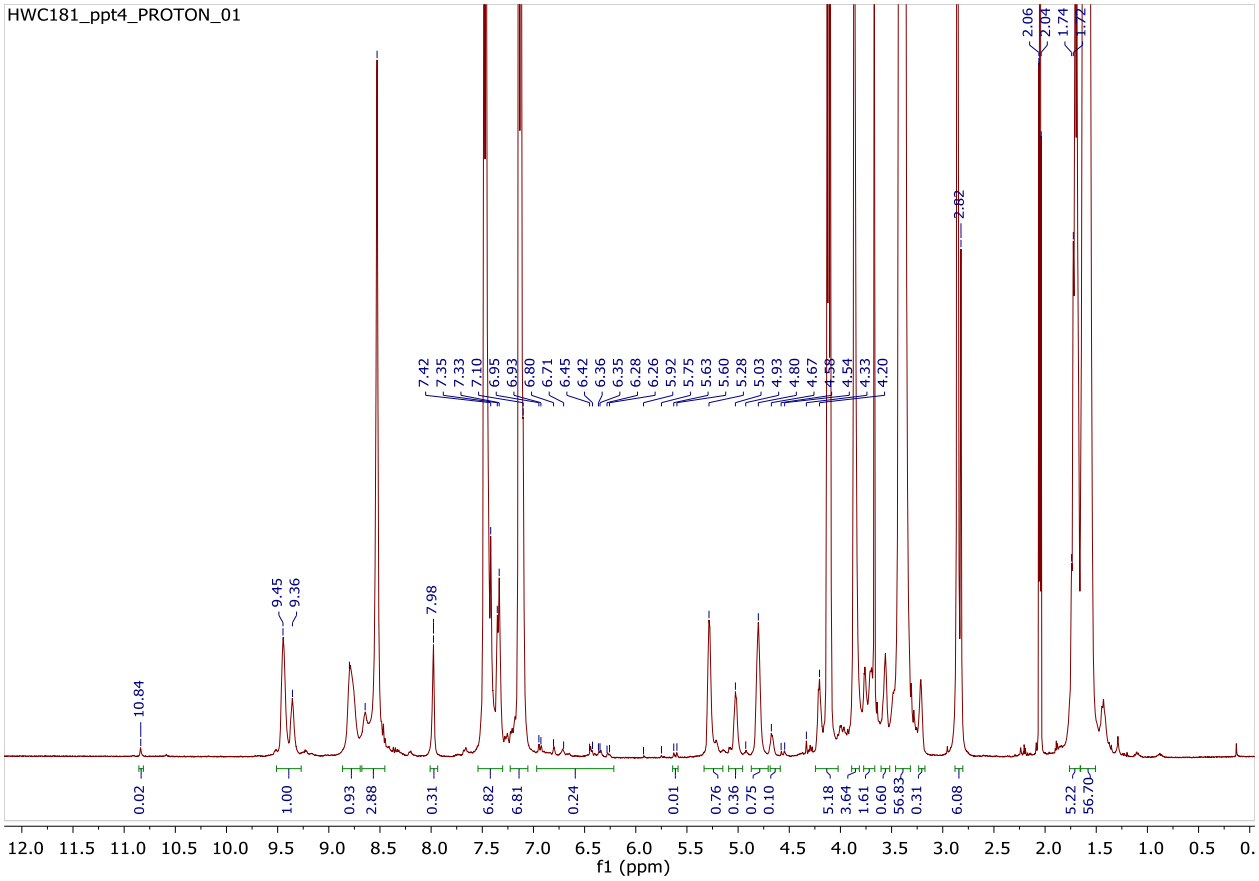

Figure 4.30. ^{1}H NMR spectrum of polyurethane formed in the presence of pyridyl cryptand after 4 precipitations in acetone-d_6 at 400 MHz

Using the signals at 9.45 and 9.36 ppm as one set of paraquat protons (4 H) all the signals between 6.95 and 6.26 as the 8 aromatic protons in the cryptand (6 H), the threading efficiency is ((0.24/6)*4)*100 = 16 %

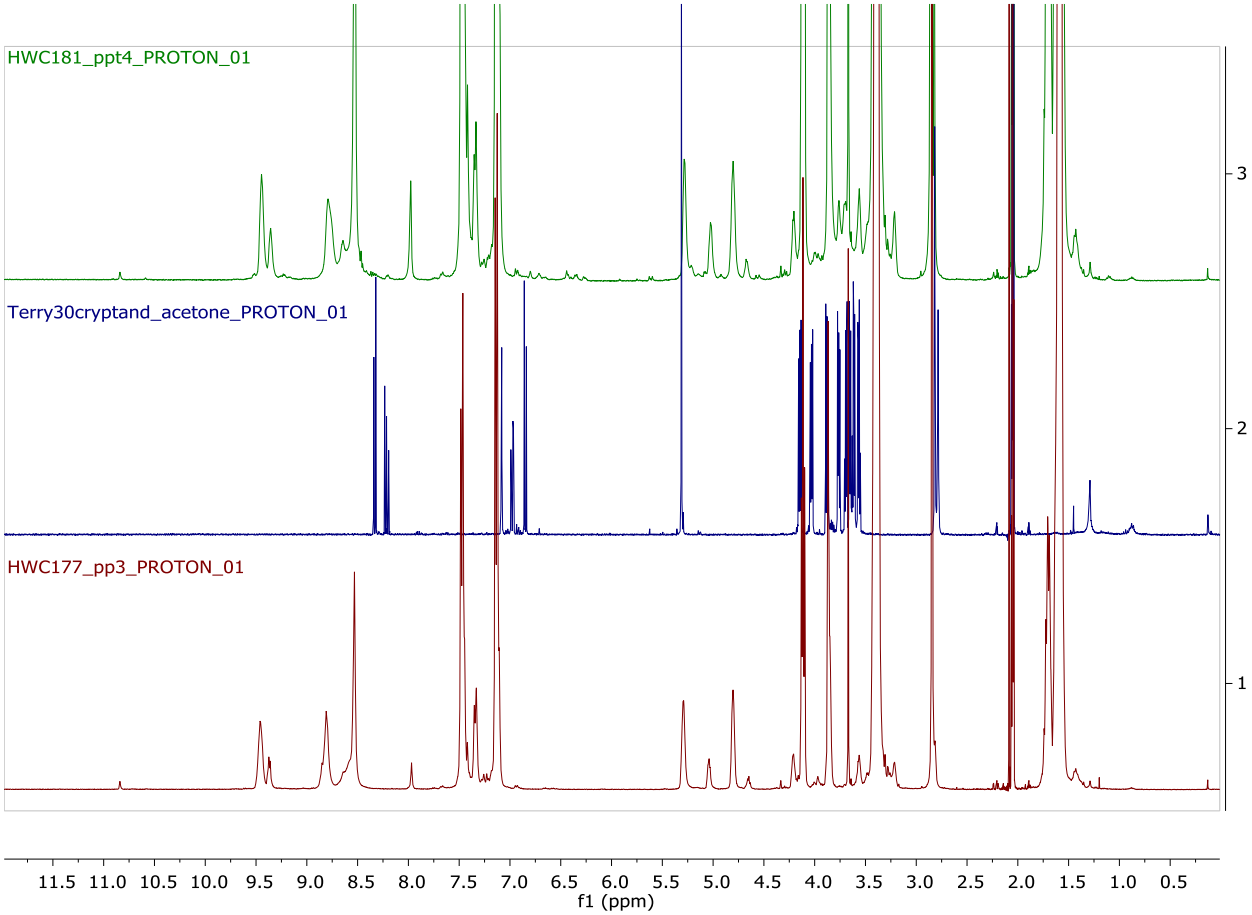

Figure 4.31. ^{1}H NMR spectra of a) the polyurethane formed in the presence of the pyridyl cryptand (top), b) the pyridyl cryptand (middle) and c) the backbone polyurethane. All spectra were obtained in acetone-d_6 at 400 MHz

Chapter 5: Conclusion and Future works

In conclusion, we devised an improved synthesis for unfunctionalized **DB24C8** and **DB30C10**. The cyclization yields were increased from 25% to more than 80% due to the use of soluble K^+ ions that act as a template. Additionally, only one step requires chromatography for purification; the final crown ether is purified by liquid-liquid extraction to remove the template. The introduction of one aromatic ring at a time allows this synthesis to be used to prepare mono-functionalized crown ethers in good yields. The removal of the protection and deprotection steps (compared to the original synthesis proposed by Pedersen in 1967[1]) simplifies the syntheses and increases overall yields.

We prepared four new rotaxanes in which **DB30C10** acts as the wheel component and a paraquat as the guest incorporated into the axle. To our knowledge, these are the first rotaxanes based on this motif. These rotaxanes where isolated and characterized by HRMS, melting point, ^1H, ^{13}C and 2-D NOESY NMR. Crystals suitable for single crystal X-ray crystallography were obtained for one rotaxane. These data demonstrated that the paraquat threads through the cavity of crown ether as opposed to wrapping around it in the “taco” conformation. This means that **DB30C10** can be used as a host for supramolecular assemblies and polymers with complex topologies.

Finally, we compared the relative threading efficiencies of five hosts; **DB24C8**, **DB30C10**, **BMP32C10**, **BPP34C10**, and a pyridiyl cryptand based on **DB30C10**. This was achieved by preparing a series of segmented poly(urethanes) with paraquat units in the backbone of the polymer in the presence of the hosts. The polymers were purified by repeated precipitation into MeOH until the integration ratio of aromatic

protons on the hosts to the paraquat signals were constant. This ratio was then used to determine the threading efficiency of the different polymers. The efficiencies were determined as 9.5%, 19%, 0.3%, 50% and 16% for **DB24C8**, **DB30C10**, **BMP32C10**, **BPP34C10**, and the pyridiyl cryptand, respectively.

Future work: Further studies on threading efficiencies with poly(urethanes)

The results obtained for the poly(urethane) pseudorotaxane chapter were contrary to our expectation. Since the pyridyl cryptand's binding constant is about 2 orders of magnitude higher than that of the crown ethers, we expected that the pyridyl cryptand would have ~100% threading. **BPP34C10** showed 50% threading upon equilibration with a highly competitive solvent. Given that the crown ethers tend to have binding constants of similar magnitude (much lower than cryptands), only a three percent difference between the threading of the **DB30C10** and the pyridyl cryptand seemed strange. The lack of threading of **BMP32C10** is also puzzling, since **BMP32C10** and paraquat have been used as the basis to form a triarm star polymer,[2] a linear polymer based on supramolecular self-assembly (AA-BB polymers where A is **BMP32C10** and B is paraquat, as well as AB polymers),[3-4] hyperbranched polymers,[5] a graft polymer [6] and a supramolecular four-armed star copolymer.[5]

On the other hand, a study by Gong and Gibson revealed that the binding constant between *N,N'*-bis(β-hydroxyethyl)-4,4'-bipyridinium hexafluorophosphate (paraquat diol) and **BMP32C10** changes based on the functionalization of the crown ether and whether the crown ether forms part of a polymer or not. The binding constant measured for **BMP32C10** diol and paraquat was 760 M^{-1}, the K_a for **BMP32C10** diester was 135 M^{-1} and the binding constant for the polyester formed form **BMP32C10** and sebacoyl chloride was 39.6 M^{-1}. All binding constants were measured by ^1H NMR at 21.8 ºC in acetone. The rationale given for the decreased binding constant in the

polymeric system was that the movement of the crown ether was restricted so that it could not as readily change its geometry to accommodate the guest.[7] Gong et al. also studied the effects of concentration and temperature on the binding constant for this system. Their investigation revealed that the K_a and the threading efficiency decreased markedly when the temperature is raised. The K_a decreased form 58.4 M^{-1} at 21.8 ºC to 17.2 M^{-1} at 54 ºC. The m/n values, or threading fraction, decreased from 34 % at 21.8 ºC to 17.7 % at 54 ºC at the lowest concentration of paraquat measured (11 mM) and from 84% at 21.8 ºC to 68 % at 54 ºC at the highest paraquat concentration measured (100 mM).[8]

Contrasting with the results obtained by Gong et al., Lee et al. showed a four to six-fold increase in association constant in their polymeric system using **BMP32C10** and paraquat. In this case, the system was comprised of a crown cantered polystyrene and a paraquat terminated poly(methyl methacrylate) or polystyrene. The polymer chains (polystyrene and poly(methyl methacrylate)) rendered the paraquat terminated chain soluble in chloroform. This enabled the authors to measure the K_a of **BMP32C10** and paraquat in chloroform for the first time.[9] The ability of the less polar solvent to substantially increase the association constant of a system was demonstrated in a recent paper by Price, Slebodnick and Gibson.[10] The K_a of a pyridiyl cryptand with dimethyl paraquat increased from $K_a = 8.34 \times 10^5$ in acetone to $K_a = 1.00 \times 10^6$ in DCM. This paraquat was rendered soluble in DCM by a change in counter ion from PF_6 to bis(trifluoromethylsulfonyl)imide (TFSI). This paper also demonstrated that the association was sensitive to variations in both the host and guest structure.[10]

In summary the complexation between even the same host and guest system is complicated. Factors that could affect the binding, as identified from the above mentioned studies include; 1) functionalization of the host and/or the guest 2) the

temperature 3) the concentration 4) whether or not the host/ guests are incorporated into a polymer 4) possibly the position of the host molecule (in the main chain vs. the chain end) 5) the solvent 6) the counter ions. Taking all of these factors together, especially the solvent polarity and the temperature, our results seem quite reasonable. The K_a of 17 M^{-1} found by Gong et al. is very low, and our maximum temperature was about 40 ºC higher than theirs, 54 ºC compared to 90-100 ºC. Our solvent system of MeCN/diglyme is also more polar, and therefore less conducive to binding than acetone. Another factor to consider is that some of the polymers were allowed to stir in the MeOH solution, into which they were repeatedly precipitated to remove excess crown ether, for excessively long times (up to 24 hrs). This probably allowed for some de-threading to occur.

To further our understanding of the threading efficiency of the hosts with the segmented poly(urethane) polypseudorotaxane in solution, some additional experiments could be performed. First, the backbone polymer, that was prepared without adding any hosts during the polymerization process, could be dissolved in acetone and the various hosts added to the solution in excess. The paper by Gibson et al. upon which this study was based performed a similar experiment.[11] The pre-formed segmented polyurethane was dissolved in acetone/DCM (30 mL/10 mL) mixture and an almost 10-fold excess of crown ether was added. The solution was allowed to stir at room temperature for 5 days before being washed extensively with hexane and DCM until the solvent that was decanted showed no more signs of crown ether by TLC.

This procedure could be performed with each of the crown ethers and the pyridyl cryptand to gain a better understanding of the threading efficiency at lower temperatures and in a solvent mixture that is more favourable to threading for future

applications. This methodology can also be easy modified to study the influence of several of the factors mentioned above on this system if desired. For example:

- The equilibration experiments could be conducted at several temperatures. For example, temperatures at which various polymerization reactions that may be used to construct supramolecular polymers could be tested
- The backbone polymer could be prepared using paraquat TFSI instead of paraquat PF_6, or the counter ions on the polymer could be exchanged after the fact. The TFSI polymer should have better solubility properties than the PF_6 polymer. If the TFSI polymer is soluble in DCM, the binding efficiencies of the crown ethers should be enhanced.
- Concentration. The effect of threading on concentration could be studied by using a 10:1, 5:1, 2:1 and 1.5:1 or 1:1 ratio of host to paraquat units. Although we have optimized several of the host syntheses (**DB24C8**, **DB30C10** and the DB30C10 pyridyl cryptand), using a 10-fold excess is quite wasteful. When the crown ethers are added *in situ*, the unthreaded crown ethers are difficult to recover because unreacted monomers are also removed during precipitation into MeOH. Using this procedure, the hexane and DCM washes should only contain crown ethers, making this approach much more atom efficient.

This methodology can also be extended to crown ethers functionalized with initiators to prepare brush polymers (Figure 5.1). A crown ether or cryptand host could be functionalized with an initiator and allowed to equilibrate with pre-formed polyurethane.

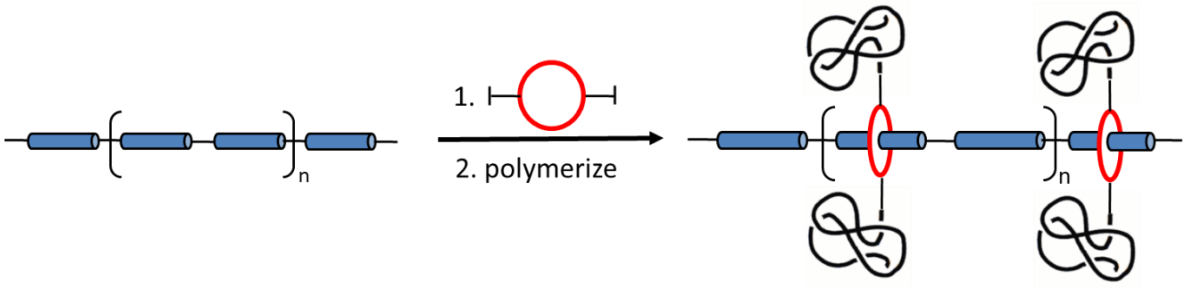

Figure 5.1. Cartoon representation of a strategy to synthesize a brunch polymer.

After the solution has been given time to equilibrate, the polymerization could be initiated. **DB30C10**, **BPP34C10** and the pyridyl cryptand would be the best choices of hosts based on the results obtained so far. Both **DB30C10** and **BPP34C10** could have initiators on either one or both the aromatic rings. Chelidamic acids functionalized with alkene, alkyne, aldehyde and alcohol groups have been prepared by a former member of our group, Dr. Price. Cryptands functionalized so that they can act as initiators for ATRP or nitroxide-mediated radical polymerization have also been prepared. However, to date we can only add one functional group to the cryptands so that they can be used to prepare pendant polymers, functionalize a chain end, or as a graft polymer, but cannot be used to make brush polymers.

Pseudocryptands

In 2011, Niu et al. synthesized pseudocryptands based on **BMP32C10** that show much higher association constants with paraquat than the unfunctionalized crown ether. Three pseudocryptands were prepared by EDCI/DMAP coupling between **BMP32C10** diol and picolinic acid (**1**), quinaldic acid (**2**) and 2-naphthyridyl carboxylic acid (**3**) (Figure 5.2). The association constants between the new hosts and paraquat are 3.1 x 10^3 M^{-1}, 12.4 x 10^3 M^{-1}, and 2.5 x 10^5 M^{-1} respectively. These association constants are between 8 and 625-fold higher than the association constant (393 M^{-1}) between un-functionalized **BMP32C10** and paraquat in the same solvent (1:1 MeCN:$CHCl_3$).[12]

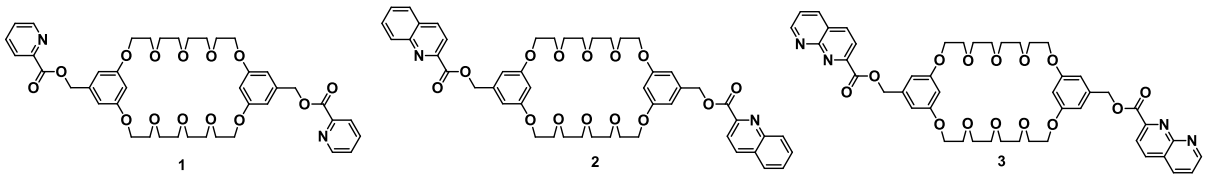

Figure 5.2. Pseudocryptands prepared by Niu et al.

The improved association constant is attributed to the fact that the heterocyclic "arms" of the pseudocryptands wrap around the guest allowing extra hydrogen bonding interactions between the H's on the guest and the N-atoms on heteroatom containing rings on the arms (figure 5.3) and π–stacking of the heterocyclic moieties. Pseudocryptands based on **DB30C10** diol have also been prepared, but unfortunately they do not show the same improvement in association constants.[13]

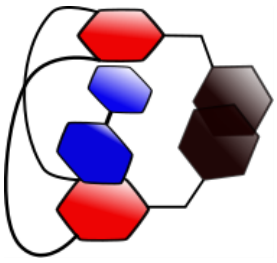

Figure 5.3. Cartoon representation of the binding between pseudocryptand **1** and paraquat, showing the pyridyl arms wrapping around the guest.

These peudocryptands are prepared in one step from **BMP32C10** diol in greater than 90% yield. The binding geometry indicates that these hosts can easily wrap around the paraquat units incorporated into the backbone of the segmented poly(urethane) instead of threading unto the backbone. Addition of pseudocryptands would be an easy way to perform a post-polymerization functionalization. The association between the pseudorotaxane and the parauqat units in the polymer should modulate several of the polymer's properties such as solubility, T_g, electronic properties, conductivity, viscosity and molecular weight.[7-8, 14] This would be a simple way to acquire several grams of a polymer with a "beads-on-a-string" configuration in order to study it's properties in detail. Additionally, the amount of threading could easily be controlled by

simply adding different amounts of the pseudocryptand. Furthermore, the nitrogens on the heterocycles could possibly be protonated reversibly; if a base can be found that will not damage the paraquat this would make these stimuli responsive materials.

Rotaxanes

Two more rotaxanes analogous to [2]rotaxane **7,** for which we obtained a crystal structure, with **BPP34C10** and pyridyl cryptand as their wheel components could be synthsized (Scheme 5.1).

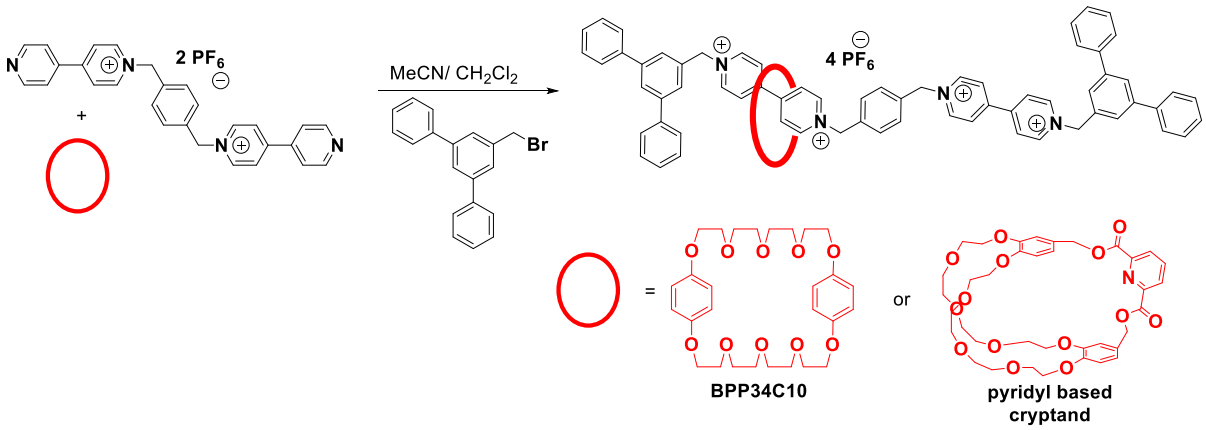

Scheme 5.1. Synthesis of rotaxnaes with **BPP34C10** and pyridyl cryptand as the wheel components

If the same synthetic method is used for their preparation, their yields (estimated in solution by ^{1}H NMR and isolated yields), as well as the amount or [2]rotaxane and [3]rotaxane isolated could shed some light on the solution threading efficiencies. If the combined yields of the **BPP34C10** rotaxanes are roughly two and a half times that of the **DB30C10** rotaxane and the yield of the pyridyl cryptand is similar to that of the **DB30C10** rotaxanes, it would be a strong indication that factors other than the K_a have an influence on rotaxane formation in solution.

DB30C10 conformation in solution

During the course of our studies, we noticed that the spectrum of **DB30C10** looks different in different solvent. Specifically, the aromatic protons appear as a singlet (or

doublet with small splitting) in $CDCl_3$, a complicated multiplet in MeCN-d_3, and two multiplets in DMSO-d_6 and acetone-d_6 (Figure 5.4).

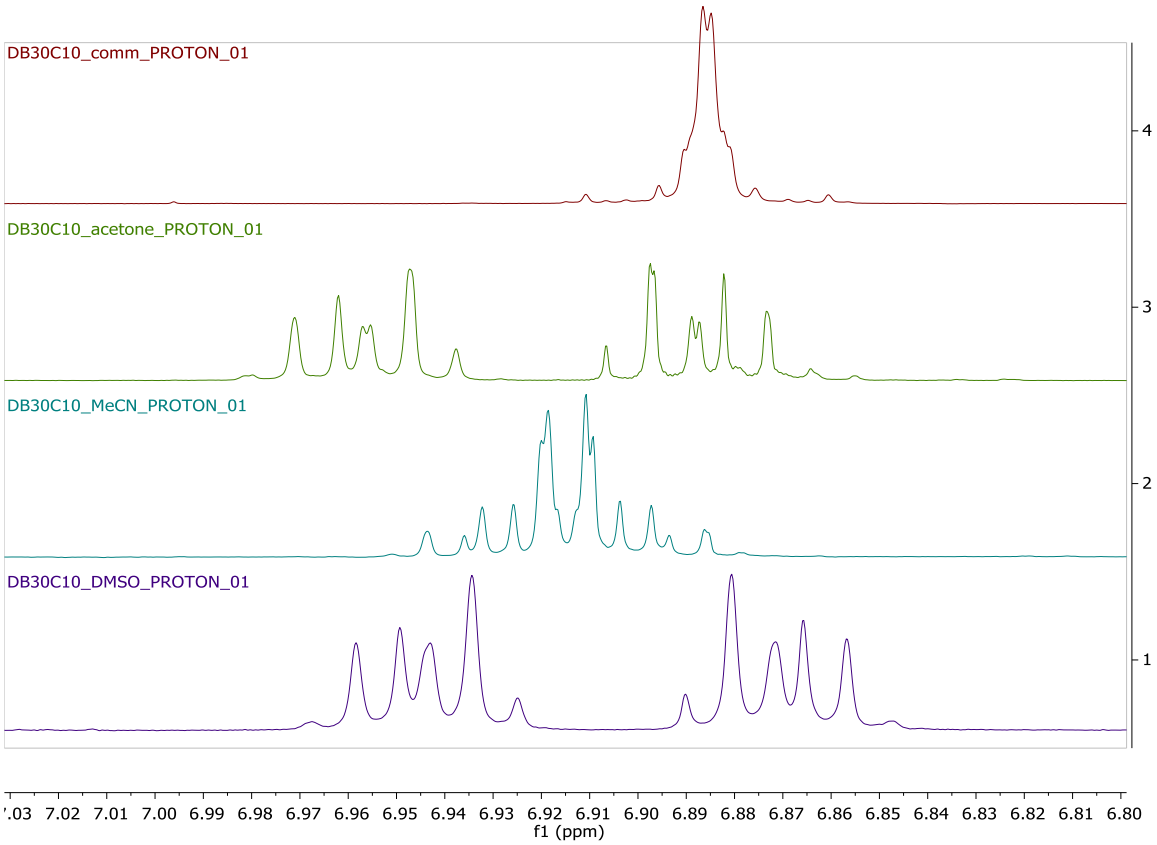

Figure 5.4. Enlarged portion of the aromatic region of the ^{1}H spectrum of **DB30C10** in a) $CDCl_3$, b) acetone-d_6, c) MeCN-d_3, and DMSO-d_6 at 400 MHz

As an ortho disubstituted benzene ring, this system should display an AA'BB' splitting pattern. The observed patterns appear to be consistent with the AA'BB' splitting. However, the J-values clearly vary quite dramatically among solvents. We have also observed that the crown ether undergoes spectral changes when forming a complex with K^+ ions. The aromatic region goes from looking like the spectrum in $CDCl_3$ (Figure 5.5) to looking more like that in DMSO-d_6 (Figure 5.8) (Figure 2.13). The ^{1}H NMR spectra of the rotaxanes all show two signals for the aromatic protons on the crown ether. The splitting patterns and chemical shifts change from the crown in DMSO-d_6

to the rotaxane as well (Figure 3.3). These observations suggest that the crown ether adopts different conformations in different solvents.

The model for the effects of solvents in host-guest complexation presented in Atwood and Steed pictures the process in a number of steps 1) desolvation of the host, 2) change in conformation of the host, 3) guest desolvation, 4) formation of the host-guest complex, 5) solvation of the complex.[15]

Complexation of **DB30C10** has been studied with a wide variety of cations. Some examples of monovalent and divalent ions that have been studied are H^+, Li^+, Na^+, K^+, Cs^+, Rb^+, Cs^+, Mg^{2+}, Ba^{2+}, La^+ and ammonium. The association constants (or stability constants of the complexes) have been measured by a variety of techniques in a number of solvents. Some techniques that have been used include NMR (various nuclei), polagraphy, potentiometry, fluorescent spectra, spectrophotometric and ion selective electrodes. Solvents in which these constants have been measured include pyridine, propylene carbonate, MeOH, acetone, nitromethane, nitrobenzene, DMSO and 50% THF/ H_2O.[16] Various studies have been performed to explore the effect of the solvent on the binding constants of the different complexes. Other effects, like that of the counter ion, ion pairing and temperature is also taken into consideration.[17-19] The dramatic variation of binding constants between solvents is consistently observed, but is usually attributed to desolvation of the cation. The effect of the solvent on the host is rarely mentioned in the studies with **DB30C10**.

In the case of **18C6**, the effect of the solvent has been explicitly studied. Gokel and Cram used the complexation **18C6** and MeCN to purify the crown ether in their synthesis published in 1974. They specifically state that they use the term “complex” loosely and that further studies into the nature of this interaction are needed.[20] Further

studies were indeed performed, including a study into the dynamics of the conformational change of **18C6** in aqueous solution,[21] several crystal structures of **18C6** with various solvents and thermodynamic constants of complexes of **18C6** with different solvents.[22]

As for **DB30C10**, a very interesting study by Chock was published in 1972.[23] The complexations of **DB30C10** with Na^+, K^+, Rb^+, Cs^+, NH_4^+ and Tl^+ in MeOH were measured using spectrophotometric titrations. The authors used a temperature jump relaxation apparatus to measure the conformational changes upon cation binding. They observed three isobestic points in their variable temperature UV-vis experiments for just **DB30C10** in MeOH. From the results of their studies, they postulated that **DB30C10** exists in at least three conformations in solution: a closed conformation, which does not bind with the cations, an open conformation which can bind with cations, and the complex.[23]

The solution conformations of benzo crown ethers (including **DB30C10**) were examined using ^{1}H NMR spectra. Careful analysis of the chemical shift changes and coupling constants of the multiplets in the ethyleneoxy signals of the crown ethers led the authors to conclude that the ether segments undergo rapid interconversion between the *syn* and *gauche* isomers in solution. This interconversion slows down in more polar solvents and upon complexation with ions. The authors also concluded that **B15C5** does not fully encapsulate the ions, and that the “wrap-around” structure observed in the crystal structure of **DB30C10**-K^+ likely also exists in solution, but not in the case of **DB30C10**-Na^+. A solution conformation of **DB30C10**-Na^+ was proposed on the basis of ^{1}H NMR and ^{13}C NMR spectra obtained in different solvents.[24]

It would be interesting to see if solution conformations for **DB30C10** in solvents of different polarity could be deduced. In addition to already mentioned ($CDCl_3$, acetone-d_6, MeCN-d_3 and DMSO-d_6), CD_2Cl_2 could be included since it is a solvent often used in our experiments. It would be interesting to see if deuterated toluene had any effect on the solution conformation, since the solvent would offer opportunity for π-π stacking with the aromatic rings of the crown ether. Other experiments that could be conducted to gain additional insight would be 2-D NOESY or ROESY spectra, and UV-vis experiments. The binding constants of **DB30C10** with different solvents could also be studied by titrating polar solvents like MeCN, acetone, DMSO, water, MeOH into a non-polar solvent that interacts with the crown ether less. These studies could potentially be performed by ITC to get thermodynamic parameters more easily, but ^1H NMR titrations might offer some insights into the solution conformations, especially since we have access to a field strength of 600 MHz, as opposed to 220 MHz. Naturally, a thorough study of the literature should be conducted to make sure that this work has not already been performed.

References:

1. Pedersen, C. J., Cyclic Polyethers and Their Complexes with Metal Salts. *J. Am. Chem. Soc.* **1967,** *89*, 7017-7036.
2. Huang, F.; Nagvekar, D. S.; Slebodnick, C.; Gibson, H. W., A Supramolecular Triarm Star Polymer from a Homotritopic Tris(Crown Ether) Host and a Complementary Monotopic Paraquat-Terminated Polystyrene Guest by a Supramolecular Coupling Method. *J. Am. Chem. Soc.* **2005,** *127*, 484-485.
3. Huang, F.; Nagvekar, D. S.; Zhou, X.; Gibson, H. W., Formation of a Linear Supramolecular Polymer by Self-Assembly of Two Homoditopic Monomers Based on the Bis(m-phenylene)-32-crown-10/Paraquat Recognition Motif. *Macromolecules* **2007,** *40*, 3561-3567.
4. Yamaguchi, N.; Nagvekar, D. S.; Gibson, H. W., Self-Organization of a Heteroditopic Molecule to Linear Polymolecular Arrays in Solution. *Angew. Chem. Int. Ed.* **1998,** *37*, 2361-2364.

5. Lee, M. Design, Synthesis and Self-Assembly of Polymeric Building Blocks and Novel Ionic Liquids, Ionic Liquid-Based Polymers and Their Properties. PhD Dissertation, Virginia Tech Polytechnic Institute and State University, Blacksburg, Va, 2010.
6. Lee, M.; Moore, R. B.; Gibson, H. W., Supramolecular Pseudorotaxane Graft Copolymer from a Crown Ether Polyester and a Complementary Paraquat-Terminated Polystyrene Guest. *Macromolecules* **2011,** *44*, 5987-5993.
7. Gong, C.; Gibson, H. W., Self-Assembly of Novel Polyrotaxanes: Main-Chain Pseudopolyrotaxanes with Poly(ester crown ether) Backbones. *Angew. Chem. Int. Ed.* **1998,** *37*, 310-314.
8. Gong, C.; Balanda, P. B.; Gibson, H. W., Supramolecular Chemistry with Macromolecules: New Self-Assembly based Main Chain Polypseudorotaxanes and Their Properties. *Macromolecules* **1998,** *31*, 5278-5289.
9. Lee, M.; Schoonover, D. V.; Gies, A. P.; Hercules, D. M.; Gibson, H. W., Synthesis of Complementary Host- and Guest-Functionalized Polymeric Building Blocks and Their Self-Assembling Behavior. *Macromolecules* **2009,** *42*, 6483-6494.
10. Price, T. L. J.; Slebodnick, C.; Gibson, H. W., Improved complexation of paraquats with crown ether-based pyridyl cryptands. *Heteroat. Chem.* **2017,** *28*, e21406.
11. Gibson, H. W.; Shen, Y. X.; Bheda, M. C.; Gong, C., Polymeric molecular shuttles: Polypseudorotaxanes & polyrotaxanes based on viologen (paraquat) urethane backbones & bis(p-phenylene)-34-crown-10. *Polymer* **2014,** *55*, 3202-3211.
12. Niu, Z.; Slebodnick, C.; Schoonover, D. V.; Azurmendi, H.; Harich, K.; Gibson, H. W., Pseudocryptand-Type [2]Pseudorotaxanes Based on Bis(metaphenylene)-32-Crown-10 Derivatives and Paraquats with Remarkably Improved Association Constants. *Org. Lett.* **2011,** *13*, 3992-3995.
13. Jones, J. W.; Price, T. L. J.; Huang, F.; Zakhorov, L.; Rheingold, A. L.; Slebodnick, C.; Gibson, H. W., Pseudocryptand Hosts for Paraquats and Diquats. *J. Org. Chem.* **2018,** *83*, 823-834.
14. Gong, C.; Ji, Q.; Subramaniam, C.; Gibson, H. W., Main Chain Polyrotaxanes by Threading Crown Ethers onto A Preformed Polyurathane: Preparation and Properties. *Macromolecules* **1998,** *31*, 1814-1818.
15. Steed, J. W.; Atwood, J. L., *Supramolecular chemistry*. second ed.; John Wiley & Sons: 2009.
16. Izatt, R. M.; Bradshaw, J. S.; Nielsen, S. A.; Lamb, J. D.; Christensen, J. J., Thermodynamic and Kinetic Data for Cation-Macrocycle Interactions. *Chem. Rev.* **1985,** *85*, 271-339.

17. Shamsipur, M.; Popov, A. I., Multinuclear NMR Study of Dibenzo-30-crown-10 Complexes with Sodium, Potassium, and Cesium Ions in Nonaqueous Solvents. *J. Am. Chem. Soc.* **1979,** *10*, 4051-4055.

18. Gholivand, M. B.; Soheila, K.; Shamsipur, M., Spectrophotometric Study of Some Alkali Earth and of Silver Complexes with Dibenzo-30-crown-10 in Methanol, Dimethylformamide and Dimethylsulfoxide solutions. *Polyhedron* **1987,** *6*, 535-538.

19. Gholivand, M. B.; Shamsipur, M., Spectroscopic Study of the Complexation of Benzo-15-crown-5 and Dibenzo-30-crown-10 with Sodium and Potassium Ions in Binary Acetonitrile-Water Mixture. *Inorg. Chim. Acta* **1986,** *121*, 53-56.

20. Gokel, G. W.; Cram, D. J., Preparation and Purification of 18-Crown-6. *J. Org. Chem.* **1974,** *39*, 2445-2446.

21. Liesang, G. W.; Farrow, M. M.; Rodriguez, L. J.; Burnham, R. K.; Eyring, E. M., Dynamics of a Conformational Change in Aqueous 18-Crown-6 by an Ultrasonic Absorbtion Method. *Int. J. Chem. Kinet.* **1978,** *10*, 471-487.

22. de Boer, J. A. A.; Reinhoudt, D. N.; Harkema, S.; van Hummel, G. J.; de Jong, F., Thermodymic Constants of Complexes of Crown Ethers and Uncharged Molecules and X-ray Structure of the 18-Crown-6(CH_3NO_2)$_2$ Complex. *J. Am. Chem. Soc.* **1982,** *104*, 4073-7076.

23. Chock, P. B., Relaxation Study of Complex Formation between Monovalent Cations and Cyclic Polyethers. *Proc. Nat. Acad. Sci. USA* **1972,** *69*, 1937-1942.

24. Live, D.; Chan, S. L., Nuclear Magnetic Resonance Study of the Solution Structures of Some Crown Ethers and Their Cation Complexes. *J. Am. Chem. Soc.* **1976,** *98*, 3769-3778.

Supplementary Figures:

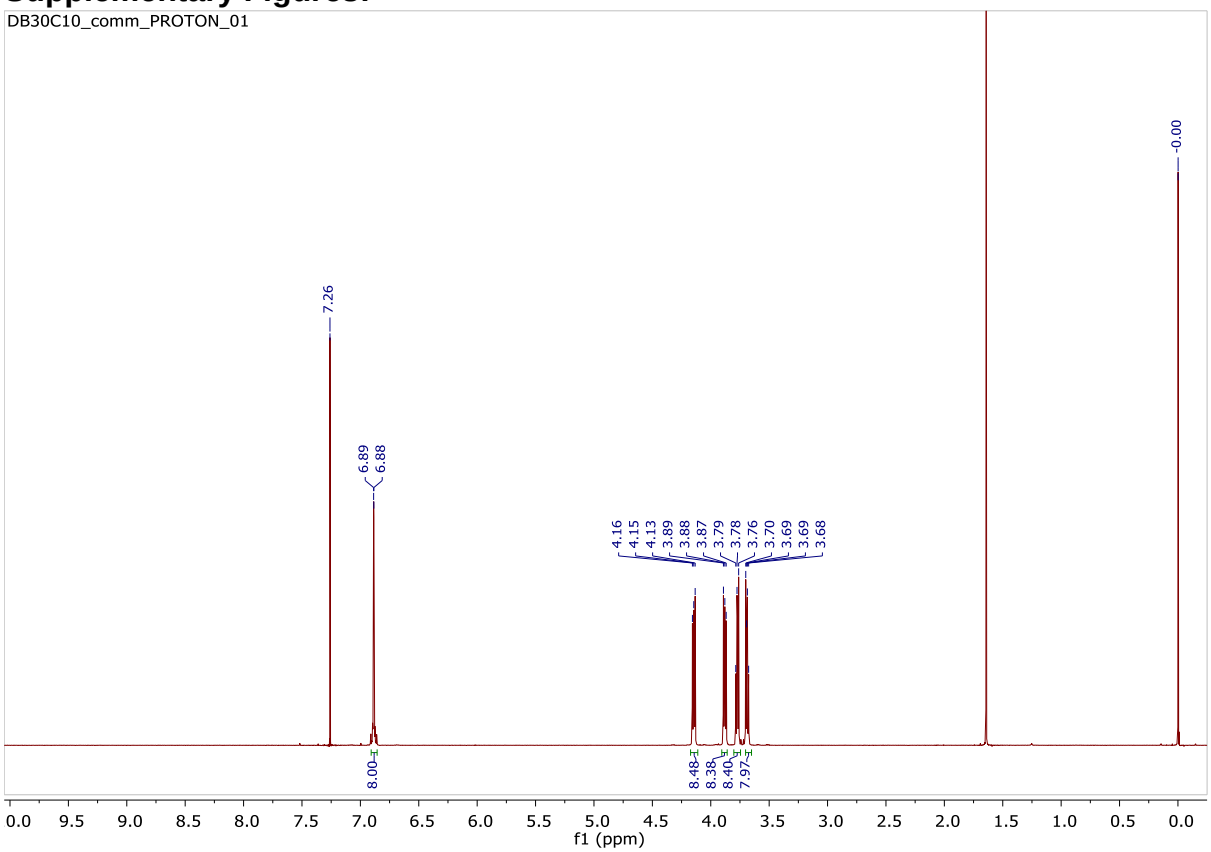

Figure 5.5. ^{1}H NMR spectrum of **DB30C10** in $CDCl_3$ at 400 MHz.

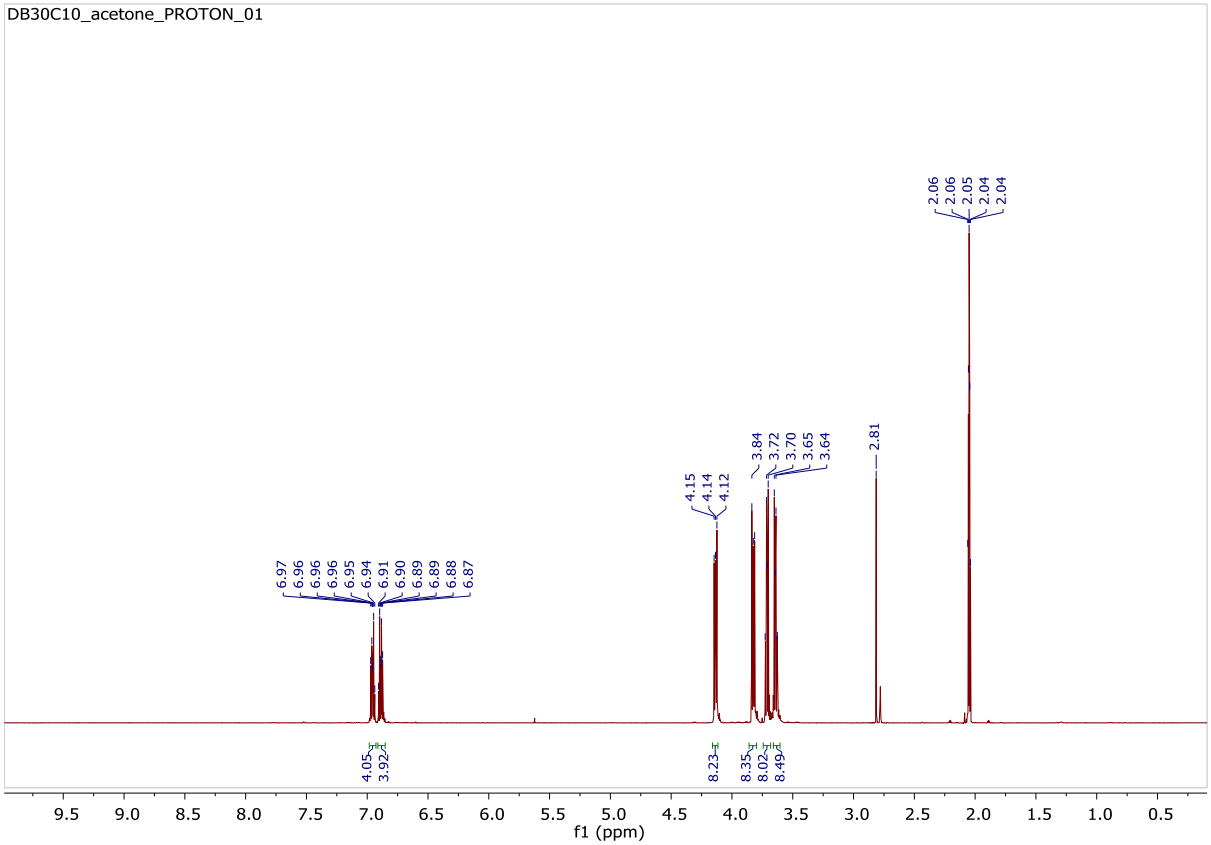

Figure 5.6. ^{1}H NMR spectrum of **DB30C10** in acetone-d_6 at 400 MHz

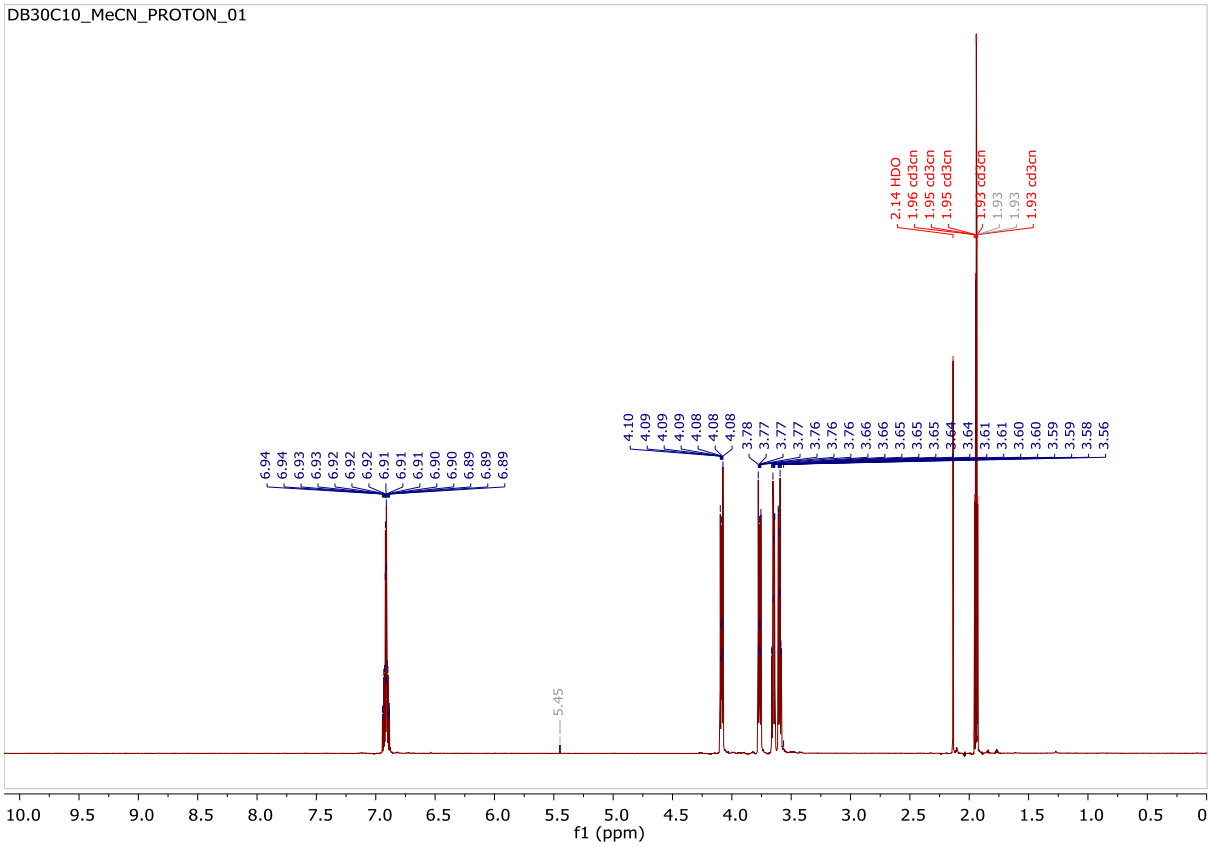

Figure 5.7. ^{1}H NMR spectrum of **DB30C10** in MeCN-d_3 at 400 MHz.

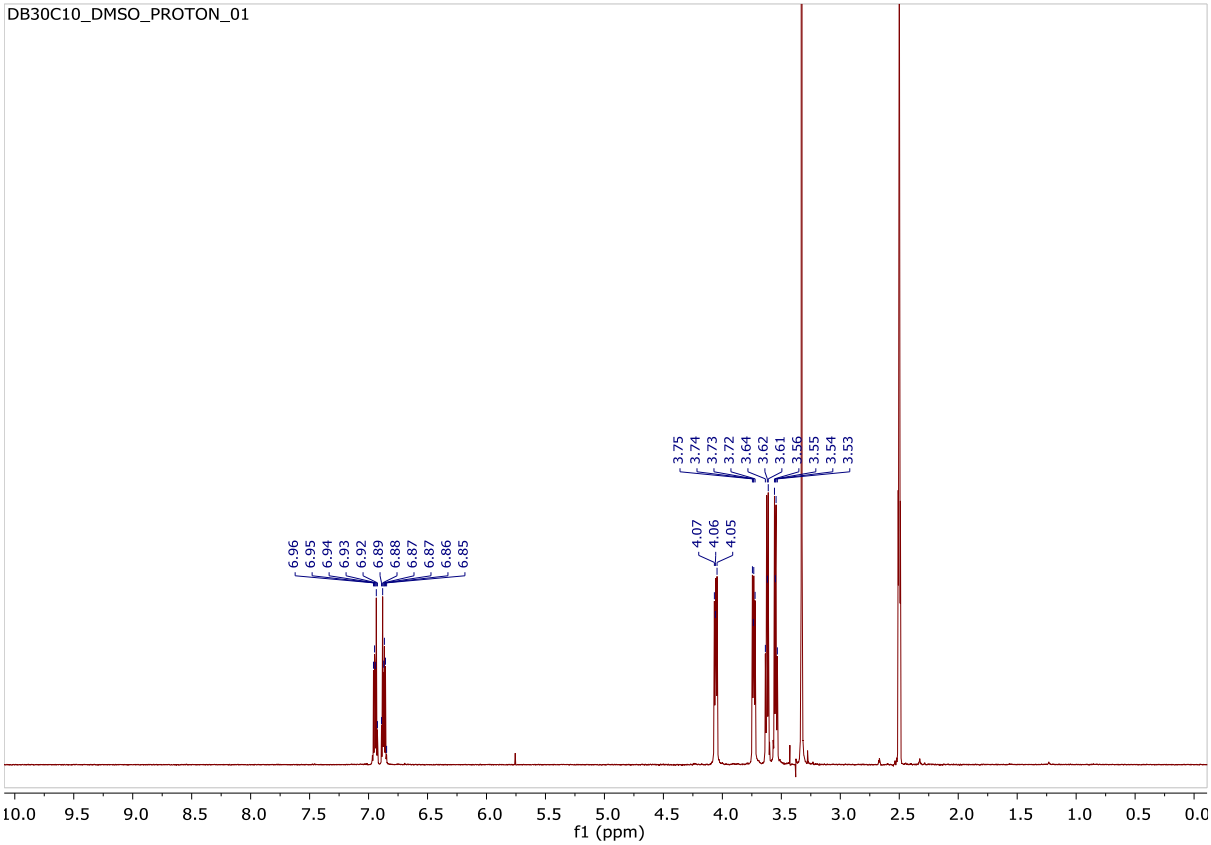

Figure 5.8. ^{1}H NMR spectrum of **DB30C10** in DMSO-d_6 at 400 MHz.